DETERMINATION OF THE THERMAL CHARACTERISTICS OF THE GROUND IN CYPRUS AND THEIR EFFECT ON GROUND HEAT EXCHANGERS

A thesis submitted for the degree of Doctor of Philosophy

by

Pouloupatis D. Panayiotis

School of Engineering and Design
Brunel University

April 2014

Abstract

Since the ancient years, human beings were using holes and caves to protect themselves from weather conditions making it the first known form of exploiting ground's heat, known as Geothermal Energy. Nowadays, geothermal energy is mainly used for electricity production, space heating and cooling, Ground Coupled Heat Pump (GCHP) applications, and many other purposes depending on the morphology of the ground and its temperature.

This study presents results of investigations into the evaluation of the thermal properties of the ground in Cyprus. The main objectives were i) to determine the thermal characteristics of the ground in Cyprus, ii) investigate how they affect the sizing and positioning of Ground Heat Exchangers (GHE) and iii) present the results for various ground depths, including a temperature map of the island, as a guide for engineers and specifiers of GCHPs. It was concluded that there is a potential for the efficient exploitation of the thermal properties of the ground in Cyprus for geothermal applications leading to significant savings in power and money as well.

Six new boreholes were drilled and two existing ones were used for the investigation and determination of i) the temperature of the ground at various depths, ii) its thermal conductivity, iii) its specific heat and iv) its density. The thermal conductivity was determined by carrying out experiments using the line source method and was found to vary in the range between 1.35 and 2.1 W/mK. It was also observed that the thermal conductivity is strongly affected by the degree of saturation of the ground.

The temperature of the undisturbed ground in the 8 borehole locations was recorded monthly for a period of 1 year. The investigations showed that the surface zone reaches a depth of 0.25 m and the shallow zone 7 to 8 m. The undisturbed ground temperature in the deep zone was measured to be in the range of 18.3 °C to 23.6 °C and is strongly dependent on the soil type. Since the ground temperature is a vital parameter in ground thermal applications, the temperature of the ground in locations that no information is available was predicted using Artificial Neural Networks and the temperature map of the island at depths of 20 m, 50 m and 100 m was generated. Data obtained at the location of each borehole were used for the training of the network.

Data for the sizing of GHEs based on the ground properties of Cyprus were presented in an easily accessible form so that they can be used as a guide for preliminary system sizing calculations. With the aid of Computational Fluid Dynamics (CFD) software the capacity of the GHEs in each location and the optimum distance between them was estimated. Additionally, the long term temperature variation of the ground was investigated.

For the first time since a limited study in the 1970's, a research focusing on the determination and presentation of the thermal properties of the ground in Cyprus has been carried out. Additionally, the use of Artificial Neural Networks (ANNs) is an innovative approach for the prediction of data at locations where no information is available. The publication of this information not only contributes to knowledge locally but also internationally as it enables comparison with other countries with similar climatic conditions to be carried out.

Statement of Copyright

Declaration

The work described in this thesis has not been previously submitted for a degree in this or any other university and unless otherwise referenced it is the author's own work.

Publications for this PhD research

- Florides, G., Pouloupatis, P. D., Kalogirou, S., Messaritis, V., Panayides, I., Zomeni, Z., . . . Koutsoumpas, K. (2013). Geothermal properties of the ground in Cyprus and their effect on the efficiency of ground coupled heat pumps. Renewable Energy, 49, 85-89.
- Kalogirou, S. A., Florides, G. A., Pouloupatis, P. D., Panayides, I., Joseph-Stylianou, J., & Zomeni, Z. (2012). Artificial neural networks for the generation of geothermal maps of ground temperature at various depths by considering land configuration. Energy, 48(1), 233-240.
- Florides, G. A., Pouloupatis, P. D., Kalogirou, S., Messaritis, V., Panayides, I., Zomeni, Z., . . . Koutsoumpas, K. (2011). The geothermal characteristics of the ground and the potential of using ground coupled heat pumps in Cyprus. Energy, 36(8), 5027-5036.
- Pouloupatis, P. D., Florides, G., & Tassou, S. (2011). Measurements of ground temperatures in Cyprus for ground thermal applications. Renewable Energy, 36(2), 804-814.

Other publications related to the research

- Florides, G. A., Christodoulides, P., & Pouloupatis, P. (2013). Single and double U-tube ground heat exchangers in multiple-layer substrates. Applied Energy, 102, 364-373.
- Florides, G., Theofanous, E., Iosif-Stylianou, I., Tassou, S., Christodoulides, P., Zomeni, Z., . . . Panayiotou, G. (2013). Modelling and assessment of the efficiency of horizontal and vertical ground heat exchangers. Energy, 58, 655-663.
- Florides, G. A., Christodoulides, P., & Pouloupatis, P. (2012). An analysis of heat flow through a borehole heat exchanger validated model. Applied Energy, 92, 523-533.

Acknowledgement

I wish to express my sincere thanks to my supervisors, Prof. Savvas Tassou and Dr. George Florides, for their invaluable support, advice and guidance during this programme of research.

I would like to thank the Research Promotion Foundation of Cyprus for funding the work 'Investigation and determination of the geothermal parameters of the ground in Cyprus, for use on the design of ground heat exchangers and heat pumps' (Contract: ΤΕΧΝΟΛΟΓΙΑ/ΕΝΕΡΓ/0308(ΒΙΕ)/15) by research grant and all our collaborators for their dedication to the project and all their support and assistance.

I would also like to acknowledge the Department of Mechanical Engineering and Materials Science and Technology of the Cyprus University of Technology and the Higher Technical Institute for allowing us to use their premises and other facilities.

Finally, I would be arrogant and selfish if I do not dedicate this thesis to my family and parents who stood by me all these years expressing my appreciation and many thanks in this way.

Contents

List of figures

List of tables

Nomenclature

∞	Infinity symbol
COP	Coefficient Of Performance of a heat pump
Cp	Specific heat (KJ/kgK)
D	Diameter (m)
D_{eq}	Equivalent diameter (m)
E_1	Exponential integral
EER	Energy Efficiency Ratio of a heat pump
ln(t)	Natural logarithm of time
L_s	Center-to-center distance between the tubes of a GHE (m)
PE	Polyethylene pipe
PN	Pipe Nominal Pressure grade (bar)
q_c	Constant heat injection rate per active length of borehole (W/m)
r	Radius (m)
R_b	Effective borehole thermal resistance (mK/W)
r_b	Radius of the borehole (m)
SDR	Standard Dimension Ratio of a pipe (outside diameter over pipe wall thickness)
t	Time (s)
$T_{(r,t)}$	Ground temperature at distance, r, from a line source after a time period, t, (˚C)
$T_{(t=0)}$	Initial temperature of the ground (˚C)
T_b	Temperature at the boundary of a borehole (˚C)
T_f	Temperature of fluid (˚C)
$T_{f(t)}$	Mean fluid temperature flowing in a GHE (˚C)
T_{fin}	Inlet fluid temperature flowing in a GHE (˚C)
T_{fout}	Outlet fluid temperature flowing in a GHE (˚C)
u	Integration variable (unitless)
α	Thermal diffusivity (m^2/s)
$\alpha t/r^2$	Dimensionless time-to-pipe ratio parameter
γ	Euler's constant = 0.5772
λ	Thermal conductivity (W/mK)
π	Mathematical constant ≈ 3.14159
ρ	Density (Kg/m^3)

Chapter 1: Introduction

Since ancient times, human beings observed that during the cold months of the year the ground temperature was higher than that of the ambient air and during the warm months, lower. The exploitation of this phenomenon and of the thermal properties of the ground is known as Geothermal Energy. Since then and following technological evolution, geothermal energy in its broad sense, has mainly been used for electricity production, space heating and cooling, Ground Coupled Heat Pump (GCHP) applications, industrial, agriculture and many other purposes depending on the properties of the ground layers and their temperature.

Geothermal energy is considered a sustainable and renewable energy source. It mainly depends on the climatic conditions of the specific location (solar radiation, mean yearly temperature, wind, rainfall, surface cover etc), the formation of the ground and its thermal characteristics, degree of saturation and geothermal gradient. Geothermal energy can minimise the use of fossil fuels and lead to reductions in pollution and greenhouse gas emissions. Also, it can lead to a reduction in the dependence of a country on imported fuel. The direct use of geothermal energy is the most common application and is usually used for the heating or cooling of buildings or for water heating purposes.

The Energy Service of the Ministry of Energy, Commerce, Industry and Tourism of Cyprus has the overall responsibility of energy matters in Cyprus, including the promotion of Renewable Energy Sources (RES). Since 2006, GCHP applications have been funded through a very generous grant scheme designed to encourage the use of RES technologies.

Partasides *et al.* (2011) reported that from evaluations of the installed geothermal systems in Cyprus, it was identified that they could offer energy savings of 40-70% for cooling and heating, depending on the size of the building and the thermal loads compared to conventional heating and cooling systems. It was also pointed out, however, that the lack of reliable information on the thermal properties of the ground in Cyprus was the main barrier in the design and application of energy efficient geothermal systems.

The knowledge of the thermal properties of the ground at the design stage assists in the correct sizing of a Ground Heat Exchanger (GHE). The Thermal Response Test (TRT) is mainly used for the in-situ determination of the thermal properties of the ground. Although, this method is relatively easy to apply and is used by many researchers to model and evaluate the response of a GHE, it is also an expensive and time consuming method to implement.

This research presents results of investigations into the evaluation of the thermal properties of the ground in Cyprus and in particular the undisturbed temperature of the ground, and thermal conductivity, specific heat and density of each type of material encountered in various locations. For the first time this information is made available in a relatively complete and reasonably accurate database. In addition, the ground temperature map of Cyprus at various depths has been established. Data for the sizing of GHEs based on the ground properties of Cyprus are also made available and can be used as a guide for preliminary system sizing calculations.

The innovation of the thesis focuses on the determination and presentation of the thermal properties of the ground in Cyprus. Additionally, it gives emphasis on the generation of the ground temperature map of Cyprus at various depths by using Artificial Neural Networks (ANNs) for the prediction of the ground temperature at locations where no information was previously available. The publication of this information not only contributes to knowledge locally but also internationally as it enables comparison with other countries with similar climatic conditions.

1.1 Main aim and objectives

The main aim of this study was to determine the thermal characteristics of the ground in Cyprus in order to investigate how they affect the sizing and positioning of Ground Heat Exchangers (GHEs) and to present the results, including a temperature map of the island at various depths as a guide for engineers.

To achieve the main aim of the study, the following specific objectives were set:

i. To estimate the temperature, thermal conductivity, specific heat and density of the ground in representative locations in Cyprus by applying established methods.

This objective is vital for the achievement of the main aim since the information collected is useful for the preparation of the temperature map of Cyprus and the determination of its influence on the sizing and positioning of GHEs.

The geology of the island and a review of the established methods to determine the thermal properties are presented. Boreholes in representative locations were drilled to analyse the formation of the ground and measure the thermal conductivity, specific heat and density of each type of material. To estimate the overall thermal conductivity of each borehole, the thermal response test was used. For this, U-tube ground heat exchangers of various hose diameters and lengths were installed in each of the boreholes. Also, the undisturbed ground temperatures in each of the boreholes at various depths were recorded for period of 12 months. For this, thermocouples were installed in each of the boreholes.

ii. To present the collected data in an easy accessible and distinctive form.

It is very important that all the data collected are presented in a comprehensible form and be easily accessible. In this way engineers can have access to a library of data related to the sizing and positioning of GHEs. Therefore, for each of the boreholes the recorded ground temperatures at various depths were plotted and the thermal properties of the characteristic ground types tabulated.

iii. To prepare the temperature map of Cyprus at various depths.

The availability of ground temperature map of Cyprus at depths of 20 m, 50 m and 100 m is very important for sizing and positioning of GHEs. Since the data collected were limited, additional data were generated using Artificial Neural Networks (ANNs) to predict the ground temperature at locations where no information was available. Various factors that could affect the temperature of the ground were considered in the training of the ANNs and the relevance of each factor was established.

iv. To examine how the ground data affect the sizing and positioning of GHEs and to determine the long term temperature variations of the ground.

A main objective of the project is to provide engineers with a useful guide for sizing and positioning GHEs in Cyprus. This will be achieved through the investigation of the influence of the temperature, thermal conductivity, specific heat and density of the ground as well as pipe diameter on the performance of GHEs using Computational Fluid Dynamics (CFD) modelling in conjunction with test data.

1.2 Structure of thesis

In Chapter 2, a general review of the geothermal energy and its exploitation is presented. The thermal properties of the ground, the factors affecting them and the calculation models developed by previous studies for their prediction are examined. A brief description of the share of geothermal energy in the world's renewable energy production is given, including the potential of geothermal energy in Cyprus.

A more detailed analysis of the thermal properties of the ground and the factors affecting the design of GHE follows in Chapter 3. The line source method, the cylindrical heat source method and the devices usually used for carrying out a Thermal Response Test (TRT) are described. The geology of the island is described and the selection of representative locations for drilling test boreholes is outlined.

Chapter 4 describes the methods, equipment used and findings related to the investigation of the temperature profile of the ground in Cyprus. Results such as the daily and monthly ground temperature distribution for each borehole location are presented graphically. Comparison of the findings with past data is also presented.

In Chapter 5, the ground temperatures recorded in Chapter 4 along with other useful data are used for the generation of the ground temperature maps of Cyprus at depths of 20 m, 50 m and 100 m using Artificial Neural Networks (ANNs). The information generated is presented in a unique way so that it is easily accessible by engineers and other interested parties.

Chapter 6 considers the factors affecting the sizing of GHEs. Using the data collected from the selected boreholes (temperature, thermal conductivity, specific heat and density of the ground) along with the pipe diameter and with the aid of Computational Fluid Dynamics (CFD) software the capacity of the GHEs in each location was estimated. Additionally, the optimum distance between GHEs and the long term temperature variation of the ground is examined. The results are tabulated and can be used as a guide for engineers designing GHEs despite the fact that some of them still need validation.

The most important conclusions arising from this study and future work are discussed in Chapter 7.

Chapter 2: Literature review

2.1 Introduction

Since the ancient times, human beings like all other living organisms on the planet were using holes and caves to protect themselves from weather conditions. Not only did they used the ground itself as a heat barrier to protect themselves against the rainfall and wind but also were exploiting the residual ground heat to keep themselves warm during the cold days of the year. Additionally, during the warm months, they were protected from solar heat and were using the lower temperature of the earth to cool themselves. This was the first known form of exploitation of the thermal properties of the ground.

Nowadays, the capacity of the ground to store heat is most widely known as Geothermal Energy. According to ASHRAE Handbook (2011), 'Geothermal energy is the thermal energy within the earth's crust'. This thermal energy exists in the rocks in depths up to 50 km on land and up to 30 km in the oceans and is also transferred in the fluids that fill the pores and fractures within them. The fluids usually in the form of water, steam or water containing large amounts of dissolved solids come to the surface naturally through the open spaces in the rocks. Where rock permeability is low, the energy extraction rate is low.

Geothermal energy is mainly used for electricity production or direct use depending on the properties of the ground layers and the temperatures produced. The following classification by temperature is used in the geothermal industry (ASHRAE Handbook, 2011):

- High temperature, $t > 150°C$
- Intermediate temperature, $90°C < t < 150°C$
- Low temperature, $t < 90°C$

For electricity production high ground temperatures are required. Areas with such capacities are not easy to exploit mostly because of the difficulty to be connected to the grid.

On the other hand, direct use of geothermal energy is possible in areas where the thermal capacity of the ground takes place in intermediate or low ground temperatures. According to data presented by Lund *et al.* (2010) in the paper "Direct utilization of Geothermal Energy 2010 Worldwide Review" at the World Geothermal Congress 2010 (WGC2010),

Geothermal Energy is directly used in 78 countries, 36 of them in Europe. The estimated installed thermal power for direct utilization at the end of 2009 was 50583 MWt while the thermal energy used is approximately 121696 GWh/year. 49% of this thermal energy is used in Ground Source Heat Pump (GSHP) applications, 24.9% for bathing and swimming, 14.4% for space heating, of which 85% is for district heating, 5.3% for greenhouse and open ground heating and the remainder for industrial process heating, aquaculture pond and raceway heating, agriculture drying, snow melting and cooling.

2.2 Ground thermal properties

The ground temperature varies with depth and is affected by the weather conditions. It is higher than that of the ambient air during the cold months of the year and lower during the warm months. At the surface, the ground is affected by short term weather variations, changing to seasonal variations as the depth increases. At the deeper layers ground temperature remains almost constant throughout the seasons and years.

Surface layer temperature varies with solar radiation, ambient temperature, wind, rain and vegetation or surface cover. Below 1 m depth and up to 8–20 m (depending on the saturation of the ground), the temperature variation is reduced and is affected by the seasonal changes only (shallow layer), while for the deeper layers the variation in the temperature is almost negligible, tending to be warmer than the ambient temperature in winter and cooler than the ambient temperature in the summer, Popiel *et al.* (2001).

Florides and Kalogirou (2005) carried out an experiment at the Athalassa area in Cyprus and discussed the factors affecting ground temperature and the temperature variation with depth. It was found that the daily temperature variations in winter only reach up to a depth of approximately 0.5 m. The temperature variation of the ground at a depth of 3 m during the year was between 15 °C to 25 °C while at a depth of 25 m the temperature remained constant at about 22 °C. The temperature measurements were also compared to calculated values using the Kasuda formula adopted by the TRNSYS program, type 501. Measured and calculated temperatures showed good agreement. A factor that can have an influence on the accuracy of simulated ground temperatures are the physical properties of the undisturbed ground which can vary from location to location.

Solar radiation is probably the most important factor affecting the temperature of the ground at the surface and shallow zones. Other climatic conditions like the wind and rain are also important. The temperature of the ground at the deeper layers is mostly affected by the structure and physical properties of the soil with the thermal conductivity being the most important. The rate of heat flow in the ground is called thermal diffusivity and is defined as the ratio of the thermal conductivity to the thermal capacity of the ground, Hepbasli et al. (2003). Another important property of the ground is the geothermal gradient which is a measure of how rapidly the temperature increases at constant heat flow and is a function of the ground thermal conductivity. Ground layers with low thermal conductivity result in higher geothermal gradients and vice versa, Kelley (2005). The thermal properties of various soil types are presented in Table 2.1 below.

Table 2.1: Thermal properties of various soil types at 20°C, ASHRAE Handbook (2011)

Soil type	Thermal conductivity (λ) (W/mK)	Dry density (ρ) (Kg/m^3)	Thermal diffusivity (α) (m^2/day)
Heavy clay, 15% water	1.4 – 1.9	1925	0.042 – 0.061
Heavy clay, 5% water	1.0 – 1.4	1925	0.047 – 0.061
Light clay, 15% water	0.7 – 1.0	1285	0.055 – 0.047
Light clay, 5% water	0.5 – 0.9	1285	0.056 – 0.056
Heavy sand, 15% water	2.8 – 3.8	1925	0.084 – 0.11
Heavy sand, 5% water	2.1 – 2.3	1925	0.093 – 0.14
Light sand, 15% water	1.0 – 2.1	1285	0.047 – 0.093
Light sand, 5% water	0.9 – 1.9	1285	0.055 – 0.12
Granite	2.3 – 3.7	2650	0.084 – 0.13
Limestone	2.4 – 3.8	2400 – 2800	0.084 – 0.13
Sandstone	2.1 – 3.5		0.65 – 0.11
Shale, wet	1.4 – 2.4	2570 – 2730	0.065 – 0.084
Shale, dry	1.0 – 2.1		0.055 – 0.074

The structure and moisture content of the ground in the Athalassa region in Nicosia was examined by Florides and Kalogirou (2004). The ground is mainly formed by calcareous sandstone and marl (details on the soil type are given in Appendix 4). Clay layers contain about 30% of water (by mass) while layers below the water table which starts at 15 m, contain about 50% of water (by mass) and has a discharge of about 2-3 m^3/h. The mean density of the undisturbed ground is about 1900 kg/m^3 and the mean specific heat capacity is about 1400 J/kg K.

Similarly, boreholes in the Agia Fyla, Agios Georgios and Saittas regions were examined by Pouloupatis et al. (2009). In the region of Agia Fyla the ground is mainly hardcore material consisting of marl, chalk and gravel. In the Agios Georgios region the ground consists of red soil, silty sand with gravels and yellow and green marl. The structure of the ground in the Saittas region is top soil up to 8 m depth and the rest, up to 178 m is diabase.

2.3 Prediction of ground temperature

For the prediction of the ground temperature behaviour several calculation models have been developed by a number of researchers. Kusuda and Achenbach (1965) presented a simplified formula describing the temperature distribution in the ground. According to that formula, the temperature of the ground is affected by the time of the year; the depth and the thermal diffusivity of the ground. Williams and Gold (1976) used this simplified formula to estimate the range of ground temperatures in Canada. For their calculations they assumed the effect of factors such as solar radiation, wind, rain, snow and water content, cancelled each other out so that the temperature variation of the ground could be estimated by using the variation of the ambient temperature only. This showed ground surface temperature to be very close to that of the ambient air, decreasing with depth. For depths below 5-6 m, ground temperature tended to stabilise with a geothermal gradient of 1 $^{\circ}$C per 50 m depth. The variation of ground temperature occurred with time lag in relation to ambient temperature reaching a 6 month lag for a 5 m depth.

Similarly, Florides and Kalogirou (2005) identified a time lag of about 160 days between the highest temperature on the ground surface and the ground temperature at 3 m depth in their tests at the Athalassa area of Cyprus. The temperature measurements were compared to the calculated values resulted from simulations performed with TRANSYS, showing general agreement.

For the prediction of the daily and annual variation of the ground surface temperature, a model based on the transient heat conduction differential equation using the energy balance equation at the ground surface as a boundary condition, was presented by Mihalakakou *et al.* (1997). The convective energy exchange between air and soil, the solar radiation absorbed by the ground surface, the latent heat flux due to ground surface evaporation and the long wave radiation were the main parameters used in the model. The model results were compared with measured temperatures of bare and short-grass covered

ground in Dublin and Athens for the period 1981 to 1990. The comparison of the predicted set of data with the measured sets, showed a very good agreement. The sensitivity of the ground temperature to different energy balance factors was also studied.

The results of numerical simulations of ground temperature distribution are not always reliable, especially when inaccurate ground property data are used. For this reason, Popiel *et al.* (2001) examined the accuracy of a simple semi-empirical formula proposed by Baggs (1983), for Australian climate conditions. The formula is based on the transient heat conduction equation in a semi-infinite solid with the exposed surface temperature varying periodically with time. Factors like structure and physical properties of the ground, surface cover, air temperature and humidity, wind, solar radiation and rainfall are taken into consideration. The ground temperature distribution for Poznan, a city in Poland, was calculated using the above formula and was compared with the temperature distribution in the ground, measured for two different ground surfaces; for a car park area up to a depth of 7 m and for a lawn area up to a depth of 17 m. The calculated and measured values showed good agreement. For the lawn area, the temperature below 1 m depth was 4 °C lower than that of the car park for summer and is recommended for cooling purposes, whereas a depth between 1.5-2 m is recommended for horizontal ground heat exchange applications. Finally, Popiel *et al.* (2001), suggested the division of the ground in Poznan into the surface zone to 1 m depth and being affected strongly by weather conditions, the shallow zone, from 1-8 m depth for dry soil and 1-20 m depth for moist heavy sandy soil and affected mostly by seasonal weather changes and the deep zone, extending from the depths of 8 or 20 m, with the ground temperature influenced only by the geothermal gradient.

A synopsis of the characteristics of the calculation models for the prediction of the ground temperature presented above is shown in Table 2.2.

2.4 Ground Heat Exchangers

For the exploitation of the ground thermal energy Ground Heat Exchangers (GHE) or Earth Heat Exchangers (EHE) are used. A GHE is usually an array of buried pipes placed either horizontally or vertically into the ground. They use the ground as a heat source when operating in the heating mode and as a heat sink when operating in the cooling mode.

Table 2.2: Calculation models for the prediction of ground temperature behaviour

Researcher	Study	Factors studied	Conclusions
Williams and Gold (1976) Florides and Kalogirou (2005)	Kasuda formula for calculating the ground temperature	• time of the year • depth of the ground • thermal diffusivity of the ground	• Simple formula with reasonable results • accuracy of the calculated results could be affected by the precision of the data related to the thermal properties of the ground and the actual weather conditions • temperature variation of the ground surface is very close to that of the ambient air decreasing with depth • variation of temperature occurs with a time lag in relation to depth
Mihalakakou *et al.* (1997)	model based on the transient heat conduction differential equation using the energy balance equation of the ground surface as a boundary condition	• convective energy exchange between air and soil • solar radiation absorbed by the ground surface • latent heat flux due to ground surface evaporation • long wave radiation • various factors involved in the energy balance equation	• very good agreement between predicted and measured sets of data • the model can be used for the prediction of the ground temperature at the surface and at various depths with sufficient accuracy • useful for the prediction of the thermal performance of buildings in direct contact with the ground and the energy efficiency of earth-to-air heat exchangers
Popiel *et al.* (2001)	simple semi-empirical formula based on transient heat conduction in a semi-infinite solid with the exposed surface temperature varying periodically with time	• structure and physical properties of the ground • ground surface cover • air temperature and humidity • wind • solar radiation • rainfall	• good agreement between calculated and measured results • depths between 1.5-2 m recommended for horizontal ground heat exchange applications • surface zone up to 1m depth, affected strongly by weather conditions • shallow zone, affected mostly by seasonal changes, reaching depths of 1-8 m for dry light soils or 1-20 m for moist heavy sandy soils • deep zone, extending from 8 or 20 m, almost constant temperature, depending on the geothermal gradient

A fluid, usually air, water or a water–antifreeze mixture transfers the heat from or to the ground. Most commonly, GHEs are either of the open type, in which groundwater or ambient air is heated or cooled by the ground and used for the air conditioning of the space, or of the closed type, where the space is heated or cooled indirectly by the ground with the aid of a heat transfer fluid.

In an open GHE system, as shown in Figure 2.1, there is direct transfer of heat between the ground, groundwater and the heating or cooling coils. The characteristic part of the system is the groundwater wells used for the extraction and injection of groundwater. Rivers or lakes can also be used for the provision of the water, Mands and Sanner (2005).

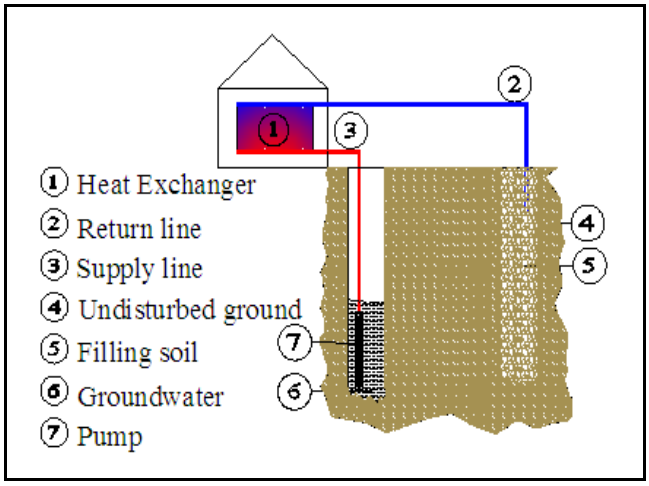

Figure 2.1: Open GHE system

In a similar way, as shown in Figure 2.2, ambient air can also be used as the heat transfer medium for air conditioning of a space. The main differences with the previous method are that the air flows in tubes buried horizontally or vertically in the ground and there is absence of heating or cooling coils.

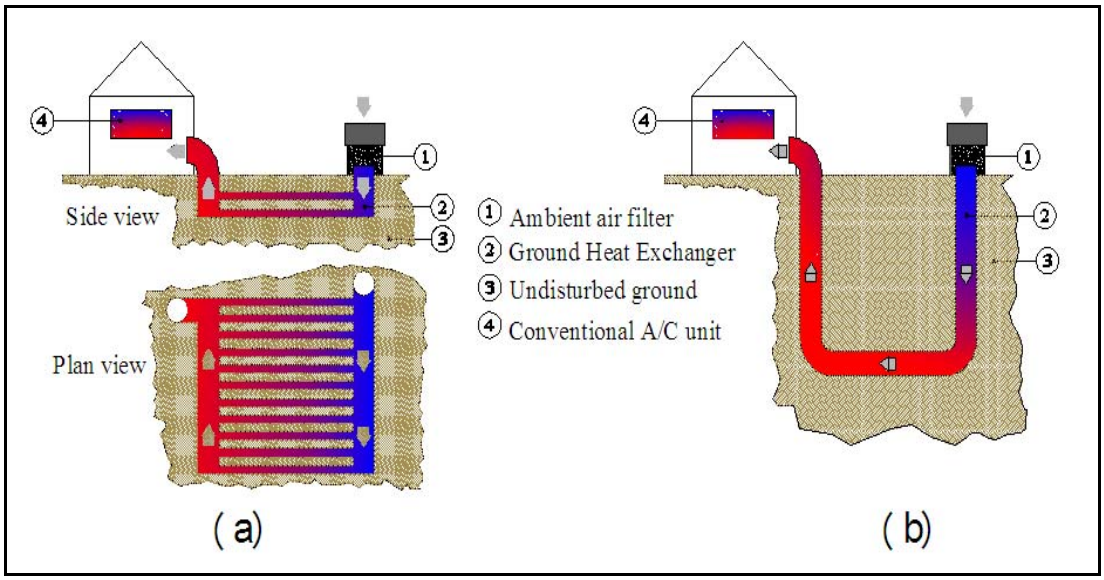

Figure 2.2: Open GHE preheating systems (a) Horizontal type and (b) Vertical type

In closed systems the ground may be used indirectly with the aid of a heat transfer fluid, circulated in the system for the air conditioning of the space. The pipes are buried in the ground either in horizontal, vertical or oblique position and a heat transfer fluid transfers the heat from the ground to the heating or cooling coils and vice versa. The heat transfer fluid usually flows through pipes made of durable materials like high-density polyethylene, polypropylene or copper. These materials are designed for a 50 year life time.

In the horizontal type, when adequate ground space is available and trenches of about 3 m deep are easy to dig, a number of pipes are connected together either in series or in parallel, as shown in Figure 2.3. It is easier and more cost effective for the system to be installed while a building is under construction; otherwise the horizontal drilling method can be used with minimal disturbance of the ground surface, for installing loops under existing constructions, Geothermal Heat Pump Consortium (2003). It is important in horizontal the type GHEs though, not to cover the ground above the heat exchanger since the main thermal recharge is mainly provided by solar radiation, Mands and Sanner (2005).

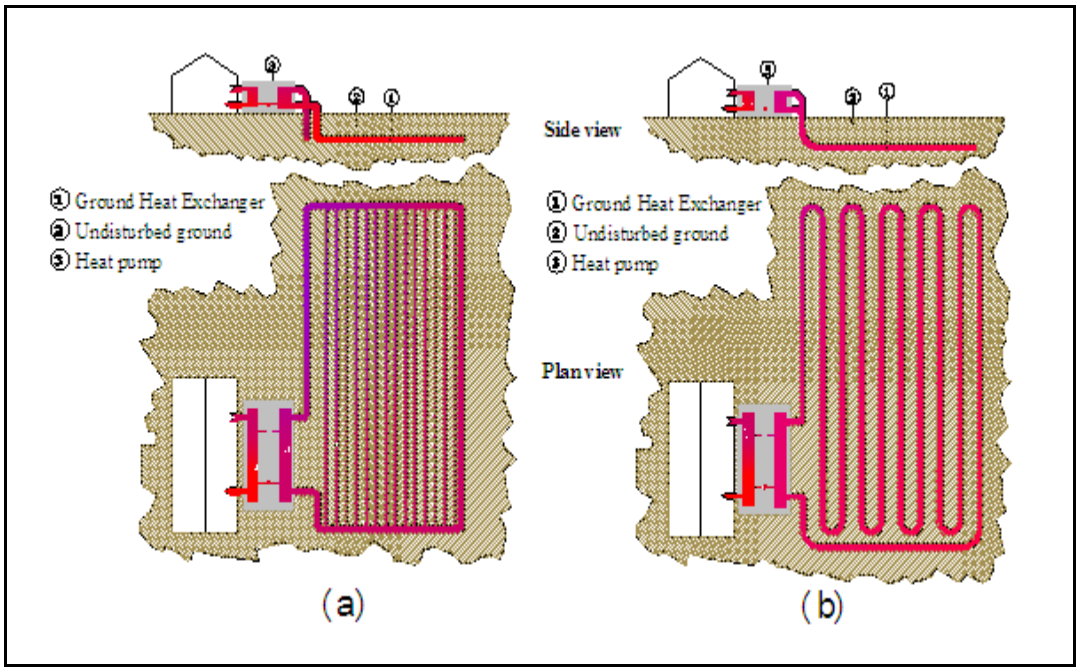

Figure 2.3: Closed system, horizontal GHE (a) in parallel and (b) in series connection

In a similar manner but with less ground space needed, pipes in a spiral shape can be laid into wide trenches. When pipes are laid horizontally the GHE is called a slinky collector (Figure 2.4(a)) and when placed vertically in narrow trenches the GHE is called Svec spiral collector (Figure 2.4(b)), Mands and Sanner (2005).

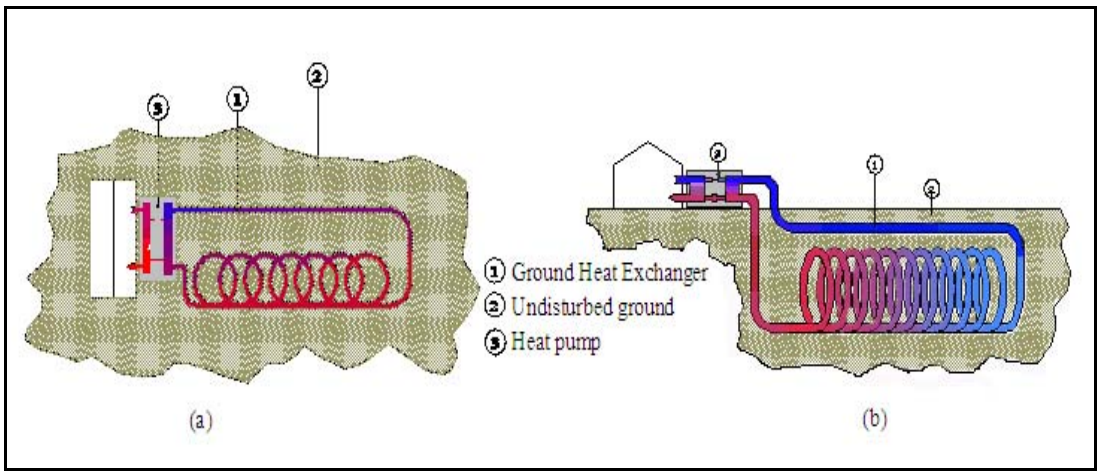

Figure 2.4: Closed GHE systems (a) Slinky shape collector and (b) Svec spiral collector

Vertical Ground Heat Exchangers (VGHEs) or Borehole Heat Exchangers (BHEs) are widely used when there is a need for sufficient heat exchange capacity under a limited ground space. Typical VGHE can be 20 m to 300 m deep, 10 cm to15 cm in diameter and have the ability to extract 40-70 W_{heat} per meter borehole depth for typical ground conditions. VGHEs are classified as U-tubes, consisting of a pair of straight pipes connected with a U-bend at the bottom, as shown in Figure 2.5, and as concentric or coaxial pipes, joined either in a very simple way with one straight pipe inside a bigger diameter pipe or forming complex configurations. A more complex configuration is formed with more than one pipes inside a bigger diameter pipe or more than one pipes placed around a central one as described by Mands and Sanner, 2005.

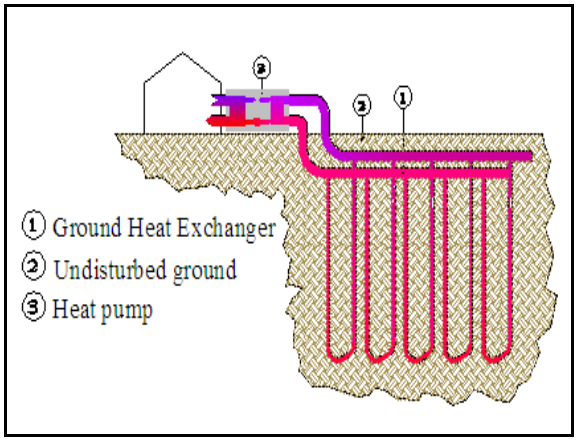

Figure 2.5: Closed system Vertical GHE

Boreholes usually are backfilled with a bentonitic clay mixture, with the possibility of using thermally enhanced additives in order to ensure good thermal contact with the ground. Due to the fact that the ground temperature increases with depth, VGHEs have the ability to exchange the required heat with the ground, with less piping than horizontal heat exchangers. VGHEs are generally more expensive to install than HGHEs. The fact that two or even three U-pipes could be installed in one borehole and the use of thermally enhanced backfilled material may reduce the number or depth of boreholes required for a specified heat extraction/rejection and lead to a reduction in the cost of the installation, Mands and Sanner (2005).

Some GHEs systems can be classified neither as open nor as closed systems. These are referred to as Miscellaneous or Unclassified GHE systems. One such system is the use of water from tunnels or mines, where the water is easily accessible and has a constant temperature. The standing column well is another type of unclassified GHE system. In this case, water is pumped from the bottom of the well and after passing through a heat pump is injected back to the well. The performance of this system for heating applications depends on the depth of the well. The deeper the well the more efficient it is. More details on the operation of GHE systems and their performance are given in section 4.3 of the thesis.

The operation of a GHE requires a continuous heat flow in the surrounding ground which takes place partly by heat conduction and to a certain degree by moisture movement. Consequently, the GHE efficiency, represented by the specific performance parameter which is the heat extraction rate per metre of hose depth, not only depends on the pipe material but also on the ground type and its thermal characteristics, Hepbasli *et al.* (2003). Table 2.3 lists the advantages and disadvantages of most GHE types.

Table 2.3: Advantages and Disadvantages of several Earth Heat Exchangers

Earth Heat Exchanger Type	Advantages	Disadvantages
Open system Ambient air or room air recirculation	Simplicity of the system High pre-heating and pre-cooling potential Low operational and maintenance costs	The influence of the pipe density on the energy gain is small Large number of pipes is required for high heat extraction rates
Closed system Horizontal type	Cost effective during building construction	Solar radiation as natural thermal recharge Not effective when the ground surface is covered
Closed system Spiral type	Less ground space required than the closed system Horizontal type	Can be used when natural thermal recharge is not vital
Closed system Vertical U-tube	Less ground space required and lower piping cost than all the other types	Higher drilling costs than the horizontal types
Heat Pump coupled to Vertical HE	Consumes less energy than air source HP The ground is more stable source than air No supplementary heat is needed in extreme ambient temperatures Less refrigerant	High initial cost

2.5 Evaluation of Ground Heat Exchanger

A number of researchers has used basic formulas to evaluate the ground heat exchanger (GHE) performance, each time taking into account different design parameters. The classic method to model the heat exchange process is through the cylindrical heat source theory proposed by Carslaw and Jaeger (1947). The method is relatively easy to apply and was used by many researchers to model and evaluate the response of ground heat exchangers. With improvements in the performance of computers, a number of software packages can now handle the finite element method and simultaneously give solutions to the arising partial differential equations for a massive cell number. Depending also on the software package, a number of modules are built-in in order to handle various forms of heat transfer at the boundaries, facilitating the formulation of the problem for a numerical solution.

De Paepe and Willems (2001) studied the performance of a ground-coupled air heat exchanger in Belgium, considering transient and three dimensional conduction heat transfer in the ground and heat transfer by convection in the pipe. They ignored the heat transfer by moisture in the ground. The heat flux from the ambient air to the surface was calculated by considering constant and uniform temperature deep in the ground. A 3D unstructured finite volume model was derived and the 'FLUENT' solver was used to obtain the numerical solutions. It was identified that the pipe affects the temperature of the ground around it up to a distance twice its diameter. Burying the pipes deeper than 2.5 m and calculating their optimal length by using the calculation model, an efficient heat exchanger can be obtained exploiting to the maximum the available ground thermal capacity.

The performance of three Earth-to-Air Heat Exchangers (EAHXs) for mid European office buildings, located at Hamm, Freiburg and Weilheim in Germany were examined and presented by Pfafferott (2003), aiming to characterise their efficiency. The main characteristics of the examined EAHXs are presented in Table 2.4.

Each of the evaluated EAHXs was shown to have certain advantages. The EAHX located at Hamm showed the outlet air temperature to be closer to the undisturbed earth temperature with Θ=0.944 and to have the smallest ratio of temperature variation with R_T = 0.28. The smallest the value of R_T the more cooling energy is supplied to the building. The system located at Freiburg supplied the highest specific energy gain based on the total surface area, h_{mean} = 51.3 kWh/m^2 per annum for heating and h_{mean} = 23.8 kWh/m^2 per

annum for cooling. The COP is the ratio of the overall energy gain supplied by the EAHX and the mechanical dissipation energy during operation time. All the tested EAHXs had high COP values mostly because of the low energy dissipation. The COP is the ratio of the energy supplied by the EAHX divided by the mechanical energy used during operation. The highest COP of 380 was obtained by the EAHX located at Weilheim due to the large pipe diameter and the low air velocity in the pipes. It was concluded that the evaluation of an EAHX depends on project-specific criteria. Pipe lengths up to 100 m and pipe diameters of around 250 mm are effective, Pfafferott (2003).

Table 2.4: Description of the main characteristics of the three EAHXs in Germany

	Hamm	Freiburg	Weilheim
Diameter (mm)	200 - 300	250	350
Total surface area of ducts (m^2)	1650	522	198
Mean air flow (m^3/h)	10300	7000	1100
Specific surface area ($m^2/(m^3/h)$)	0.16	0.075	0.18
Air speed (m/s)	≈ 2.2	5.6	1.6
Soil type	Dry, rocky	Dry, gravel	Moist, clay
Hours of operation (h)	3701	4096	3578
Specific heating energy gain (kWh/m^2 per annum)	16.8	51.3	16.2
Specific cooling energy gain (kWh/m^2 per annum)	13.5	23.8	12.1
RT (K/K) = $(T_{outmax}–T_{outmin})/(T_{inmax}–T_{inmin})$	0.28	0.47	0.36
h_{mean} ($W/(m^2K)$)	5.5	5.0	3.2
Θ (K/K) = $(T_{in}–T_{out})/(T_{in}–T_{earth})$	0.944	0.766	0.804
COP (kW_{hth}/kW_{hmech})	88	29	380

Nam *et al.* (2008) developed a numerical model to predict heat exchange rates for a ground-source heat pump system. The model combined a heat transport model with ground water flow and a heat exchanger model with an exact shape. FEFLOW was adopted to calculate the heat exchange rate between the ground heat exchanger and the surrounding ground and to estimate the distribution of subterranean temperature. FEFLOW is an analysis code that uses the finite element method for the simulation of heat and material transport in the ground based on the three preservation equations for mass momentum and energy conservation. Comparison between experimental results and numerical analysis showed a good agreement. Finally, the developed model was used to predict the heat exchange rate for an actual office building in Japan.

Cui *et al.* (2008) used a numerical model for the simulation of the ground heat exchangers in alternative operation modes over a short time period for ground-coupled heat pump applications. A two-dimensional transient heat conduction was used as the

finite element model and the commercial code ANSYS was used to perform the transient numerical simulations of heat transfer in the borehole domain. The ANSYS program can automatically generate a finite element model that consists of nodes and elements dealing with arbitrary geometries and non-homogenous media. For a simplified analysis, a symmetrical arrangement of the two legs of the U-tube inside the borehole was assumed. Then only half of the borehole domain was modelled because of the axisymmetric configuration. An adiabatic boundary condition was applied to the symmetric plane on the centre of the borehole. The borehole domain is physically divided into three regions, the inner is the pipe wall; the middle is the grout backfilled in the borehole and the outer region is the soil surrounding the borehole. The governing equations for each region in the borehole domain were represented with cylindrical coordinates. The comparisons with experimental results showed a reasonable agreement within the range of ±6.5%. The variation of the U-tube pipe wall temperatures demonstrated that the discontinuous operation mode and the alternative cooling/heating modes could effectively alleviate the heat build-up in the surrounding soil.

Schiavi (2009) analyzed simulated Thermal Response Test data in order to evaluate the effect of a three-dimensional model in determining the actual value of the soil thermal conductivity and borehole thermal resistance. These values are necessary for the design of geothermal energy storage systems. For the 3D system simulation the finite element method, implemented within the Comsol Multiphysics environment, was adopted. The analysis confirmed that the Line Source Model applied to the Thermal Response Test represents a sufficiently accurate approach for the U-tube configuration.

Kim *et al.* (2010) developed a numerical model for the simulation of temperature changes in a borehole heat exchanger (BHE). The model calculated the thermal power transferred from heat pumps to BHEs while considering the nonlinear relationship between the temperature of the circulating fluid and the thermal power. To simulate the vertical closed-loop ground heat pump (GHP) system, three modules were added to the 3D numerical simulator TOUGHREACT. The modules calculated the heat transfer between the U-tube and the circulating fluid, the circulation of the fluid in the BHE and the rate of energy transfer from a heat pump to a BHE. The developed model was validated by comparison with two experimental datasets and was used for the BHE design of an actual system that was numerically evaluated with respect to the temperatures of the circulating fluid at the

BHE inlet and outlet, the heat pump efficiency, the heating power and electric power of the heat pumps.

Eslami-nejad and Bernier (2011) presented an analytical model to predict steady-state heat transfer in double U-tube boreholes with two independent circuits operating with unequal mass flow rates and inlet temperatures. For the modelling it was assumed that the heat capacities of the grout and pipe inside the borehole were negligible, the ground and the grout were homogeneous and their thermal properties were constant, the borehole wall temperature was uniform over the borehole depth, heat conduction in the axial direction was negligible and the combined fluid convective resistance and pipe wall thickness conduction resistances were assumed to be equal in both circuits. This two-region model was validated experimentally and was in very good agreement with experimental data in the steady-state regime. The proposed model was then used to study a double U-tube borehole configuration with one circuit linked to a ground-source heat pump operating in the heating mode and the other to thermal solar collectors.

Concluding from what was described before, the thermal performance of GHEs is strongly dependent on the thermal properties of the ground in relation to depth. Pipe depth, pipe length and pressure drop in the pipe increase the thermal capacity of the system while the pipe diameter, air flow and air speed, are factors affecting negatively the earth-to-air heat exchangers when they are increased. Although moisture in the ground is another factor that was widely studied, it appeared to have almost negligible influence on the total heat transfer in the ground, Gauthier (1994) and Puri (1986).

2.6 Ground Coupled Heat Pumps

Ground Coupled Heat Pumps (GCHP) or Geothermal Heat Pumps (GHP), are heat pumps coupled to GHEs, to improve the heat pump efficiency. They are used mostly for the air conditioning of a space and/or water heating purposes. They exchange heat between indoor air (for space heating or cooling) or water (for heating or cooling water) and a liquid (either water or a water-coolant mixture) circulating in the closed loop heat exchanger.

GCHP systems are more efficient than conventional heat pump systems because of the improved efficiency of their compressors. This can be achieved since the ground temperature is more stable than that of ambient air providing cooler condensation

temperatures during cooling operation and warmer evaporating temperatures during heating operation. Unlike air source units, GCHP systems do not need auxiliary heat, for defrost cycles or backup electric resistance heat, at extreme outdoor air temperatures, Collins *et al.* (2001).

The improved efficiency and the lower running cost of GCHP systems over conventional heat pump systems can make them an attractive choice for air conditioning and water heating provided the installation cost is not excessive, Collins *et al.* (2001).

For the effective sizing of a GCHP and related GHE, specific ground thermal characteristics are required. Several models based on Fourier's law of heat conduction can be used for this purpose. The most widely used is the thermal response test, first presented by Mogensen in 1983 and used by Sanner *et al.* on several boreholes. This method requires a specified heat load to be applied on a borehole through a circulating fluid, measuring its temperature changes and allowing calculation of the thermal conductivity of the borehole. The formula calculating the thermal conductivity of the system, including the influence of the groundwater flow and grouting, takes into account the heat exchanged, the length of the borehole and the slope of the curve of temperature against logarithmic time. From the thermal response test, the borehole thermal resistance can be calculated. Results of thermal response tests carried out in 5 different locations in Germany are listed in Table 2.5. The differences in the thermal conductivities are due to the differences in the geology of the locations, Sanner *et al.* (2000).

Table 2.5: Results of various thermal response tests carried out in Germany

Location	Geology	Thermal conductivity λ_{eff} (W/mK)	Resistance R_b K/(W/m)
Attenkirchen	Quarternary and tertiary silt and clay	1.62	0.50
Erfurt	Mesozoic sediments	2.78	0.18
Langen	Quarternary and tertiary sand and clay	2.79	0.11
Minden	Marly clay	2.51	0.12
Werne	Cretaceous marl, clayey	1.45	0.11

Pahud and Matthey (2001) carried out thermal response tests for several boreholes to investigate the effect of the filling materials on the borehole thermal performance. Fill materials like standard bentonite and cement mixture, bentonite and cement with quartz

sand as additive or plain quartz sand were used. The use of spacers to keep the plastic pipes apart from each other and close to the borehole wall was also investigated. The use of quartz sand as a filling material showed an increase in the thermal performance by 30%. With a common heat extraction rate of 50 W per meter of borehole length, the temperature gain in a heat pump evaporator was +2 K. In Switzerland, boreholes of 100-200 m deep and pipe diameters of 10-15 cm are used for residential buildings. They are sized for a heat extraction rate of 50 W per meter length of borehole.

2.7 Environmental aspects of geothermal energy

Geothermal energy is considered a sustainable and renewable energy source able to replace fossil fuels and lead to reductions in pollution and greenhouse gasses emissions. Also, for many countries geothermal energy leads to a reduction in their dependence on imported fuel. According to data presented by Rybach at the World Geothermal Congress 2010, in 2008 geothermal power production exceeded by more than three times that produced by photovoltaics, Rybach (2010).

Although geothermal energy has the largest capacity amongst the renewable energy sources as stated by Rybach (2010) its current growth is slow in comparison to wind and solar PV. Nowadays, the development of geothermal energy is based on the increasing deployment of GCHPs mainly due to the fact that this technology is mature and the systems can be installed in most ground formations.

The Energy Service of the Cyprus Ministry of Commerce, Industry and Tourism has the overall responsibility for Energy matters and specifically for preparing and implementing programmes for energy conservation, the promotion of renewable energy sources (RES). The Government of Cyprus being aware of the benefits of geothermal energy and in order to increase the share of energy from renewable sources promotes geothermal energy systems through a Scheme that provides financial incentives for the utilization of RES for heating and cooling. However, the lack of data for the thermal properties of the ground in Cyprus was one of the main barriers to the design of efficient geothermal systems, the implementation of the support scheme in the field of geothermal energy and the calculation of the share of energy from renewable sources for heating and cooling.

The use of geothermal systems for the air conditioning of buildings in Cyprus had a significant increase in the last few years. The technology is already used in hospitals, hotels, industrial buildings and households. From evaluations of the installed geothermal systems in Cyprus, it was observed that the use of geothermal systems can offer an energy saving between 40-75% for heating and cooling of buildings compared to conventional systems. In 2006 the applications submitted for grant support were only 14 reaching 55 in February 2010. Since then, the increase in the installed capacity has been rising steadily, Partasides *et al*. (2011).

The knowledge of the thermal behaviour of the ground at various locations and depths is valuable for improving the design of geothermal applications in Cyprus. As discussed previously, the thermal behaviour of the ground depends on many factors and varies in different locations. This is the reason that each location is considered unique and its thermal behaviour needs to be investigated or predicted.

The measurement of the thermal behaviour of the ground at a specific location is costly and in many cases might be unaffordable. On the other hand, prediction is easier, faster and more economic. This is the reason that calculation models have been developed for this purpose.

The provision of important information on the structure of the ground in different areas of the island and the definition of their thermal characteristics are of significant importance. One of the objectives of the thesis is to draw maps that will indicate the temperature of the ground at different locations and depths in Cyprus in order to assist in the efficient design of geothermal systems. Furthermore, this will also support the future drawing of isothermal and thermal conductivity maps of the island and provide appropriate information to consultants to improve design accuracy and techno-economical studies.

2.8 Summary

GHEs are used for the utilisation of the ground's thermal capacity for air conditioning and domestic water heating. The temperature of the earth is always higher than that of the ambient air in winter when the ground can be used as heat source and lower in summer when the ground can be used as a heat sink.

For the prediction of the ground thermal capacity, several calculation models were presented. The temperature variation of the ground surface is found to be very close to that of the ambient air, decreasing with depth and tending to stabilise after a certain depth which depends on ground lithology (i.e. the characterisation of a rock in all those visible features that in the aggregate impart individuality to the rock). The variation of the ground temperature occurs with a time lag from the variation of the ambient air temperature. The time lag is a function of the depth from the surface.

An array of buried pipes in the ground, either horizontally or vertically, can be used for the heat exchange process. GHEs are classified as open or closed systems and can be used either for the preheating or precooling of a heat exchange fluid or can be coupled to heat pumps to improve the efficiency of operation.

For the prediction of the thermal performance of GHEs several calculation models were presented and validated against experimental results. These models can also be used for system sizing. The thermal performance of GHEs is strongly dependent on the thermal properties of the ground and their variation with depth.

The reduction in gas and oil supplies and the increase in energy prices will increase the economic attractiveness of geothermal energy. Research and development and the application of geothermal energy systems is expected to increase in the future.

Limited information in the area of space cooling using geothermal energy is reported. According to Lund et al. (2010), space cooling is reported only in five countries, amounting to 56 MWt and 281 TJ/yr. In warm climates and especially in the Eastern Mediterranean countries like Greece, Italy Egypt, Turkey and Middle East where the climatic conditions are similar to the ones in Cyprus, geothermal energy is reported to be used mainly for space heating, in greenhouses and aquaculture, for bathing, in spas etc. In addition to this, Iran reported the installation of GCHPs in demonstration projects for the evaluation of their efficiency under different climatic conditions.

Chapter 3: Estimation of the thermal conductivity of the ground in Cyprus

3.1 Introduction

Ground Coupled Heat Pumps (GCHP) performs better than Air Coupled Heat Pumps for heating and cooling because the ground has a lower temperature than the atmosphere in the summer and vice-versa in winter. To exploit effectively the heat capacity of the ground, Ground Heat Exchangers (GHE) are used. Therefore, information on the temperature and other thermal properties of the ground are essential for the sizing of GHE and GCHPs.

As mentioned in Chapter 2, the temperature of the ground at the deeper layers is mostly affected by the structure and physical properties of the soil with the thermal conductivity being the most important.

3.2 Definitions

For the better understanding of this chapter some definitions of the main properties of the ground are introduced. According to ASHRAE Terminology of Heating, Ventilating, Air Conditioning and Refrigeration (2000-2003):

Density is defined as '*the mass per unit of volume*' of a substance and is measured in kg/m^3.

'*Thermal conductivity is the time rate of steady-state heat flow through unit thickness of unit area of a homogeneous material, induced by a unit temperature gradient in a direction perpendicular to that unit*' and is mainly measured in W/mK.

'*Thermal diffusivity is the physical quantity that determines the rate of heat propagation in transient-state processes*'. It is the quotient of the division of thermal conductivity by the product of density and specific heat ($\lambda/\rho C_p$) and it is measured in m^2/s.

'*Specific heat is the quantity of heat required to raise the temperature of a given mass of any substance by one degree*'. Specific heat is measured in kJ/kgK.

Permeability, κ, is a measure of the ability of porous materials like rocks to allow fluids to pass through them and is defined as '*the time rate of water-vapour transmission through unit area of flat material of unit thickness induced by unit vapour pressure difference between two specific surfaces, under specified temperature and humidity conditions*'. It is measured in Darcy (d), were 1 Darcy = 10^{-12} m^2.

Another important factor is the porosity of a substance. Porosity describes the fraction of the volume of all the pores in a material, where the pores may contain air, water or a combination of both. In the case that the pores are air-filled, the substance is set to be at its dry state (0% degree of saturation). In the case where the pores are water-filled, the substance is set to be at its saturated state (100% saturation). Between the dry and saturated state of a substance, water and air or moisture may exist to some extent, defining its degree of saturation.

3.3 Thermal Response Tests

In small plants such as for residential house applications, the thermal properties usually are estimated or calculated with the aid of calculation models. In such a case, the morphology of the ground in the area, the thermal conductivity, density and specific heat capacity of the different soil formations as well as the temperature of the ground at various depths are usually available from the Geological Survey Departments of each country or by geologists that perform geotechnical studies in the area. Unfortunately in Cyprus the available data are limited due to the limited interest in the previous decade in the exploitation of geothermal energy for heating and cooling applications.

For the design of large scale applications it is important that the thermal properties of the ground and especially the thermal conductivity of the borehole should be measured on site. A pilot borehole should be drilled and a GHE should be installed of approximately the size (in diameter and depth) of the actual GHE. Water or heat-transfer fluid heated at a constant rate is circulated in the GHE and data are collected. This method for the in-situ determination of the thermal properties of the ground is known as the Thermal Response Test (TRT).

Information on the thermal properties of the borehole and its surroundings can be obtained by evaluating the increase or decrease of the temperature of the heat transfer fluid versus

time. The greater the change in the temperature of the heat transfer fluid between the input and output leg of the GHE, the more conductive the borehole is. Also, the thermal resistance of the borehole can be obtained by evaluating the temperature difference between the heat transfer fluid and the surrounding ground. As the difference in the temperature between the heat transfer fluid and the surrounding ground increases, the less conductive is the borehole. Mogensen (1983) is reported as the first investigator who proposed the TRT as a method to determine the in-situ values of ground thermal conductivity. He circulated chilled heat-transfer fluid through the GHE at a constant heat extraction rate. The outlet fluid temperature was recorded continuously during the test and was compared with the results of a mathematical model simulating the heat transfer process of the borehole and its surroundings.

Another method for estimating the thermal properties of the ground is to collect rocks or drill chipping samples from the borehole or obtain rock samples from locations that are lithologically identical or similar to the ones of the borehole. The collection of rock samples from the borehole may not always be feasible. Sometimes, the necessary equipment is not available but mostly the small diameter of the borehole (around 15 – 20 cm) and its depth (where it usually reaches at least 100 m) obstruct the extraction of the required samples. Chipping samples can be easily collected from other locations but their thermal properties and especially the thermal conductivity may not always match the values for the actual borehole due to the difference in density and saturation levels.

Yun and Santamarina (2008) investigated the effect of thermal conduction in dry soils. According to their study, the contact quality and number of contacts per unit volume in granular materials in relation to the presence or not of liquids or cementing agents in the pores are the main factors affecting their thermal conductivity. Although, the thermal conductivity of minerals is higher than 3 W/mK the thermal conductivity of dry soils made of minerals is less than 0.5 W/mK. This is due to the presence of air in the dry soils and its low thermal conductivity of 0.026 W/mK. The improvement of the interparticle contacts of dry soils and the reduction of their porosity enhance their thermal conductivity. Table 3.1 shows the factors that determine the thermal conductivity of soils as presented by Yun and Santamarina (2008), based on selected previous studies.

Table 3.1: Factors that determine the thermal conductivity of soils

Factor	Features
Mineralogy	As the thermal conductivity of the solid increases the bulk thermal conductivity increases as well
Particle size	The bigger the particle the higher the thermal conductivity
Applied pressure	The higher the contact pressure the higher the thermal conductivity
Density/Gradation	The decrease of porosity leads to higher thermal conductivity
Water content	The higher the water content the higher the thermal conductivity
Pore fluid	The higher the thermal conductivity of the saturating pore fluid the higher the bulk thermal conductivity

Because of the above mentioned variations, the TRT gives more accurate results concerning the thermal properties of a borehole in relation to the sample collection method. A number of approaches can be employed for the case of TRTs to determine the thermal characteristics of the borehole and hence of the ground. According to ASHRAE HVAC Applications (2003) these methods are based on the line source method, the cylindrical heat source method or the numerical method.

3.3.1 Line source method

For the determination of the thermal conductivity of solids in a laboratory environment, Stalhane and Pyk (1931) devised the so-called single-probe method. The line source method is actually based on this method and since then this method became popular especially in Europe where it is the most widely used method for calculating the thermal properties of the ground and for the design of Borehole Heat Exchangers (BHEs). Initially, the thermal properties of the probe material were ignored in the calculations and the method was known as the line-source approximation. Ingersoll and Plass (1948) applied the line source model to the design of GHE. Blackwell (1954) introduced the analytical method where the probe material and a possible contact resistance at the probe surface were taken into account. Blackwell also reported that the determination of the thermal conductivity and diffusivity at the same time using this method wasn't possible. The influence of the contact resistance on the thermal diffusivity was significant.

According to the theory of the simplified line source method, constant heat flow rate per active length of borehole should be supplied to the ground and the change in ground temperature at a defined distance from the line source after a time period should be recorded. Ingersoll and Plass (1948) suggested Eq. (1) for the calculation of the temperature change in the ground

$$T_{(r,t)} - T_{(t=0)} = \frac{q_c}{4\pi\lambda} \int_{\frac{r^2}{4\alpha t}}^{\infty} \frac{e^{-u}}{u} du = \frac{q_c}{4\pi\lambda} E_1\left(\frac{r^2}{4\alpha t}\right) \quad \text{(Eq. 1)}$$

where:

$T_{(r,t)}$ – ground temperature at a distance (r) from the line source after a time period (t)

$T_{(t=0)}$ – initial temperature of the ground

q_c – constant heat injection rate per active length of borehole in W/m

λ – thermal conductivity of the ground

u – integration variable (unitless)

E_1 – exponential integral

The undisturbed ground temperature should be obtained before the beginning of the test. This can be achieved by circulating the fluid in the borehole heat exchanger and measuring its inlet and outlet temperature. At the beginning of the process the inlet and outlet temperature, as expected, differs. After a few hours, the temperature difference finally reaches its lowest value and stabilises. The time required for the temperature to become constant depends on the thermal properties of the borehole and the undisturbed ground.

The thermal front is defined as the distance that the heat injected from the line source can reach in the horizontal direction. The vertical effect of the heat dissipation from the line source is ignored. When the dimensionless time-to-pipe ratio parameter $\alpha t/r^2$ reaches large values, the exponential integral (E_1) can be approximated with Eq. (2) below. The larger the time that heat is injected in the ground, the bigger the radius of influence.

$$E_1\left(\frac{r^2}{4\alpha t}\right) = \ln\left[\frac{4\alpha t}{r^2}\right] - \gamma \quad \text{(Eq. 2)}$$

where:

γ – Euler's constant = 0.5772

When the parameter $\alpha t/r^2$ reaches values equal or greater than 20 Eq. (2) can give a maximum error of 2.5% while when it reaches values equal or greater than 5 the maximum error increases to 10%. Therefore, the above condition means that the accuracy increases as the thermal front reaches further beyond the borehole wall, Gehlin (2002).

The thermal resistance between the fluid in the probes and the boundary of the borehole is known as the effective borehole thermal resistance, R_b and is defined by Eq. (3). The effective borehole thermal resistance takes into account both the geometrical parameters of the borehole heat exchanger (pipe diameter, length and spacing, number of pipes) and the physical parameters (thermal conductivity of the materials, flow rate in the borehole, fluid properties, etc.) Pahud and Matthey (2001).

$$R_b = (T_f - T_b)/q_c \qquad \text{(Eq. 3)}$$

where:

T_f – temperature of the fluid in the probe

T_b – temperature at the boundary of the borehole

Hence, the fluid temperature at the boundary of the borehole as a function of time is given by Eq. (4), arising by the substitution of Eq. (1) and (2) into Eq. (3).

$$T_{f(t)} = \frac{q_c}{4\pi\lambda} * \left[\ln\left(\frac{4\alpha t}{r_b^2} \right) - \gamma \right] + q_c R_b + T_{(t=0)} \qquad \text{(Eq. 4)}$$

In a U-tube GHE used in TRTs the fluid temperature ($T_{f(t)}$) is given by the arithmetic mean of the inlet (T_{fin}) and outlet fluid temperature (T_{fout}) flowing in the GHE ($T_{f(t)}$=½(T_{fin}+T_{fout})).

Eq. (4) can be rearranged in a linear form as:

$$T_{f(t)} = \frac{q_c}{4\pi\lambda} \ln(t) + q_c \left[R_b + \frac{1}{4\pi\lambda} \left(\ln\left(\frac{4\alpha}{r_b^2} \right) - \gamma \right) \right] + T_{(t=0)} \qquad \text{(Eq. 5)}$$

Although the line source method has been used by researchers in many different ways, the method has been used for the determination of the thermal conductivity of the borehole by calculating the slope of the line resulting from plotting of the fluid temperature against the natural logarithm of time (ln(t)).

3.3.2 Cylindrical heat source method

Several researchers (Carlsaw and Jaeger (1959), Deerman and Kavanaugh (1991) and Kavanaugh and Rafferty (1997)) have used this method in order to determine the thermal properties of the ground and especially the thermal conductivity and diffusivity. In this method, a single loop GHE is represented as a cylindrical source. The two pipes of the GHE are represented in the calculations as a single coaxial pipe with an equivalent diameter. The equivalent diameter is based on the diameter of the U-tube GHE and the centre-to-centre distance between the two tubes and is calculated by Eq. (6) below:

$$D_{eq} = \sqrt{2D * L_s} \qquad D \leq L_s \leq r_b \qquad \text{(Eq. 6)}$$

where:

D_{eq} – equivalent diameter (m)

D – diameter of the U-tube (m)

L_s – center-to-center distance between the two tubes (m)

r_b – radius of the borehole (m)

Katsura *et al.* (2008) proposed a method for calculating the temperature of the ground for heat extraction or heat injection purposes via multiple GHEs. In their study they treated soil as an infinite isotropic constant solid and a vertical ground heat exchanger (borehole) as a hollow cylinder in the infinite soil.

Thus, assuming that the u-tube GHE is presented by a hollow cylinder, the effective borehole thermal resistance R_b can be calculated by modifying Eq. (3) above as:

$$R_b = \frac{\ln(r_2 / r_1)}{2\pi\lambda} \qquad \text{(Eq. 7)}$$

where r_1 and r_2 are the internal and external radii of the hollow cylinder respectively. The thermal conductivity of the borehole can be calculated with the aid of Eq. (6) and by solving Eq. (7) with respect to λ.

3.3.3 TRT measurement devices

Thermal Response Tests using mobile measurement devices for the recording of the data were first introduced in Sweden and USA in 1995. Two similar devices were constructed

independently at Lulea University of Technology, Sweden, as reported by Eklof and Gehlin (1996) and at Oklahoma State University, USA as reported by Austin (1998). The two devices were based on Mogensen's concept but with heated circulated fluid instead of chilled.

The schematic diagram in Figure 3.1 depicts the main parts of a typical TRT measurement device. Usually a buffer tank containing hot or chilled fluid acting as the heat carrier fluid is employed. A circulator is used for the circulation of the heat carrier fluid in the GHE. The heat carrier fluid is usually heated by electric heating elements or is being heated or chilled by a heat pump. With the aid of sensors installed, the inlet and outlet temperatures of the heat carrier fluid, its flow rate and the energy input to the system are automatically recorded by data loggers. The system requirements can vary depending on the purpose the TRT is performed. In some cases more data might be collected like the temperature of the heat carrier fluid in the buffer tank, the temperature of the ground at several depths and distances from the borehole and so on. Also many other instruments or devices might be used if necessary for controlling the inlet temperature of the heat carrier fluid in the GHE and/or its flow, the energy input to the system etc.

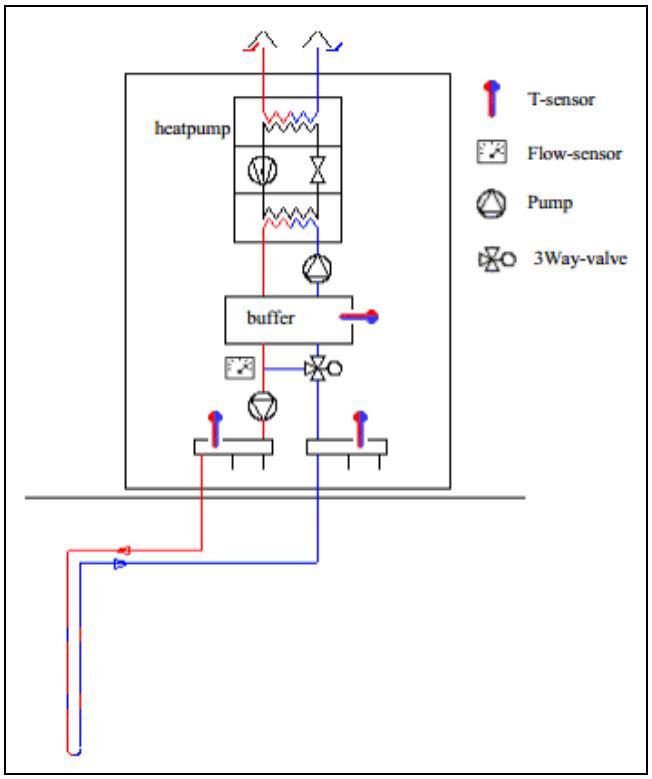

Figure 3.1: Schematic diagram of the main parts of a typical TRT measurement device, Witte *et al.* (2002)

3.4 The Cyprus case

Cyprus is an island located in the eastern Mediterranean. Geologically, Cyprus is situated between the Anatolian platform and the African one. It consists of four main geological zones, the Kyrenia terrane, the Troodos terrane, the circum Troodos sedimentary succession and the Mammonia terrane, as indicated in Figure 3.2, the Geological Survey Department of the Republic of Cyprus (GSDC) (2012).

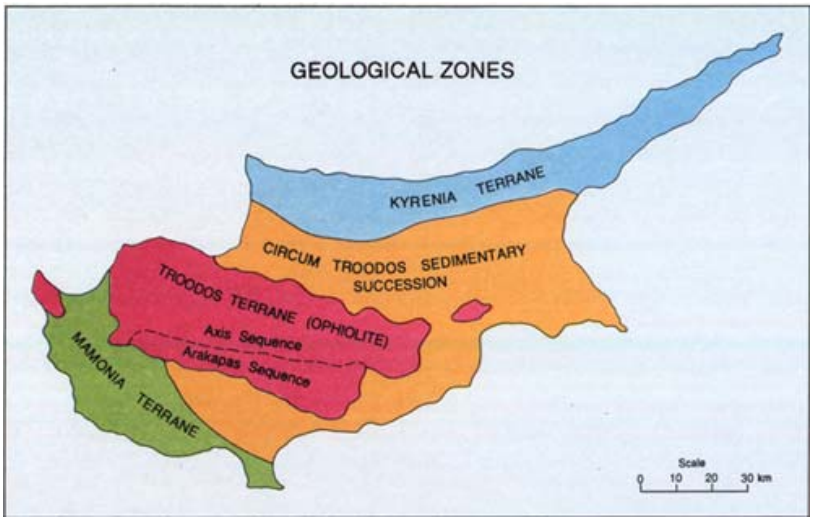

Figure 3.2: Main geological zones of Cyprus, GSDC (2012)

Research to estimate the thermal properties of the ground in Cyprus was performed in the early 1970s by Morgan (1973). In his PhD thesis he reported the geothermal gradient measured at 33 boreholes in Cyprus. The measurements were made for new and/or existing air filled and water filled boreholes. Although he studied 33 boreholes, useful results were extracted from less than half of the boreholes. The investigations were based on laboratory measurements on drill chipping samples from the boreholes. The form of the samples did not allow for the use of transient methods such as the needle probe method or the quasi-steady-state method for the calculation of the thermal conductivity. Lees (1892) and Beck (1957) described a steady state method for the calculation of thermal conductivity by using a form of divided bar apparatus (see Jessop, 1970). Morgan, used a newer version of this apparatus for his experiments. The idea was based on the investigation of the effective thermal conductivity of a two component system as proposed by Woodside and Messmer (1961). The assumption was that, if the thermal conductivity of a two component system was measured and the thermal conductivity of one of the two components was known, then the thermal conductivity of the other component could be

calculated. In Morgan's experiments, the two component system was assumed to consist of the chip sample and the brass bars of the apparatus.

For the accurate determination of the thermal conductivity of a borehole, the natural porosity of the rocks of the borehole should be known in order to select the porosity of the chip samples collected and tested. Therefore, rock samples were collected from areas lithologically identical or similar to the ones for each of the 33 tested boreholes. All Morgan's findings from his research in Cyprus are presented in Appendix 1. The underlined values represent the thermal conductivity of the chip samples collected from within the depth range in the borehole. Values from lithologically equivalent disc samples are presented in rounded brackets while values from lithologically equivalent chip samples are presented in square brackets. Assumed values are not marked. Morgan assumed that the samples were representative and only measurement errors were considered.

Since then, no study was reported on the investigation of the geothermal properties of the ground in Cyprus until 2008. Florides and Kalogirou (2008) investigated the geothermal properties of the ground in a new-drilled borehole in the Athalassa region in Nicosia. The borehole was drilled in 2006 and it was 20 cm in diameter and 50 m in depth. Drill chipping samples were selected during drilling from various depths of the borehole and tested to define the soil type. The geological data of the borehole are presented in Table 3.2. It was found that the mean density of the undisturbed ground was about 1900 kg/m^3 and the mean specific heat capacity around 1400 J/kgK.

Table 3.2: Geological data of the borehole in Athalassa region, Florides and Kalogirou (2008)

Depth (m)	Type of material	Density ρ (Kg/m^3)
0-1	Fill material such as gravels, sands and silt with specific heat of 1200 J/kg·K	1950
1-15	Yellowish-creamy, fine to coarse-grained weak to moderately cemented, calcareous sandstone. According to sieve analysis the results are 15-30% silt and the rest sand	1660
15-21	Khaki, marly calcarenite grading to calcarenitic marl (clay 15-20%, silt 45-50%, sand 30-40%)	
21-24	Fine grained moderately cemented calcareous sandstone	
24-29	Khaki, marly calcarenite grading to calcarenitic marl (clay 15-25%, silt 45-50%, sand 30-40%)	
29-32	Khaki, sandy marl (fine sand 5-10%, clay 25-30%, silt 60-65%)	
32-50	Grayish marl (fine sand 5-10%, clay 30-40%, silt 50-65%)	1400 1560

For the determination of the thermal conductivity of the borehole a U-tube GHE made of polyethylene pipe 32 mm in external diameter was installed at the full depth of the borehole. Then the borehole was backfilled with bentonitic clay. The TRT method used was based on the line source method. The tests were carried out by injecting constant heat energy into the borehole through the GHE with water acting as the heat carrier fluid. An in-line 2.8 kW electric heating coil was employed for the heat generation. The inlet and outlet temperatures of the water, its flow rate in the GHE and the input energy were recorded by an Omega OMB-DAQ 55/65 USB data acquisition module every 15 minutes. 20 thermocouples were also placed in the middle of the borehole at various depths so as to record the ground temperature. Figure 3.3 depicts the set up of the equipment used in the experiment.

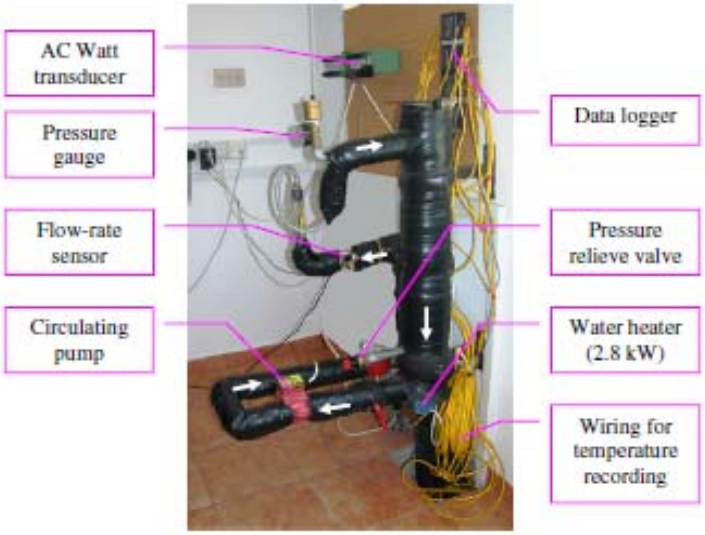

Figure 3.3: Equipment used for the determination of the thermal conductivity of the borehole drilled in Athalassa region in Nicosia, Florides and Kalogirou (2008)

By plotting the water temperature against the natural logarithm of time, Ln(t), the ground thermal conductivity and the effective borehole thermal resistance were calculated. The results of the experiments are presented in Table 3.3.

Table 3.3: Results of the experiments carried out by Florides and Kalogirou (2008) in the Athalassa region in Nicosia

Number of hours for which data are discarded hours	Thermal conductivity, λ W/mK	Effective borehole thermal resistance, Rb K/(W/m)
0	1.6300	0.2583
25 (for $\alpha t/r^2 \geq 5$)	1.4655	0.2409
100 (for $\alpha t/r^2 \geq 20$)	1.6050	0.2574

According to the researchers, the accuracy of the collected data could be affected mainly by daily heat flux penetration through the ground which gradually increases the temperature of the top layers and the variation of the heating coil injection rate per active length of borehole. The tests however, showed that the effect of the above factors was negligible. The authors also concluded that the steady state method is not suitable for estimating the thermal conductivity and effective thermal resistance of a borehole because of deviation of the results by between 5% and 25% in relation to those obtained using the line source method.

At the start of this PhD investigation, two new shallow boreholes were drilled in 2008 in the south coast of Cyprus; one in the Ariel region and the other in the Ayia Phyla region, in the town of Limassol. The locations are shown in Figure 3.4. They were selected mainly because of the specific ground formation in the area. Drill chipping samples were collected during the drilling of the boreholes to characterise the soil types. Hardcore material like marl, chalk and gravel are prevalent in these areas. The findings are listed in Table 3.4.

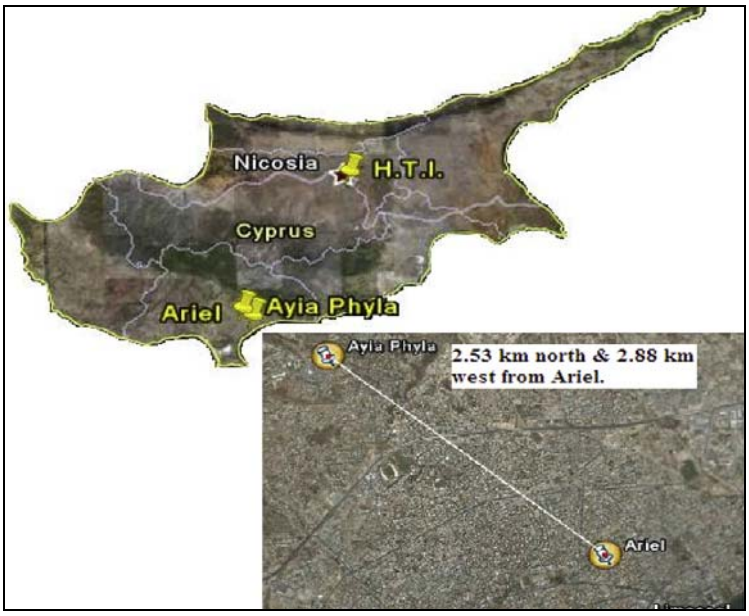

Figure 3.4: Google earth map showing the positions of the two boreholes in respect to the one drilled in the Athalassa region in Nicosia, Pouloupatis *et al.* (2011)

Table 3.4: Geological data for the boreholes in Ayia Phyla and Ariel regions in Limassol, Pouloupatis *et al.* (2011)

Location	Type of material
Ayia Phyla	Hardcore material (marl, chalk and gravel)
Ariel	Hardcore material (marl, chalk and gravel)

In the Ayia Phyla region a borehole 10 cm in diameter and 7.7 m in depth was drilled. A U-tube GHE made of polyethylene pipe with 32 mm external diameter was installed to the depth of 7 m in order to gain the required experience. The borehole was backfilled with the soil extracted during drilling. Thermocouples were placed at various depths on the borehole's wall on the undisturbed ground. In the Ariel region the borehole was 10 cm in diameter and 7 m in depth and it was drilled only for measuring the temperature of the ground at various depths. The thermocouples were placed on the central axis of the borehole which was backfilled with the soil taken out during the drilling operation. No heat exchanger was placed in this borehole, Pouloupatis *et al.* (2011). These boreholes proved to be very shallow and obviously could not be used to extract useful information about the thermal conductivity of the ground.

Because of the high cost of drilling and the necessity to perform in situ TRT to determine the thermal conductivity of full depth boreholes, funding was sought to support the work. In 2008 the Energy Service of the Ministry of Commerce, Industry and Tourism of the Republic of Cyprus in collaboration with the Cyprus Institute of Energy and the Cyprus University of Technology funded a project for the determination of the thermal parameters of the ground in two locations in Cyprus, in the Agios Georgios region of Limassol and in Saittas. I participated in this project by organising and executing the TRTs and collecting and analysing the necessary data. The Agios Georgios region was selected because of its interesting geological formation. Also it was close to the two previous boreholes drilled in Ayia Phyla and Ariel which were not deep enough and could not be used for measurements. Unconsolidated clay and silt are the main soil types in the area. Saittas, is a mountainous region and the ground is mainly formed by diabase.

Table 3.5: Borehole lithology in Agios Georgios, Limassol and Saittas regions

Agios Georgios - Limassol		Saittas	
Type of material	Depth m	Type of material	Depth m
Red soil	0-4	Top soil	0-8
Silty sand with some gravels	4-16		
Yellow marl	16-38	Diabase	8-178
Green marl	38-120		

The borehole in Agios Georgios was about 15 cm in diameter and 120 m in depth. A double U-tube GHE made of polyethylene pipe with 40 mm external diameter (3.7 mm

thickness) was installed down to the entire depth of the borehole. Thermocouples attached to the GHE were also placed in the borehole before it was backfilled with thermo-cement.

The borehole drilled in Saittas was also 15 cm in diameter but with a depth of 178 m. In both boreholes the thermal conductivity of the drill chipping samples collected during drilling were determined by Geoliving Energy the Swiss company that was responsible for the drilling and the determination of the thermal properties of the ground. Thermal response tests were also carried out for the determination of the thermal conductivity and effective thermal resistance of the boreholes. All results are tabulated in Table 3.9.

Finally, a Project funded by the Research Promotion Foundation of Cyprus that was undertaken by the Cyprus University of Technology and other collaborators provided the opportunity to gather and publish similar information for six new-drilled boreholes. This project was designed in order to fulfil the purpose of this study and I acted as the main researcher to perform and coordinate the technical and scientific actions of the project. The sites were selected based on geologic conditions, prevailing weather conditions and population density in order to include seaside, inland, semi-mountain and mountainous locations. For this study the drilling sites were located in the regions of Lakatamia in Nicosia, Kivides in Limassol, Meneou in Larnaca, Agia Napa in Famagusta, Geroskipou and Prodromi in Paphos. Figure 3.5 depicts the geological map of Cyprus with the locations of the 6 new-drilled boreholes and the 2 boreholes drilled in Agios Georgios in Limassol and in Saittas region.

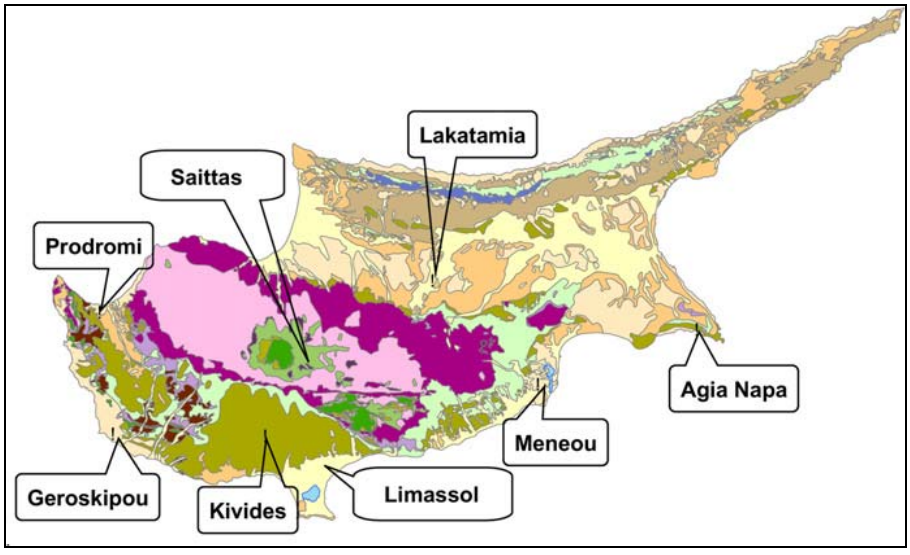

Figure 3.5: Geological map of Cyprus with the 8 borehole locations, Florides *et al.* (2011)

Table 3.6 presents all relevant information for the boreholes. In most of the boreholes more than one GHE were installed. This would allow the examination of the effect of the GHE length, diameter or type on the result of the thermal conductivity tests.

Table 3.6: Borehole and equipment installation details, Florides *et al.* (2011)

Location	Depth /Diam m	Ground heat exchangers	Filling material
Agia Napa Famagusta	100.5/0.2	PE100, PN16, 32x3 mm, 2Ux100 m	bentonitic clay
Meneou Larnaca	97/0.2	PE100, PN16, 32x3 mm, 1Ux97 m PE100, PN16, 40x3 mm, 1Ux97 m PE80, PN16, 40x3 mm, 1Ux97 m	bentonitic clay
Lakatamia Nicosia	160/0.23	PE100, PN16, 32x3 mm, 1Ux160 m 1Ux100 m	bentonitic clay and cement
Kivides Limassol	196/0.15	PE100, PN16, 32x3 mm, 1Ux196 m 1Ux96 m	bentonitic clay
Geroskipou Pafos	100/0.2	PE100, PN16, 32x3 mm, 1Ux100 m PE100, PN16, 25x3 mm, 1Ux100 m	bentonitic clay
Prodromi Paphos	100/0.2	PE100, PN16, 32x3 mm, 1Ux100 m	bentonitic clay
Agios Georgios Limassol	120/0.152	PE100, PN16, 40x3.7 mm, 2Ux120 m	bentonitic clay
Saittas Limassol	178/0.152	PE100, PN16, 40x3.7 mm, 1Ux178 m	bentonitic clay

As in the previous cases, drill chipping samples were collected during drilling (Figure 3.6). The drill chipping samples were used by the Geological Survey Department of the Ministry of Agriculture and Natural Resources of the Republic of Cyprus (GSDC) to identify the geological layers. The ground layers mostly include sandy marls, chalk, limestones and sandstones. Figure 3.7 depicts the borehole lithology at the six selected locations based on the GSDC findings.

Figure 3.6: Drill chipping samples collected during drilling

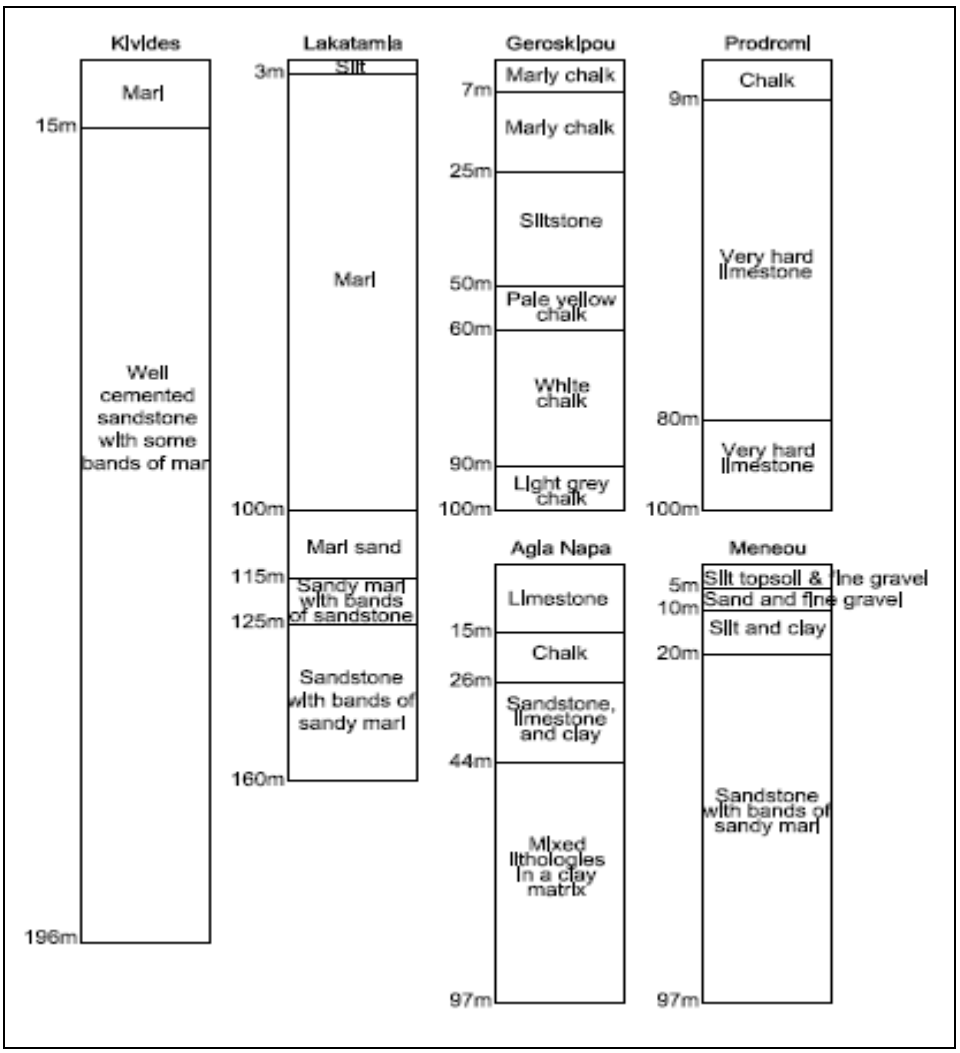

Figure 3.7: Borehole lithology at the six selected locations

Additionally, samples from areas lithologically identical or similar to those of the boreholes were collected from nearby areas for analysis. For every sample, a number of thermal conductivity measurements were made using the Hukseflux TPSYS02 thermal sensor device. The device could measure the thermal conductivity of soils, thermal backfill materials, sediments, etc with the aid of needle probes. The measurement principle is that of a non-steady state probe or transient line source where the thermal conductivity of the sample is determined by the temperature response to heating. After an initial transition period, the temperature rise close to the heater depends only on the thermal conductivity of the surrounding medium, and no longer on heat capacity. The Measurement and Control Unit (MCU) controls the process while a software installed on a PC analyses the data and presents the results (see Figure 3.8). The needle probes used were designed for measure thermal conductivities in the range 0.1 to 6 W/mK while the accuracy of the system is ±(3% + 0.02) W/mK. This method of measurement is fast and independent of sample size, (www.hukseflux.com).

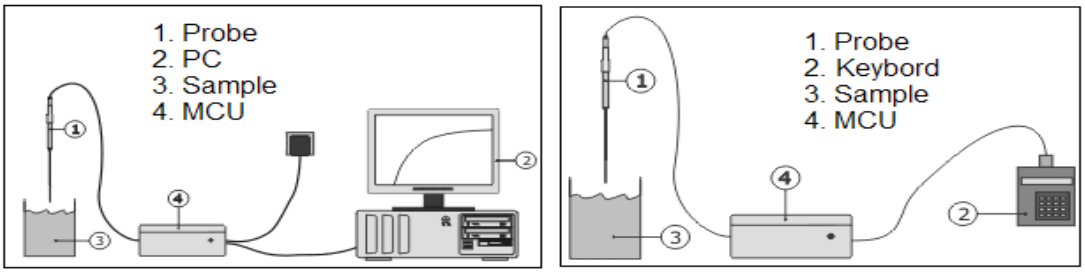

Figure 3.8: The Hukseflux TPSYS02 device in (a) standard and (b) field configurations (www.hukseflux.com).

To measure the thermal conductivity of a rock sample a hole 3 mm in diameter and 150 mm in depth should be drilled in the sample. With this method, in order to prevent convective heat flow between the needle probe and the hole wall, the hole diameter should match the probe diameter and the hole should be sealed at both ends. Since the needle probe diameter was very thin and it was difficult to drill such a hole in hard samples, the larger diameter hole drilled (5 mm) was filled with conductive materials such as heat conducting paste. The measured values using the Hukseflux TPSYS02 thermal sensor are presented in Table 3.7.

Table 3.7: Measured values using the Hukseflux TPSYS02 thermal sensor device

Specimen	Type of material	Absorption %, WA24	λ	ρ	Condition
			W/mK	kg/m^3	
1	Chalk	15.9	0.73	2030	dry
					100% saturated
2	Chalk	10.3	0.77	2160	dry
					100% saturated
3	Chalk	4.7	0.87	2420	dry
			1.54		100% saturated
4	Chalk	3.0	0.9	2580	dry
					100% saturated
5	Chalk	8.2	0.7	2270	dry
			1.33		100% saturated
6	Chalk	5.1	0.83	2440	dry
			1.05		100% saturated
7	Chalk	5.6	1.07	2070	dry
			1.45		100% saturated
8	Marl	34.7	0.51	1720	dry
			1.45		100% saturated

All values of Table 3.7 are lower than those expected. This is because hard rock specimens present problems in drilling and as experienced thin needle probes cannot give accurate results due to the difference between needle and hole diameter. Needle probes on the other hand can be used reliably for the determination of the thermal conductivity of soft materials like moist clay, sands, polystyrene and powders.

For more accurate and consistent results, the Isomet 2104 portable heat transfer analyzer was bought (Figure 3.9) and used to repeat the tests performed with the Hukseflux thermal device. The Isomet 2104 analyzer is a device that uses surface probes for direct measurement of thermophysical properties, thermal conductivity and volumetric heat capacity of a wide range of materials. The measurement principle is based on the temperature response of the sample to heat flow impulses. The heat flow is induced by electrical heating using a resistor heater. The surface probe assures a direct thermal contact with the surface of the sample. The accuracy of the instrument when measuring thermal conductivity in the range 0.015 to 0.7 W/mK is 5% of the reading +0.001 W/mK, while in the range 0.7 to 6.0 W/mK it is 10% of the reading. The instrument has a repeatability of 3% of the reading +0.001 W/mK, Applied Precision Ltd.

Figure 3.9: Isomet 2104 portable heat transfer analyzer with surface probe, Applied Precision Ltd.

The measurements were performed on various samples in their dry and water saturated state. All results measured with the Isomet 2104 portable heat transfer analyzer with a surface probe are shown in Table 3.8.

Table 3.8: Isomet 2104 portable heat transfer analyzer results

Specimen	Type of material	λ	Cp	ρ	Condition
		W/mK	W/kgK	kg/m^3	
1	Reef limestone	1.22	654	2232	dry
		1.74	906	2347	100% saturated
2	Reef limestone	1.51	718	2125	dry
		1.94	962	2234	100% saturated
3	Chalk	1.58	729	2304	dry
		1.70	733	2402	100% saturated
4	Marly chalk	0.75	1020	1591	dry
		1.22	961	1862	100% saturated
5	Marl	0.50	806	1832	dry
		0.99	767	2155	100% saturated
6	Calcarenite	0.78	784	2075	dry
		1.19	757	2461	100% saturated
7	Calcarenite	0.36	296	1359	dry
		0.80	527	1777	100% saturated
8	Gypsum	1.23	717	2301	dry
		1.19	753	2301	100% saturated
9	Ochre	0.72	690	2174	dry
10	Lava (lower horizon)	0.80	751	1997	dry
		0.97	805	2020	100% saturated
11	Lava (upper horizon)	0.82	749	2119	dry
		0.98	756	2225	100% saturated
12	Lava (basal group)	1.45	596	2728	dry
13	Gabbro	1.97	675	2749	dry
14	Werlite	2.65	630	2941	dry
15	Hartzbourgite	2.34	645	2708	dry
16	Plagiogranite	2.81	586	2893	dry
		3.16	703	2893	100% saturated
17	Diabase	3.76	522	3264	dry
		3.73	603	3264	100% saturated
18	Iron pyrite	9.06	392	4093	dry
19	Umber (silisified)	2.97	642	2773	dry
		3.14	690	2773	100% saturated
20	Pyroxenite	2.02	660	2718	dry
21	Serpentinite	2.29	641	2588	dry

The thermal conductivity of each type of sample is not constant. Due to the fact that the specific weight of the samples also varies. Samples collected from the surface appear to be less dense than the ones collected from deeper in the ground. Also it must be stated that, as expected, materials which absorb water attain a higher conductivity than when they are dry

since water with higher conductivity replaces the air. Materials like gypsum in a crystalline form or diabase do not absorb water therefore their conductivity remains the same. Small differences observed in the table are due to the accuracy of the measurement and the uniformity of the material.

To perform the in situ TRT a device comprising the electrical heaters (2 x 3 KW coils) circulating pump, flow meter electrical panel and measuring equipment was constructed. A lightweight hot water storage tank was also utilised. For every borehole a number of TRTs were carried out in order to determine the average thermal conductivity of the ground and the average temperature of the undisturbed ground. Figure 3.10 depicts the device used for the tests. The line source method was employed for the determination of the thermal conductivity of the boreholes. The tests were carried out by injecting a constant thermal energy into the boreholes. The inlet and outlet temperatures of the heat carrier fluid, its flow and the input energy from the electric heating coil were recorded over a certain period. The mean heat carrier fluid temperature was plotted against the natural logarithm of time, Ln(t), and from the plot the ground thermal conductivity was calculated. The specific plots for the two tests carried out at the Geroskipou region are illustrated in Figures 3.11 and 3.12.

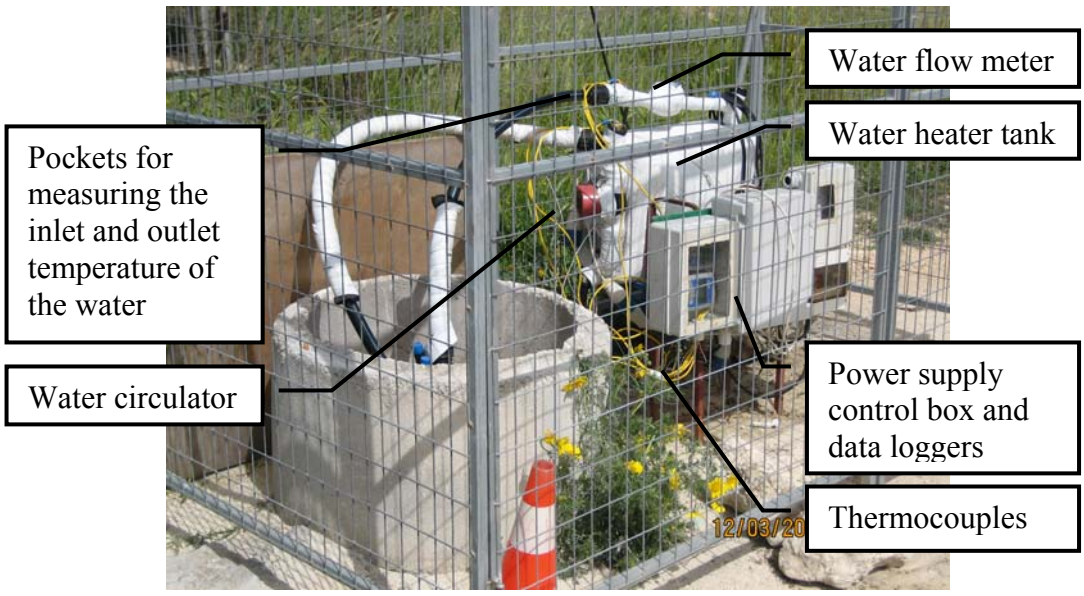

Figure 3.10: The equipment used for the tests

Figure 3.11 shows the input and output temperatures of the circulating fluid. As expected, the temperature in the larger diameter tube (32 mm) is maintained at a slightly lower temperature although the input energy injected during the test was slightly higher than the

case of the 25 mm tube. This shows that a bigger diameter tube is more efficient in dissipating heat in the ground.

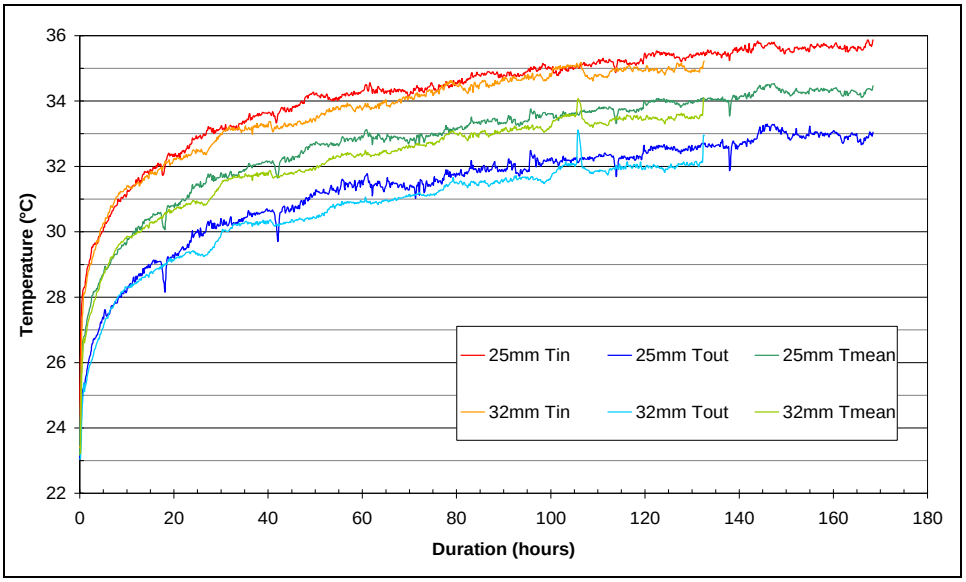

Figure 3.11: Input, output and mean temperature of circulating fluid for the 25 mm and 32 mm diameter tube in Geroskipou-Paphos

Figure 3.12, illustrates the logarithmic relation between the mean tube temperature and heating time, from which the thermal conductivity of the ground can be calculated. Both relations give a very close result of 1.40 and 1.45 W/mK in the case of the 25 and 32 mm diameter tube respectively. The slight difference observed is mainly due to injected thermal energy variations (which depended on the grid voltage variation according to the time of day and load demand of the area) and also to small differences in the ground saturation level since the tests were carried out in different months. Details of all the tests carried out and their results are shown in Table 3.9.

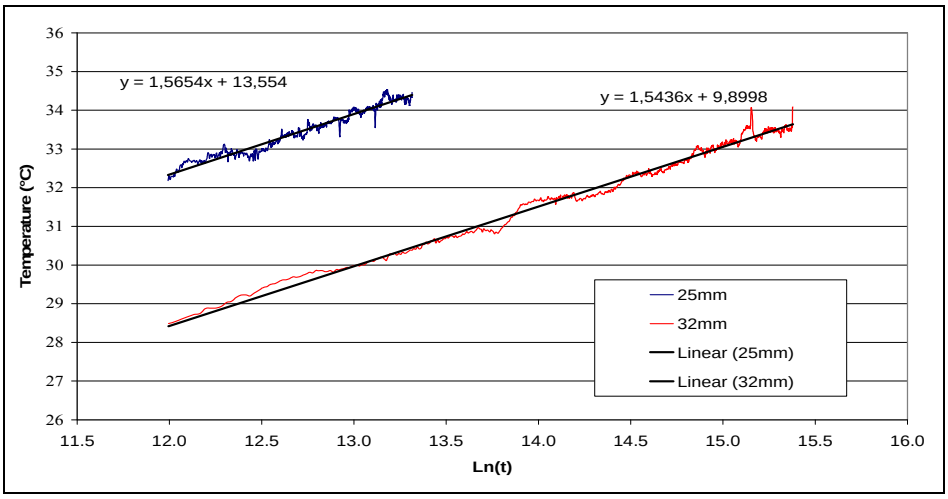

Figure 3.12: Logarithmic relation between the mean tube temperature and heating time for the tests carried out at Geroskipou-Paphos

Table 3.9: Details of the TRTs carried out in the 8 borehole locations

Place	Date	GHE Diam./Depth	Heater		Initial Temp	T_{in} at 50 hours	T_{out} at 50 hours	dT at 50 hours	T_{in} at 80 hours	T_{out} at 80 hours	Thermal conductivity, λ
		mm/m	W	W/m		°C	°C	°C	°C	°C	W/mK
Agia Napa	Jan. 09	32/100	2813	28.1	23.5	35.1	31	4.1	36.2	31.9	1.58
	Feb. 10	2x32/100	5190	51.9	22.4	41.8	35.7	6.1	43.2	36.6	1.88
Lakatamia	Nov. 09	32/160	5710	35.7	23	37	31.2	5.8	-	-	1.68
	Dec. 09	32/60	2865	47.75	23.4	40.3	37.7	2.6	41.5	38.4	1.77
Geroskipou	May 10	25/100	2746	27.5	24	35	31.8	3.2	35.5	32.5	1.40
	Mar. 10	32/100	2820	28.2	21.5	33.4	30.4	3	34.5	31.5	1.45
	Dec. 11	25/100	2730	27.3	23.1	31.1	34.2	3.1	31.8	34.5	1.35
	Dec. 11	32/100	2780	27.8	23.5	31.7	34.7	3	32.5	35.5	1.45
Meneou	Oct. 09	32/100	5875	58.75	22	35.5	32.8	2.7	37.2	34.4	1.72
	Jan. 10	40/100	2505	25.05	22.3	32	28	4	33	28.5	1.39
Prodromi	Jun. 10	32/100	2678	26.78	24	32.5	30.6	1.9	-	-	1.87
Tests carried out with the instruments of Geoliving energy company											
Limassol	Jun. 08	32/120	5000	41.6	22.1	38.5	32	6.5	-	-	1.7
Saittas	Jun. 08	40/178	9238	51.9	18.6	35	28	7	-	-	2.1

Furthermore an attempt is made to compare the results of the thermal conductivity measurements in this project to those by Morgan (1973). In order to do this, boreholes drilled in nearby areas of similar lithological structure were identified. In Figure 3.13 the 8 boreholes drilled for the purposes of this study (blue marks) and the 33 boreholes used by Morgan (red marks) are plotted on the geological map of Cyprus. As shown, comparison can be made for the borehole drilled in Prodromi in Paphos with Morgan's boreholes in stations CY28 and CY 30. Also the borehole in Lakatamia and Morgan's borehole in station CY18 could have been compared but the geological data of this borehole were not published.

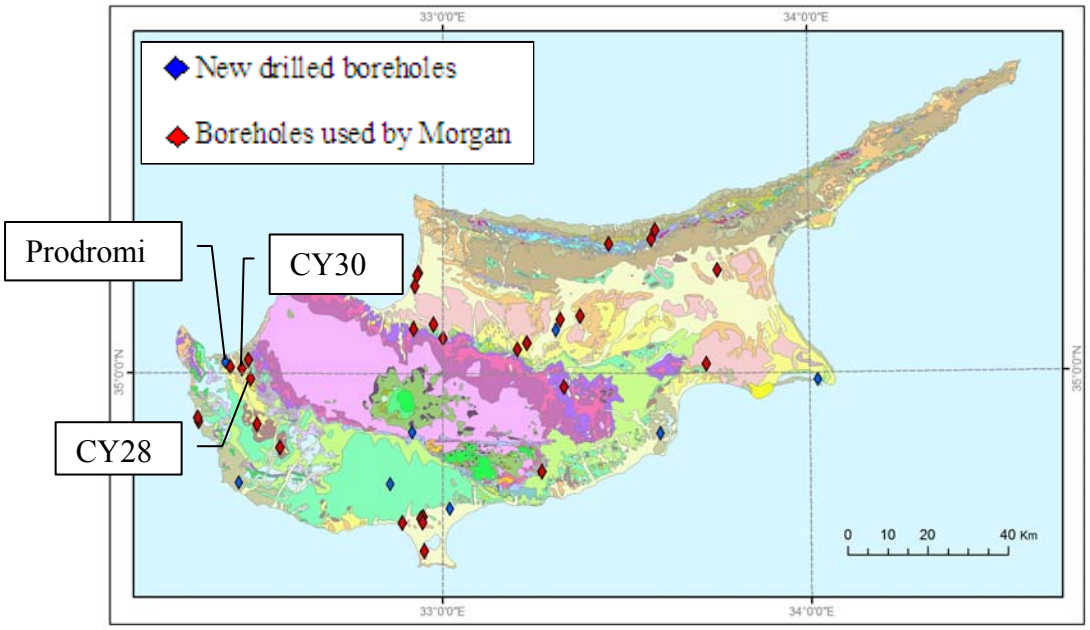

Figure 3.13: Geological map of Cyprus depicting the borehole locations

Table 3.10 presents the thermal conductivities of the two boreholes examined by Morgan and the borehole in Prodromi. Although the depths of the boreholes vary and in some cases are much deeper than 100 m, depths up to approximately 100 m have been considered for comparison.

A closer examination of the lithology (Table 3.10) shows that the ground layers at Prodromi are not very similar to CY28 B/H PB56 and CY30 B/H PB 50. Therefore, it can be concluded that the geology in nearby areas can vary and each location should be examined individually to establish its properties.

Additionally, in Table 3.10 a comparison can be made between the calculated value (1.6 to 1.9 W/mK), resulting from the values measured with the Isomet 2104 portable heat transfer analyzer (Table 3.8), and the TRT value (1.87 W/mK) for the borehole at Prodromi. These values show a reasonable agreement considering that the water level in the drilled borehole was at a depth of about 80 m and that there was a high degree of saturation in the layers above the water.

Table 3.10: Comparison of the thermal conductivities of the two boreholes referred to by Morgan with the borehole in Prodromi

Borehole location	Depth m		Type of material	Thermal conductivity, λ W/mK	
	From	To		Range of material type (Refer to Table 3-8)	Average of borehole
Prodromi, Paphos	0	9	Chalk	1.58 - 1.7	1.6 - 1.9 (TRT Result 1.87)
	9	80	Very hard limestone	1.51 - 1.94	
	80	100	Very hard limestone	1.94	
CY 28 B/H PB56	0	182.9	Gravel, Clay, Gravel, Marl, Marl with chalk, Limestone	1.43	1.43
CY 30 B/H PB50	0	12.2	Marls	1.42	1.4
	12.2	27.4		1.43	
	27.4	33.5		1.47	
	33.5	45.7		1.36	
	45.7	57.9		1.40	
	57.9	67.1		1.45	
	67.1	77.4		1.44	
	77.4	88.7		1.49	
	88.7	100.6		1.48	

3.5 Summary

Knowledge of the thermal behaviour of the ground at various locations and depths is important for the design of geothermal applications in Cyprus as of determines the efficiency of ground coupled heat pumps for heating and cooling of buildings.

The line source method is an easy way of determining the thermal conductivity of a borehole and under certain circumstances the thermal diffusivity and thermal capacitance.

Drill chipping samples can be used to define the soil types of the borehole but not for the determination of their thermal properties. The determination of the thermal properties can be done by using core samples collected from the boreholes or from areas lithologically identical to the ones of the borehole. The thermal conductivity of each sample can vary due to variation in the specific weight and degree of saturation of the sample. Samples collected from the surface appear to be less dense than the ones collected from locations deeper in the ground. The geology of neighbouring areas can vary so each location should be investigated individually for accurate results.

In general, the thermal conductivities of the drilled boreholes were found to be in the range 1.35 to 2.1 W/mK. The variation is mainly due to the degree of saturation of the ground.

When the thermal conductivity of a borehole (the combination of the backfilled material in the drilled hole and the surrounding undisturbed ground) is low, using standard heat exchangers could result in long borehole lengths. Therefore one should investigate the possibility of using heat exchangers that will minimize the resistance of the thermal flow between the ground and the heat carrier fluid.

Chapter 4: The temperature profile of the ground in Cyprus

4.1 Introduction

Further to the determination of the thermal parameters of the ground in Cyprus discussed in the previous chapter, the determination of the temperature profile of the ground is also very important. In this chapter, the recorded ground temperatures at the selected sites in relation to depth, time of year, geology and altitude are presented and discussed. The effect of the ground temperature on the efficiency of Ground Coupled Heat Pumps (GCHP) is also examined.

As previously mentioned in Chapter 2 of this thesis, studies showed that the ground is divided in zones depending on its temperature variation in relation to depth and time. At the surface zone, the ground is affected by short term weather variations (hourly variations), changing to seasonal variations (monthly) in the shallow zone. At the deeper layers (deep zone) the ground temperature is not affected by weather variations. The temperature of the ground in the deep zone is constant throughout the seasons and years and is usually higher than that of the ambient air during the cold months of the year and lower during the warm months.

4.2 Ground zones in Cyprus

The structure and physical properties of the ground are factors affecting the temperature, in all zones. The temperature of the ground is a function of the thermal conductivity, geothermal gradient, water content and water flow rate through the borehole. In Cyprus, Florides and Kalogirou (2005) studied the fluctuations of the ground temperature with depth in the borehole drilled in Athalassa region in Nicosia. It was found that the temperature variations in the surface zone in winter reached the depth of approximately 0.5 m. For our study, we have also measured the ground temperature for the period of May 2006 to May 2007, at Athalassa region and found that the ground temperature in the surface zone varied in phase with the ambient air temperature while as the depth increased the maximum or minimum temperatures occurred with a time delay, Pouloupatis *et al.* (2011). In the deep zone the ground temperature remains unaffected by the ambient air temperature variations. Figure 4.1 below depicts the recorded ground temperatures in various depths against time for the certain period. The three zones of the ground can be

distinguished as well as the time delay of the minimum or maximum in the ground temperature at various depths.

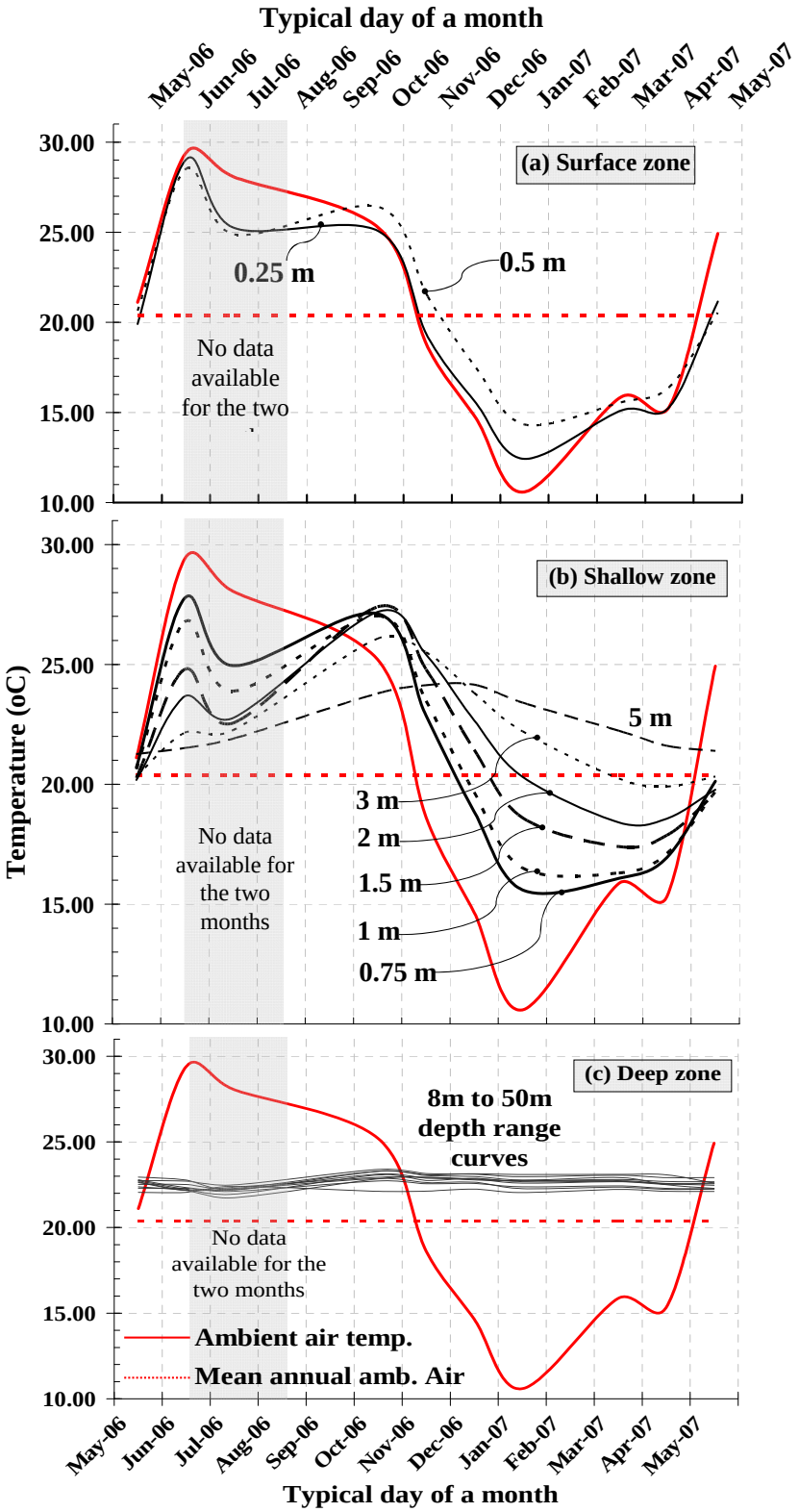

Figure 4.1: Mean monthly ground temperature at the (a) Surface zone, (b) Shallow zone and (c) Deep zone in the Athalassa region in Nicosia for the period May 2006 to May 2007

In Figure 4.1(a) the curves representing the depths of 0.25 m and 0.5 m follow the path of the ambient air fluctuation very closely stating clearly the surface zone that reaches approximately the depth of 0.5 m. The curves in Figure 4.1(b) representing the depths from 0.75 m to 5 m indicate the shallow zone in which longer time is needed for these layers to be affected by the ambient temperature. The shallow zone extends up to the depth of 8 m. From the depth of 8 m and deeper, Figure 4.1(c), the ground temperature is almost constant showing negligible fluctuations as happens typically in deep zones.

4.3 Ground Coupled Heat Pumps

The exploitation of the ground thermal capacity and the difference in temperature between ambient air and ground can be accomplished via Ground Heat Exchangers (GHE). A GHE is usually an array of buried pipes installed either horizontally or vertically into the ground. They are either open or closed type systems with air, water or a water–antifreeze mixture, acting as the heat carrier fluid exchanging heat with the ground. The ground acts as a heat source when heating is required while when cooling is required the ground acts as a heat sink. GHEs can contribute to the air conditioning of a space, for water heating purposes and also for improving the efficiency of heat pumps coupled to them, called Ground Coupled Heat Pumps (GCHP).

The main operation of single-stage vapour compression cycle heat pumps is to extract heat from a source and transfer it at a higher temperature to the sink. Air, water and ground are the main sources that heat can be extracted from and transferred to as well. Heat pumps are classified mainly based on their heat source and sink and their thermodynamic cycle. The most popular type of heat pump is the common air-to-air heat pump or air-cooled heat pump. These heat pumps use the atmosphere as heat source and/or sink and they exchange heat with ambient air. All refrigeration equipment, including air conditioners, used for heating and cooling purposes are considered as heat pumps.

Air-cooled heat pumps use refrigerants as heat carrier fluids for the heat exchange process. The refrigerants have the ability to change state, from liquid to gas when heated and usually they boil at low temperature. In the heating mode of an air-cooled heat pump, the refrigerant flowing in the evaporator absorbs heat from the environment and evaporates (changes state from liquid to gas) at low pressure. Then, an electrically driven compressor is used for the compression of the refrigerant aiming to the increase of its temperature.

Therefore, the refrigerant at this stage is at high pressure and temperature and flows through a condenser and exchanges heat with a lower temperature medium. Having its temperature dropped the refrigerant returns to the liquid stage and after passing through an expansion valve, it becomes liquid at low temperature and pressure. The process described above is depicted in Figure 4.2. Most commonly, heat pumps are designed to reverse their cycles to deliver heating and cooling as well.

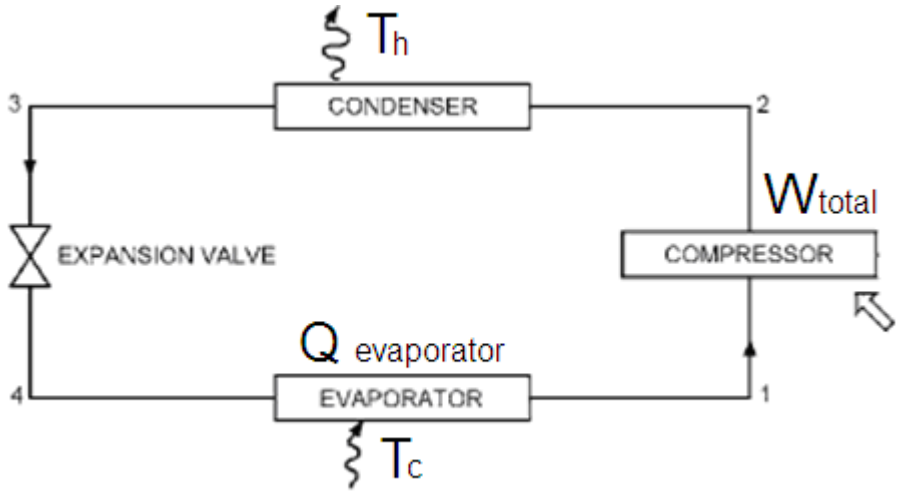

Figure 4.2: Theoretical single-stage vapour compression refrigeration cycle, ASHRAE Handbook (2009).

The efficiency of heat pumps is defined by the Coefficient of Performance (COP) in the heating mode and the Energy Efficiency Ratio (EER) in the cooling mode. As stated in the ASHRAE handbooks (2001), COP or EER *'is the ratio of the rate of net heat output to the total energy input expressed in consistent units and under designated rating conditions or is the ratio of the refrigerating capacity to the work absorbed by the compressor per unit time*'.

$$\mathrm{COP} = \frac{\text{Rate of net heat output}}{\text{Total energy input}} = \frac{\text{Refrigerating capacity}}{\text{Work absorbed by the compressor}} \qquad (1)$$

Sometimes the efficiency is described by the Seasonal Performance Factor, which is the average efficiency of the pump over the heating and cooling period, or the Seasonal Energy Efficiency Ratio for cooling (SEER), which is the total cooling output of an air conditioner during its normal annual usage period for cooling divided by the total electric energy input during the same period.

Most heat pumps use a vapour compression or an absorption thermodynamic cycle. For a mechanical vapour compression system as described above, the total energy input is usually in the form of work to the electrically driven compressor and fans. Similarly, the rate of net heat output can be expressed by the total heat delivered by the evaporator. Therefore, Eq. (1) can be expressed as:

$$\mathrm{COP} = \frac{Q_{\mathrm{evaporator}}}{W_{total}} \tag{2}$$

The Carnot cycle usually expresses the ideal reversible refrigeration cycle. It consists of two isothermal processes, heat exchange at constant temperature in the evaporator and condenser and two adiabatic processes, temperature increase during compression and temperature drop during expansion. By reversing the entire cycle the heat engine is converted into a refrigerator with the maximum possible efficiency. The Theoretical Coefficient of Performance of the Carnot refrigeration cycle is given by:

$$\text{Theoretical COP} = \frac{T_c}{T_h - T_c} \tag{3}$$

where:

T_c - is the temperature of the cold reservoir (room to be cooled)

T_h - is the temperature of the hot reservoir (ambient air)

Eq. (3) shows that the smaller the difference between T_h and T_c, the greater the performance coefficient.

Heat pumps actually differ from the ideal cycles in many respects. Pressure drops occur everywhere in the system except in the compression process and heat transfers occur between the refrigerant and its environment in all components. All of these cause irreversibilities within the system, each one requiring additional power into the compressor. For a non idealised refrigerator the actual thermodynamic Coefficient of Performance is always less than that of the Carnot cycle and at the best cases is 0.8 to 0.9 of the Carnot Coefficient of Performance, Vrachopoulos (2000).

GCHPs, or Ground Source Heat Pumps (GSHP) or Geothermal Heat Pumps (GHP), are heat pumps coupled to GHEs. The difference of GCHPs with common air-cooled heat pumps lies in the way they exchange heat in the evaporator. GCHPs exchange heat with

the ground instead of the atmosphere. The rest of the process remains the same. Because of the difference mentioned above, it is expected that GCHPs would have some additional parts that comprise the ground loop system. Besides the GHE which is considered as part of the system, a heat carrier fluid circulator and an additional heat exchanger are required. The additional heat exchanger is responsible for the heat exchange process between the refrigerant in the main system and the heat carrier fluid in the ground loop system while the heat carrier fluid circulator is responsible for the circulation of the heat carrier fluid in the GHE and therefore for the heat exchange process in the ground, Healy and Ugursal (1997), Christofides et al. (2009). Figure 4.3 depicts a typical GCHP system.

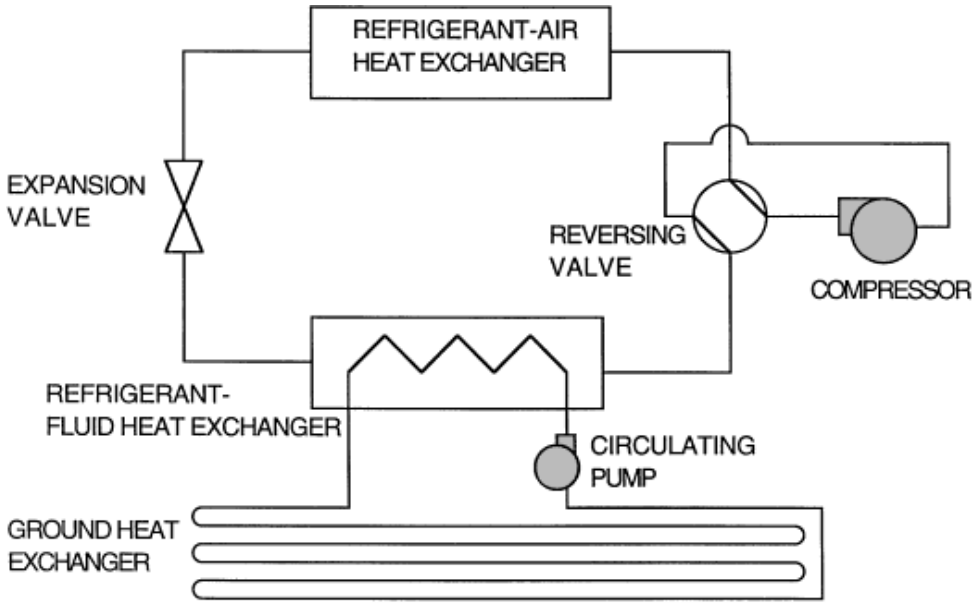

Figure 4.3: Schematic diagram of a Ground Coupled Heat Pump,
Healy and Ugursal (2009)

As mentioned above and also shown in Figure 4.1, the temperature of the ground provides a more steady and reliable source than the ambient air for the heat exchange process. Because of that, GCHPs could have improved efficiencies compared with common air-cooled heat pumps. Researches proved that the use of GCHPs could result in CO_2 reductions up to 54% in relation to common water to air heat pumps Healy and Ugursal (1997), Christofides et al. (2009).

4.4 Ground temperature determination in Cyprus

As mentioned in Chapter 3, Morgan (1973) in his PhD study was the first known researcher who measured and reported the geothermal gradient for 33 boreholes in Cyprus,

Appendix 1. For this study, the ground temperatures were recorded for 8 locations and are presented in Appendix 2. The locations of the boreholes are shown in Figure 3.5 in Chapter 3.

For the temperature recording, two methods were used. Firstly, thermocouples were fitted at the various depths in each of the boreholes as shown in Table 4.1. The Omega thermocouples used were of the K type and were twisted/shielded thermocouple wires ideal for systems sensitive to induced voltages and electrical noise. They were also moisture, abrasion, chemicals and UV light resistant, Omega Engineering Inc. All the data were recorded using DaqPRO data loggers at 30 minute intervals.

DaqPRO is an eight-channel, compact, stand-alone, portable data acquisition and logging system with built-in analysis functions. It is capable for measuring voltage, current, temperature and pulses and it has a variety of selectable ranges for each input. Moreover, it can be connected to a PC through the DaqLAB software. The above instrument has an accuracy of 0.5°C, Fourier systems Ltd (2007).

Table 4.1: Borehole and equipment installation details

Location	Depth /Diam (m)	Thermocouple positions (m)
Agia Napa Famagusta	100.5/0.2	Ambient, 0, 0.25, 0.5, 0.75, 1, 3, 5, 7, 8, 9, 10, 11, 15, 20, 40, 60, 80, 100
Meneou Larnaca	97/0.2	Ambient, 0, 0.25, 0.5, 0.75, 1, 3, 5, 7, 8, 9, 10, 11, 15, 17, 37, 57, 77, 97
Lakatamia Nicosia	160/0.23	Ambient, 0, 0.25, 0.5, 0.75, 1, 3, 5, 7, 8, 9, 10, 11, 15, 10, 20, 30, 40, 50, 60, 70, 80, 90, 100, 110, 120, 130, 140, 150, 160.
Kivides Limassol	196/0.15	Ambient, 0, 0.25, 0.42, 0.67, 0.92, 3, 5, 7, 8, 9, 10, 15, 26, 46, 76, 96, 126, 146, 176, 196.
Geroskipou Pafos	100/0.2	Ambient, 0, 0.25, 0.5, 0.75, 1, 3, 5, 7, 8, 9, 10, 20, 40, 60, 80, 100.
Prodromi Paphos	100/0.2	Ambient, 0, 0.25, 0.5, 0.75, 0.95, 3, 5, 7, 8, 9, 10, 15, 20, 40, 60, 80, 90, 100.
Limassol	127/0.152	N/A
Saittas Limassol	178/0.152	Ambient, 0, 0.25, 0.5, 0.75, 1, 3, 5, 7, 10, 50, 100, 150, 185.

A second method was used for checking and increasing the accuracy of measurements. An immersible thermocouple wire connected to an Omega HH41 digital thermometer was used. The 500 m long thermocouple wire was wound on a small portable spool and immersed in one of the legs of the U-tube heat exchanger installed in each borehole which was permanently filled with water. While lowering the thermocouple wire the temperature of the water in the tube (and therefore the ground temperature) was recorded at the same depths where the K-type thermocouple wires were installed. This procedure was done slowly so as to prevent water movement in the GHE. The small PVC pipe diameter used for the GHE also prevented water movement due to temperature differences caused by small density variations. The measured temperature with the HH41 thermometer was corrected by using a formula provided by the manufacturer and giving an accuracy of 0.2°C for the temperature range of 10°C - 30°C. By using the same instrument and thermocouple wire all data were directly comparable with the same inherent errors.

The borehole drilled in Prodromi region in Pafos was selected as a reference borehole for the analysis of the recorded data that follows. The main reason for this was because this borehole was close to another 2 boreholes used by Morgan in his study and comparison is possible.

As expected the surface zone was affected by the ambient air temperature and the solar radiation and it reached the depth of about 0.25 m as clearly shown in Figures 4.4(a), (b) and (c). The hourly fluctuations of the ground temperature were more prevalent at depths closer to the surface and followed the ambient air temperature pattern. In the winter period the ambient air temperatures and the temperatures of the surface zone were colder than in the spring period. Therefore the curves of Figure 4.4(a) were shifted to the left in relation to the ones of Figure 4.4(b). Similarly, the curves shifted to the right in the summer period as shown in Figure 4.4(c), because of warmer ambient air and surface zone temperatures. The impact of the weather conditions on the ground temperature was diminishing with the increase in depth and this was proved by the tendency of the curves to join at a depth of about 0.25 m.

From the 0.25 m depth and downwards to about 8 m depth is the shallow zone. Only seasonal variations were observed with the daily weather variations not being of any importance. As shown in Figure 4.5, the ground temperature range at the depth of 0.5 m was within the range of 13.7°C to 25.8°C and reduces as the depth increases, reaching to

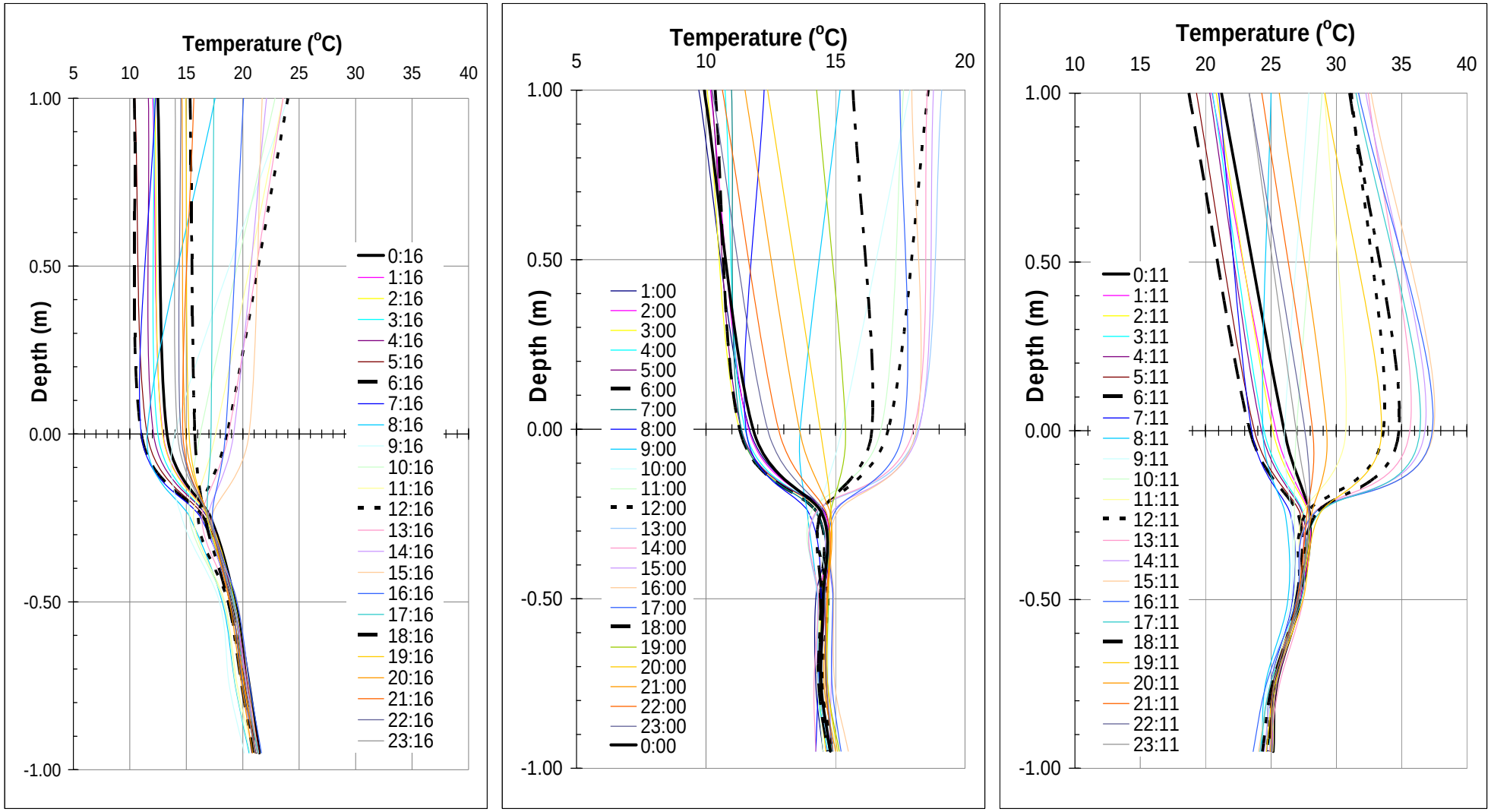

(a) winter (b) spring (c) summer

Figure 4.4: Top layer temperature distribution at Prodromi for (a) 6 November, 2009 [winter], (b) 13 March, 2010 [spring] and (c) 15 July, 2010 [summer]

the range of 20.8°C to 21.3°C at the depth of 8 m. Finally, the ground temperature in the deep zone remained almost constant throughout the year as expected with 21.77°C being the minimum temperature recorded at 100 m depth while the maximum one was 21.91°C, a difference that lies in the accuracy range of the instrument which is 0.2°C.

The geothermal gradient which as mentioned in Chapter 2 is a function of the ground thermal conductivity is indicated by the slope of the curves representing the temperature distribution in the ground. Based on the collected data, the geothermal gradients of the 8 boreholes examined were between 1°C to 1.5°C per 100 m. This is clearly shown in the graphs of the ground temperature plotted against depth of each borehole in Appendix 2.

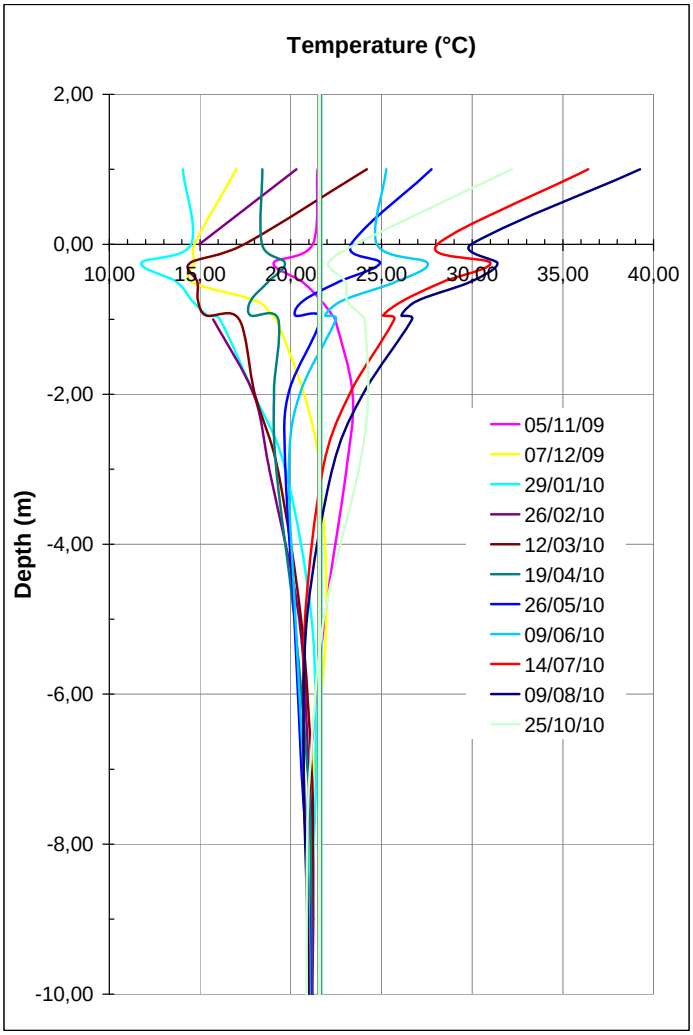

Figure 4.5: Borehole temperature distribution at Prodromi
for the period of January, 2009 to May, 2010

Figure 4.6 depicts the minimum and maximum ground temperatures recorded at the eight borehole locations for the period between October 2009 and 2010. As can be seen, the

ground temperature in the deep zone was constant throughout the year. Agia Napa was the warmest of the examined locations and Saittas the coldest. The mean minimum ground temperature in the deep zone in Agia Napa region was 23.1°C and the mean maximum 23.6°C. Similarly, the mean ground temperature in the deep zone in Saittas region was 18.3°C. The semi-mountainous location represented by the borehole in Kivides region was on average 0.5°C warmer than the one in Saittas region (18.6°C – 18.8°C). The deep zone temperature distribution in the rest of the data collection locations lay between the ones in Agia Napa and Saittas regions. The deep zone temperature distribution of the boreholes examined proved that the lithology of the ground was the most important factor affecting the geothermal characteristics of the boreholes and not their location (near the sea or inland).

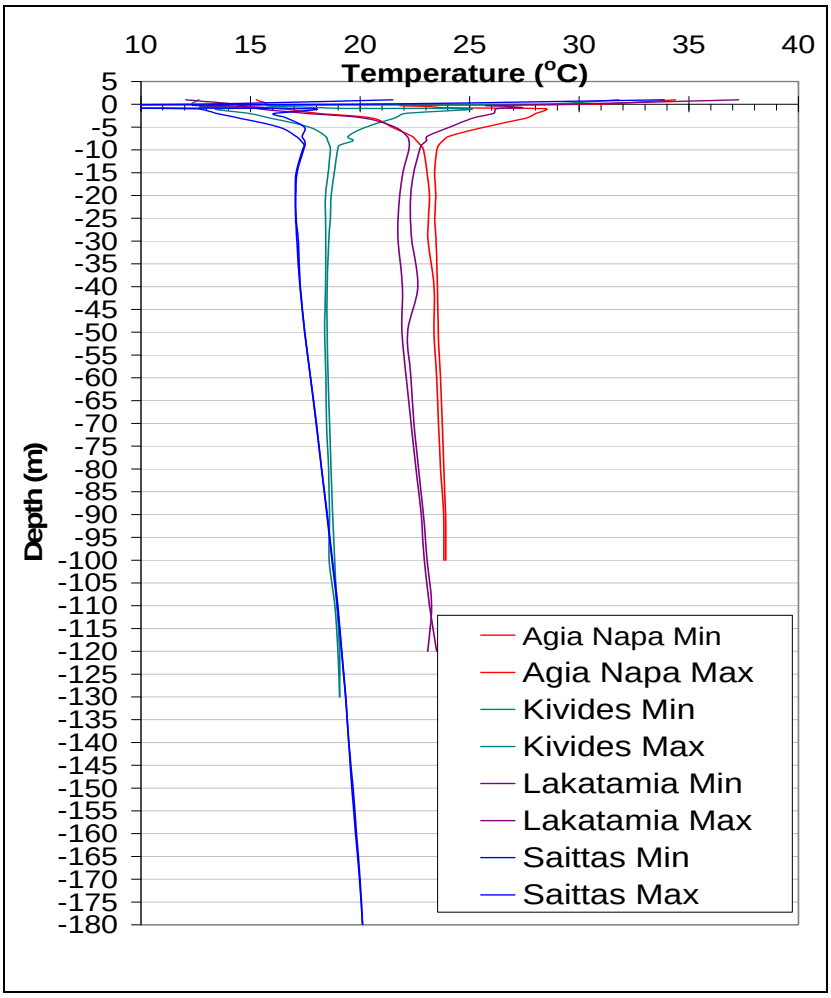

Figure 4.6: Minimum and maximum ground temperature distribution at Saittas, Kivides, Lakatamia and Agia Napa locations for the period between October, 2009 and 2010

A comparison of the ground temperatures recorded at Prodromi in May, 2010 against the ground temperatures recorded by Morgan in May, 1971, in three nearby locations, is

presented in Figure 4.7. According to the depicted curves, the ground temperatures recorded by Morgan 39 years ago are very close to the ones recorded today. This proves that the lithology of the ground is the most important factor affecting the geothermal characteristics of a location and not the weather.

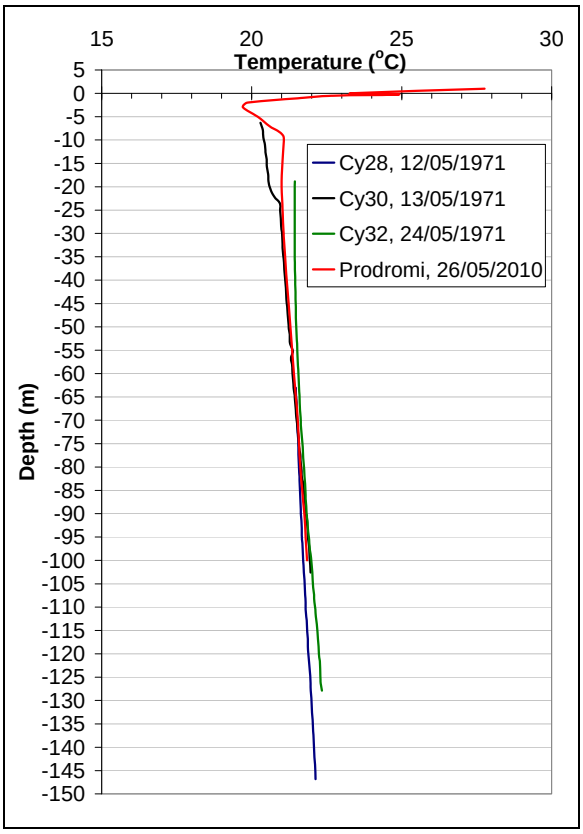

Figure 4.7: Comparison between the ground temperature distribution at Prodromi and the three nearby locations recorded by Morgan in May, 1971

4.5 Testing of a GCHP in Cyprus

As mentioned above, GCHPs exchange heat with the ground instead of the atmosphere resulting to a higher COP and EER than those of the common air-cooled heat pumps. In order to investigate the efficiency of a GCHP in relation to the ground characteristics, the GHE fitted in the borehole in the Athalassa region in Nicosia was coupled to a water to air GCHP (details of the GCHP are given in Appendix 3). K-type thermocouples were placed in the middle of the 20 cm of diameter and 50 m deep borehole to record the temperature of the ground at several depths. A k-type thermocouple was also used to record the ambient air temperature. The GHE was made of polyethylene pipe, 32 mm external diameter. More details of the borehole were presented in Chapter 3. All data were recorded at 15 minute intervals, using an Omega OMB-DAQ 55/65 USB data acquisition module.

The deep zone temperature was at 22.6°C while the mean annual ambient air temperature of the region was 19.5°C.

A typical office of 27.65 m^2 floor area next to the borehole was used for testing the water to air GCHP. The heating and cooling needs of the office were calculated to be 2.5 kW and 4.3 kW respectively. During the experiment, in the summer period, the room temperature was kept between 22°C and 24°C with a relative humidity of about 38%. The latent heat of the room was negligible since there were no occupants in the room and therefore it was ignored in the calculations. During the winter period the room temperature was kept at about 23°C.

The experiment was carried out during typical days early in October, 2008 and by the end of January, 2009. Figure 4.8 depicts the temperature variation of the water at the inlet and outlet of the GHE, the intake and delivered air temperature of the GCHP, the temperature variation of the ground at the depth of 50 m and the recorded ambient air temperature variation in October.

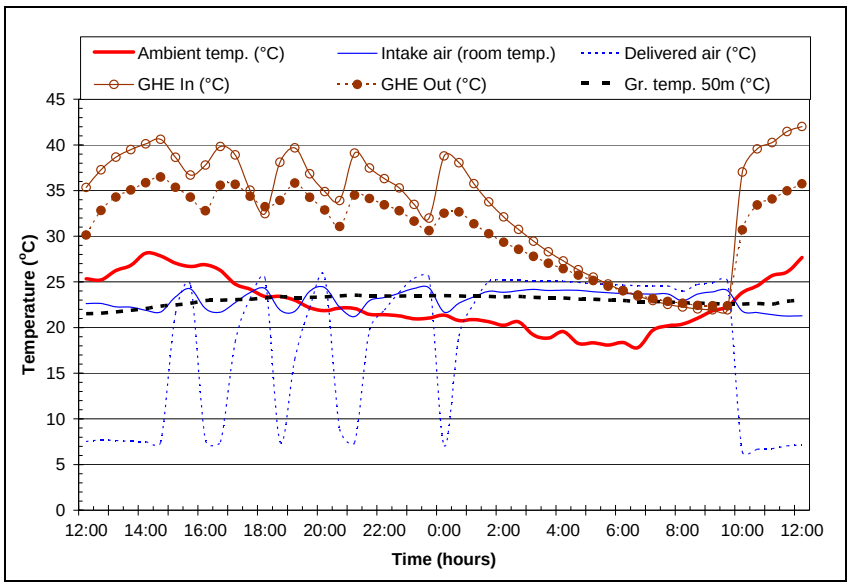

Figure 4.8: Temperature data during a typical day early in October of 2008

The air handling unit of the GCHP was continuously re-circulating the room air therefore the intake to the GCHP air temperature coincided with the room temperature. During the measurements the range of the room temperature was between 21.5°C and 24°C and the average room temperature was 23.0°C. The compressor of the GCHP was working continuously between 10:00 and 15:00 and intermittently between 15:00 and midnight to

satisfy the cooling load. From 0:00 of the next day till 10:00 the compressor was not in operation. When the compressor of the GCHP was on the delivered air temperature was between 6°C – 8°C. Also, depending on the operation of the compressor of the GCHP the temperature of the fluid entering the GHE varied between 22°C – 42.0°C. Similarly, the return temperature of the fluid varied between 22.4°C – 36.5°C. The temperature difference between the inlet and return fluid of the GHE was about 6°C while the difference was almost zero when the compressor was not in operation.

Figure 4.9 depicts the variations in the sensible capacity of the GCHP, the rejected heat to the ground by the ground heat exchanger and the input power to the GCHP when the entering air temperature to the GCHP was 23°C and the entering fluid temperature varied between 10°C – 40°C. These values were calculated using the data collected during the experiment in October. It also shows the calculated sensible capacity over the input power ratio and the trend of the curves when the entering fluid temperature rises to 50°C. Under these circumstances the calculated sensible capacity over the power input ratio was between 2.52 and 2. On average, the entering fluid temperature was calculated to be 30.7°C with the sensible capacity over the power input ratio being close to 2.2. In the case that the capacity of the GHE was higher so that the entering fluid temperature to the GCHP was lower and close to that of the ground, about 25°C, the sensible capacity over the power input ratio of the GCHP would improve and reach 2.4.

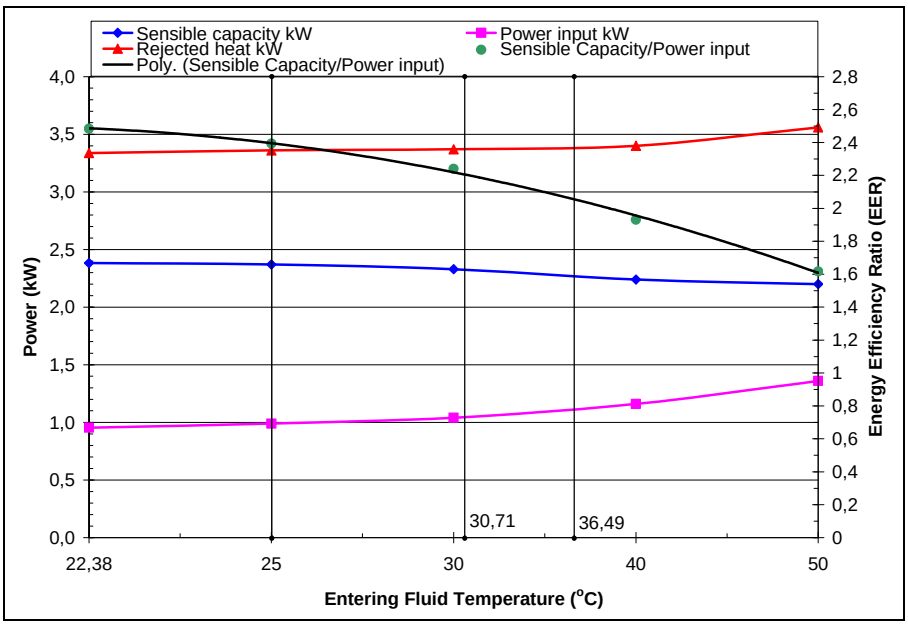

Figure 4.9: GCHP results for a room temperature of 23°C for a typical day early in October of 2008

Similar were the operating conditions during the experiment carried out in January. The GCHP was working periodically to satisfy the heating load, continuously during the night-time when the load was high and intermittently during the daytime where the heating requirements were less. The room temperature was about 23.0°C. When the compressor of the GCHP was in operation, the delivered air temperature was about 35°C. The temperature difference between the inlet and return fluid of the GHE was about 4°C. Figure 4.10, depicts the variations in the total capacity of the GCHP, the heat absorbed by the ground through the GHE and the input power to the GCHP when the range of the entering fluid temperature was between 10°C – 25°C and the entering air temperature was 23°C (room temperature). These values were calculated using the data collected during the experiments carried out in January. It also shows the calculated COP.

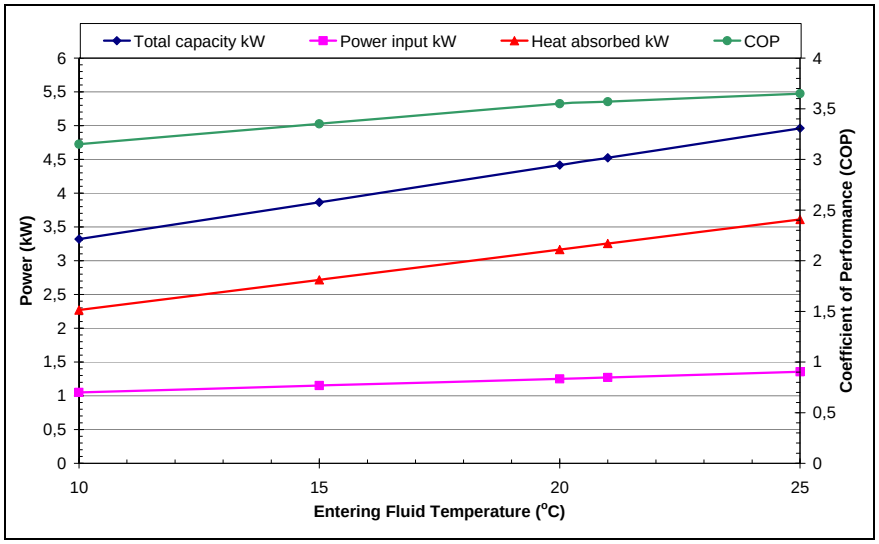

Figure 4.10: Heat pump results for a room temperature of 23°C for a typical day by the end of January of 2009

According to the data collected, the entering fluid temperature to the GCHP was almost constant and close to 20°C. At those conditions, the calculated COP was 3.55. According to the plot above, the COP of the GCHP would be slightly improved and reach 3.6 when the entering fluid temperature to the GCHP was close to that of the ground, about 22°C. This would occur in the case that the capacity of the GHE was higher. As shown on the graph, the COP of the pump had a small variation range of only 0.5 for an entering fluid temperature range between 10°C to 25°C.

The results of the tests showed that in summer, when the demand is for cooling load, the lower the ground temperature the higher the GCHP efficiency. Similarly in winter, when

the demand is for heating load, the efficiency of the GCHP is higher when the ground temperature is as high as possible.

The effect of the ground temperature and the capacity of the GHE on the efficiency of a GCHP were further investigated. The theoretical efficiencies of three typical GCHPs with different capacities were plotted in respect to the entering fluid temperature as shown in Figure 4.11(a) and (b). It is clearly shown that in the cooling mode, the EER of the GCHP increases as the entering fluid temperature decreases. In this case, the lower the ground temperature, the higher the EER is. In the heating mode, the COP of the GCHP increases as the entering fluid temperature increases. It can also be seen that higher ground temperature improves the COP. Figure 4.11(a) and (b) also depict the range of the ground temperature measured in Cyprus and the ground temperature measured in northern Germany, Mahfouf and Viterbo, (2001).

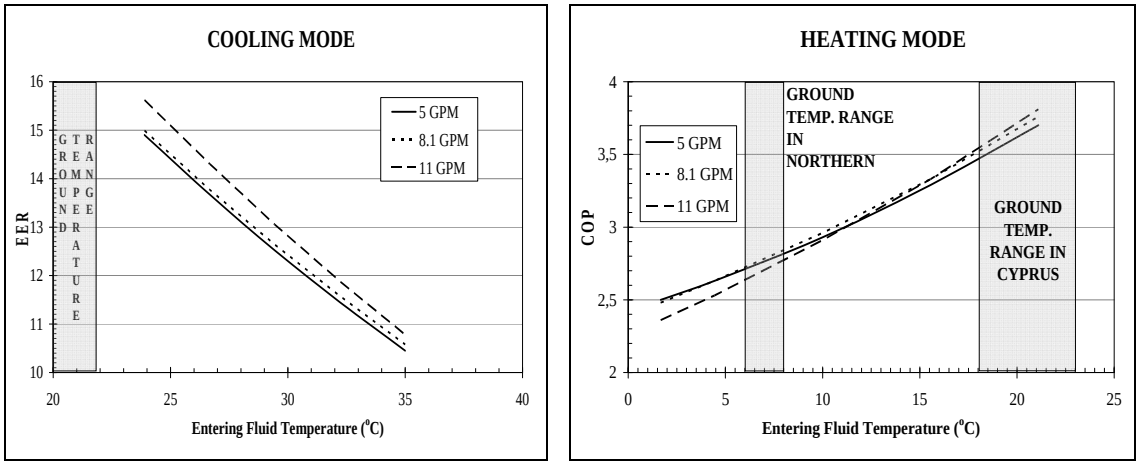

(a) (b)

Figure 4.11: GCHP efficiencies in respect to the entering fluid temperature for (a) cooling mode and (b) heating mode

It is clearly shown that, provided that the same kind of heat pump is used, the ground temperature in Cyprus would ensure a higher COP for heating that the ground temperature in northern Germany. Also, the ground temperature in Cyprus is lower than the required ground temperature when cooling is needed ensuring high EER of the GCHPs. In Cyprus, steady ground temperatures unaffected by weather conditions are achieved only in the deep zone, at depths below 8 m from the ground surface. As described above, the temperature of the ground in the shallow zone is affected by seasonal variations. Therefore, vertical GHEs

are expected to be more efficient and more reliable when coupled to GCHPs than the horizontal ones.

4.6 Summary

According to the results obtained in the 8 borehole locations in Cyprus the surface zone reaches a depth of 0.25m. The shallow zone penetrates to 7 - 8 m and there after the deep zone follows. The deep zone temperature is constant throughout the year and based on the data recorded from the 8 borehole locations is within the range of 18.3°C - 23.6°C. A temperature difference of about 5°C was recorded.

The data collected can be used by the Engineers in sizing the GHEs and clearly indicate that there is a potential for the efficient use of GCHPs in Cyprus leading to significant savings in power and in some cases in money, depending on the initial and running cost.

The ground temperatures in Cyprus indicate that the vertical GHEs are more efficient than the horizontal ones.

Chapter 5: Generation of Ground Temperature Maps of Cyprus using Artificial Neural Networks

5.1 Introduction

As mentioned mainly in chapters 3 and 4, the knowledge of the thermal properties of the ground is very important for engineers of geothermal systems for the heating and cooling of buildings. In Cyprus, this information is not easily available and for this purpose a test borehole should be drilled and probes should be installed for logging the temperature profile of the ground at each specific location. Knowing the ground formation and the temperature profile of the borehole, other useful information like the thermal conductivity and diffusivity of the borehole can be estimated. This is a time consuming and expensive process which in the majority of cases is not followed. Instead, the rule of thumb or solutions applied to similar cases or even over-sizing of the system is used, leading to expensive or sub-optimal insatallations.

This chapter presents an attempt to create the temperature profile of the island of Cyprus using Artificial Neural Networks (ANNs) that should inform and ease the work of engineers. It is believed that this would be a valuable tool for the estimation of the geothermal potential of a prospective site. Three geothermal maps depicting the temperature profile of the island at depths of 20m, 50m and 100m were created by using ANNs.

5.2 Geothermal maps

Since the ancient times humans were excited by the challenge of creating machines that could think and act like humans. Despite the prediction of French philosopher-mathematician Rene Descartes in 1637 that this would be impossible, in 1950 the British mathematician and computer pioneer Alan Turin declared that one day machines could be developed to act as humans. The passing of the years proved that neither of them was completely correct. Powerful computers were developed that can do calculations in a much faster manner than the human brain and more accurately, but are not capable enough in mimicking the human brain. Usually, computers follow a serial processing method and only supercomputers equipped with several processors can process several algorithms at the same time in a similar manner to the human brain. The human brain not only can

perform several operations at the same time but is also capable to understand them. It does not only follow the rules of logic but reasoning and factors like emotions, perception, awareness, evaluation, etc are also involved, Kalogirou (2001).

The ability of a computer to perform and act like the human brain is referred to as Artificial Intelligence (AI). AI is employed in Expert Systems and Artificial Neural Networks (ANNs). Expert Systems use pre-established rule systems to process the data giving them the ability to 'decide' by interpreting data and choosing among alternatives.

As described by Kalogirou (2000; 2001; 2003), ANNs mimic somewhat the learning process of the human brain. Instead of complex rules and mathematical routines, they are able to learn key information patterns within a multi-information domain. They differ from the traditional modelling approaches in that they are trained to learn solutions or can learn from examples rather than being programmed to model a specific problem in a mathematical way. ANNs are widely accepted as a technology offering an alternative way to tackle complex and ill-defined problems since they are able to handle noisy and incomplete data and once trained can perform predictions at very high speed.

Although the concept of artificial neural network analysis has been developed nearly 60 years ago it is only in the last 30 years that application software has been developed to handle practical problems. They have been applied successfully in various fields of mathematics, engineering, medicine, economics, meteorology, psychology, neurology amongst others. Some of the most important applications are in sound and speech recognition and the analysis of medical signatures, in weather forecasting amongst many others.

A number of researchers have worked on the development of geothermal resource maps for various locations of the world. Most of these studies are published in the transactions of Geothermal Resources Council in the United States, and concern mostly deep geothermal formations. Blackwell *et al.* (2010) summarised the results of a new Enhanced Geothermal System (EGS) assessment based on the use of Bottom Hole Temperatures (BHT). Aiming to create a more accurate temperature to depth geothermal map of North America, 5800 new heat flow points were recorded and introduced to the map created in 2004 using only 323 points. Using this method, more data could be used for the prediction of the temperature of the ground where no data were available. Sares *et al.* (2009) compiled

existing geothermal data with oil and gas data and data from new geothermal points to produce new maps of heat flow and geothermal gradient for Colorado. Similarly, Richards *et al.* (2009) used oil and gas wells to collect ground temperatures and in combination with existing data from research covering the period 1970 to 1990 for Texas, developed a series of temperature maps at depths ranging from 2134 m to 4267 m for Texas.

Moeck *et al.* (2010) presented a 3D geological model developed primarily from a detailed geological map for west-central Nevada. The information used was based on surface data instead of subsurface data collected from wells or seismic data as most 3D models do. This technique, called 3D geological mapping, involves the digitisation of a geological map and selected cross-sections that are correlated.

Yousefi *et al.* (2010) presented the geothermal resources map for Iran showing the 18 most promising geothermal areas in the country. A combination of geological, geochemical and geophysical datasets were used and the Geographic Information System (GIS) based map showed that 8.8% (144,815km^2) of Iran can be defined as having geothermal potential. Similar studies were performed for Algeria, Kedaid (2007) and for Turkey, Kaftan *et al.* (2011).

It should be noted that in most of the above studies, specialized software was used for the construction of geothermal resource maps. Only Kaftan *et al.* (2011) used ANNs. They used two different types of ANNs to investigate the applicability and performance of these networks for estimating the structure parameters as location, depth, and density contrasts. The networks were applied first to synthetic gravity data and then real data obtained from the Seferihisar geothermal area in Western Turkey. The results showed that the proposed ANN schemes give similar characteristics and are good candidates for evaluation of structure parameters with one of the models being faster and provides slightly better performance.

Alvarez del Castillo *et al.* (2012) developed an ANN for modelling two-phase flows in geothermal wells. The ANN model was used for the prediction of void fractions under geothermal two-phase flow conditions. The inputs were pressure, wellbore diameter, steam quality, fluid densities and viscosities and other dimensionless numbers. The ANN model was successfully validated by efficiently correlating the input variables to the desired output, using a comprehensive worldwide database with production wellbore data sets.

Bassam *et al.* (2010) used an ANN for the estimation of the static formation temperatures in geothermal wells and Arslan (2011) for the optimization of a Kalina cycle power generation system from medium temperature geothermal resources.

ANNs have also been used in the past for the time series reconstruction of precipitation records with acceptable accuracy (Kalogirou *et al.,* 1997) and in the drawing of isohyets i.e., contour lines of equal rainfall (Kalogirou *et al.,* 1998). In this chapter an ANN was trained to estimate the temperature of the ground at depths of 20, 50 and 100 meters in various locations in Cyprus and to assist in the generation of the geothermal maps (isolines or contours of constant temperature).

5.3 Artificial Neural Network principles

It is estimated that the human brain has around 100 billion interconnected neurons forming networks, known as neural networks. Each neuron processes and transmits information through electrical and chemical signals organised in groups known as subsystems. The main part of typical neuron as shown in Figure 5.1 is formed by a cell body called the soma and in which the cell nucleus is contained, the neuron dendrites and an axon. The axon of each neuron is a special cellular extension of the soma responsible for the transmission of information to other neurons and also carries information back to it. The information is received by the synapses, a special connection that permits a neuron to pass an electrical or chemical signal to another neuron. Dendrites are thin structures that arise from the soma branching multiple times and are able to receive the information from the axon of another neuron via the synapses. The soma of a neuron frequently gives rise to multiple dendrites, but never to more than one axon, although the axon may branch hundreds of times before it terminates. Each neuron is estimated to receive information from as many as 10,000 other neurons.

Artificial Neural Networks aim to simulate some properties of the biological neural networks by trying to solve particular tasks. According to Haykin (1994), a neural network is a massively parallel distributed processor that has a natural propensity for storing experiential knowledge and making it available for use. Interconnected artificial neurons forming a network are transferring information among others. As stated by Kalogirou (2001; 2003), ANN models represent a new method in system prediction because they

operate like a “black box” model requiring no detailed information about the system and have the ability to handle large and complex systems with many interrelated parameters.

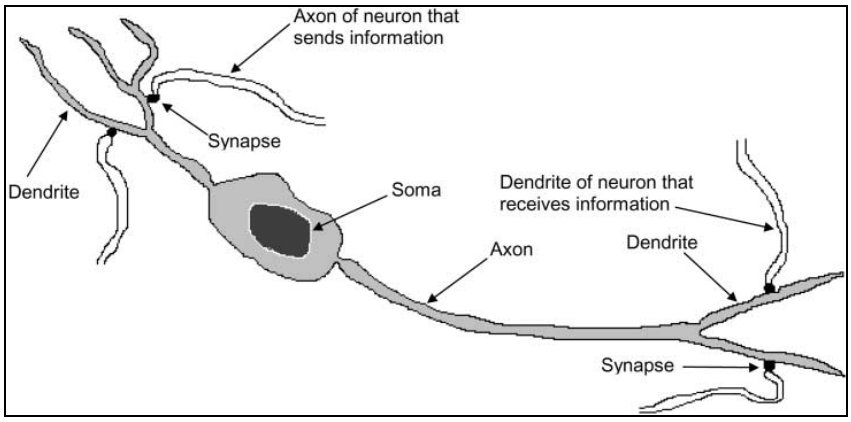

Figure 5.1: A simplified model of a biological neuron, Kalogirou (2001)

ANNs can have many inputs but only one output. In a typical network, there are three layers of neurons, the input, the hidden and the output one. The input layer receives input from the outside world, its neurons transfer the information to the hidden layer or layers and hence the output layer receives the information from the hidden layers and passes its output to the outside world and in some cases back to the preceding layers. In a simple network, connection weights representing the synapses in a biological network help in the connection of each single neuron to other neurons of the previous layer. Knowledge is usually stored as a set of connection weights, Kalogirou (2001; 2002).

Training is the process of modifying the connection weights (controllable parameters in the form of numbers) using a learning method aiming for the desired output. The weights before training contain random information that is turned into meaningful information when training finishes. In order to train a network a specific set of data containing an input, a desired output and a training algorithm is required. Each single neuron, as depicted in Figure 5.2, receives weighted activation from other neurons through its incoming connections and adds them up. The result of the summation is then passed through an activation function representing the output of the neuron. For each of the outgoing connections, this activation value is multiplied by the specific weight and transferred to the next neuron. The output of an ANN is a dependent variable for each corresponding input and is compared to the training pattern, i.e. the desired output. If there is a difference between them, the connection weights are altered aiming to minimise the difference. The network runs repeatedly through all the input patterns until the difference between its

output and the desired output is within the required tolerance. When the training is finished the network holds the weights unchanged and is used for decision taking, pattern identification or for defining associations in new input data sets not used in the training. As stated by Haykin (1994), learning or training is the process by which the free parameters of a neural network are adapted, through a continuing process of simulation by the environment in which the network is embedded. The type of learning is determined by the manner in which the parameter changes take place. Neocleous (1998) also stated that '*learning can be achieved through any change in any characteristic of a network until meaningful results are achieved*'.

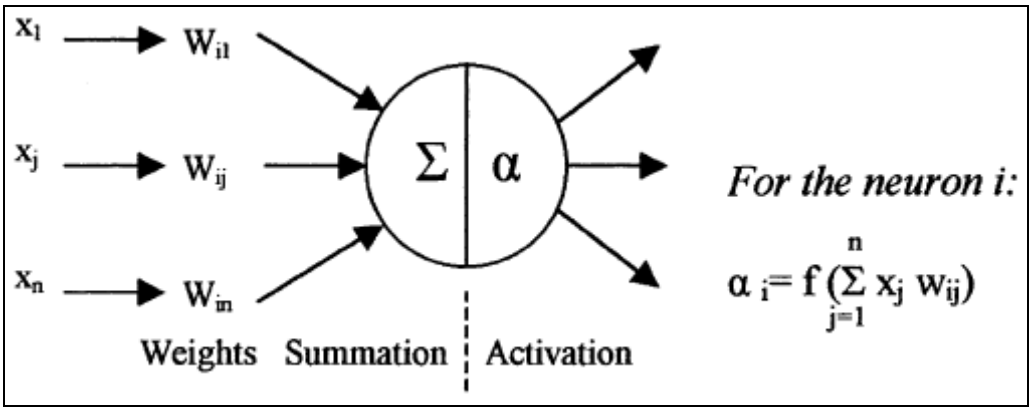

Figure 5.2: Information processing in a single neuron of an ANN, Kalogirou (2001)

Kalogirou (2001), refers to the architecture of ANNs as *'the arrangement of neurons into layers and the connection patterns between layers, activation functions and learning methods'* aiming to the computational transformation of its input into an output. For a successful ANN a good model needs to be build. This requires a clear understanding of the problem and identifying the most important variables in the process that can be used to predict its behaviour. As soon as the model is built based on a predicted output, the model's output is then simulated using different scenarios and the control variables are modified until the desired output is obtained.

5.4 Model selection and archived data used

The archived data of the ground temperature recorded at the boreholes, described in Chapter 4, were used for the training of the selected artificial neural network. The architecture, among those tested, that gave the best results and was adopted for the present work, is shown in Figure 5.3. This architecture has been used in a number of engineering problems for modelling and prediction, with very good results, and it is a feed-forward

architecture composed of five layers, three of which are hidden. There are different activation functions in each layer. Different activation functions were applied to the hidden layers in order to detect different features in a pattern processed through the network. Nine element inputs were used corresponding to the values of the input parameters listed below. The learning procedure was implemented by using the back-propagation algorithm. For the training of the network, a learning rate and a momentum factor needed to be specified by the user. Both of these constant terms were specified at the start of the training cycle and determine the speed and stability of the network. For this purpose, the learning rate was set to a constant value of 0.1 and the momentum factor to 0.3. The weights were initialized to a value of 0.3. For the training of the ANN the back-propagation learning algorithm was used as described by Kalogirou *et al.* (1999) and Kalogirou and Bojic (2000). In the layers below, $\alpha_{(pi)}$ represents the activation for each node and β_i the weighted average obtained by combining all input numerical information from upstream nodes.

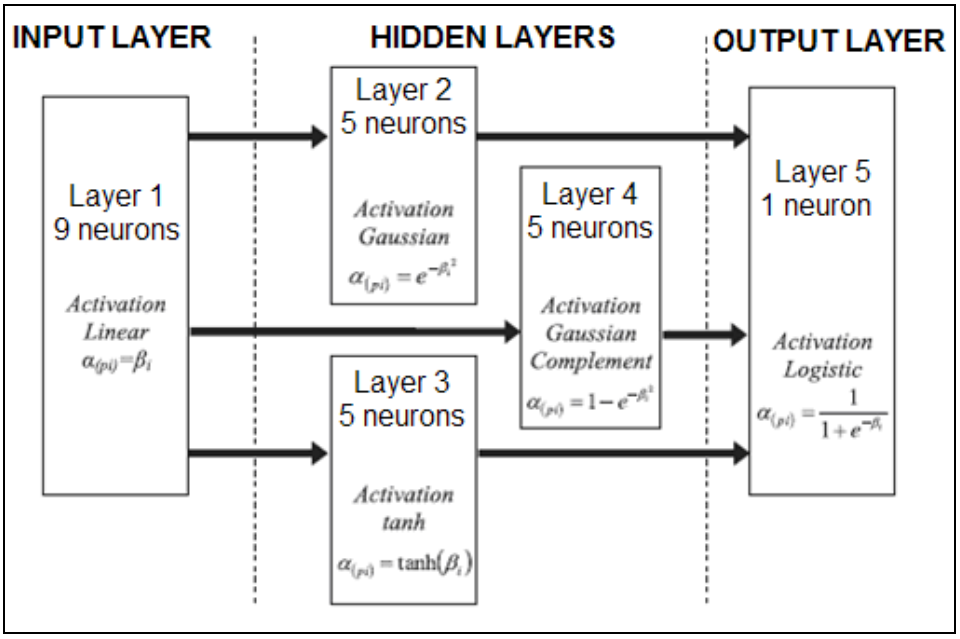

Figure 5.3: Employed neural network architecture

The parameters selected to be used for the training of the network were;

1) The lithology class at the area of each borehole,
2) The borehole elevation,
3) The mean, minimum and maximum ambient air temperature at the location of the borehole,
4) Rainfall at the location of the borehole,
5) The x and y coordinates for each borehole, measured from some reference point,
6) The depth at which temperature is recorded (20, 50 and 100 meters) and
7) The ground temperature at the previous depth.

All these parameters are considered to affect in some respect the temperature of the ground. As described in Chapter 4, the ground temperature is affected by seasonal variations up to a maximum depth of 8 m, therefore, as the depths considered in this work exceed this figure, the ground temperature at those depths is constant year round and depends on the prevailing ambient temperature at the location of the borehole. The parameters were chosen by trial and error giving the best results. The significance and degree to which they affect the thermal conductivity of the ground and hence its thermal diffusivity on the geothermal gradient of a borehole was described in Chapter 3. For this reason, the lithology of the ground in the borehole area, which describes the thermal properties, was used in the training data set. The x and y coordinates of each borehole were measured from some reference point, chosen randomly to be at the left bottom side of the island map, as shown in Figure 5.4.

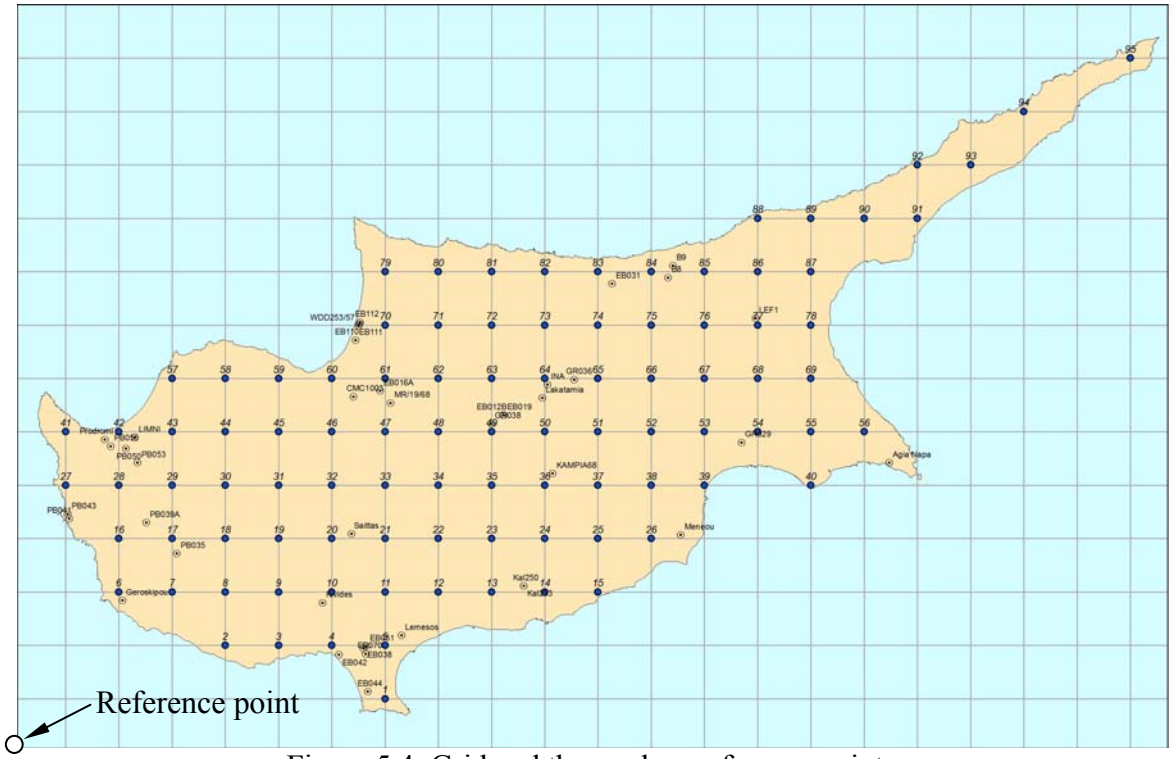

Figure 5.4: Grid and the random reference point

The required data throughout the depth of each borehole were not available for all the 41 boreholes. By eliminating the cases where data were not available 112 patterns were left. From those, 90 patterns were used for the training of the network and 22 (20%) were randomly selected for its validation. A sample of the data used for the training and validation of the ANN is shown in Table 5.1. As can be seen, except from the lithology class, all other data represent real values. The coordinates are distances in meters measured from the reference point. The ambient temperatures and precipitation were obtained from

the Cyprus Meteorological Service. All data were normalized in the range [0-1] before being used in the ANN to increase prediction accuracy.

Table 5.1: Sample of the data used for the training and validation of the ANN

Lith. Class	Elev. m asl	Mean Annual Amb. Temp. °C	Min. Annual Amb. Tem. °C	Max. Annual Amb. Temp. °C	Rainfall mm	East m	North m	Depth m	Ground Temp. °C
14	52	17.88	11.57	25.83	300	193322	71772	20	23.31
16	734	18.43	10.34	28.13	350	151823	106462	20	15.90
16	369	18.36	10.34	28.13	350	152719	108685	20	15.80
8	330	18.25	9.08	27.64	400	120892	80701	20	20.05
…	…	…	…	…	…	…	…	…	…
14	52	17.88	11.57	25.83	300	193322	71772	50	23.32
16	734	18.43	10.34	28.13	350	151823	106462	50	16.50
…	…	…	…	…	…	…	…	…	…
14	52	17.88	11.57	25.83	300	193322	71772	100	23.72
16	734	18.43	10.34	28.13	350	151823	106462	100	17.24
…	…	…	…	…	…	…	…	…	…

For the data used, it should be noted that borehole elevation is the actual elevation above sea level (asl) and is inherently considered by the actual temperatures recorded for each borehole because the borehole is located at the particular elevation. The map of Cyprus used provided topographic contours at steps of 50 m. The borehole elevation was used in an attempt to improve the network mapping and thus be able to predict the unknown cases more accurately. The same applies to the other physical or meteorological parameters used as inputs to the network, like the lithology class of the borehole, the ambient air temperature and the rainfall at the area where the borehole is located.

The lithology class at the grid points was obtained from the corresponding geological map. Since ANNs understand numbers and not text labels, a number is used to identify each lithology class as shown in Table 5.2. As can be seen, a total of 22 different classes were used in this work, which represents the main lithology classes encountered in Cyprus.

After the network was trained and achieved a satisfactory level of performance, it was used to predict the ground temperatures at various depths at a number of points all over Cyprus where recorded data were not available. This was done in order to be able to obtain information for the whole island, which would be able to be used to produce the required maps. For this purpose, a 10x10 km grid was drawn over a detailed topographic map of

Table 5.2: Lithology class employed in this work

Lithology class	Lithology
1	Clay
2	Silts and clays
3	Sand
4	Sands and gravels
5	Gravels
6	Calcarenite
7	Sandstone
8	Sandstones and marls
9	Gypsum
10	Marl over gypsum
11	Marl
12	Chalk and Marl
13	Chalk
14	Limestones and chalks over clay lithologies
15	Limestone over chalk
16	Limestone
17	Basalt
18	Basalt and Diabase
19	Diabase
20	Gabbro
21	Serpentinite
22	Hurzburgite

Cyprus as shown in Figure 5.4 and the lithology class; elevation; mean, minimum and maximum ambient air temperature; rainfall and the x and y coordinates for each borehole, measured from the reference point were recorded. A total of 95 grid points were obtained in this way.

The training was stopped when the average error obtained by comparing the actual and the ANN modelled data remained constant for 100,000 events; i.e. about 890 iterations through all data (epochs) in the training dataset. This was considered a good value enabling the network to learn the input patterns satisfactorily and to give good predictions while avoiding overtraining. The correlation coefficient obtained between the predicted and training data set was 0.9889, which was very close to 1, indicating an accurate mapping of the data. Once a satisfactory degree of input-output mapping was achieved, the network training was frozen and a set of completely unknown test data was applied for verification. The validation of the network was performed by using the "unknown" data for 22 cases. The correlation coefficient for the unknown cases was 0.9253. The prediction error was confined to be lower than 1.74°C, which is considered quite adequate.

Finally, in order to broaden the database, the 22 patterns used for the validation of the technique were embedded into the training data set and a new training of the network was performed. The architecture of the network, the momentum, the learning rate and the initial weight values were the same as in the validation phase. The correlation coefficient for the training dataset was equal to 0.9918, which was again a satisfactory value. An improvement from the previous training value (0.9889) was expected due to the increase in the amount of data used. It was anticipated that the accuracy of prediction would also be increased due to the increased amount of data used to train the ANN. In fact, the mapping of the data was satisfactory and according to the results presented in Table 5.3 which show the prediction accuracy for all 112 data patterns, only four data points were above 5% deviation from the actual measured values. This is related to the correlation coefficient for the training dataset. A closer to 1 correlation coefficient would result in fewer point deviations with the risk the network to be overtrained. The prediction error for all 112 data patterns is shown graphically in Figure 5.5 and is generally considered to be satisfactory.

Table 5.3: Accuracy of ANN data mapping

Accuracy range	Percentage of data in range	Number of data
0-5%	96.4	108
5-10%	1.8	2
10-15%	1.8	2

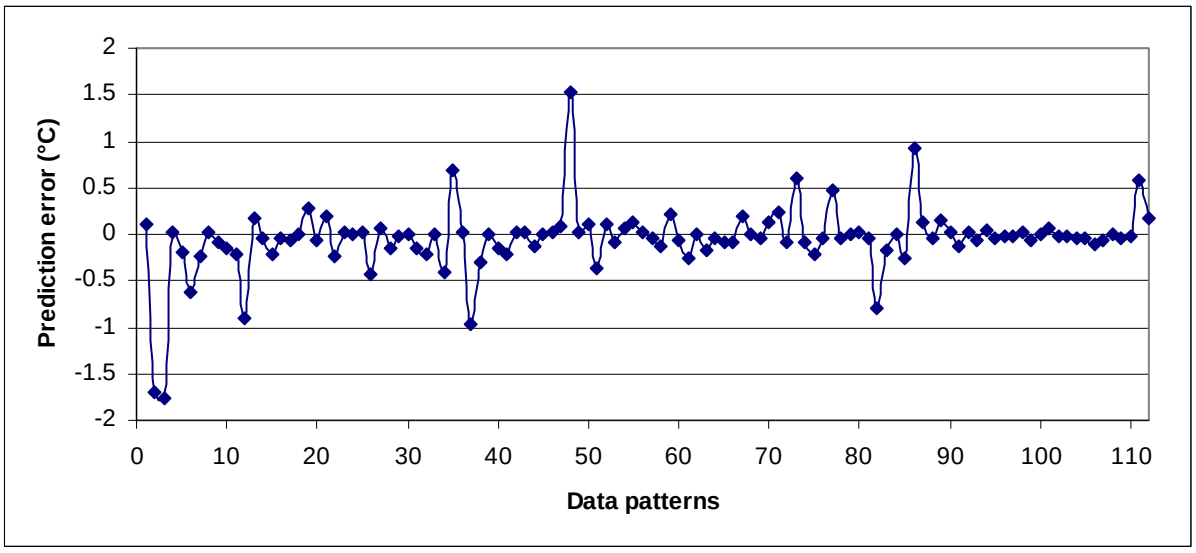

Figure 5.5: Prediction error of the ANN for all 112 data patterns

5.5 Geothermal maps of Cyprus – ground temperatures

As mentioned before, a 10x10 km grid was drawn over a detailed topographic map of Cyprus and the lithology class; elevation; mean, minimum and maximum ambient air temperature; rainfall and the x and y coordinates for each borehole, measured from the reference point were recorded. This information was then supplied to the trained network and by doing so the temperature at the same depths as above was predicted at each grid-point. The x and y coordinates and the estimated temperatures at the three depths for both the original boreholes (41 boreholes) and the grid-points (95 in total), were then used as input to a specialized contour drawing software in order to draw the geothermal maps. The maps were drawn using ArcGIS 3D Analyst software by the Geological Survey Department using the Natural Neighbour algorithm. The maps obtained, one for each depth considered, are shown in Figures 5.6 to 5.8 for the depths of 20, 50 and 100 meters respectively. It should be noted that on these maps, dots which do not fall on the actual grid-points i.e. intersection of the grid lines, represent the actual location of the 41 boreholes.

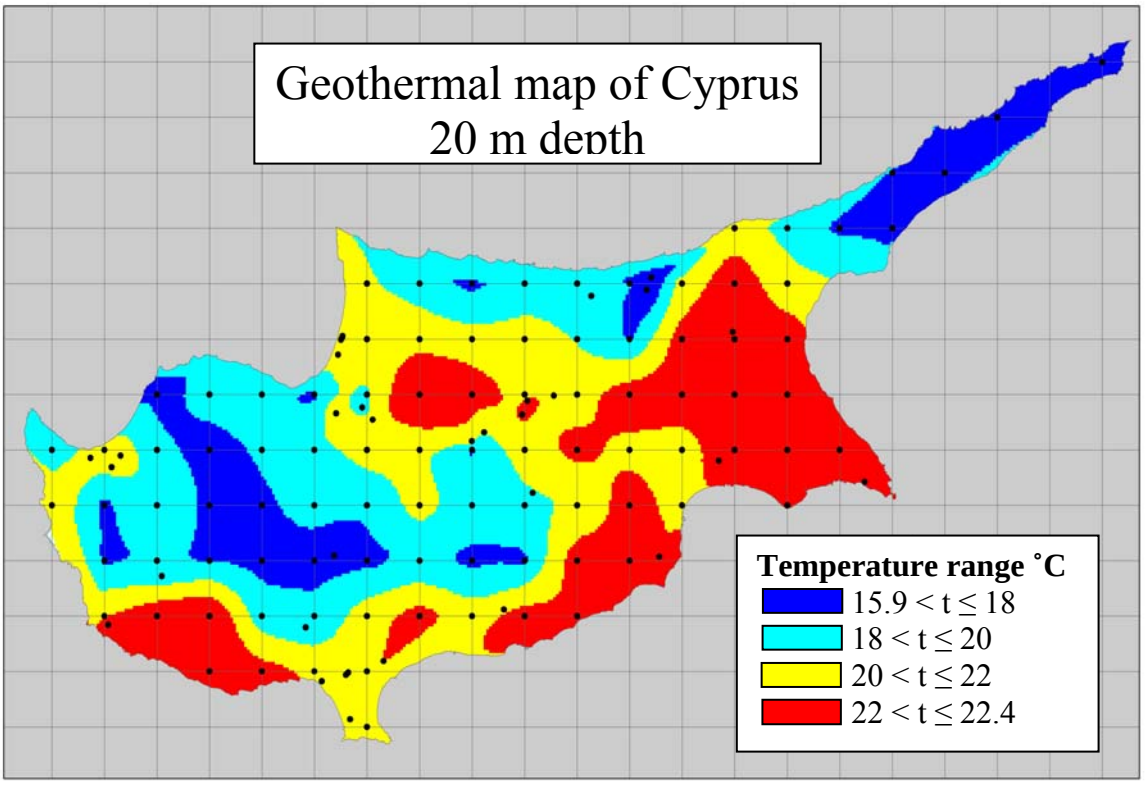

Figure 5.6: Geothermal map for the depth of 20 m

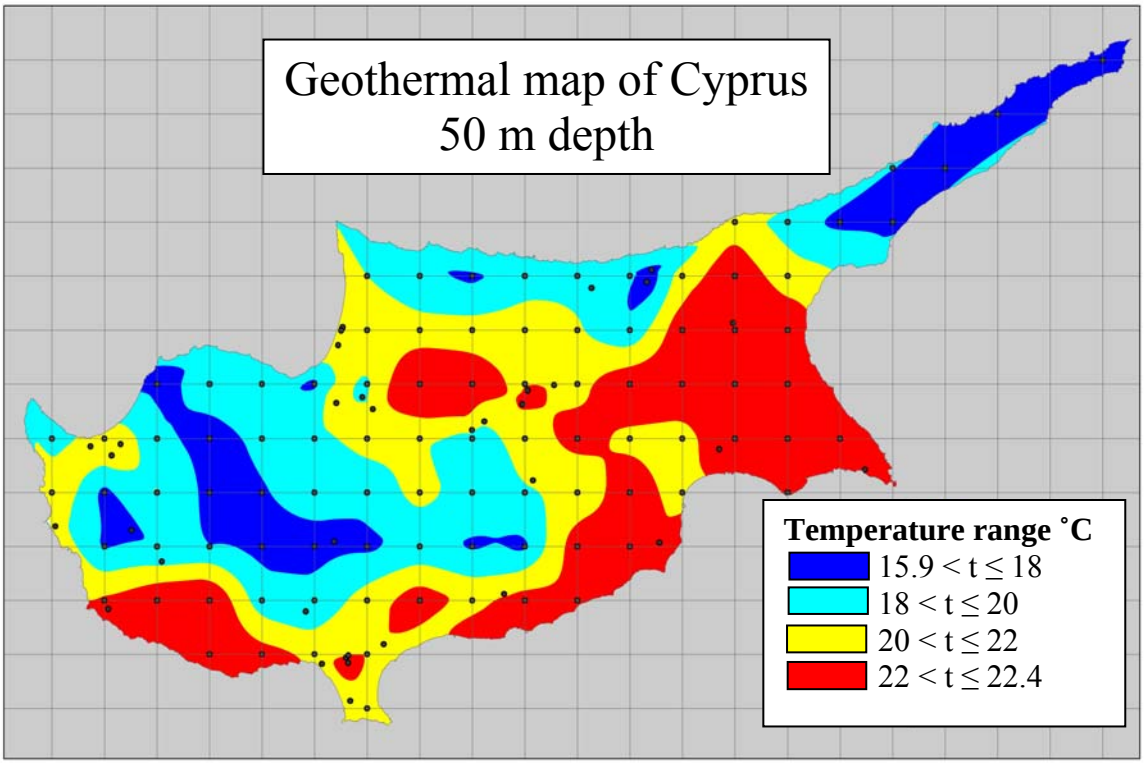

Figure 5.7: Geothermal map for the depth of 50 m

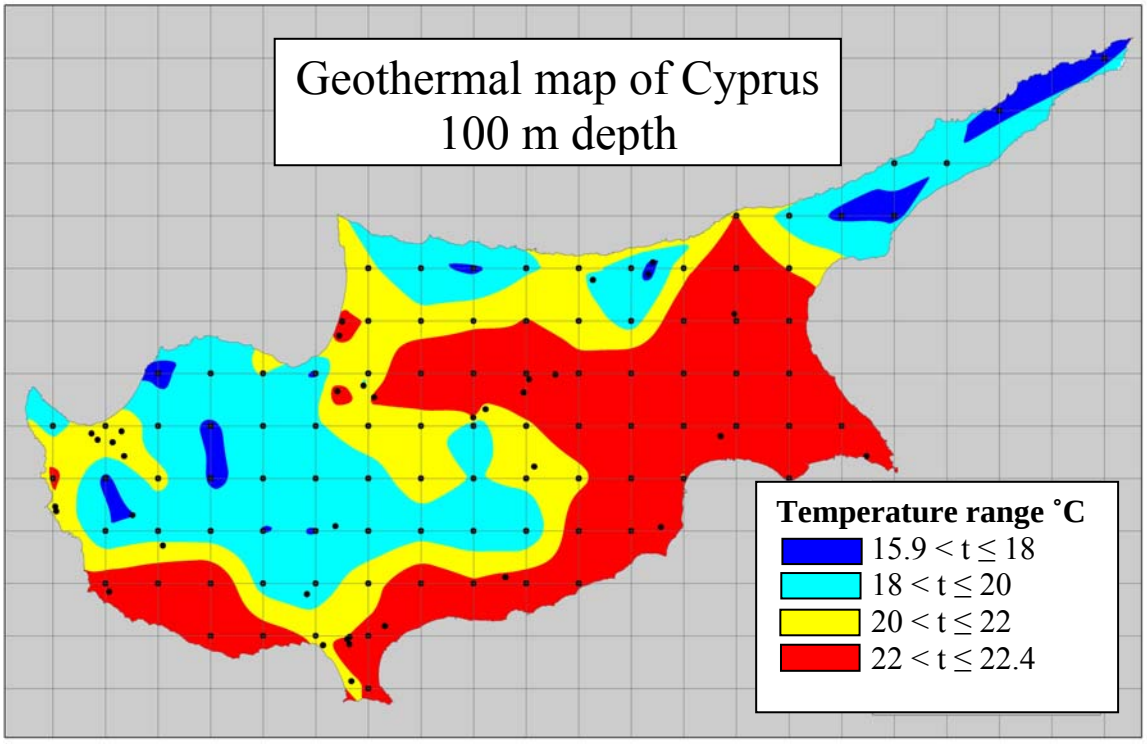

Figure 5.8: Geothermal map for the depth of 100 m

5.6 Summary

In this chapter the use of Artificial Neural Networks for the generation of geothermal maps at different ground depths in Cyprus was examined. Various network architectures were investigated and the one that gave the best results was adopted. This architecture has been used in a number of engineering problems for modelling and prediction, with very good results. Based on the results and the accuracy of the ANN used, it is believed that the proposed method of explicitly involving the lithology class, elevation, ambient temperature and rainfall in drawing geothermal maps, produced valid maps of temperatures at the depths of 20 m, 50 m and 100 m. These maps will be a helpful tool for engineers designing geothermal systems in Cyprus.

The above described procedure can be repeated when new data is available to improve the accuracy of the maps. The more data available (inputs to the ANN) the more accurate the calculations and hence the results (outputs of the ANN) leading to more accurate maps.

Also, for the more accurate evaluation of the potential of a site, additional information on the thermal properties of the ground that influences the specific heat extraction rates would be needed. Thus, thermal conductivity and/or thermal diffusivity maps would be more helpful if could be drawn.

The maps are indicative but offer a good approximation which can safely be used for preliminary design purposes. It was mentioned in Chapter 3 that even if the formation of the ground is identical in several locations, each location is unique and are subjected to its special characteristics.

Chapter 6: Design of GHEs in Cyprus by using a Computational Fluid Dynamics software module

6.1 Introduction

In this chapter the effect of the thermal characteristics of the ground on the sizing of GHEs in Cyprus is investigated. Also, the long term temperature variation of the ground around the boreholes is examined since this affects the positioning of the GHEs.

A main objective of the project is to provide engineers with a useful guide for sizing and positioning GHEs in Cyprus. This is achieved through the investigation of the influence of the temperature, thermal conductivity, specific heat and density of the ground as well as pipe diameter on the performance of GHEs using Computational Fluid Dynamics (CFD) modelling in conjunction with test data. The results are tabulated and can be used as a guide for engineers designing GHEs.

6.2 Model analysis

As discussed in Chapter 2, a vertical GHE mainly consists of a descending and an ascending leg of polyethylene pipe connected at their ends with a U-joint. Usually a borehole with a diameter of 0.1 m - 0.2 m and a depth of 100 m is drilled in the ground, the heat exchanger is placed in position and the borehole is filled with thermally enhanced bentonitic clay or silica sand. The result is a good contact between the pipe and the ground and therefore the heat transfer fluid, usually water, circulating in the pipes can be cooled or heated depending on its temperature relative to the adjacent ground.

Over the years various analytical, numerical and hybrid models have been developed and used to estimate the heat transfer in and around boreholes and calculate the required borehole depth by predicting the short and long term performance of GHEs. Classic analytical solutions used for dimensioning vertical ground heat exchangers include the line and the cylindrical source models which have been presented by Ingersoll and Plass (1948), Blackwell (1954), Carslaw and Jaeger (1959), Deerman and Kavanaugh (1991), Kavanaugh and Raffety (1997) and many others as described in more detail in Chapter 3.

Eskilson and Claesson (1998), Muraya (1994), Zeng *et al.* (2003), Michopoulos and Kyriakis (2009) and Lee (2011) amongst others, presented related numerical models based on finite difference, finite volume and finite element methods. Numerical models give accurate solutions and are good for theoretical analysis but have limited flexibility and need extensive computational time. Depending on the complexity of the model the running time may vary from several hours to many days. Numerical models, therefore, are difficult to be incorporated into building simulation programs at present.

Analytical models, although less precise than numerical models due to the modelling assumptions made when deriving the analytical solutions for GHEs, are preferred in most practical applications because of their superior computational time and flexibility for parameterized design. The need to combine precision with computational speed has given rise to the so called hybrid models that can provide a feasible alternative as described by Eskilson (1987), Yavuzturk (1999) and Yavuzturk *et al.* (1999). Such models are used to calculate special temperature response functions numerically. These response functions can then be incorporated into the building simulation software as databases and hence can be used without the inherent disadvantages of numerical models.

There are short and long term responses of GHE which are determined using different approaches and simplifications. When determining the long term responses of a GHE, the geometry of the borehole is modelled either as a line or as a cylindrical source with finite or infinite lengths, therefore neglecting the borehole thermal details. Eskilson's (1987) g-function approach is considered as the state of the art in this field. Short term response functions on the other hand, retain the actual geometry of the borehole but an equivalent diameter is used for simplifications instead of considering a U-tube with two legs. The short term g-functions developed by Yavuzturk *et al.* (1999) are regarded as the state of the art in determining the short term response of GHEs. Both long and short term response g-functions have been implemented in various building simulation and ground loop design software including TRANSYS, Energy Plus and GLEHEPRO as reported by Javed *et al.* (2009).

Yang *et al.* (2010) summarized in detail the most typical models of the vertical ground heat exchangers currently available, including the heat transfer processes outside and inside the boreholes.

Comparisons between numerical, analytical and hybrid modelling have been almost exhaustively made by numerous studies. Some indicative cases were described by Cui *et al.* (2008) and Bauer *et al.* (2011). Cui *et al.* (2008) used a numerical model in cylindrical coordinates for the simulation of the GHEs in alternative operation modes over a short time period for GCHP applications. Comparisons made between their numerical models with analytical results show that the finite line source model is not capable of modelling the GHEs within a time period of few hours.

Schiavi (2009) analyzed simulated Thermal Response Test (TRT) data in order to evaluate the ability of a three-dimensional model in determining the soil thermal conductivity and borehole thermal resistance. These values are necessary for the design of the storage capacity of the geothermal energy system. The finite element method within the Comsol Multiphysics environment was adopted. The simulated area covered only half of the symmetrical area of the system, the area was considered practically infinite in the radial direction in order to respect the Line Source Condition, while in the axial direction it was limited by two adiabatic surfaces placed at the soil surface and at the simulated depth of the heat exchanger. The analysis confirmed that the Line Source Model applied to the TRT represents a sufficiently accurate approach in the modelling of the U-tube configuration.

Kim *et al.* (2010) developed a numerical model for the simulation of temperature changes in a borehole heat exchanger (BHE). The model calculated the thermal power transferred from heat pumps to BHEs while considering the nonlinear relationship between the temperature of the circulating fluid and the thermal power. To simulate the vertical closed loop GCHP system, three modules were added to the 3D numerical simulator TOUGHREACT. The modules calculated the heat transfer between the U-tube and the circulating fluid, the circulation of the fluid in the BHE and the rate of energy transfer from a heat pump to a BHE. The developed model was validated by comparison with two experimental datasets and was used for the BHE design of an actual system that was numerically evaluated with respect to the temperatures of the circulating fluid at the BHE inlet and outlet, the heat pump efficiency and the heating power and electric power of heat pumps for different combinations.

Eslami-nejad and Bernier (2011) presented an analytical model to predict steady state heat transfer in double U-tube boreholes with two independent circuits operating with unequal mass flow rates and inlet temperatures. For the modelling it was assumed that: i) the heat capacities of the grout and pipe inside the borehole were negligible, ii) the ground and the grout were homogeneous, iii) their thermal properties were constant, iv) the borehole wall temperature was uniform over the borehole depth, v) heat conduction in the axial direction was negligible and vi) the combined fluid convective resistance and pipe wall thickness conduction resistances were assumed to be equal in both circuits. This two-region model was validated experimentally and was found to be in very good agreement with experimental data in the steady state regime. The proposed model was then used to study a double U-tube borehole configuration with one circuit linked to a GCHP operating in the heating mode and the other to thermal solar collectors.

With the increase of computer power a number of software packages are capable nowadays of handling the finite element method and simultaneously provide solutions to the arising partial differential equations for a massive cell number. Depending also on the software package, a number of modules are build-in in order to handle various forms of heat transfer at the boundaries, facilitating the formulation of the problem.

A number of design tools for the design of GHEs have been developed in the last decade and are available either for free or to buy. Right-Loop is a module for sizing geothermal systems for residential applications, Wrightsoft Corporation. Similarly, GLHEPRO can be used for the design of GHEs mainly for commercial applications, GLHEPRO 4.0 Users' Guide, (2007). Based on Eskilson's methodology, Eskilson (1987), it can predict the temperature response of the GHE to monthly heating and cooling loads and peak demands over a number of years by automatically adjusting the GHE size on user's specified GCHP entering fluid temperatures. Several other software are available that not only can provide engineers with an easy and quick way to design GHEs, but also give them the opportunity to perform economic analyses and do comparisons between other technologies.

Amongst these software is GLD, the one selected for use in this study. GLD Premier 2012 Edition is a "Geothermal Design Studio" modular program that provides the user with flexibility in the design process and customization based on designer preferences, The Ground Loop DesignTM Premier 2012 Edition User's Manual, (2012). Two

separate theoretical models, the cylindrical source model and the line source theory model are included within the GLD framework. The cylindrical source model allows for quick length or temperature calculations based on limited data input while the line source theory that is more popular throughout Europe, is more detailed and generates monthly and/or hourly temperature profiles over time, given monthly loads and peak data and/or hourly loads data. It is also able to model the impact of balanced and unbalanced loads on loopfield performance and length requirements. Users also have the option to directly compare the results of the two models using an identical input data set. Although the outputs of the two models do not always agree, they do give the designer more information on which to base a final system design.

GLD can also calculate the evolution of the borehole wall temperature over time when heat at a constant rate is extracted from the borehole. Using a dimensionless G-function, it models the temperature variations taking into account the ratio of the borehole radius and length and the physical layout of the bore field. GLD also employs its own internal borehole superposition model, allowing users to draw their own grid in the GridBuilder and then automatically determine the required G-function.

GLD was chosen for this study because it allows users to do more 'what if' modelling and perform multiple design simulations to optimize geothermal systems. It can also be easily integrated with other commercial software programmes like AutoCAD, Carrier HAP, etc allowing data to be easily imported or exported. Finally, it enables designers to compare different types of systems such as vertical and horizontal GHEs.

6.3 Ground Heat Exchanger design

In order to provide engineers with a useful guide for sizing and positioning GHEs in Cyprus, the heating and cooling load of a typical house, along with the thermal characteristics of the ground in the 8 selected locations were used as input data in the GLD computational fluid dynamics software. As mentioned in the GLD's User Manual (2012), although GLD utilizes the best theoretical models available today, because the calculations involve a large number of input parameters, the most accurate results will naturally arise from the most accurate input parameters. Figure 6.1 shows the number of parameters affecting the design of geothermal systems.

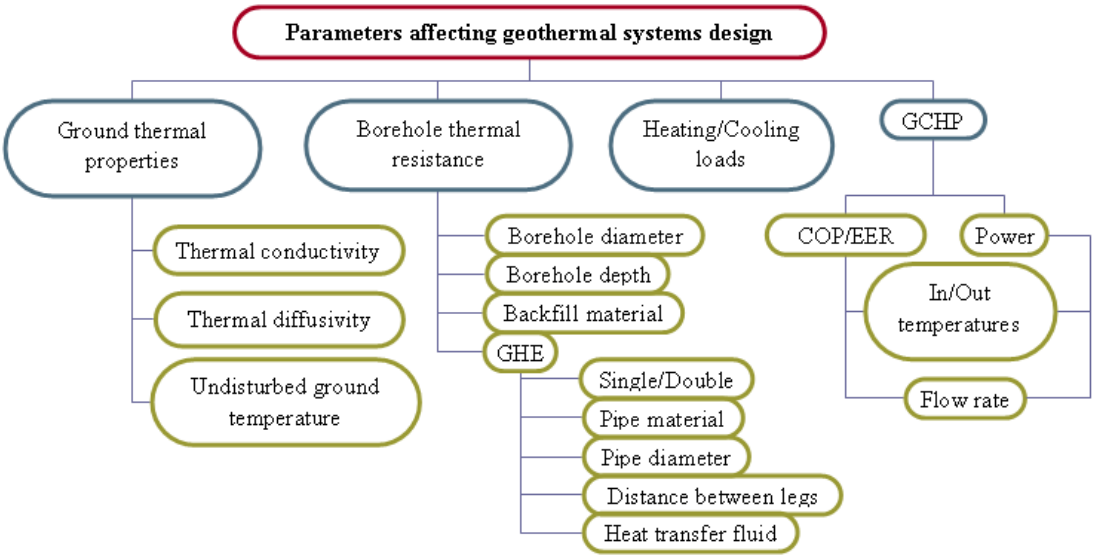

Figure 6.1: Parameters affecting geothermal systems design

The thermal data presented in Tables 3.8 and 3.9 and Appendix 2 of the thesis for the 8 representative locations in Cyprus were used in the simulations. These are considered accurate enough to give reliable results. Amongst the most important factors required as inputs are the thermal conductivity and thermal diffusivity of the lithologies forming each borehole. Although GLD suggests typical values of thermal conductivity and diffusivity for different types of rocks and soil, it strongly recommends that soil tests should be performed to obtain these values. This is due to the fact that thermal conductivity in particular has a large effect on the calculated bore length. Also, it is recommended to perform thermal conductivity tests especially for commercial projects since non-published empirical studies showed that different values arise from weighted average calculations and empirically-derived thermal conductivity results.

The layer calculator in GLD allows designers to use data from a drilling log to produce a quick weighted-average calculation for thermal conductivity, thermal diffusivity and borehole thermal resistance. The line source model technique is used for the calculations. The thickness of each type of soil forming the borehole is required along with the thermal conductivity and diffusivity as shown in Figure 6.2. The undisturbed ground temperature is also an input requirement and it refers to the temperature of the ground in the deep zone, where seasonal effects are negligible.

For the calculation of the borehole thermal resistance some more information is required such as the GHE pipe type and diameter. Hence, the designer needs to select between a

single or double u-tube GHE in each of the boreholes and then the distance between the legs. Having selected the above, as well as the borehole diameter and the thermal conductivity of the backfill material, GLD calculates the thermal resistance of the borehole. The layer calculator and the information required are shown in Figure 6.2.

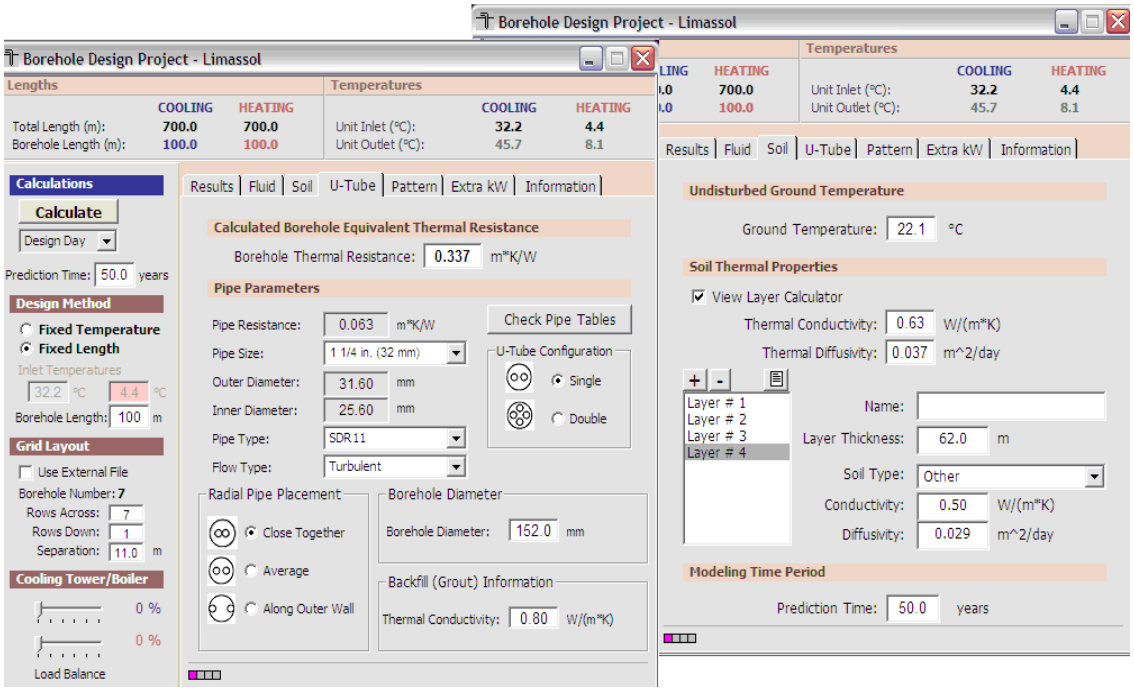

Figure 6.2: Borehole Design Module, Soil Thermal Properties and Borehole Equivalent Thermal Resistance calculator

Table 6.1 shows the average thermal conductivity and thermal diffusivity of the ground in each borehole location in Cyprus in relation to the depth and the undisturbed ground temperature as calculated by GLD. The ground thermal properties of the various types of soil used in the calculations are those measured by Isomet 2104 heat transfer analyzer and presented in Table 3.8 in chapter 3. It was assumed that in the boreholes, a 32 mm single U-tube GHE was installed and that its pipes were close together in the middle of the borehole. The thermal conductivity of the backfill material (bentonitic clay) was 0.8 W/mK. In Saittas and Limassol where the borehole diameter was 0.15 m, the borehole thermal resistance was calculated by GLD to be 0.337 mK/W while in the rest of the locations where the borehole diameter was 0.2 m, the borehole thermal resistance was calculated to be 0.418 mK/W. According to the calculated values of the average thermal conductivity of the ground and borehole thermal resistance in each location, the thermal conductivity of the borehole was estimated.

Table 6.1: Thermal properties of the boreholes in each location as calculated by GLD

Location	Borehole depth (m)	Undisturbed ground Temp. (˚C)	Ground thermal conductivity (W/mK)	Ground thermal diffusivity (m^2/day)
Agia Napa	100	23.4	0.97	0.056
Meneou	97	22.6	0.92	0.048
Geroskipou	100	22.4	1.1	0.057
Prodromi	100	21.3	1.32	0.073
Lakatamia	100	22.7	0.56	0.032
	160		0.73	0.047
Kivides	100	18.7	0.58	0.036
	196		0.58	0.036
Limassol	100	22.1	0.63	0.037
	120		0.61	0.036
Saittas	100	18.3	1.4	0.074
	178		1.42	0.076

According to the calculations, Lakatamia and Kivides are the locations that have the lower borehole thermal conductivity while Saittas has the highest. This is due to the fact that the thermal conductivity of the soil forming the ground is low in the first case and high in the latter.

It is also important to mention that the thermal conductivity of the ground in Lakatamia region is increased significantly with depth, from 0.56 W/mK for a100 m borehole to 0.73 W/mK for a 160 m borehole. This is due to the fact that the structure of the ground below 100 m depth changes (see Figure 3.7) and that the saturation level increases due to the presence of flowing water. The above combination results in the increase of the thermal conductivity of the borehole.

The thermal conductivity of the bentonitic clay used as backfill material was lower than some of the soils or rocks forming the boreholes. In such a case, the bentonitic clay acts as an insulator rather than a conductive material affecting the heat exchange process. Although the soil taken out of the borehole during drilling is preferred to be used as

backfill material, this is not always feasible as discontinuities in filling and flowing water may impact negatively on the integrity of the borehole. Bentonitic clay has the ability to expand and completely fill the borehole and hold firmly the GHE in place.

In the Borehole design module, designers have the option to decide if the design is to be based on a fixed borehole length or a fixed heat carrier fluid temperature. In the fixed temperature mode, the required length of the bores is calculated based on the desired temperatures of the heat carrier fluid. In the fixed length mode, the inlet temperature to the GHE is calculated when the length of the GHEs is preset. In both cases, GLD needs as input the borehole grid to be used.

The positioning of the boreholes forming the grid to satisfy a typical house load is very important taking into account the common way houses are built in Cyprus. Most are semi-detached, two houses built in the same plot and attached to each other on one side, Figure 6(c), or are linked-detached, with a short distance between them, Figure 6(b). In both cases, the only available space for drilling boreholes is a 3-4 m region at the edge of the plot. Rarely, houses are detached (Figure 6.3(a)) having enough land space free for drilling as many boreholes as needed and positioning them without any limitation.

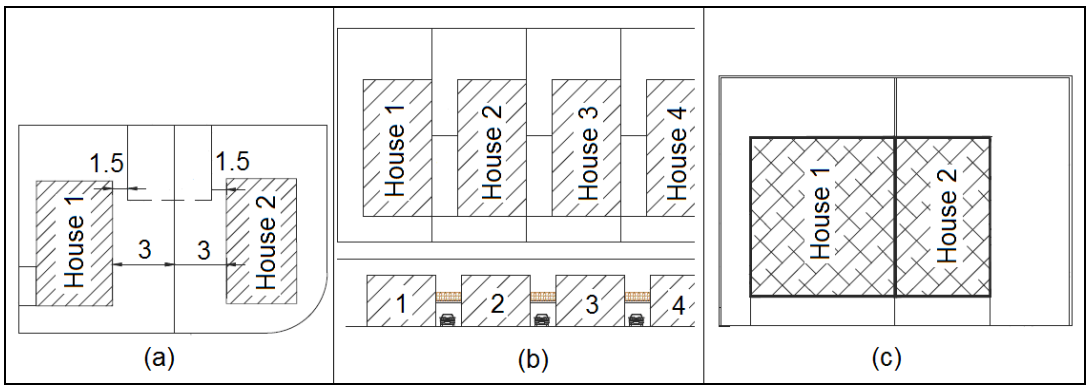

Fifure 6.3: Typical positioning of houses in plots, (a) detached, (b) linked detached (c) semi-detached, (http://www.moi.gov.cy).

For design purposes, the heating and cooling load of a typical house is needed. As shown in Figure 6.4, the selected typical house is a three bedroom, two storey house of a total useful floor area of 190.07 m². In one side, the house is attached to another house, and there is available land space of at least 4 m in the other three sides. The house is made of reinforced concrete pillars and beams while the walls are made of red and sandy clay bricks. All parts of the house were thermally insulated as stated by the law. Extruded

polystyrene was used for the thermal insulation while double glazed aluminium framed windows were used. The U values of the elements of the house are tabulated in Table 6.2.

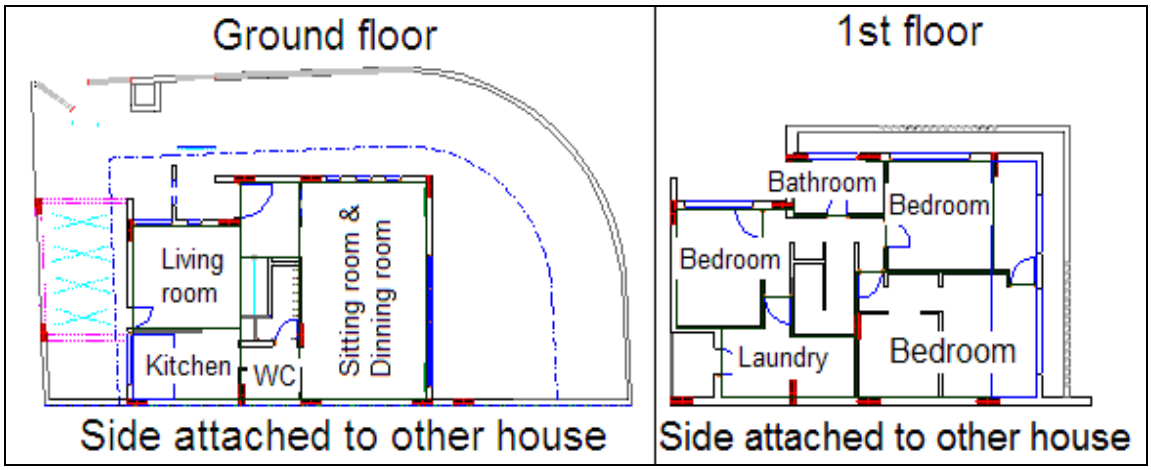

Figure 6.4: Plan views of the typical house used in the calculations

Table 6.2: U-values of the elements of the house

Name of the elements of the house	**Element description**	**U-value (W/m^2K)**	**Thermal capacitance (kJ/m^2K)**
External wall	10 cm brick 3 cm extruded polystyrene 10 cm brick	0.581	119
External beams & pillars	20 cm reinforced concrete 3 cm extruded polystyrene	0.765	224
Exposed roof	15 cm reinforced concrete 5 cm concrete 5 cm extruded polystyrene 5 cm loose lightweight rock	0.424	236
Floor in contact with ground	15 cm reinforced concrete 10 cm lightweight concrete 3 cm extruded polystyrene 3 cm granite ceramic	0.421	200
Exposed floor	15 cm reinforced concrete 10 cm lightweight concrete 3 cm extruded polystyrene 3 cm granite ceramic	0.546	132
External door	5 cm Massif wood	2.29	14
Openings: frame ≤ 25% opening area	Aluminium frame 4 mm glass 12 mm air gap 4 mm glass	2.6	N/A
Openings: frame > 25% opening area		3.2	

The possible available grids, their performance and the long term temperature variation of the ground in the 8 selected locations are examined based on the loads of the typical house as calculated according to the weather conditions of Limassol. In the absence of any regulations in Cyprus related to the calculation of the energy use in buildings for

heating, cooling and the design of their mechanical services, the Methodology for Assessing the Energy Performance of Buildings (MAEPB) in Cyprus is considered as the most appropriate guide to be used for the estimation of the heating and cooling loads of the house.

According to the legislation in Cyprus, since 1st of January 2010, all new buildings and all existing buildings of useful floor area over 1000m² that undergo major renovation should amongst others, have a certificate for their energy performance. For issuing certificates the Energy Service of the Ministry of Energy, Commerce, Industry and Tourism of Cyprus developed the MAEPB and a calculation tool.

The main characteristic of MAEPB is that it is used for comparison rather than absolute calculation to encourage consistency between repeated evaluations. The comparison is done between the characteristics of the actual building in consideration and the ideal characteristics of a reference building. The formulation used for the calculation of the heating and cooling loads of a building is based on monthly loads and monthly average ambient temperature, solar radiation, wind speed, etc. Despite the fact that MAEPB is not recommended for design purposes, its outputs are within 5-10% of those from professional design software.

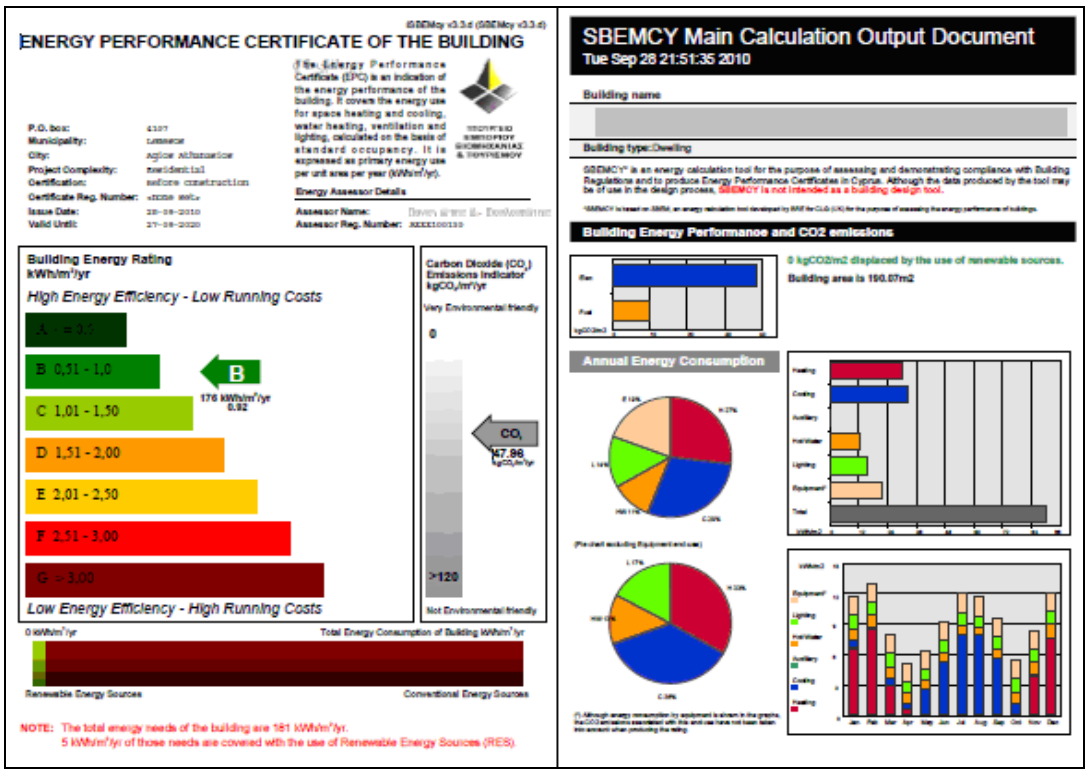

Figure 6.5: The Energy Performance Certificate and the main calculations output of the typical house in Limassol

For GLD, monthly or hourly load data are necessary for the calculation of monthly or hourly inlet temperatures for the ground heat exchangers and evaluate heat pump performance. For the house under consideration, the monthly load data obtained from the Interface for Simplified Building Energy Model for Cyprus (iSBEM-CY) and shown in Table 6.3 were imported into the month-by-month load screen of GLD. According to the calculations a cooling load appears also in the winter because of the increase of the desired temperature in the house due to solar radiation and internal loads. In practice, those loads are considered of no consequence especially in January, February, November and December and for this reason are not considered in the monthly loads in GLD. For comparing the performance of the GHEs in the different locations without being affected by the load variations due to weather conditions, the same load data were assumed in all locations.

Table 6.3: Heating and cooling loads of the typical house used in the calculations

Month	Cooling load (kWh)	Cooling peak load (kW)	Heating load (kWh)	Heating peak Load (kW)
January	~~157.89~~	~~0.2~~	1252.58	13.52
February	~~14.52~~	~~0.02~~	1622.21	15.87
March	137.43	0.185	555.19	12.54
April	99.32	0.138	108.57	11.33
May	482.86	4.67	0.00	0.00
June	1003.00	11.38	0.00	0.00
July	1508.43	14.83	0.00	0.00
August	1483.09	16.18	0.00	0.00
September	1048.94	11.07	0.00	0.00
October	214.93	0.29	12.18	8.46
November	~~35.44~~	~~0.05~~	731.30	12.24
December	~~9.24~~	~~0.01~~	1430.17	14.73

In order to proceed with the calculations, a GCHP (ground coupled heat pump) should be selected. The GCHP will be coupled to the GHEs and the characteristics of the boreholes and heat pump performance will determine the desired number of GHEs required for the application. The selection of the heat pump was made based on the characteristics of the TRTs in each location investigated. As shown in Table 3.9 in Chapter 3, the temperature of the water exiting the GHE did not exceeded 38.4 ˚C in the case of Lakatamia for a single U-tube GHE and 36.6 ˚C in the case of Agia Napa for a double U-tube GHE. The GCHP to be selected should have similar inlet temperatures in order to perform efficiently. Table 6.4(a) shows the Capacity and Power of the selected GCHP in kW based on the entering

water temperature at a certain flow rate. The water flow rate in the GHEs during the TRTs was between 10.5 – 12 L/min. Therefore, in a geothermal system of about 5 to 7 GHEs the nominal system flow should to be between 52.5 – 84 L/min. Table 6.4(b), tabulates the factors affecting the capacity and power required by the GCHP when the water temperature entering the unit deviates from the design value. Similarly, Table 6.4(c) shows the factors affecting the capacity and power required by the GCHP when the system flow rate deviates from the nominal one which is 43.5 L/min. The above factors are given by the GCHP manufacturers, (more details are given in Appendix 3).

Table 6.4(a): Heat Pump Specification

Flow rate (L/min)	Cooling mode			Heating mode		
	Entering Water Temp. (˚C)	Capacity (kW)	Power input (kW)	Entering Water Temp. (˚C)	Capacity (kW)	Power input (kW)
30.3	21.1	18.2	3.17	-1.1	12.6	4.23
	32.2	16.5	4.04	10	15.8	4.3
	43.3	14.8	4.91	21.1	18.9	4.37
56.8	21.1	17.9	2.88	-1.1	13.1	4.27
	32.2	16.6	3.72	10	16.5	4.32
	43.3	15.2	4.57	21.1	19.9	4.38

Table 6.4(b): Heat Pump Temperature corrections

Cooling mode			Heating mode		
Entering Water Temp. (˚C)	Capacity Factor	Power factor	Entering Water Temp. (˚C)	Capacity factor	Power factor
10	0.795	0.975	15.6	1.089	0.591
21.1	1	1	26.7	1.045	0.795
32.2	1.206	1.022	37.8	1	1
			48.9	0.955	1.205

Table 6.4(c): Heat Pump Flow corrections (Nominal flow 43.5 L/min)

Cooling mode			Heating mode		
% of nominal flow	Capacity Factor	Power factor	% of nominal flow	Capacity factor	Power factor
69.6	0.970	0.955	69.6	1.002	1.021
100	1	1	100	1	1
130	1.032	1.003	130	1	0.979

Based on the selected heat pump and its specifications and assuming a system flow rate of 11.4 L/min/3.5 kW of peak cooling load and a 100 m fixed borehole length, the minimum number of boreholes to be drilled in each of the locations in order to satisfy the heating and cooling loads of the house is calculated. The results are tabulated in Table 6.5. Increasing the system flow rate per peak load means that more heat will be injected to or absorbed by the ground, necessitating measures to be taken to increase the borehole's capacity. Such measures can be: greater distance between the boreholes, an increased number of boreholes, deeper boreholes, installing 2 u-tube GHEs in a single borehole, larger pipe diameter or a combination of the above.

Very good agreement was observed between the expected number of boreholes for some of the locations based on the TRT results and the results from the GLD calculations. For example, in Agia Napa, the borehole capacity was calculated from the TRT to be 2.81 kW. In this case, the expected number of boreholes to satisfy the 16.2 kW cooling load of the house under consideration would be 5.7. With GLD model, six boreholes were found to be needed to satisfy the load. In most locations 6 boreholes were found to be needed to satisfy the load. In Lakatamia 7 boreholes were estimated because Lakatamia is the location with the lower ground thermal conductivity and diffusivity. Although Kivides have also a low borehole thermal conductivity, 6 boreholes are sufficient because the undisturbed ground temperature is lower, 18.7 ˚C compared to 22.7 ˚C for Lakatamia. In Saittas, the location with the most conductive and diffusive ground and the one with the lower undisturbed ground temperature than the rest of the locations, only 4 boreholes were estimated to satisfy calculated loads. Similar is the case in Prodromi but since the undisturbed ground temperature is slightly higher than Saittas, 21.3˚C instead of 18.3 ˚C, the boreholes determined were increased to 5.

Table 6.5 also show that the increase in the temperature over a 50 year period is low, the maximum being 1.4 ˚C in Kivides when the distance between the boreholes is 3 m. As the distance between the boreholes increases, the estimated ground temperature over the 50 year period decreases reaching 0 ˚C at a distance 10 m to 11 m apart. But when increasing the distance between the boreholes the unit inlet temperature showed a slight decrease of about a 1˚C depending on the location. This resulted in an increase of up to 0.2 units in the system COP in the cooling mode and a decrease of up to 0.1 units in the respective one in the heating mode.

Table 6.5: Calculated number of boreholes required for a single row grid

Location	Total Length (m)	Boreholes	Minimum distance between the boreholes (m)	Estimated ground temp. change over 50 years (˚C)	Cooling mode		Heating mode	
					System COP	Unit inlet/outlet temp. (˚C)	System COP	Unit inlet/outlet temp. (˚C)
Agia Napa	600	6	3	+0.9	4.5	42/47.7	3.7	14.4/11.2
			10	0	4.7	41/46.4	3.6	13.6/10.4
Meneou	600	6	3	+0.8	4.7	41.1/46.5	3.6	13.7/10.5
			10	0	4.9	40.1/45.5	3.6	12.9/9.7
Lakatamia	700	7	3	+1.1	4.6	41.1/46.5	3.7	14.5/11.3
			11	0	4.9	39.8/45.1	3.6	13.5/10.3
Limassol	600	6	3	+1.3	4.6	42.3/47.7	3.6	13.1/9.9
			11	0	4.8	41/46.3	3.5	11.9/8.7
Saittas	400	4	3	+1	5	41.6/46.9	3.3	7.2/4.2
			10	0	5.2	40.5/45.8	3.2	6.3/3.3
Kivides	600	6	3	+1.4	5.2	40/45.2	3.4	9.2/6.1
			11	0	5.5	38.5/43.7	3.3	8.1/5
Geroskipou	600	6	3	+0.8	4.8	39.8/45.2	3.6	13.8/10.6
			10	0	5	39.1/44.4	3.6	13/9.9
Prodromi	500	5	3	+0.7	4.8	41.9/47.3	3.5	10.9/7.8
			10	0	4.9	41.2/46.5	3.4	10.3/7.1

The modelling results also showed that in some cases the distance between the boreholes could be less than 3 m. Although a short distance between boreholes can save space, too short a distance is not desirable as drilling cannot be guaranteed to be entirely vertical. The greater the depth of the borehole, the larger the deviation from vertical could be and if boreholes are too close to each other, the effectiveness of the GHEs will be reduced. Therefore, it is desirable to keep the distance between boreholes as large as practically possible, particularly for deep boreholes. For 100 m deep boreholes and a 3 m distance between them the deviation from vertical should be less than 0.5 degrees.

As mentioned above, the thermal conductivity of the bentonitic clay used as backfill material was lower than most of the soils or rocks forming the boreholes. This results in higher thermal resistance of the borehole when the pipes are placed close together in the middle of the borehole as opposed to the wall of the borehole. The modelling results, shown in Table 6.6, show that for the minimum distance between the boreholes shown in Table 6.5, as the pipes are moved towards the borehole wall the system efficiency increases as expected because of the reduction in the thermal resistance. The change in the unit inlet temperature, reduced in the cooling mode and increased in the heating mode, is the parameter affecting system COP in the degree shown in Tables 6.4(a) to 6.4(c). Also, important is the balance between the heat rejected and absorbed by the GHE and the heat pulse rate since heat could be built up in the area resulting in a ground temperature change over the passing of the years. The movement of the pipes from the centre of the borehole to the borehole wall did not affect the change in the ground temperature over the 50 year period modelled. In all cases improved system efficiency in the cooling and heating mode was observed when the pipes are placed close to the borehole wall and that is the case that it should be preferred.

Fewer boreholes may be used in a system if they are deeper. The deeper the borehole, the longer the GHE resulting in more heat to be injected to or absorbed from the ground. This doesn’t necessarily mean that doubling the depth of a borehole will double the capacity of the borehole as well. The capacity will depend on the thermal properties of the ground in the deeper layers. Table 6.7(a) shows a comparison between the number and depth of boreholes in a particular location when the distance between the boreholes is the minimum possible. The same comparison is shown in Table 6.7(b) but this time the distance between the boreholes is increased so the ground temperature wouldn’t change over a 50 year period.

Table 6.6: Spacing between the legs of the GHE

Location	Total Length (m)	Leg spacing	Cooling mode		Heating mode	
			Unit inlet/outlet temp. (˚C)	System COP	Unit inlet/outlet temp. (˚C)	System COP
Agia Napa	600	CT*	41.9/47.3	4.5	14.4/11.2	3.7
		A*	37.2/42.5	4.9	17/13.7	3.8
		BW*	33.7/39	5.3	18.9/15.6	3.9
Meneou	600	CT*	41.1/46.5	4.7	13.7/10.5	3.6
		A*	36.4/41.7	5.1	16.1/12.9	3.8
		BW*	32.7/38	5.5	18.2/14.9	3.9
Lakatamia	700	CT*	41.1/46.5	4.6	14.5/11.3	3.7
		A*	37/42.3	5	16.6/13.4	3.8
		BW*	33.9/39.2	5.3	18.4/15.1	3.9
Limassol	600	CT*	42.3/47.7	4.6	13.1/9.9	3.6
		A*	39.3/44.6	4.8	14.7/11.4	3.7
		BW*	36.4/41.7	5.1	16.1/12.9	3.8
Saittas	400	CT*	41.6/46.7	5	7.2/4.2	3.3
		A*	36.9/42.1	5.7	9.3/6.2	3.4
		BW*	32.8/37.9	6.1	11.4/8.2	3.5
Kivides	600	CT*	40/45.2	5.2	9.4/6.3	3.4
		A*	35.2/40.4	5.7	11.5/8.4	3.5
		BW*	31.8/36.9	6.1	13.6/10.4	3.6
Geroskipou	600	CT*	39.8/45.2	4.8	13.8/10.6	3.6
		A*	35.2/40.5	5.3	16.2/13	3.8
		BW*	31.8/37	5.6	18.2/14.9	3.9
Prodromi	500	CT*	41.9/47.3	4.8	10.9/7.8	3.5
		A*	36.5/41.8	5.3	13.8/10.6	3.6
		BW*	32.3/37.5	5.7	18/15.9	3.8

Table 6.7(a): Comparison of borehole capacity in relation to their depth for the minimum distance between the boreholes

Location	Borehole length (m)	Boreholes	Total Length (m)	Minimum distance between the boreholes (m)	Ground temp. change over 50 years (˚C)	System COP Cooling	System COP Heating
Lakatamia	100	7	700	3	+1.1	4.6	3.6
	160	4	640	3	+1	4.6	3.6
Limassol	100	6	600	3	+1.3	4.6	3.6
	120	5	600	3	+1.3	4.6	3.6
Saittas	100	4	400	3	+1	5	3.3
	178	3	534	3	+0.6	6	3.4
Kivides	100	6	600	3	+1.4	5.2	3.4
	196	3	588	3	+1.2	5.2	3.4

In Kivides by almost doubling the borehole length (from 100 m to 196 m), half boreholes were calculated to be needed to satisfy the specific cooling and heating loads, resulting also in the reduction of the total length of the GHEs by 12 m. No change in the system COP was observed. Similarly, in Lakatamia, the system COP and the ground temperature change over a 50 year period were not affected even if the borehole depth increased 1.6 times (from 100 m to 160 m), the number of boreholes reduced from 7 to 4 and the total length of GHEs reduced by 60 m. Although the case in Saittas was similar to the one in Kivides, the GHE length increased from 100 m to 178 m, the number of boreholes estimated could only be limited to 3 increasing the total GHE length by 134 m. The result was the increase of the COP in the cooling mode from 5 to 6 and in the heating mode from 3.3 to 3.4. The thermal properties of the ground deeper than 100 m is the main factor affecting. The more improved is the average thermal conductivity and diffusivity of the ground around the borehole the less total length of GHE is required resulting in less boreholes needed as in the cases of Kivides and Lakatamia. In the case of Limassol, although the increase in the depth of the borehole was only 20 m the number of boreholes was reduced by 1 keeping the total GHE length needed unchanged. This is because the

average thermal conductivity and diffusivity of the ground around the borehole remained unchanged.

Table 6.7(b): Comparison of borehole capacity in relation to their depth without affecting the ground temperature over a 50 year period

Location	Borehole length (m)	Boreholes	Total Length (m)	Distance between the boreholes (m)	System COP Cooling	System COP Heating
Lakatamia	100	7	700	11	4.9	3.6
	160	4	640	10	4.8	3.6
Limassol	100	6	600	11	4.8	3.5
	120	5	600	11	4.8	3.5
Saittas	100	4	400	10	5.2	3.2
	178	3	534	8	6.1	3.4
Kivides	100	6	600	11	5.5	3.3
	196	3	588	10	5.4	3.3

Aiming to keep the temperature of the ground unaffected over a 50 year period a comparison is made between the increase in the borehole length and distance between the boreholes. It is observed that the increase in the length of the boreholes had a negligible impact on the distance required between the boreholes and the system COP except from the case of Saittas for the same reasons explained above. Also, the number of boreholes and total length of GHE needed had the same response as in the previous modelling shown in Table 6.7(a).

Another way to minimise the number of boreholes in a system is to use GHEs with bigger pipe diameter. The effect on the borehole performance when the 32 mm GHEs were replaced by 40 mm GHEs were simulated and the results are listed in Table 6.8. A small increase in the system COP in the cooling mode, between 0.2 to 0.5 units was determined. In the heating mode, if not unchanged, the system COP had a minor increase of 0.1 units. The increase in the pipe diameter reduced the thermal resistance of the borehole since the heat exchange surface increased (approximately 5 m² in each borehole). But the most

Table 6.8: Comparison of the 100 m borehole capacity in relation to pipe diameter

Location	Pipe Diam. (mm)	Boreholes/Total Length (m)	Distance between the boreholes (m)	Ground temp. change Over 50 years (˚C)	System COP Cooling mode	System COP Heating mode
Agia Napa	32	6/600	3	+0.9	4.5	3.7
	40	6/600	3	+0.9	4.7	3.7
	40	5/500	4	+0.5	4.5	3.6
Meneou	32	6/600	3	+0.8	4.7	3.6
	40	6/600	3	+0.9	4.9	3.7
	40	5/500	3	+1.1	4.5	3.6
Lakatamia	32	7/700	3	+1.1	4.6	3.7
	40	7/700	3	+1.2	4.8	3.7
	40	6/600	3	+1.4	4.5	3.7
Limassol	32	6/600	3	+1.3	4.6	3.6
	40	6/600	3	+1.2	4.8	3.6
Saittas	32	4/400	3	+1	5	3.3
	40	4/400	3	+0.9	5.5	3.3
Kivides	32	6/600	3	+1.4	5.2	3.4
	40	6/600	3	+1.3	5.5	3.5
	40	5/500	3	+1.6	4.9	3.4
Geroskipou	32	6/600	3	+0.8	4.8	3.6
	40	6/600	3	+0.8	5.1	3.7
	40	5/500	3	+0.9	4.7	3.6
Prodromi	32	5/500	3	+0.7	4.8	3.5
	40	5/500	3	+0.8	5.1	3.6

significant observation is that the boreholes could be reduced by one except from the cases of Limassol, Saittas and Prodromi. The changes in pipe diameter in combination with the thermal properties of the ground in these three locations were not sufficient for the further reduction in number of boreholes. The reduction of the borehole had almost negligible impact on the system COP and the temperature change over a 50 years period.

Combinations of the results shown in Tables 6.1 – 6.8 are also graphically presented below. In Figure 6.6, the correlation between the thermal properties of the ground and the borehole thermal resistance at each location is plotted against the total length required to satisfy the load of the house. Similarly, in Figure 6.7, the parameters affecting the thermal resistance of a borehole, like pipe and borehole diameter, the distance between the GHE legs and the number of GHEs in the borehole were plotted against the borehole resistance. The backfill material is assumed to be bentonitic clay with thermal conductivity of 0.8 W/mK.

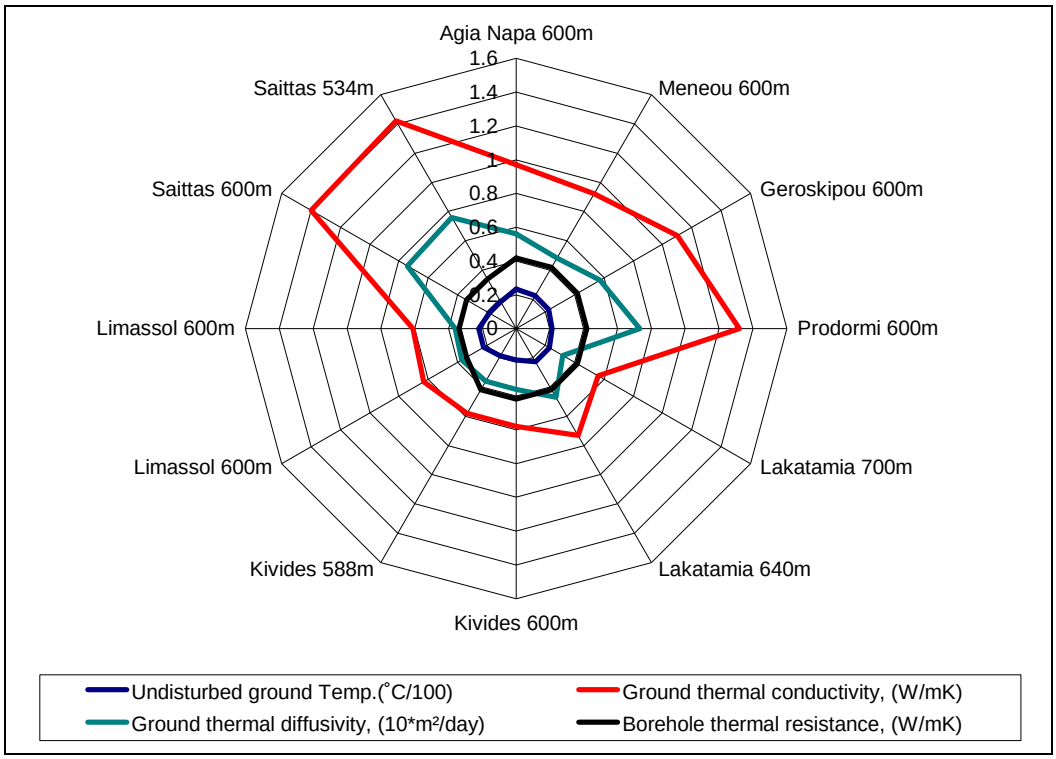

Figure 6.6: Graphical representation of the ground thermal properties and borehole thermal resistance against the total length required in each location for the heating and cooling load of the typical house

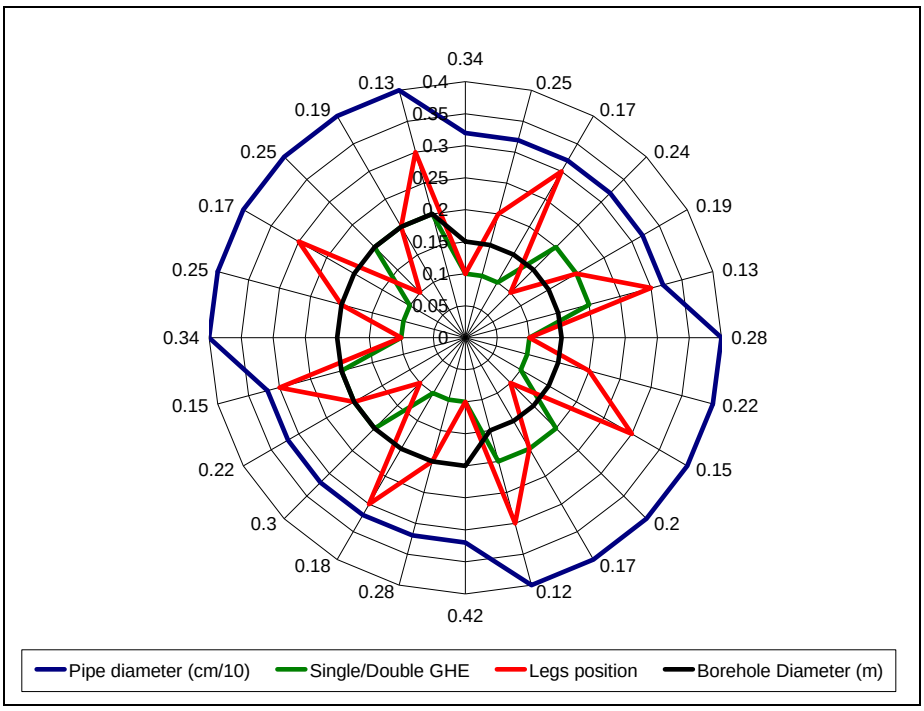

Figure 6.7: Parameters affecting the borehole resistance

Since the single row grid is not always feasible to be used because of the limitation in the length of the plot, the reverse 'L' shape is often utilized as shown in Figure 6.8. Assuming the same conditions as in the single row grid calculations, 11.4 L/min/3.5 kW system flow rate, 100 m deep boreholes and the same GCHP, the minimum number of boreholes and the distance between them required to satisfy the heating and cooling loads of the house is calculate and the results are tabulated in Table 6.9.

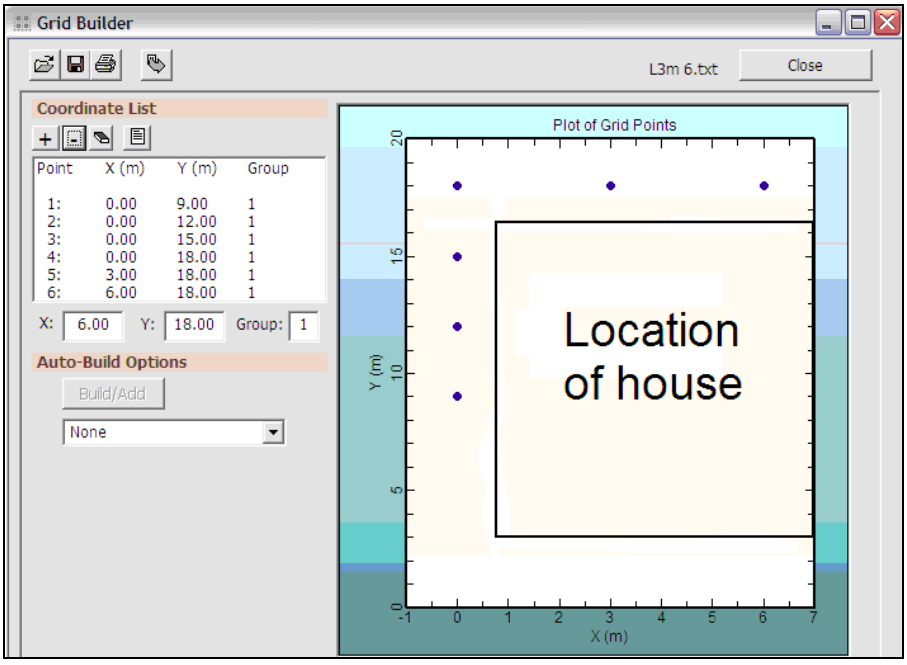

Figure 6.8: Typical reverse shape 'L' grid, GLD Grid Builder (2012).

Table 6.9: Reverse 'L' grid characteristics

Location	Pattern	Boreholes	Minimum distance between the boreholes	Ground temp. change over 50 years (˚C)	System COP Cooling	System COP Heating
Agia Napa	SR	6	3	+0.9	4.5	3.7
	L	6	3	+0.4	4.7	3.6
Meneou	SR	6	3	+0.8	4.7	3.6
	L	6	3	+0.3	4.8	3.6
Lakatamia	SR	7	3	+1.1	4.6	3.7
	L	7	3	+0.4	4.8	3.6
Limassol	SR	6	3	+1.3	4.6	3.6
	L	6	3	+0.4	4.7	3.6
Saittas	SR	4	3	+1	5	3.3
	L	4	3	+0.4	5.1	3.2
Kivides	SR	6	3	+1.4	5.2	3.4
	L	6	3	+0.4	5.4	3.3
Geroskipou	SR	6	3	+0.8	4.8	3.6
	L	6	3	+0.3	4.9	3.6
Prodromi	SR	5	3	+0.7	4.8	3.5
	L	5	3	+0.4	4.9	3.5

It is obvious that the reverse 'L' shape grid does not offer any significant advantages apart from the flexibility in the installation that gives to engineers by increasing the available space and therefore the number of boreholes or the distance between them. The change in the system COP is insignificant while in none of the locations the number of boreholes could be reduced. It is worth mentioning the reduction in the ground temperature change observed over the 50 years period.

Engineers should also be aware of the possibility that two independent geothermal systems could be installed close to each other affecting their performance. This may happen in the case that an engineer who designs a geothermal system for a new build house has not been informed of the presence of a geothermal system in the adjacent house.

A determination of how this affects the performance of the systems and the possible ways to avoid it follows. Since it is not possible to simulate in GLD the operation of the geothermal system of two houses, it is assumed that a single grid is used to serve the loads of two typical houses entered in Zone Manager as two different zones. The same pump as before was assigned to each zone and both of them connected to a grid. The two most important grids of interest are: the 2 single row grids 3 m apart to each other as shown in Figure 6.9(a) and a similar grid but with a vertical offset of 1.5 m as shown in Figure 6.9(b). The results of the calculations are tabulated in Table 6.10.

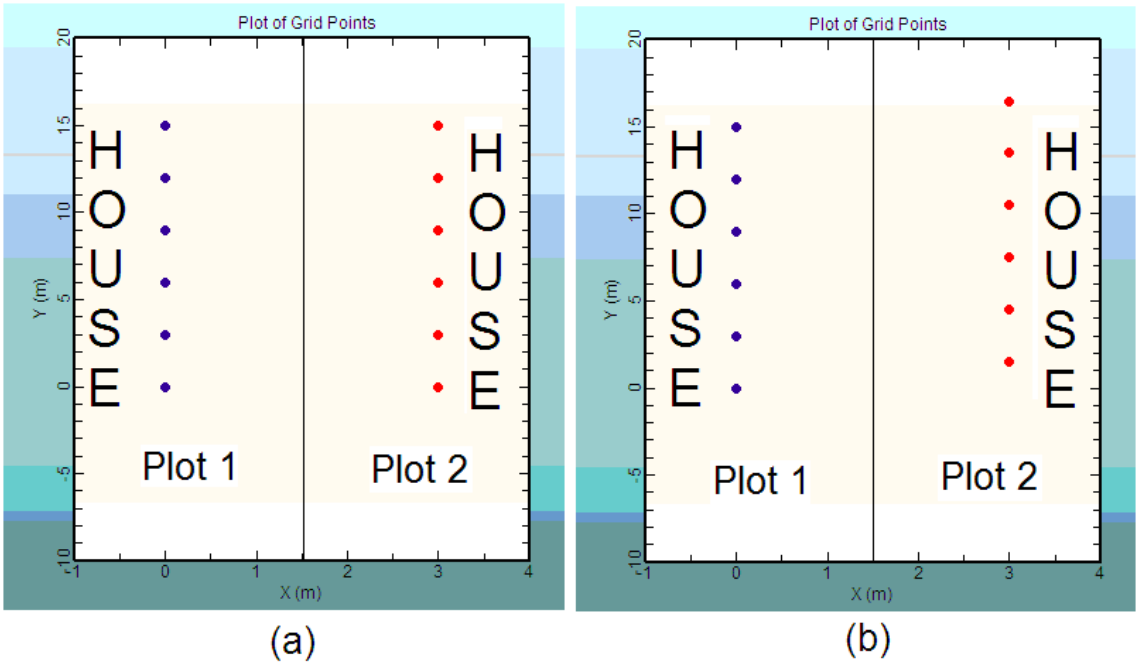

(a) (b)

Figure 6.9: (a) 2 single row grids 3 m apart to each other and (b) 2 single row grids 3 m apart to each other with a vertical offset of 1.5 m

Table 6.10: Effects on the operation of two independent geothermal systems when their single row grids are positioned close to each other

Pattern	**Boreholes per grid**	**Minimum distance between the boreholes**	**Ground temp. change over 50 years (˚C)**	**System COP Cooling**	**System COP Heating**
SR	6	3	+1.3	4.6	3.6
2SR	6	3	+0.7	4.7	3.5
2SRO	6	3	+0.7	4.7	3.5

According to the results, the effect on the system COP is minor as it is the change in the temperature of the ground over a 50 years time. As mentioned before, it is desirable to keep the distance between boreholes as large as practically possible keeping the balance between heating and cooling system COP.

Closing this section, the effect of the weather conditions on the design of a geothermal system is also determined. This is done by calculating the heating and cooling loads of the selected house based on the weather conditions in Lakatamia, Kivides and Saittas and comparing it with the previous results. According to MAEPB Methodology for Assessing the Energy Performance of Buildings, Cyprus is divided in 4 regions as per the prevailing climatic data. Zone 1, accounts for the sea-side locations like Agia Napa, Meneou, Limassol, Geroskipou and Prodromi, Zone 2, for the inland locations like Lakatamia, Zone 3, for the semi-mountainous like Kivides and Zone 4, for the mountainous locations like Saittas. The calculation results are shown in Table 6.11.

Table 6.11: Comparison of the heating and cooling loads in the 4 different climatic zones and the geothermal system required to satisfy the loads

Location	**Load (kWh)** **Cooling** **Heating**	**Peak Load (kW)** **Cooling** **Heating**	**Number of Boreholes/Total length (m)**	**System COP** **Cooling** **Heating**	**Ground temp. change over 50 years (˚C)**
Limassol	6195.08 5712.21	16.18 15.87	6/600	4.6 3.6	+1.3
Lakatamia	6129.76 7382.32	11.56 20.78	5/500 (7/700)*	4.8 (4.6)* 3.1 (3.7)*	+1.4 (+1.1)*
Kivides	7053.50 8294.65	10.97 21.51	5/500 (6/600)*	5.4 (5.2)* 2.9 (3.4)*	+1.6 (+1.4)*
Saittas	2136.39 26885.40	10.82 23.94	5/500 (4/400)*	7.6 (5)* 2.7 (3.3)*	-1.8 (+1)*

***In the brackets are shown the results of the calculations obtained considering the loads calculated based on the weather conditions in Limassol and presented in Table 6.5.**

According to the results in Table 6.11 and as it was expected, the heating load is higher and the cooling load lower in the cooler zones. In the locations except from Limassol, 5

boreholes, 500 m in total length were needed to satisfy the new loads. The impact of the weather conditions caused significant increase in both the total and peak heating loads. Consequently, the system COP in the heating mode had a slight drop. The drop in the peak cooling load in the three locations resulted in an increase of the system COP in cooling mode even if the total cooling load in Kivides increased. The change in loads due to weather conditions was sufficient to reduce the number of boreholes needed in Lakatamia and Kivides and increase them in Saittas. The change in the ground temperature over a 50 years time was considerably decreased in Saittas where it dropped from +1 ˚C to -1.8 ˚C.

The large amount of parameters involved in the design of geothermal systems, their variability and the interaction between them demonstrates that each case and application should be considered individually.

The temperature map of Cyprus produced by using artificial neural networks and presented in Chapter 5 is of a major assistance since the undisturbed ground temperature is now known and can be eliminated from the list of assumptions.

6.4 Summary

In determining the number of boreholes required and the heating and cooling performance of ground source heat pumps it is important that accurate data are used in simulations. It is preferable that data specific to the location and application are obtained from in-situ investigations and measurements.

Because of the large number of parameters affecting the design of geothermal systems graphical presentations were drawn showing the interaction between them. These show that one can arrive at a satisfactory result in various ways by considering the specific parameters.

Bentonitic clay as backfill material although is essential to be used should be avoided when the thermal conductivity of the ground is higher than the bentonitic clay since it acts as an insulator and reduces borehole efficiency. Enhanced bentonitic clay or even the drill chipping material taken out from the borehole during drilling improves borehole performance.

The efficiency of a geothermal system depends on the borehole thermal resistance which should be as low as possible. Apart from the backfill material, the distance between the pipes of the GHE influences borehole efficiency. The thermal resistance of the borehole is at its minimum when the pipes touch the borehole wall. The heat exchange between the pipes and the borehole wall increases as the pipe diameter increases. The heat exchange process between the pipes and the ground also improves as the borehole depth is increased.

The degree that each of these factors alone or in combination affects the system efficiency is strongly dependant on the thermal properties of the ground. Thermal conductivity and diffusivity of the ground and the temperature of the undisturbed ground are the most important factors.

The selection of the GCHP should be made in accordance to the thermal properties of the ground and on the results of the TRTs. Its performance is also dependant on the grid of boreholes to be used. The number of boreholes in relation to the distance between them also affects the temperature variation of the ground in the long run.

For the most of the 8 tested locations in Cyprus, about 6 boreholes of 3 m apart from each other are required to satisfy the 16.2 kW peak cooling load and the 15.87 kW peak heating load of a typical house. In all cases, the ground temperature variation in 50 years period is negligible. This is due to the fact that the load in the summer and winter balances out. When there is a big difference between the heating and cooling load (12.5 times greater) as in Saittas when the weather data for Saittas were used, the balance between the two periods is inevitable and significant temperature change occurs (from +1 ˚C to -1.8˚C).

Chapter 7: Conclusions and recommendations for future work

7.1 Introduction

Geothermal energy is the thermal energy within the earth's crust which can be used for a variety of purposes including space heating or cooling. It is considered a sustainable and renewable energy source able to minimise the use of fossil fuels resulting in the reduction in the dependence of a country on imported fuel, reductions in pollution and greenhouse gas emissions.

Since 2006, in Cyprus, Ground Coupled Heat Pump (GCHP) applications have been funded through a very generous grant scheme. The evaluation of the installed geothermal systems for cooling and heating showed that significant energy savings could be achieved if more energy efficient systems were designed.

Due to the lack of reliable information on the thermal properties of the ground for geothermal applications, the main aim of the study was to determine the thermal characteristics of the ground in Cyprus in order to investigate how they affect the sizing and positioning of Ground Heat Exchangers (GHEs) and to present the results, including a temperature map of the island at various depths as a guide for engineers.

To achieve the main aim of the study some more specific objectives were set resulting in the following conclusions:

i. To estimate the temperature, thermal conductivity, specific heat and density of the ground in representative locations in Cyprus by applying established methods.
ii. To present the collected data in an easy accessible and distinctive form.
iii. To prepare the temperature map of Cyprus at various depths.
iv. To examine how the ground data affect the sizing and positioning of GHEs and to determine the long term temperature variations of the ground.

In this chapter, all the useful conclusions resulted from the project are summarised along with suggestions for possible future work to be done to enrich and support the geothermal energy in Cyprus.

7.2 Main conclusions

1. According to literature, the ground is separated into 3 zones based on its temperature and how it is affected by weather conditions. At the surface, the ground is affected by short term weather variations, changing to seasonal variations as the depth increases. At the deeper layers ground temperature remains almost constant throughout the seasons and years and is strongly dependant on the soil type.

For the investigation of the thermal characteristics of the ground in Cyprus, 8 boreholes were drilled in selected sites based on geologic conditions, prevailing weather conditions and population density. The thermocouples fitted at various depths of each of the boreholes recorded the temperature of the ground monthly for a period of 1 year and showed that:

a. The surface zone reaches a depth of 0.25 m and that the soil temperature is very close to the ambient air temperature.
b. The shallow zone penetrates to 7 - 8 m and thereafter the deep zone follows.
c. The variation in the ground temperature in the surface and shallow zones occurs with a time lag compared to the ambient air temperature.
d. The time lag, which is a function of the depth from the surface, diminishes as the depth increases.
e. The temperature of the ground in the deep zone is always higher than that of the ambient air in winter and lower in summer.
f. Heat pumps can be coupled to GHEs to improve their efficiency of operation since the heat exchange process is done with the steady temperature of the ground and not the variable one of the ambient air.

2. Depending on the temperature of the ground mainly in the deep zone, geothermal energy is classified into high ($t > 150\ ^{\circ}C$), intermediate ($90\ ^{\circ}C < t < 150\ ^{\circ}C$) and low temperature ($t < 90^{\circ}C$). The undisturbed ground temperature at depths up to 200 m in the 8 locations was measured to be in the range of 18.3 °C to 23.6 °C and in combination with the geology of the island Cyprus is classified as a low temperature ground heat source.

3. When the ground temperature is low the utilisation of its thermal capacity is mainly done with the aid of GHEs. They are arrays of pipes buried in the ground and depending on the use their placement can be done horizontally or vertically. The performance of horizontal GHEs is affected by the temperature variations occurring in the shallow zone

where they are installed while Vertical GHEs are more reliable since the temperature of the ground in the deep zone is constant. It is concluded that in Cyprus Vertical GHEs:

a. Are more efficient than the horizontal ones.
b. They require less space to be installed.
c. Less piping is required therefore reduced piping cost.
d. Their installation is more expensive due to the high cost of deep drilling.

4. To define the several soil or rock types forming the ground, drill chipping samples were collected during drilling. But to determine the thermal characteristics of each layer and more specific the thermal conductivity, the thermal diffusivity, the thermal capacitance and the density, core samples from the boreholes or lithologically identical locations were collected. Measurements were made in their dry and saturated state and the following were concluded:

a. The ground layers in the selected locations mostly include sandy marls, chalk, limestones and sandstones.
b. The thermal characteristics of a sample can very since are strongly dependant on their specific weight and degree of saturation.
c. The lithology and thermal characteristics of neighbouring areas can vary therefore in situ determination is recommended for accurate results.
d. Accurate instruments are recommended to be used in the determination of the thermal characteristics of the samples for accurate and consistent results.

5. The thermal response test (TRT) based on the line source method was used for the determination of the thermal conductivity of the drilled boreholes in the 8 locations. In most of the boreholes more than one GHE were installed allowing for the examination of the effect of the GHE length, pipe diameter or type on the result of the thermal conductivity tests. To perform the in situ TRT a lightweight hot water storage tank equipped with two electrical heaters 3 KW each, a circulating pump, a flow meter, an electrical panel and measuring equipment were utilised. For every borehole a number of TRTs were carried out in order to determine the average thermal conductivity of the ground. The results showed that:

a. The thermal conductivity of the ground in the 8 locations was measured in the range of 1.35 - 2.1 W/mK.
b. The change in the degree of saturation of the ground affected the results of the tests carried out.

c. The bigger the pipe diameter of the GHE is, the more improved is the heat exchange process.
d. In locations of low ground thermal diffusivity and hence poor heat dissipation, an increase or decrease of the temperature of the ground could occur in the long run.

6. The data collected related to the temperature of the ground in Cyprus and its thermal properties obtained from the in situ investigations are unique since such data are presented for the first time. In this way engineers can have access to a library of data related to the sizing and positioning of GHEs. The tables and graphs offer a comprehensible form of data easily accessible on the web.

Furthermore, the information collected from the 8 locations was used as data sets for training Artificial Neural Networks (ANNs) to predict the temperature of the ground at locations where no information is available. The generation of the temperature maps of Cyprus at the depths of 20 m, 50 m and 100 m were plotted. This is an innovative approach for the prediction of data with very good results, previously used in a number of engineering problems. The publication of this information enables comparison with other countries with similar climatic conditions to be carried out.

7. For the prediction of the thermal performance of GHEs and for the geothermal system design several calculation models and tools were presented and validated against experimental results. It is recommended to select the appropriate one for each case based on the formulation used and to use accurate data and more preferably data collected from in situ investigations. GLD Premier 2012 Edition, a Computational Fluid Dynamics (CFD) software, was chosen for this study because amongst others it allows users to:
a. To directly compare the results of the cylindrical source model and the line source theory model included within the GLD framework.
b. To do more ‘what if’ modelling and perform multiple design simulations to optimize geothermal systems.
c. To draw their own borehole grid.
d. To import the desired heat pumps characteristics.
e. To compare different types of systems such as vertical and horizontal GHEs.
f. To easily import or export data from or to other commercial software programmes.

8. The performance of GCHPs depends on a large number of parameters amongst them the thermal properties of the ground, the borehole resistance and the thermal load to be satisfied. With the aid of GLD Premier 2012 Edition software the effect of those parameters on the capacity of the GHEs in each location, the optimum distance between them and the long term temperature variation of the ground were examined. The data collected related to the thermal properties of the ground in each location were used as inputs to the software. The study showed that:

a. The system performance is strongly dependent on the desired peak load to satisfy, the borehole thermal resistance and the thermal properties of the ground.
b. The borehole resistance should be the minimum possible.
c. The thermal conductivity of the backfill material should be higher than the ground thermal conductivity. Enhanced bentonitic clay or even the drill chipping material taken out from the borehole during drilling is suggested to be used.
d. The borehole diameter should be the less possible.
e. The borehole thermal resistance decreases with the increase in the pipe diameter of the GHE.
f. The pipes of the GHE is recommended to be the closest possible to the borehole wall than close to each other in the middle of the borehole.
g. The doubling of the borehole depth and the length of the GHE, improves the borehole efficiency but does not necessarily result to the reduction by half of the number of boreholes since the heat exchange process also depends on the properties of the ground at the deeper layers.
h. 2 GHEs in a single borehole improve the heat exchange process between water and ground.
i. It is most likely to have a change in the temperature of the ground over the passing of the years if the cooling and heating loads are not balanced. For the locations examined this change could reach the +1.6 ˚C.
j. The change in the system flow rate per peak load means a change in the heat injected to or absorbed by the ground and a possible change in the temperature of the ground over the passing of the years especially if the diffusivity of the ground is poor.
k. The distance between the boreholes is desirable to be as large as practically possible to avoid the effects from the deviation from vertical, particularly for deep boreholes. For 100 m deep boreholes, the distance between them is recommended to be around 7 m.
l. Despite the large number of parameters involved and the interaction between them a desired result can be achieved in various ways by considering the specific parameters.

7.3 Recommendations for future work

Further to the work done for this project and its findings, some more work is proposed to be done to enrich and support the geothermal energy in Cyprus

First, despite the accuracy of the temperature maps drawn, further improvement could be achieved with the enrichment of the input data sets of ANNs. The creation a library or database in where engineers could easily import related data when they acquire such is proposed.

In addition to the temperature maps of Cyprus, the thermal conductivity and thermal diffusivity maps of the island are proposed to be drawn as well. A project entitled 'Investigation and determination of the geothermal parameters of the lithologies in Cyprus, for the compilation of the geothermal map of the island' already deals with the analysis of the thermal properties of the ground in a number of locations in Cyprus.

Finally, the collected data could be used by the relevant authorities of Cyprus for adopting installation guidelines, regulations or even legislation related to geothermal applications.

References

Álvarez del Castillo, A., Santoyo, E. & García-Valladares, O. 2012, "A new void fraction correlation inferred from artificial neural networks for modelling two-phase flows in geothermal wells", *Computers and Geosciences,* vol. 41, pp. 25-39.

Arslan, O. 2011, "Power generation from medium temperature geothermal resources: ANN-based optimization of Kalina cycle system-34", *Energy,* vol. 36, no. 5, pp. 2528-2534.

ASHRAE Terminology of Heating, Ventilating, Air Conditioning, and Refrigeration, Terms and definitions, 2000, 2001, 2002 and 2003, CD-ROM, ASHRAE Handbook, *American Society of Heating, Refrigerating and Air-Conditioning Engineers, Inc.*

Austin, W.A. 1998, "Development of an in-situ system for measuring ground thermal properties" master's thesis, Oklahoma State University, in Gehlin, S. 2002, "Thermal Response Test, Method Development and Evaluation", PhD Thesis, Department of Environmental Engineering, Division of Water Resources Engineering, Lulea University of Technology, ISSN: 1402-1544.

Baggs, S.A. 1983, "Remote prediction of ground temperature in Australian soils and mapping its distribution", *Solar Energy,* vol. 30, no. 4, pp. 351-366.

Bassam, A., Santoyo, E., Andaverde, J., Hernández, J.A. & Espinoza-Ojeda, O.M. 2010, "Estimation of static formation temperatures in geothermal wells by using an artificial neural network approach", *Computers and Geosciences,* vol. 36, no. 9, pp. 1191-1199.

Bauer, D., Heidemann, W. & Diersch, H.-.G. 2011, "Transient 3D analysis of borehole heat exchanger modeling", *Geothermics,* vol. 40, no. 4, pp. 250-260.

Beck, A.E., Anglin, F.M. & Sass, J.H. 1971, "Analysis of heat flow data- in situ thermal conductivity measurements", *Can.J.Earth Sci.,* vol. 8, no. 1, pp. 1-19.

Blackwell, D.D., Richards, M., Batir, J., Frone, Z. & Park, J. 2010, "New geothermal resource map of the Northeastern US and technique for mapping temperature at depth", *Transactions - Geothermal Resources Council*, pp. 283.

Blackwell, J.H. 1954, "A transient-flow method for determination of thermal constants of insulating materials in bulk part I - Theory", *Journal of Applied Physics,* vol. 25, no. 2, pp. 137-144.

Carslaw H.S. & Jaeger J.C., 1959. "Conduction of heat in solids", 2nd edition. Great Britain: Oxford Science Publications, in Chapter A32: Geothermal Energy, CD-ROM, 2003 ASHRAE HVAC Applications, *American Society of Heating, Refrigerating and Air-Conditioning Engineers, Inc.*

Carslaw, H.S. & Jeager, J.C. 1947, "Conduction of Heat in Solids, Oxford Univ. *Press*, pp. 386.

2009 ASHRAE Handbook, Fundamentals, Chapter 2, Thermodynamics and refrigeration cycles, *American Society of Heating, Refrigerating and Air-Conditioning Engineers, Inc*, ISBN 978-1-933742-54-0.

2011 ASHRAE Handbook, HVAC Applications, Chapter 34, Geothermal Energy, *American Society of Heating, Refrigerating and Air-Conditioning Engineers, Inc*, ISBN 978-1-936504-07-7.

Christofides, A.C. Ksanthopoulos, S & Spyrou, S. 2009, "Εφαρμογή γεωθερμικής αντλίας θερμότητας μεταβλητης παροχής ψυκτικού μέσου (VRV) με οριζόντιο γεωεναλλάκτη" [Variable Refrigerant Volume (VRV) geothermal heat pump coupled to a horizontal ground heat exchanger] *Proceedings of the 9th National Conference for Renewable Energy Sources, Geroskipou, Cyprus*, pp. 525-532.

Collins, T., Parker, S.A. & Baxter, V. 2001, *Assessment of Hybrid Geothermal Heat Pump Systems, Technology Installation Review*.

Cui, P., Yang, H. & Fang, Z. 2008, "Numerical analysis and experimental validation of heat transfer in ground heat exchangers in alternative operation modes", *Energy and Buildings,* vol. 40, no. 6, pp. 1060-1066.

De Paepe M. & Willems N. 2001, "3D Unstructured modelling technique for ground-coupled air heat exchanger", 7th REHVA World Congress, Napoli.

Deerman, J.D. & Kavanaugh, S.P. 1991, "Simulation of vertical U-tube ground-coupled heat pump systems using the cylindrical heat source solution", *ASHRAE Transactions,* vol. 97, no. 1, pp. 287-295.

Eklöf, C. & Gehlin, S. 1996, "TED - A mobile equipment for thermal response test", master's thesis, Lulea University of Technology, in Gehlin, S. 2002, "Thermal Response Test, Method Development and Evaluation", PhD Thesis, Department of Environmental Engineering, Division of Water Resources Engineering, Lulea University of Technology, ISSN: 1402-1544.

Eskilson, P. & Claesson, J. 1988, "Simulation model for thermally interacting heat extraction boreholes", *Numerical heat transfer,* vol. 13, no. 2, pp. 149-165.

Eskilson, P., 1987, "Thermal analysis of heat extraction boreholes", PhD thesis, Department of Mathematical Physics, Lund University, Sweden.

Eslami-Nejad, P. & Bernier, M. 2011, "Coupling of geothermal heat pumps with thermal solar collectors using double U-tube boreholes with two independent circuits", *Applied Thermal Engineering,* vol. 31, no. 14-15, pp. 3066-3077.

Florides, G. & Kalogirou, S. 2005, "Annual ground temperature measurements at various depths", *8th REHVA World Congress*.

Florides, G. & Kalogirou, S. 2008, "First in situ determination of the thermal performance of a U-pipe borehole heat exchanger, in Cyprus", *Applied Thermal Engineering,* vol. 28, no. 2-3, pp. 157-163.

Florides, G., & Kalogirou, S. (2004). Measurements of ground temperature at various depths. *Proceedings of the 3rd International Conference on Sustainable Energy Technologies.*

Florides, G.A., Pouloupatis, P.D., Kalogirou, S., Messaritis, V., Panayides, I., Zomeni, Z., Partasides, G., Lizides, A., Sophocleous, E. & Koutsoumpas, K. 2011, "The geothermal characteristics of the ground and the potential of using ground coupled heat pumps in Cyprus", *Energy,* vol. 36, no. 8, pp. 5027-5036.

Fourier Technologies Ltd. 2007, "DaqPRO user guide, 8th edition".

Gauthier, C. 1994, "Transfer de chaleur et d'hulite dans le sol", Internal report, Group de recherché THEMAUS in De Paepe M. & Willems N. 2001, "3D Unstructured modelling technique for ground-coupled air heat exchanger", 7th REHVA World Congress, Napoli.

Gehlin, S. 2002, "Thermal Response Test, Method Development and Evaluation", PhD thesis, Department of Environmental Engineering, Division of Water Resources Engineering, Lulea University of Technology, ISSN: 1402-1544.

Geological Survey Department, Ministry of Agriculture and Natural Resources and Environment, viewed 18 July 2012 from:
http://www.moa.gov.cy/moa/gsd/gsd.nsf/dmlIntroduction_en/dmlIntroduction_en?OpenDocument

"*Geothermal Heat Pump Consortium*", viewed 2003 from http://www.geoexchange.org.

Haykin, S. 1994, "Neural Networks, A comprehensive Foundation", *McMillian College Publishing Company*, pp. 198-203.

Healy, R.F. & Ugursal, V.L. 1997, "Performance and economic feasibility of ground source heat pumps in cold inmate", *International Journal of Energy Research,* vol. 21, no. 10, pp. 857-870.

Hepbasli, A., Akdemir, O. & Hancioglu, E. 2003, "Experimental study of a closed loop vertical ground source heat pump system", Energy Conversion and Management, vol. 44, no. 4, pp. 527-548.

Holzfeind, W. 2009, "Ground Response Test Analysis" Report, Geoliving Energy, ACRenergiebohr ag, Husarenweg 10, CH-7303 Mastrils.

Ingersoll, L.R. & Plass, H.J. 1948, "Theory of the ground pipe heat source for the heat pump", *Heating, Piping and Air Conditioning,* vol. 20, no. 7, pp. 119-122.

ISOMET2014, Portable system for measurement of heat transfer properties of materials, 2011, Applied Precision Ltd,
http://www.appliedp.com/download/catalog/isomet_pc_en.pdf.

Javed, S., Fahlén, P. & Claesson, J. 2009, "Vertical ground heat exchangers: A review of heat flow models", *Proceedings of the 11th International Conference on Thermal Energy Storage, Effstock 2009.*

Jessop, A.M., 1070, "The effect of environment on divided bar measurements", *Tectonophysics*, vol. 10, pp. 39-49.
Kaftan, I., Salk, M. & Senol, Y. 2011, "Evaluation of gravity data by using artificial neural networks case study: Seferihisar geothermal area (Western Turkey)", *Journal of Applied Geophysics,* vol. 75, no. 4, pp. 711-718.

Kalogirou, S., Neocleous, C., Michaelides, S. & Schizas, C. 1997, "A time series reconstruction of precipitation records using artificial neural networks",*Proc. EUFIT'97,* vol. 3, pp. 2409-2413.

Kalogirou, S., Neocleous, C., Michaelides, S. & Schizas, C. 1998, "Artificial neural networks for the generation of isohyets by considering land configuration", *Proceedings of the Engineering Applications of Neural Networks (EANN'98) Conference,* vol. 3, pp. 383-389.

Kalogirou, S.A. & Bojic, M. 2000, "Artificial neural networks for the prediction of the energy consumption of a passive solar building", *Energy,* vol. 25, no. 5, pp. 479-491.

Kalogirou, S.A. 2000, "Applications of artificial neural-networks for energy systems", *Applied Energy,* vol. 67, no. 1-2, pp. 17-35.

Kalogirou, S.A. 2001, "Artificial neural networks in renewable energy systems applications: A review", *Renewable and Sustainable Energy Reviews,* vol. 5, no. 4, pp. 373-401.

Kalogirou, S.A. 2003, "Artificial intelligence for the modelling and control of combustion processes: A review", *Progress in Energy and Combustion Science,* vol. 29, no. 6, pp. 515-566.

Kalogirou, S.A., Panteliou, S. & Dentsoras, A. 1999, "Modeling of solar domestic water heating systems using Artificial Neural Networks", *Solar Energy,* vol. 65, no. 6, pp. 335-342.

Kasuda, T. & Archenbach, P.R. 0000, "Earth temperature and thermal diffusivity at selected stations in the United States", *ASHRAE Transactions,* vol. 71, no. PART 1, pp. 1965.

Katsura, T., Nagano, K. & Takeda, S. 2008, "Method of calculation of the ground temperature for multiple ground heat exchangers", *Applied Thermal Engineering,*vol. 28, no. 14-15, pp. 1995-2004.

Kavanaugh, S.P. & Rafferty, K. 1997, "Ground-source heat pumps, design of geothermal systems for commercial and institutional buildings", *ASHRAE, Inc.*, pp. 72-113.
Kedaid, F.Z. 2007, "Database on the geothermal resources of Algeria", *Geothermics,* vol. 36, no. 3, pp. 265-275.

Kelley, S. 2005, "Temperatures in the Kiowa Drill Hole", *Denver museum of Nature & Science*. Retrieved from http://www.dmns.org/.

Kim, S., Bae, G., Lee, K. & Song, Y. 2010, "Field-scale evaluation of the design of borehole heat exchangers for the use of shallow geothermal energy", *Energy,* vol. 35,

no. 2, pp. 491-500.

Lee, C.K. 2011, "Effects of multiple ground layers on thermal response test analysis and ground-source heat pump simulation", *Applied Energy,* vol. 88, no. 12, pp. 4405-4410.

Lees, C.H. 1892, "On the thermal conductivity of crystals and other bad conductors", Phil. Trans. R. Soc. London., A, 183, 481-509 in Morgan P, 1973, "Terrestrial heat flow studies in Cyprus and Kenya", PhD thesis, Geology department, Imperial College, University of London.

Lund, J.W., Freeston, D.H. & Boyd, T.L., 2011, "Direct Utilization of Geothermal Energy 2010 Worldwide Review", *Proceedings the World Geothermal Congress 2010*.

Mahfouf, J.-. & Viterbo, P. 2001, "Land surface assimilation", *ECMWF Meteorological Training Course Lecture Series*, pp. 1-23.

Mands, E. & Sanner, B. 2005, "*Shallow Geothermal Energy*" UBeG GbR viewed in 18 April 2014 from http://www.ubeg.de/Downloads/ShallowGeothEngl.pdf.

Michopoulos, A. & Kyriakis, N. 2009, "Predicting the fluid temperature at the exit of the vertical ground heat exchangers", *Applied Energy,* vol. 86, no. 10, pp. 2065-2070.

Mihalakakou, G., Santamouris, M., Lewis, J.O. & Asimakopoulos, D.N. 1997, "On the application of the energy balance equation to predict ground temperature profiles", *Solar Energy,* vol. 60, no. 3-4, pp. 181-190.

Moeck, I., Hinz, N., Faulds, J., Bell, J., Kell-Hills, A. & Louie, J. 2010, "3D geological mapping as a new method in geothermal exploration: A case study from central Nevada", *Transactions - Geothermal Resources Council*, pp. 742.

Mogensen, P. 1983, "Fluid to duct wall heat transfer in duct system heat storages", *Document - Swedish Council for Building Research*, pp. 652.

Morgan P, 1973, "Terrestrial heat flow studies in Cyprus and Kenya", PhD thesis, Geology department, Imperial College, University of London.

Muraya, N.K. 1994, "Numerical modelling of the transient thermal interface of vertical U-tube heat exchangers", *Numerical modelling of the transient thermal interference of vertical U-tube heat exchangers*.

Nam, Y., Ooka, R. & Hwang, S. 2008, "Development of a numerical model to predict heat exchange rates for a ground-source heat pump system", *Energy and Buildings,* vol. 40, no. 12, pp. 2133-2140.

Neocleous, C., 1998, "A neural network architecture composed of adaptively defined dissimilar single-neurons", PhD thesis, Department of Mechanical Engineering, Brunel University.

Omega Engineering Inc., "*UL Listed Twisted Shielded Extension Grade Thermocouple Wire*" viewed in 18 April 2014 from
http://www.omega.com/Temperature/pdf/EXPP-K-TWSH-UL.pdf.

Omega Engineering Inc., "USB Data Acquisition Modules for Thermocouples Process Signals, OMB-DAQ-54, OMB-DAQ-55 and OMB-DAQ-56" viewed in 18 April 2014 from http://www.omega.com/pptst/OMB-Daq55.html.

Pahud, D. & Matthey, B. 2001, "Comparison of the thermal performance of double U-pipe borehole heat exchangers measured in situ", *Energy and Buildings,* vol. 33, no. 5, pp. 503-507.

Partasides, G., Lizides A., Kassinis S., Florides G., Pouloupatis P., Kalogirou S., …, Koutsoumpas K. 2011, "Investigation and determination of the geothermal parameters of the ground in Cyprus for the exploitation of geothermal energy and the impact of the results in the design of the geothermal systems", *Proceedings, Thirty-Sixth Workshop on Geothermal Reservoir Engineering, Stanford University, California*.

Pfafferott, J. 2003, "Evaluation of earth-to-air heat exchangers with a standardised method to calculate energy efficiency", *Energy and Buildings,* vol. 35, no. 10, pp. 971-983.

Popiel, C.O., Wojtkowiak, J. & Biernacka, B. 2001, "Measurements of temperature distribution in ground", *Experimental Thermal and Fluid Science,* vol. 25, no. 5, pp. 301-309.

Pouloupatis D.P., Florides G. & Tassou S. 2009, "Measurements of Ground Temperatures in Cyprus for Ground Thermal Applications", *Proceedings of the 9th National Conference for Renewable Energy Sources, Geroskipou, Cyprus*, pp. 525-532.

Pouloupatis, P.D., Florides, G. & Tassou, S. 2011, "Measurements of ground temperatures in Cyprus for ground thermal applications", *Renewable Energy,* vol. 36, no. 2, pp. 804-814.

Puri V. 1986, "Feasibility and performance curves for intermittent earth tube heat exchangers", A.M. Soc. Agricul. Eng. Vol 29, pp. 526-532.

Richards, M., Stepp, P., Blackwell, D. & Kweik, A. 2009, "Eastern Texas geothermal mapping", *Transactions - Geothermal Resources Council*, pp. 843.

Rybach, L. 2010, "The Future of Geothermal Energy and Its Challenges", *Proceedings World Geothermal Congress 2010, Bali, Indonesia*.

Sanner, B., Reuss, M., Mands, E. & Müller, J. 2000, "Thermal response test-experiences in Germany", *Proceedings Terrastock 2000,* vol. 1, pp. 177-182.

Sares, M.A., Berkman, F.E. & Watterson, N.A. 2009, "Statewide geothermal resource mapping in Colorado", *Transactions - Geothermal Resources Council*, pp. 867.

Schiavi, L. 2009, "3D Simulation of the thermal response test in a U-tube borehole heat exchanger", *Proc COMSOL Conference*.

School of Mechanical and Aerospace Engineering, Oklahoma State University, "*GLHEPRO 4.0 Users Guide*", 2007, viewed 18 April 2014 from http://www.hvac.okstate.edu/glhepro/.

Stalhane, B. & Pyk, S. 1931, "New method for determining the coefficients of thermal conductivity", *Teknisk Tidskrift,* vol. 61, no. 28.

The Cyprus Institute of Energy, "*Grant schemes for the promotion of electrical power generation, 2013*", viewed in 18 April 2014 from http://www.cie.org.cy/#sxedia-xorhgiwn-odhgoi.

The Ground Loop Design™ Premier 2012 Edition, 2012, "User's Manual".

Town planning and Housing Department, Ministry of Interior, 2011, "Οδηγός ερμηνείας πολεοδομικών κανονισμών" [Town planning regulations guide], ISBN 978-9963-50-060-4, viewed in 18 April 2014 from http://www.moi.gov.cy .

"*TPSYS02 PC controlled thermal conductivity measurement system*", Hukseflux Thermal Sensors, viewed in 18 April 2014 from http://www.hukseflux.com/product/tpsys02?referrer=/product_group/thermal-conductivity.

Vrachopoulos, M. 2000, *Ψυκτικές διατάξεις,* [Refrigeration configurations], ION Publishers, ISBN: 960-411-094-2.

Williams, G.P. & Gold, L.W. 1976, "Ground temperatures", *Canadian Building Digest,* vol. 180, pp4, *Institute for Research in Construction*.

Witte, H.J.L., Van Gelder, G.J. & Spitler, J.D. 2002, "In situ measurement of ground thermal conductivity: A Dutch perspective", *ASHRAE Transactions*, pp. 263.

Woodside, W. & Messmer, J.H. 1961, "Thermal conductivity of porous media. I. Unconsolidated sands", *Journal of Applied Physics,* vol. 32, no. 9, pp. 1688-1699.

Woodside, W. & Messmer, J.H. 1961, "Thermal conductivity of porous media. II. Consolidated rocks", *Journal of Applied Physics,* vol. 32, no. 9, pp. 1699-1706.

Wrightsoft HVAC Software Solutions, Right-Loop™, "*Geothermal Design Worksheets for Accurate Calculations*" viewed in 18 April 2014 from http://www.wrightsoft.com/products/right-loop.aspx.

Yang, H., Cui, P. & Fang, Z. 2010, "Vertical-borehole ground-coupled heat pumps: A review of models and systems", *Applied Energy,* vol. 87, no. 1, pp. 16-27.

Yavuzturk, C. 1999, "Modeling of vertical ground loop heat exchangers for ground source heat pump systems" PhD thesis, Graduate College, Oklahoma State University.

Yavuzturk, C., Spitler, J.D. & Rees, S.J. 1999, "A transient two-dimensional finite volume model for the simulation of vertical U-tube ground heat exchangers", *ASHRAE Transactions,* vol. 105, no. 2, pp. 465-474.

Yousefi, H., Noorollahi, Y., Ehara, S., Itoi, R., Yousefi, A., Fujimitsu, Y., Nishijima, J. & Sasaki, K. 2010, "Developing the geothermal resources map of Iran",*Geothermics,* vol. 39, no. 2, pp. 140-151.

Yun, T.S. & Santamarina, J.C. 2008, "Fundamental study of thermal conduction in dry soils", *Granular Matter,* vol. 10, no. 3, pp. 197-207.

Zeng, H., Diao, N. & Fang, Z. 2003, "Heat transfer analysis of boreholes in vertical ground heat exchangers", *International Journal of Heat and Mass Transfer,* vol. 46, no. 23, pp. 4467-4481.

Appendix 1

The data collected and the results tabulated or plotted by Morgan (1973) for the locations used for comparison in Chapter 3 are presented unchanged in this section.

A complete set of information is contained in the attached CD-ROM.

Appendix 4

TABULATIONS AND PLOTS OF CYPRUS HEAT FLOW DATA AND RESULTS

A4.1 Tabulations of Temperature and Conductivity Data

A full tabulation of the Cyprus temperature and conductivity data used in this study is given below. For each borehole the temperature-depth is given first followed by the conductivity data. The heat flow station numbers are given followed by the borehole number and in the case of the temperature data this is followed by the date on which the temperature log was carried out. Depths (DEPTH) are given in metres, temperature (TEMP) in degC. Conductivities (COND) are given in W m^{-1} $^{o}C^{-1}$, with the depth range (REGION) in metres over which the conductivity value was used. Values determined from measurements on chip samples collected from within the depth range in the borehole are underlined, assumed values are not marked, values from lithologically equivalent disc samples are indicated by rounded brackets and values from lithologically equivalent chip samples by square brackets.

CYPRUS 28 B/H PB56 12 MAY 1971

DEPTH	TEMP	DEPTH	TEMP	DEPTH	TEMP	DEPTH	TEMP
63.06	21.47	64.65	21.48	66.23	21.50	67.82	21.50
69.40	21.51	70.99	21.52	72.57	21.53	74.13	21.55
75.71	21.56	77.30	21.56	78.88	21.57	80.47	21.58
82.05	21.59	83.64	21.60	85.19	21.61	86.78	21.62
88.36	21.63	89.95	21.64	91.53	21.66	93.12	21.67
94.70	21.67	96.29	21.69	97.84	21.70	99.43	21.71
101.01	21.73	102.60	21.74	104.18	21.76	105.77	21.77
107.35	21.78	108.91	21.80	110.49	21.80	112.07	21.82
113.66	21.84	115.24	21.85	116.83	21.87	118.41	21.87
120.00	21.89	121.55	21.91	123.14	21.93	124.72	21.95
126.31	21.96	127.89	21.97	129.48	21.99	131.06	22.01
132.62	22.01	134.20	22.03	135.79	22.04	137.37	22.06
138.96	22.07	140.54	22.08	142.13	22.09	143.71	22.11
145.27	22.12	146.85	22.13				

CYPRUS 28 B/H PB56 CONDUCTIVITY DATA

REGION	COND
0.0	182.9 [1.43]

CYPRUS 29 B/H PB53 13 MAY 1971

DEPTH	TEMP	DEPTH	TEMP	DEPTH	TEMP	DEPTH	TEMP
69.71	20.60	72.88	20.59	76.02	20.59	79.19	20.60
82.36	20.60	85.50	20.61	88.67	20.61	91.84	20.64
95.01	20.66	98.15	20.69	101.32	20.72	104.49	20.74
107.66	20.84	110.79	20.87	113.96	20.94	117.13	20.98
120.30	21.02	123.44	21.05	126.61	21.06	129.78	21.09
132.92	21.09	136.09	21.09	139.26	21.08	142.43	21.08
145.57	21.08	148.74	21.08	151.91	21.08	155.08	21.10
158.22	21.09	161.39	21.09	164.56	21.10	167.73	21.10
170.87	21.10	174.04	21.10	177.21	21.10	180.35	21.10
183.52	21.10	186.69	21.10	189.86	21.14	193.00	21.19
196.17	21.25	199.34	21.32	202.51	21.32	205.65	21.47
208.82	21.89	211.99	21.99	215.16	22.03		

CYPRUS 29 B/H PB53 CONDUCTIVITY DATA

REGION	COND
0.0	228.6 [1.43]

CYPRUS 3[illegible] B/H PB50 13 MAY 1971

DEPTH	TEMP	DEPTH	TEMP	DEPTH	TEMP	DEPTH	TEMP
6.28	2[illegible].29	7.86	20.37	9.45	20.39	11.[illegible]0	20.44
12.59	20.46	14.14	20.50	15.73	20.51	17.31	20.55
18.87	20.56	20.45	20.62	22.01	20.74	23.59	20.94
25.18	20.95	26.73	20.97	28.32	20.98	29.87	21.01
31.46	21.02	33.04	21.03	34.63	21.05	36.21	21.08
37.76	21.09	39.35	21.11	40.93	21.13	42.52	21.15
44.10	21.16	45.69	21.18	47.27	21.20	48.86	21.22
50.41	21.24	52.0[illegible]	21.27	53.58	21.28	55.17	21.30
56.75	21.31	58.34	21.35	59.92	21.36	61.48	21.38
63.06	21.40	64.65	21.43	66.23	21.45	67.82	21.47
69.40	21.49	70.99	21.52	72.57	21.54	74.13	21.57
75.71	21.58	77.30	21.62	78.88	21.63	80.47	21.66
82.05	21.67	83.64	21.72	85.19	21.74	86.78	21.77
88.36	21.79	89.95	21.81	91.53	21.83	93.12	21.86
94.70	21.87	96.29	21.90	97.84	21.92	99.43	21.93
101.01	21.95	102.60	21.96				

CYPRUS 3[illegible] B/H PB50 CONDUCTIVITY DATA

REGION		COND	REGION		COND	REGION		COND
0.0	12.2	1.42	12.2	27.4	1.43	27.4	33.5	1.47
33.5	45.7	1.36	45.7	57.9	1.40	57.9	67.1	1.45
67.1	77.4	1.44	77.4	88.7	1.49	88.7	100.6	1.48
100.6	112.8	1.40	112.8	121.9	1.41			

A4.2 Plots of Heat Flow Data and Results

The data and results from each Cyprus heat flow station are given in the plots below with brief geological information from the boreholes. Temperatures are given in degC with depths in metres. The conductivity data, in W m^{-1} $^{o}C^{-1}$, are given as a step function against depth indicating the depth ranges for which the values were used. Temperature gradients (TEMP GRADIENT), in degC km^{-1}, calculated from adjacent temperature data are plotted as a step function at the corresponding depths. These values have been smoothed to remove oscillations derived from the digital nature of the data, and the curves are discontinuous where off-scale values were calculated. Heat flow values, in mW m^{-2}, calculated by the Bullard reduction method are plotted over the depth range from which data were taken for the fits. Assuming that the data in these ranges follow a normal distribution, error bars are given on the ends of the heat flow plots indicating $\pm$ 3·09 times the standard errors of the least squares fits, and the probability that an observation will fall outside this zone is 1 in 500 (Topping, 1962, p.61).

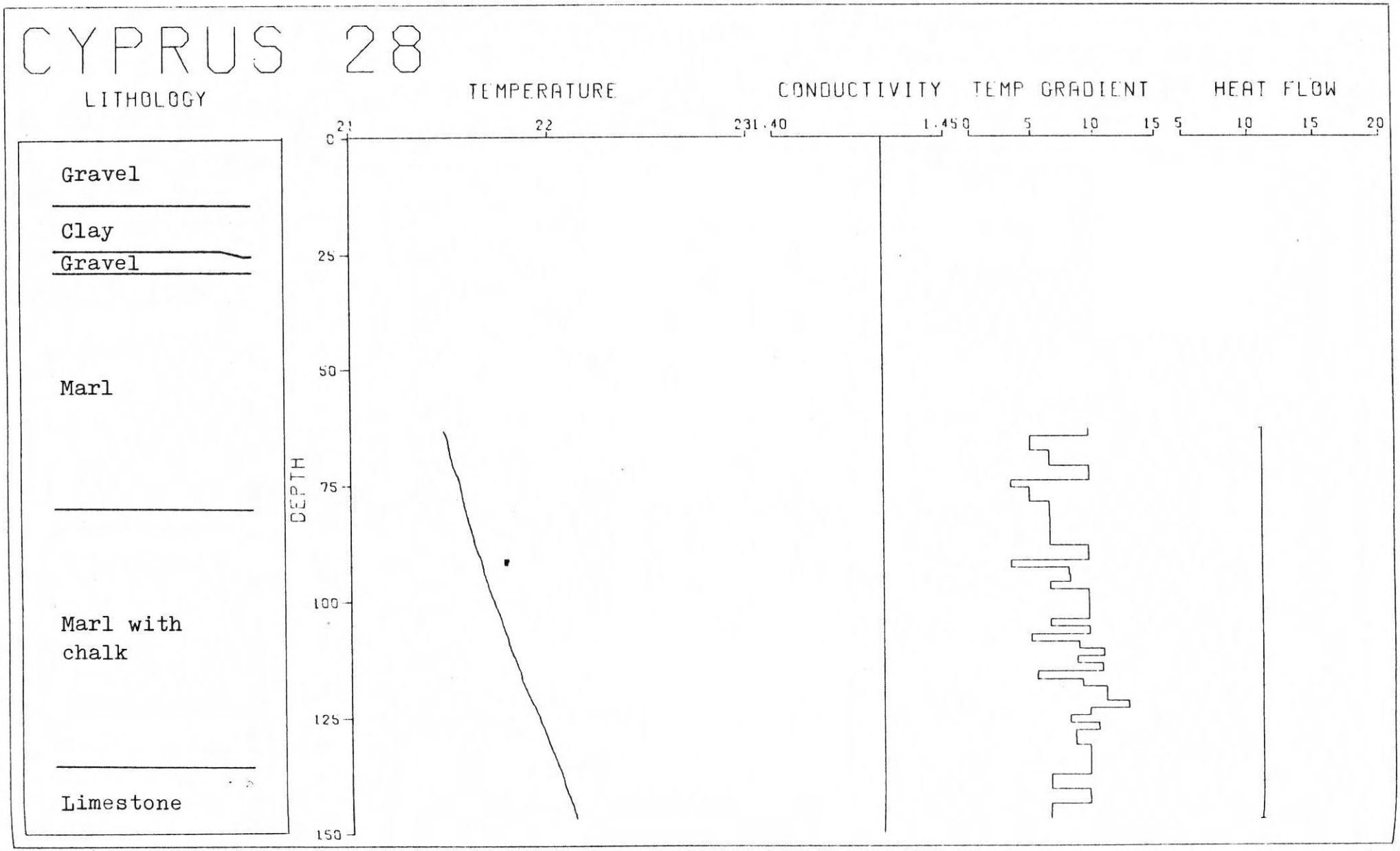
CYPRUS 28
LITHOLOGY
TEMPERATURE
CONDUCTIVITY
TEMP GRADIENT
HEAT FLOW
21
22
23
1.40
1.45
0
5
10
15
5
10
15
20
0
25
50
75
100
125
150
DEPTH
Gravel
Clay
Gravel
Marl
Marl with
chalk
Limestone

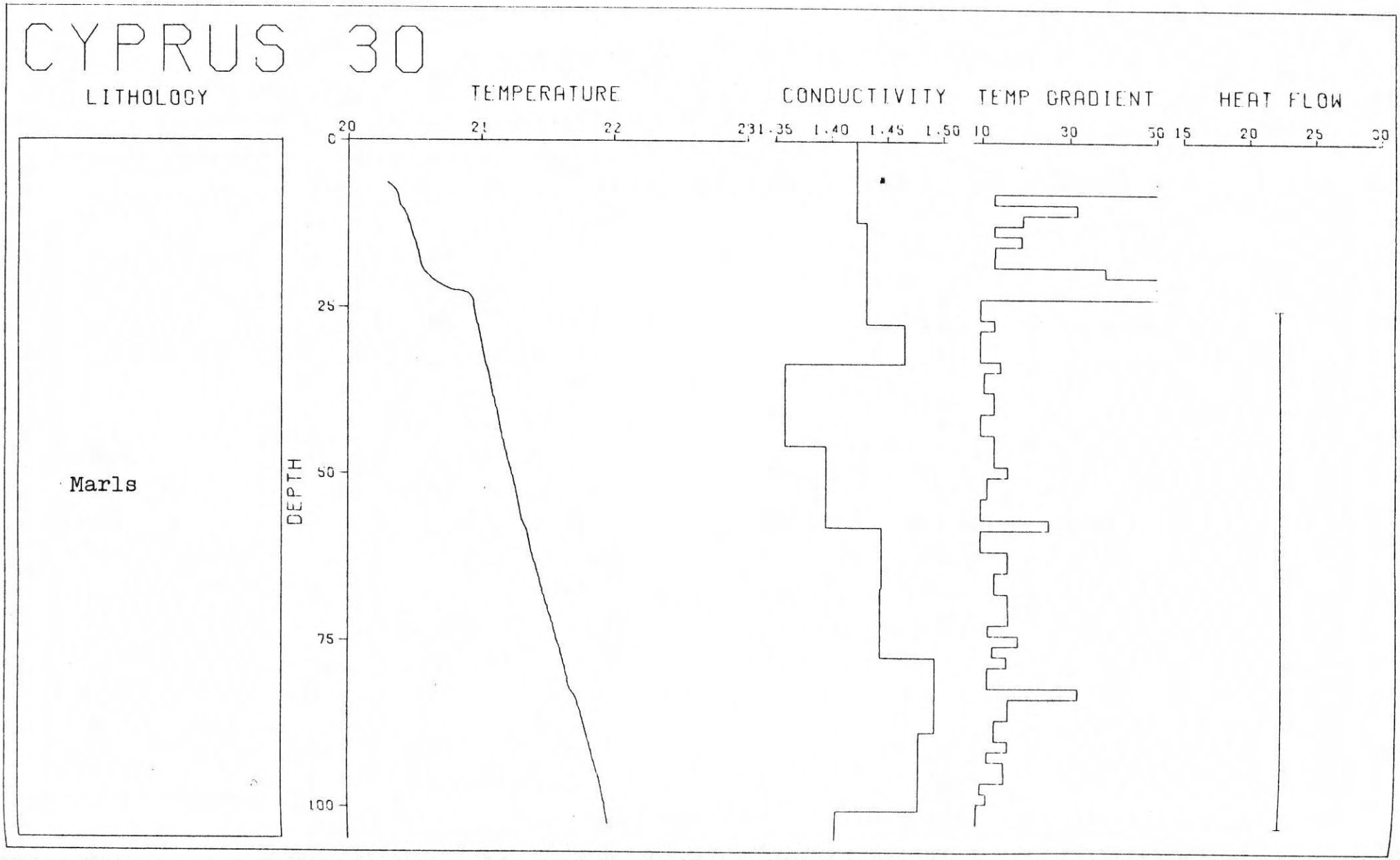
CYPRUS 30
LITHOLOGY
TEMPERATURE
CONDUCTIVITY
TEMP GRADIENT
HEAT FLOW
20
21
22
23
1.35
1.40
1.45
1.50
10
30
50
15
20
25
30
0
25
50
75
100
DEPTH
Marls

Appendix 2

The temperatures of the ground recorded in the selected locations for the period October 2009 to October 2010 are presented in this section.

The attached CD contains a complete set of records while a printed version follows for the:

1. Top layer temperature distribution, Saittas 31 October, 2010.
2. Borehole temperature distribution, all locations.
3. Boreholes temperature comparison, November, 2009 to October, 2010.

TOP LAYER TEMPERATURE
SAITTAS, 31 October, 2010

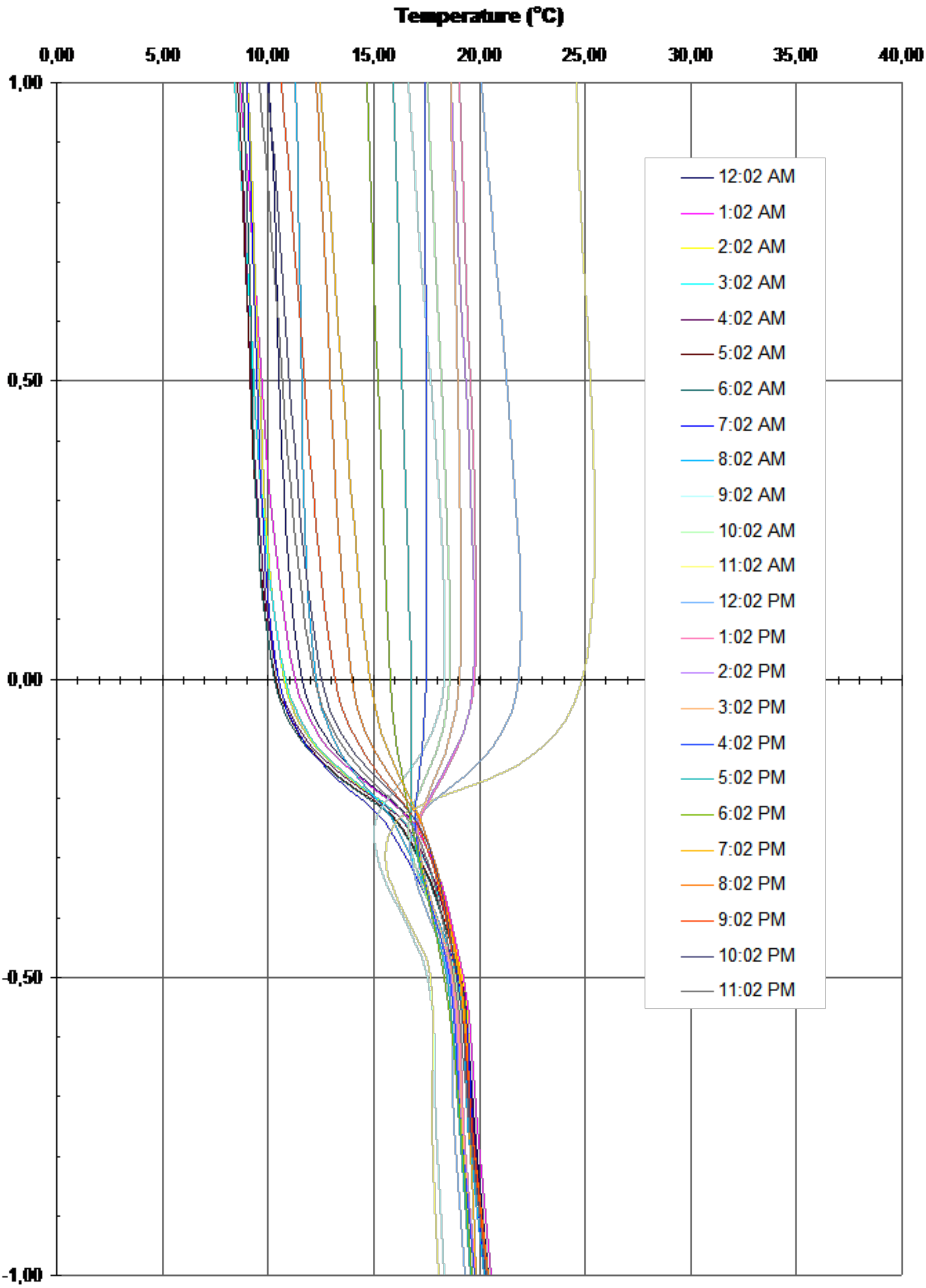

BOREHOLE TEMPERATURE
AGIA NAPA

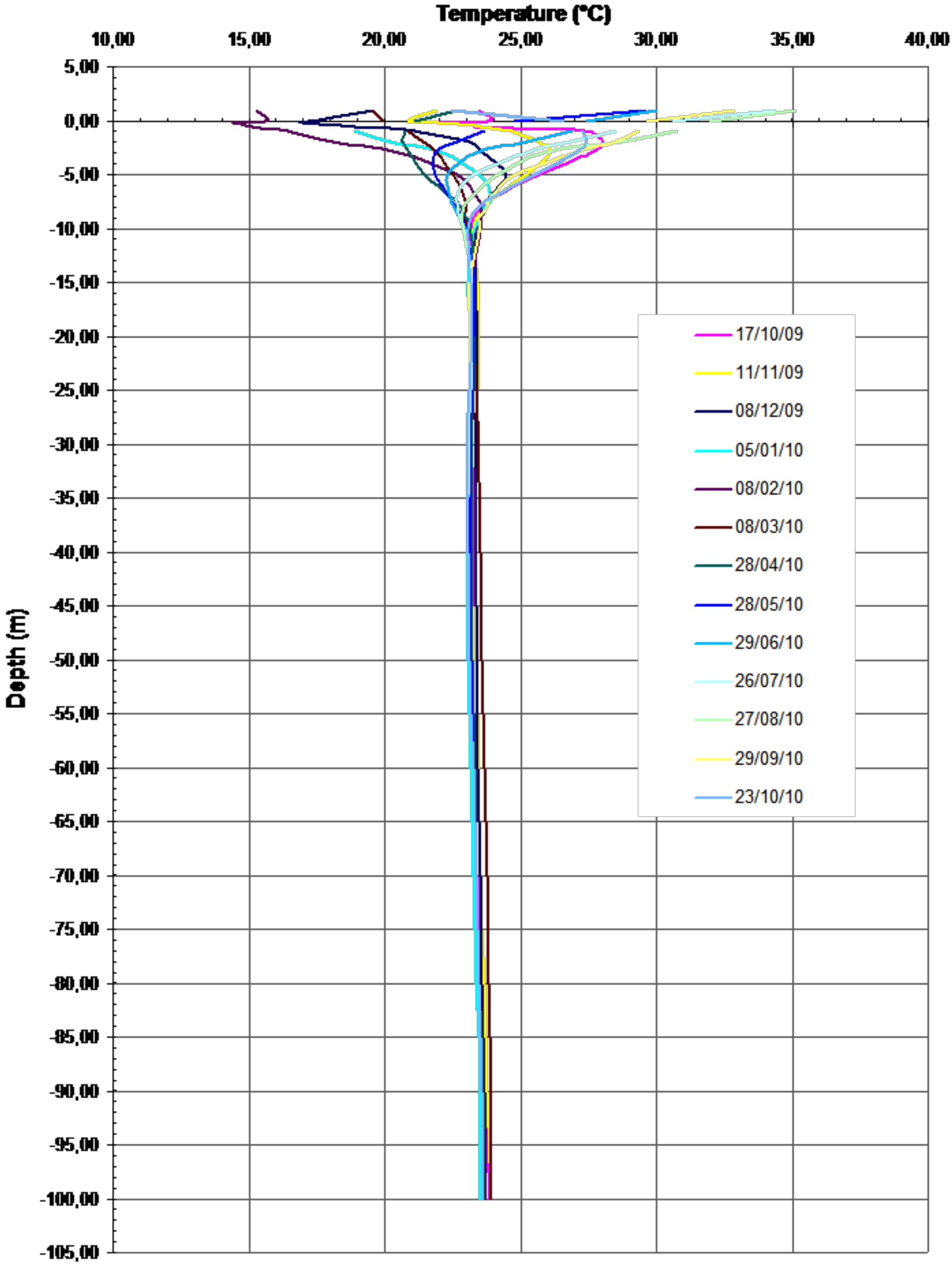

BOREHOLE TEMPERATURES
MENEOU

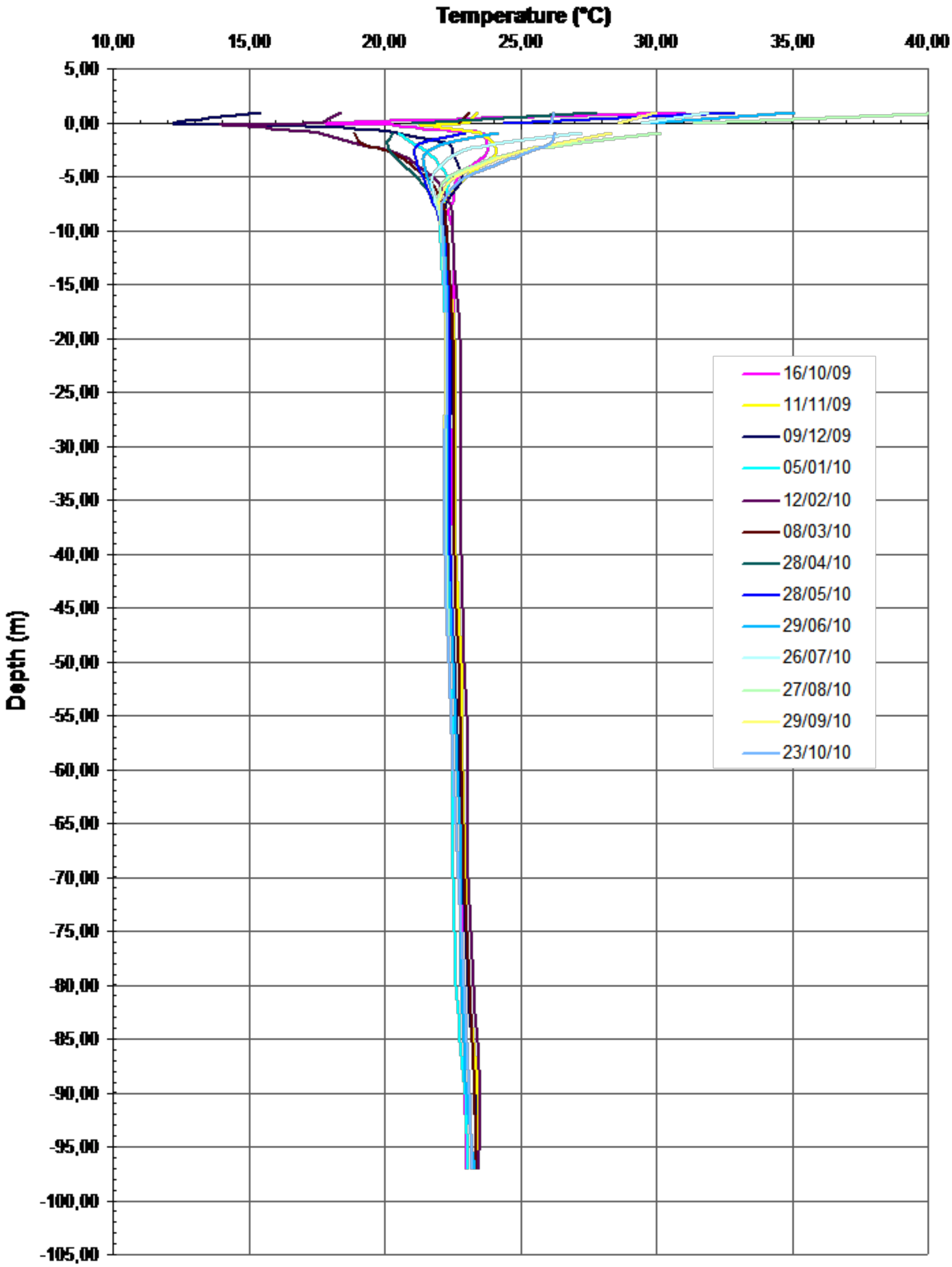

BOREHOLE TEMPERATURES
LAKATAMIA

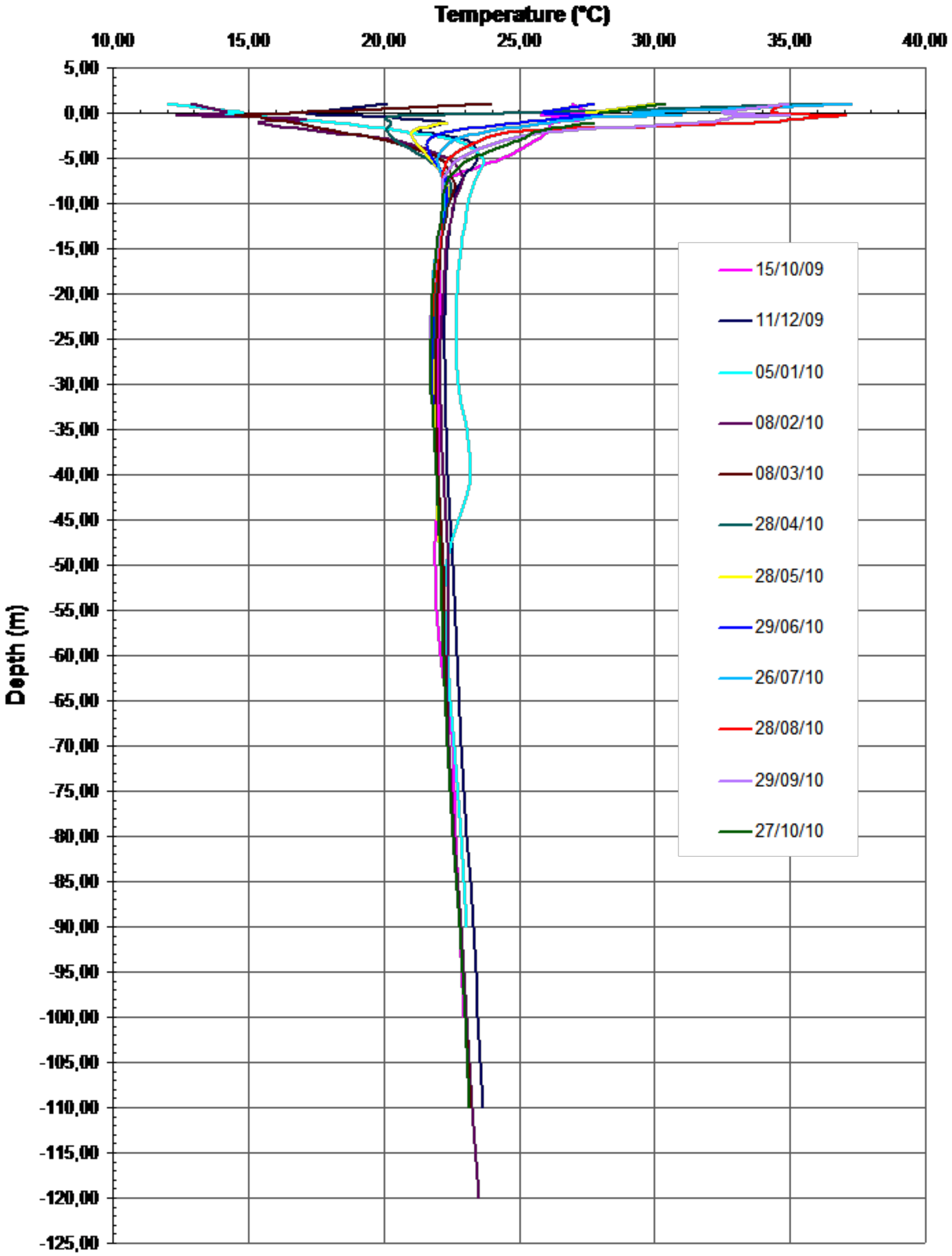

BOREHOLE TEMPERATURES
KMDES

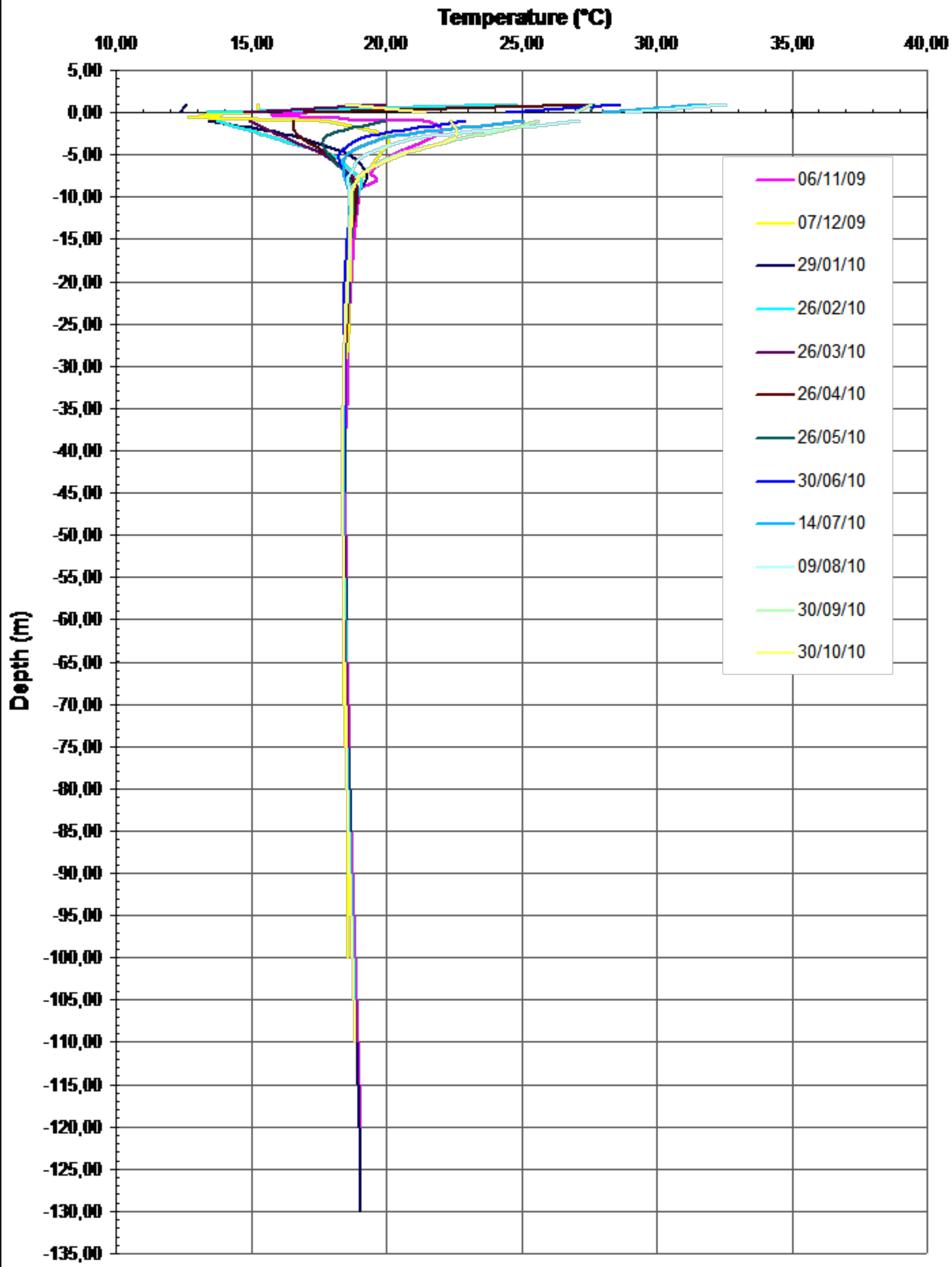

BOREHOLE TEMPERATURES
GEROSKIPOU

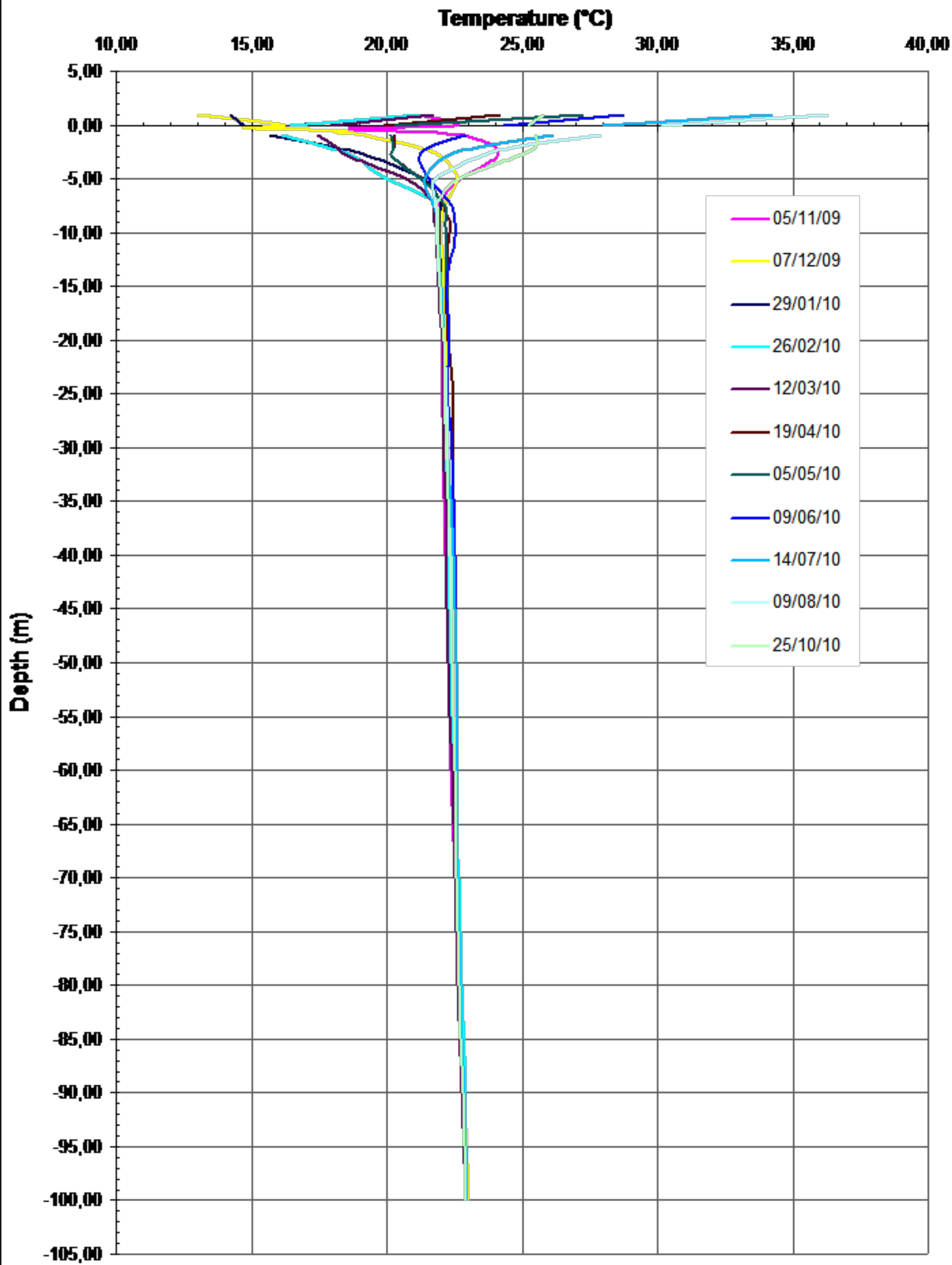

BOREHOLE TEMPERATURES
PRODROMI

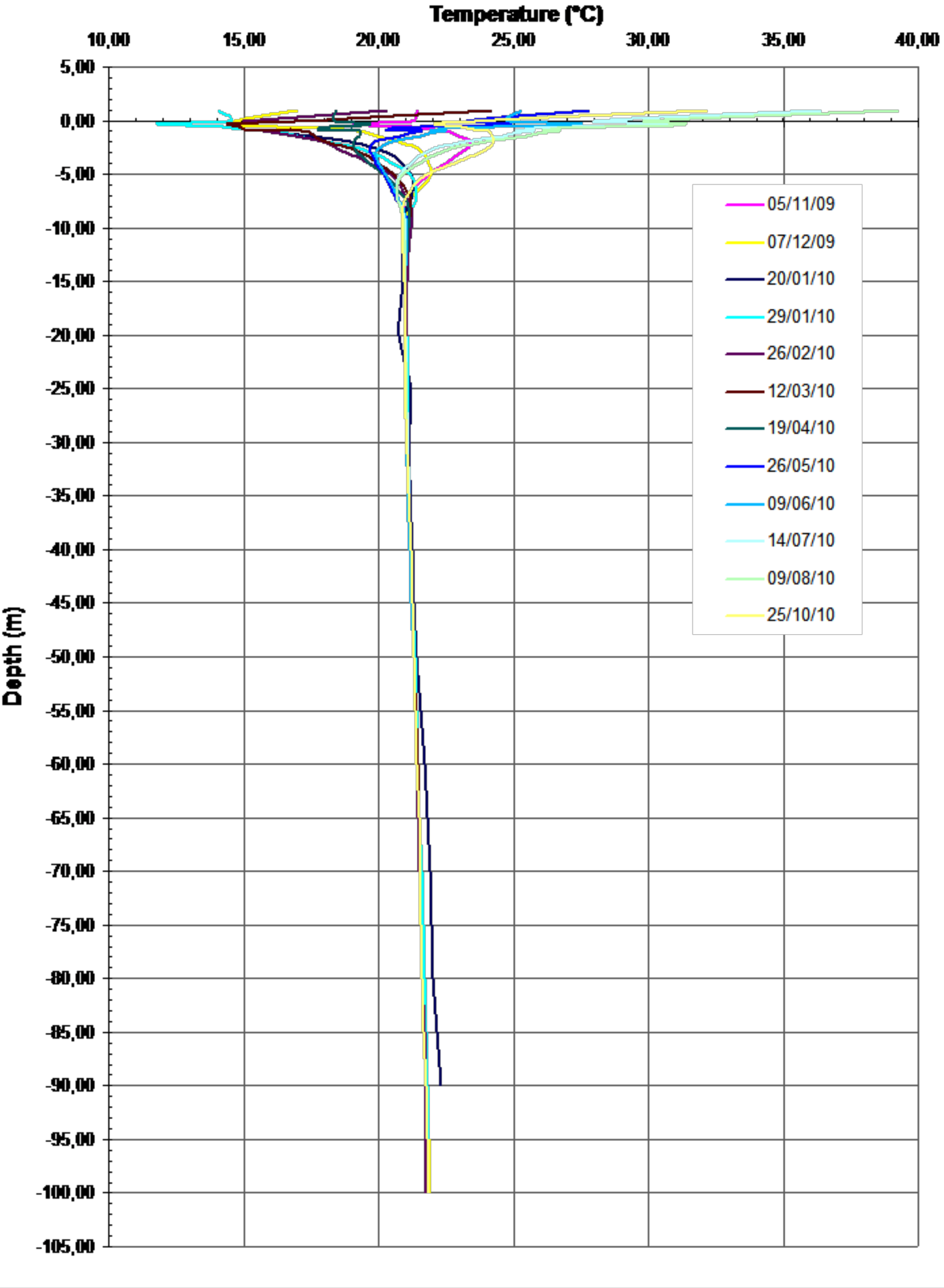

BOREHOLE TEMPERATURES
SAITTAS

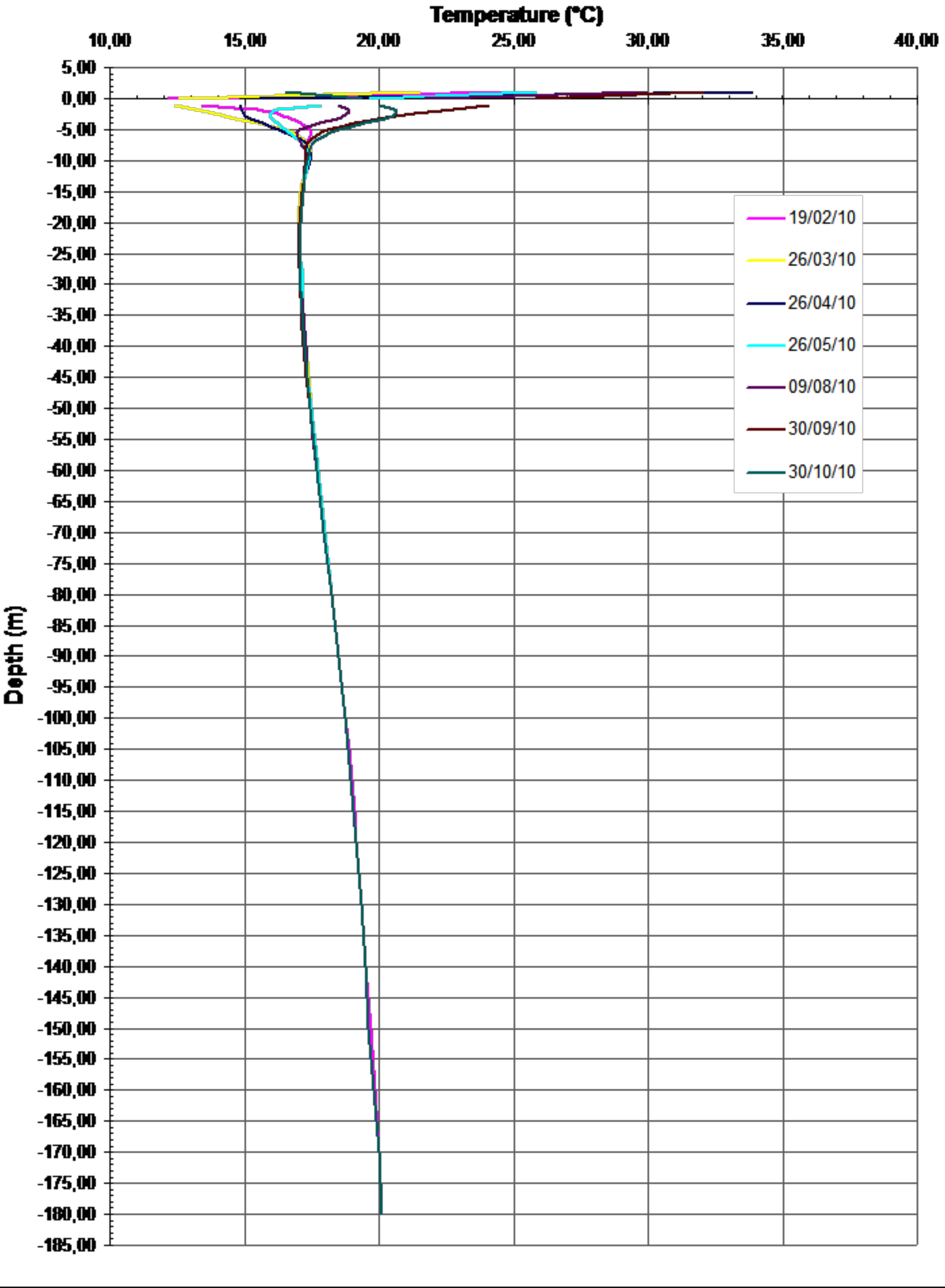

BOREHOLE TEMPERATURES
LIMASSOL

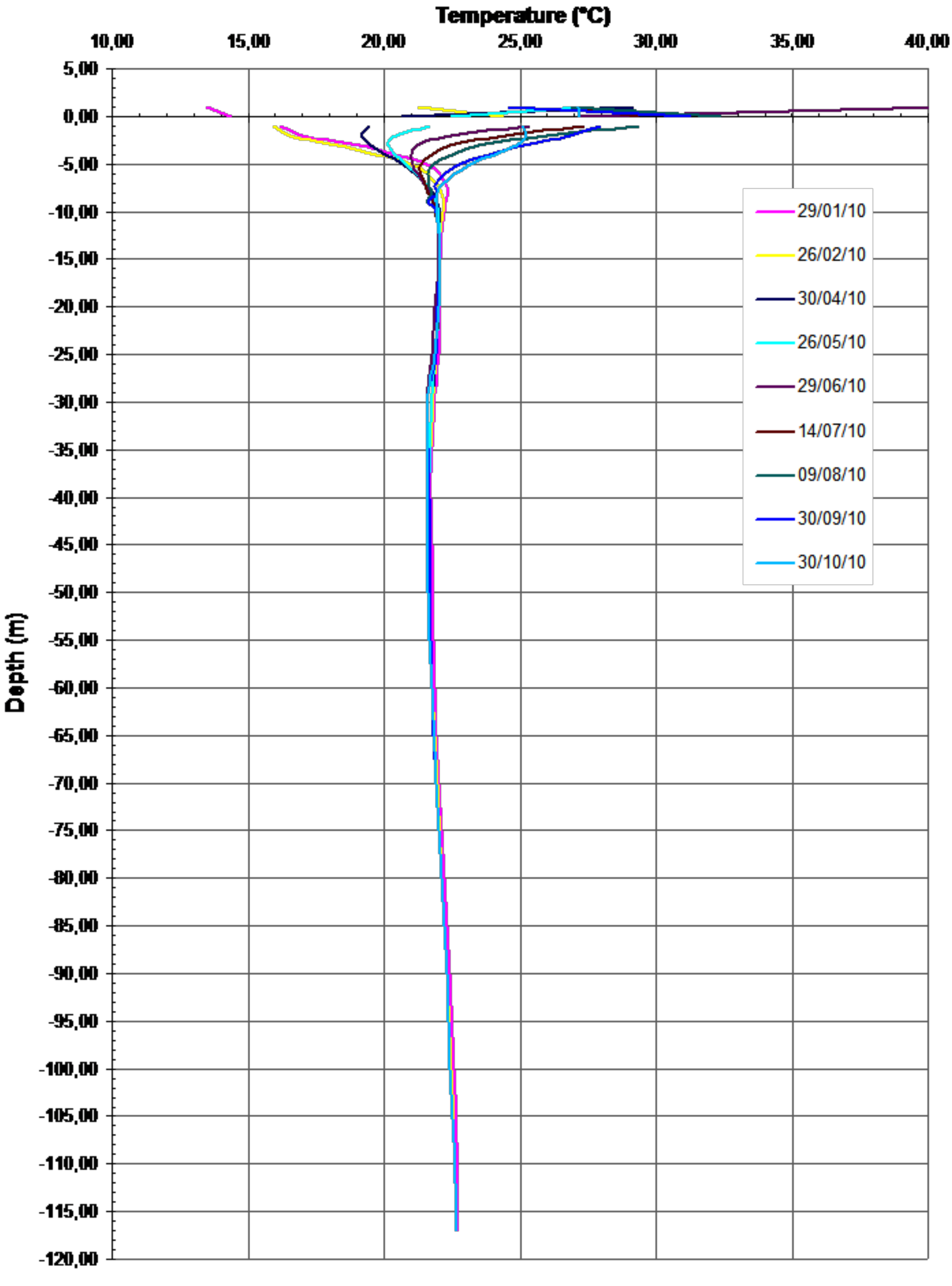

BOREHOLES TEMPERATURE CMPARISON
NOVEMBER 09

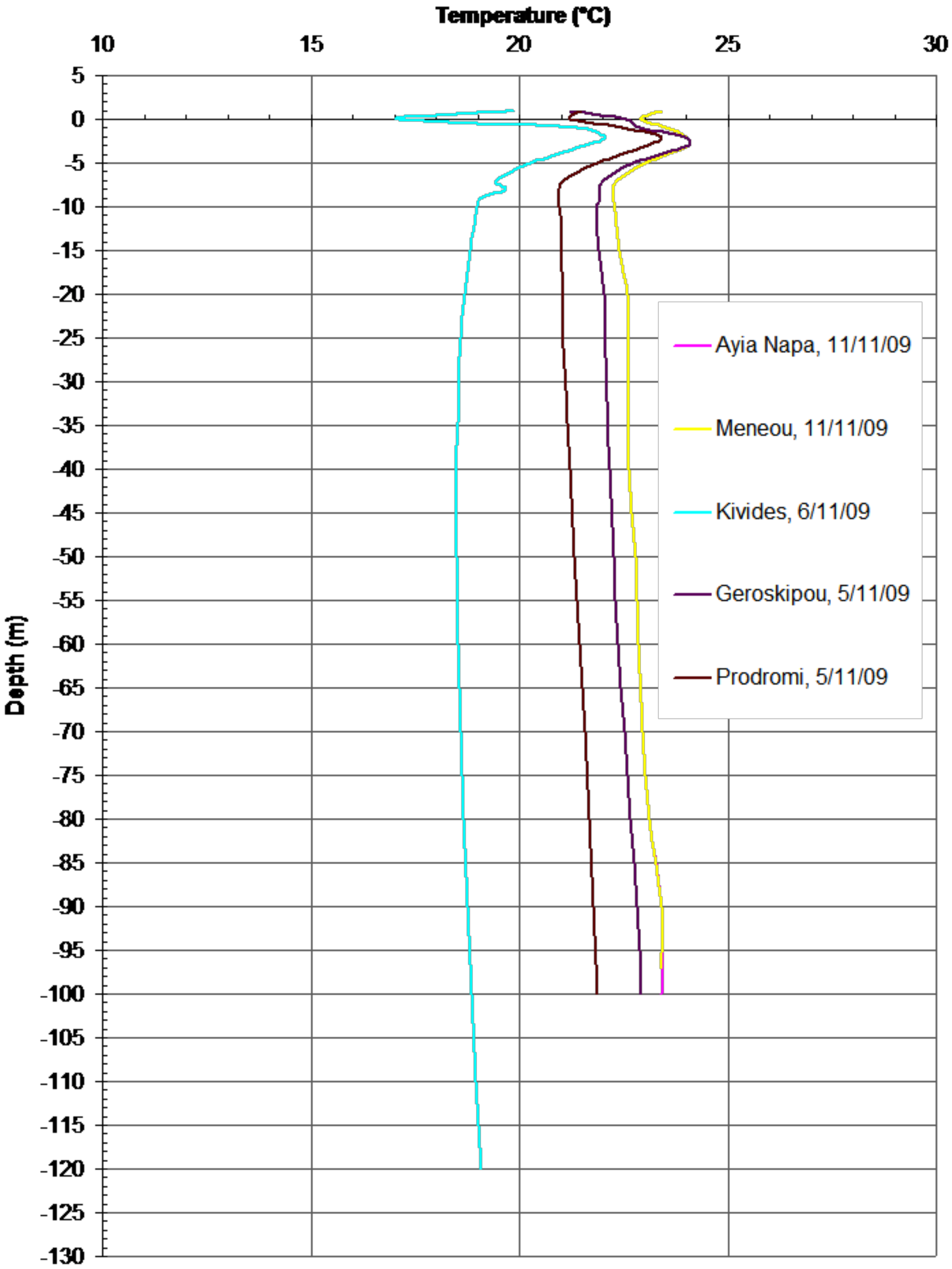

BOREHOLES TEMPERATURE CMPARISON
DECEMBER 2009

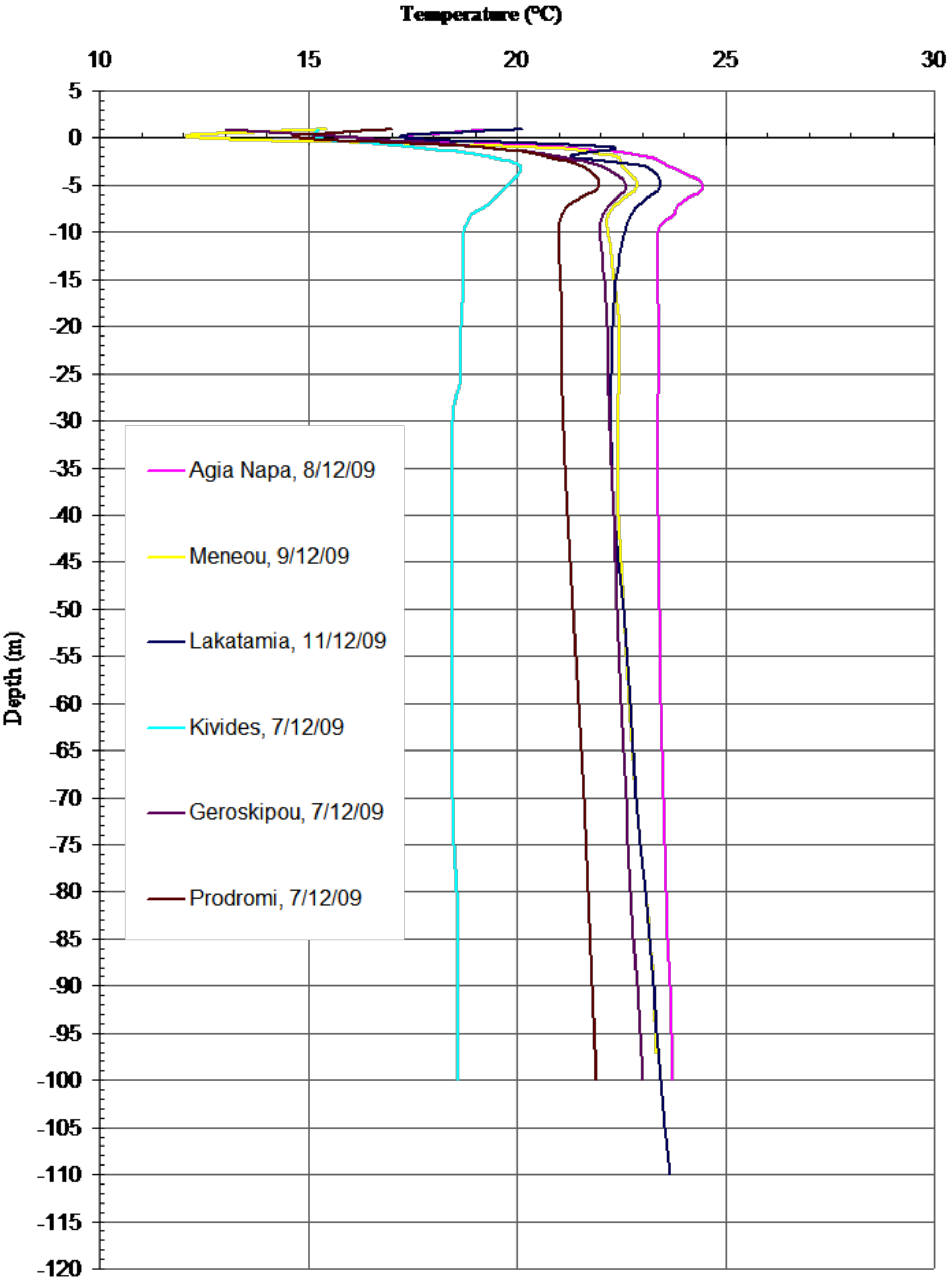

BOREHOLES TEMPERATURE CMPARISON
JANUARY 2010

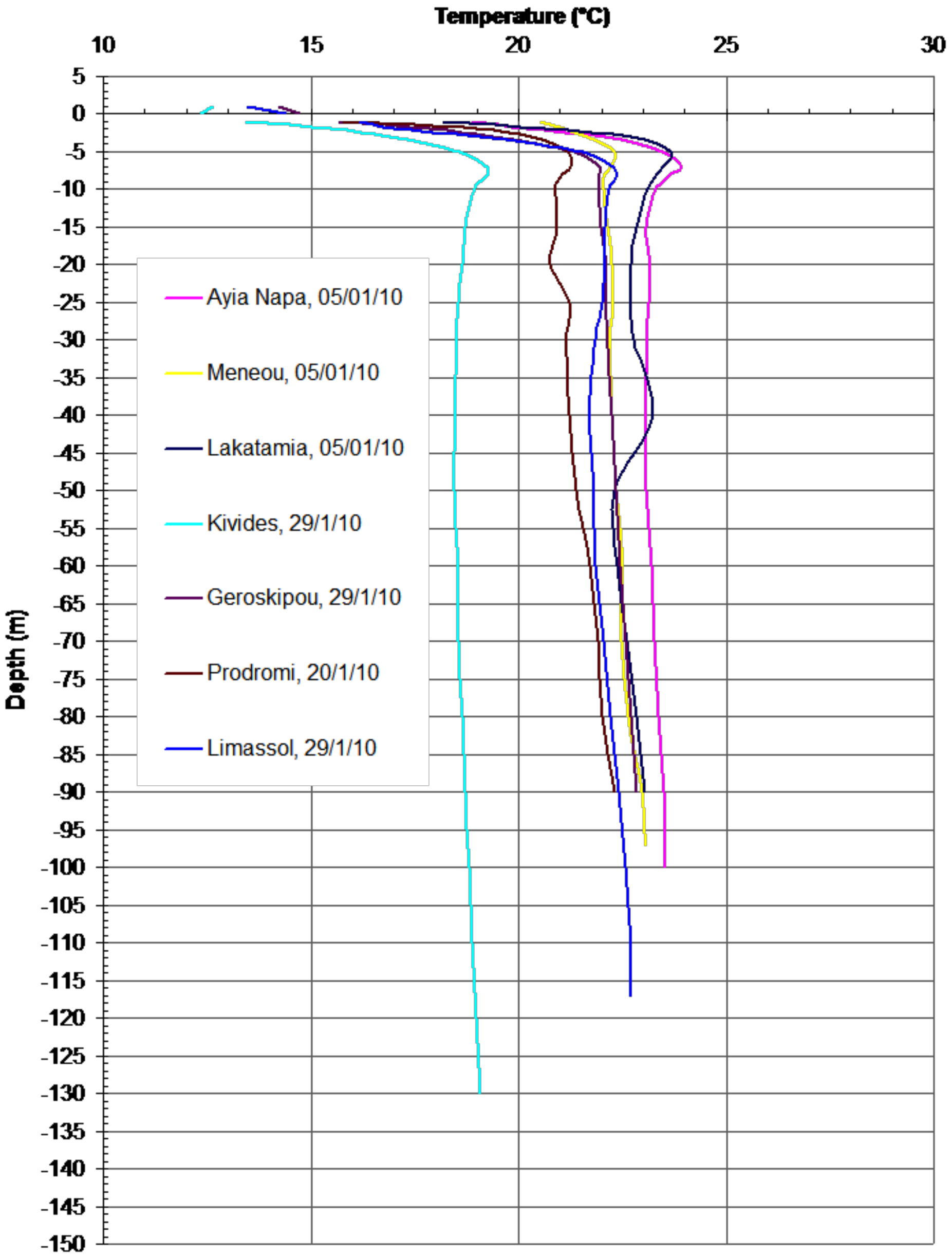

BOREHOLES TEMPERATURE CMPARISON
FEBRUARY 2010

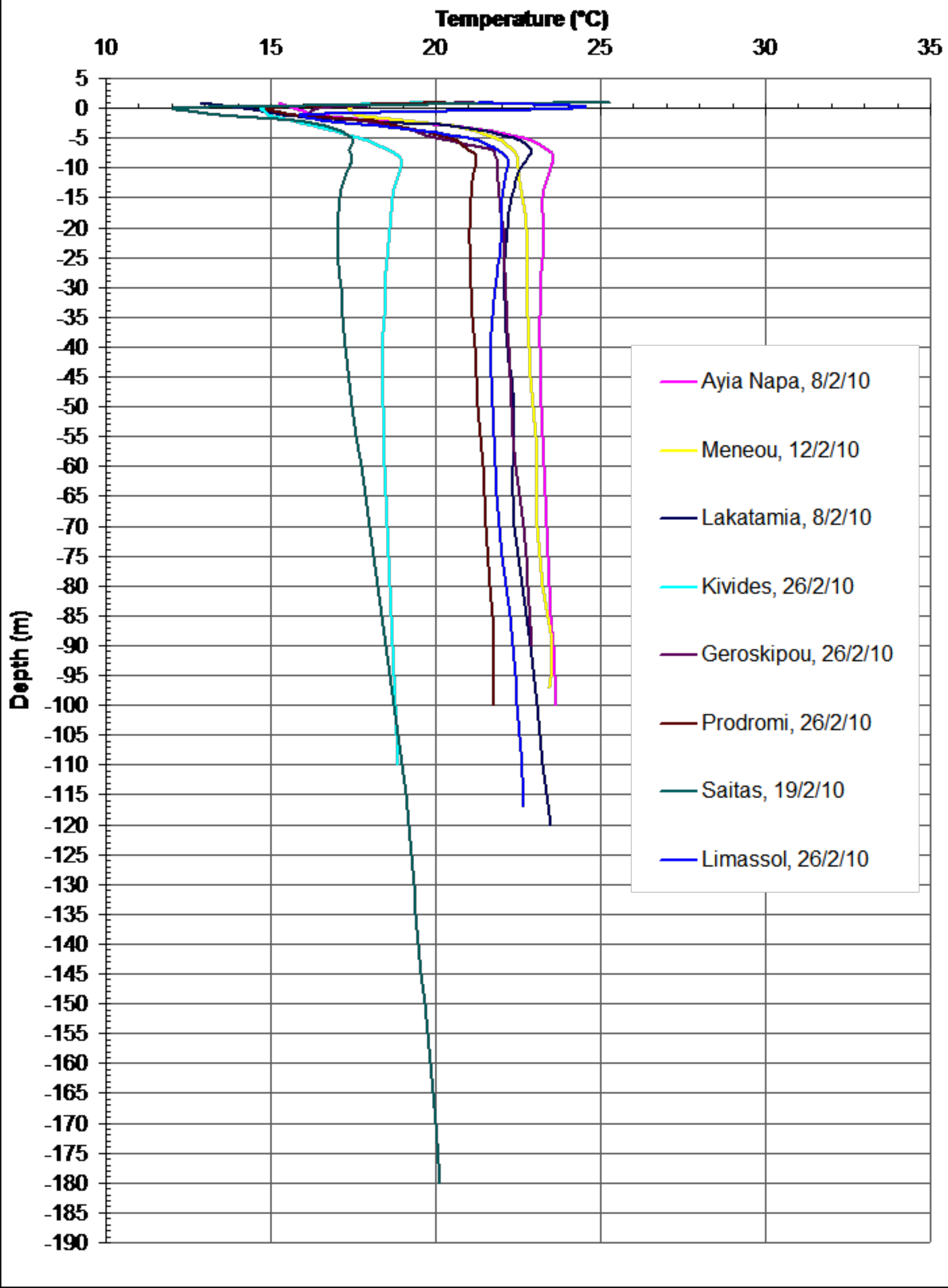

BOREHOLES TEMPERATURE CMPARISON
MARCH 2010

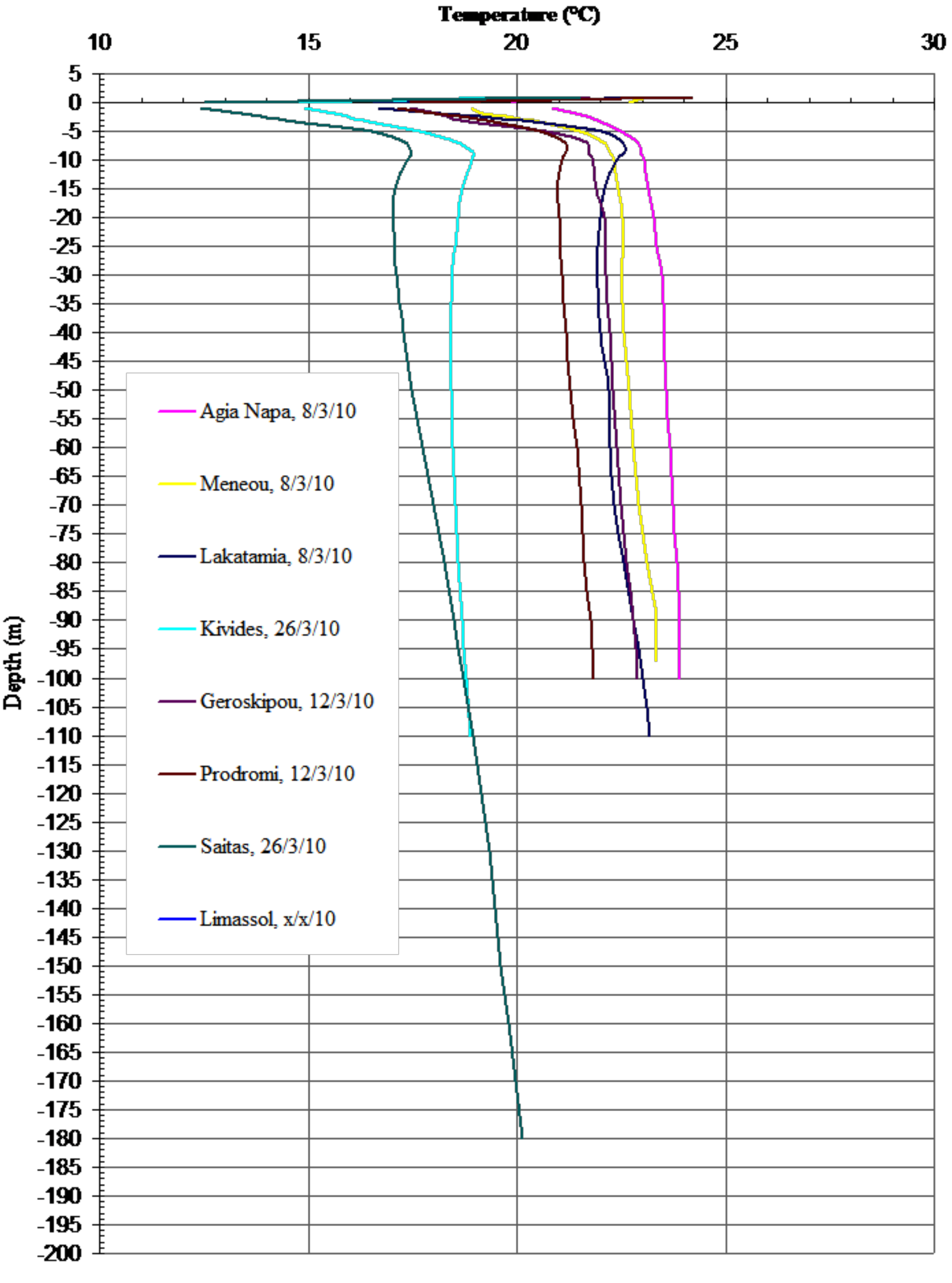

BOREHOLES TEMPERATURE CMPARISON
APRIL 2010

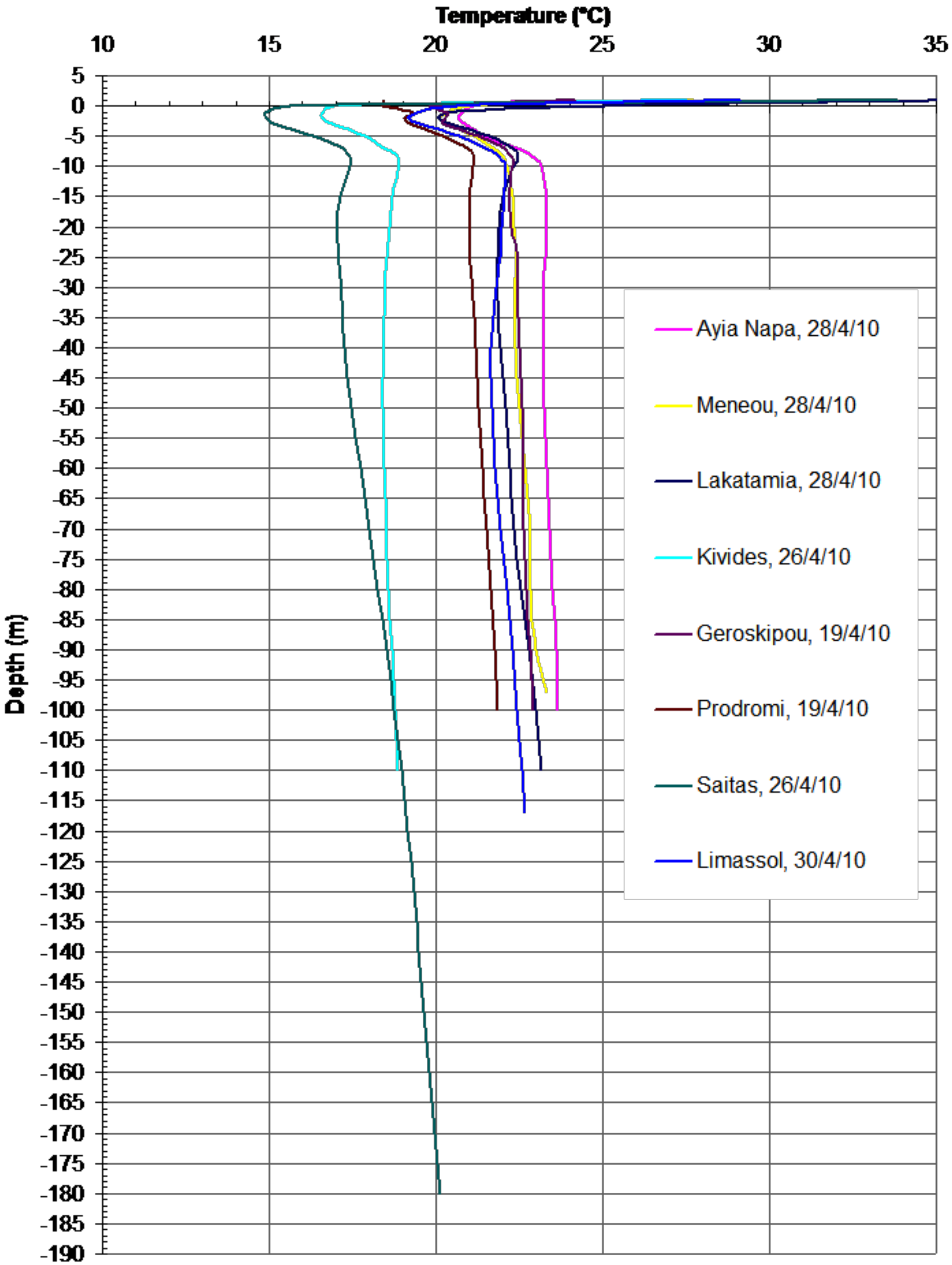

BOREHOLES TEMPERATURE COMPARISON
MAY 2010

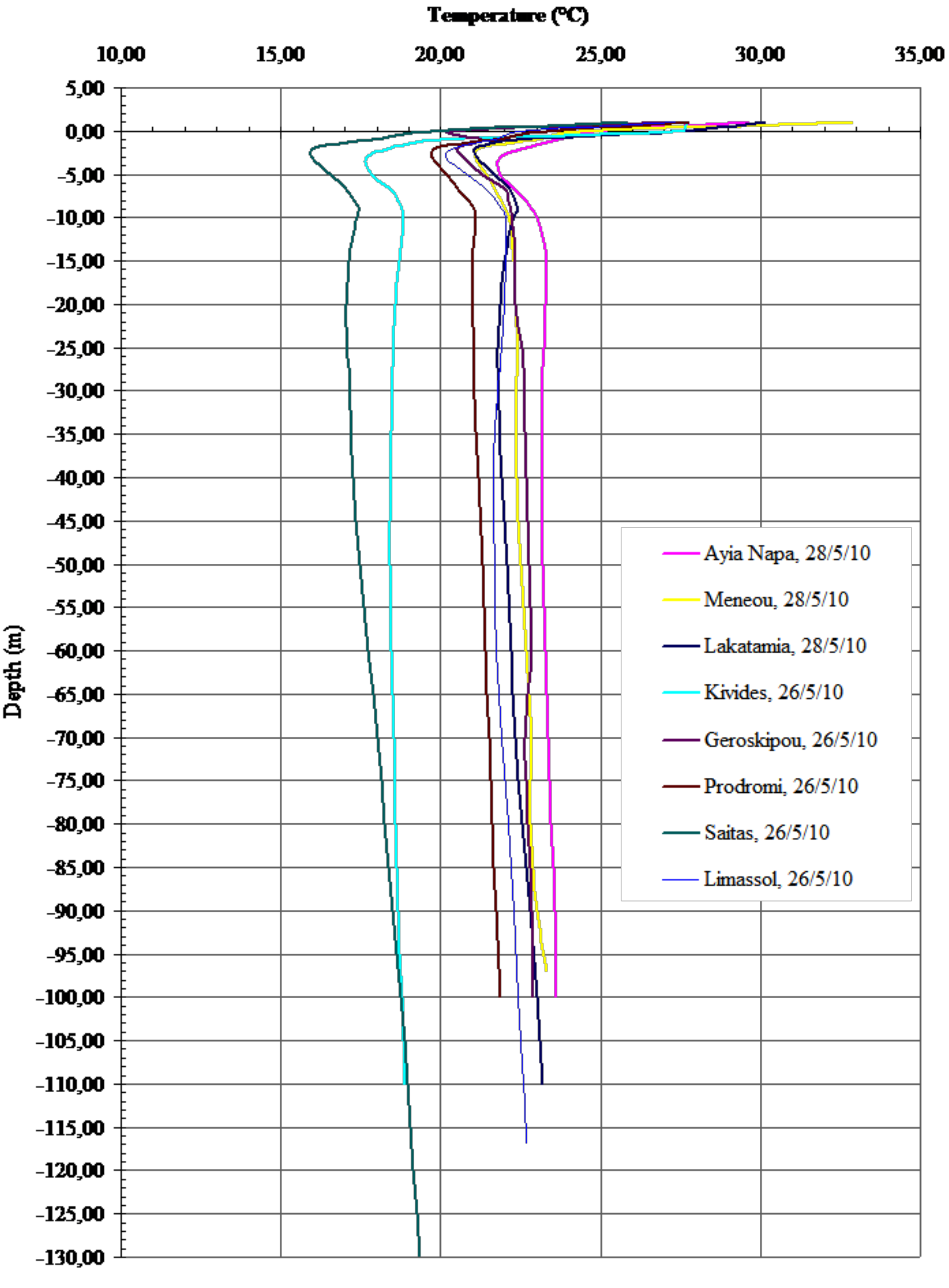

BOREHOLES TEMPERATURE COMPARISON
JUNE 2010

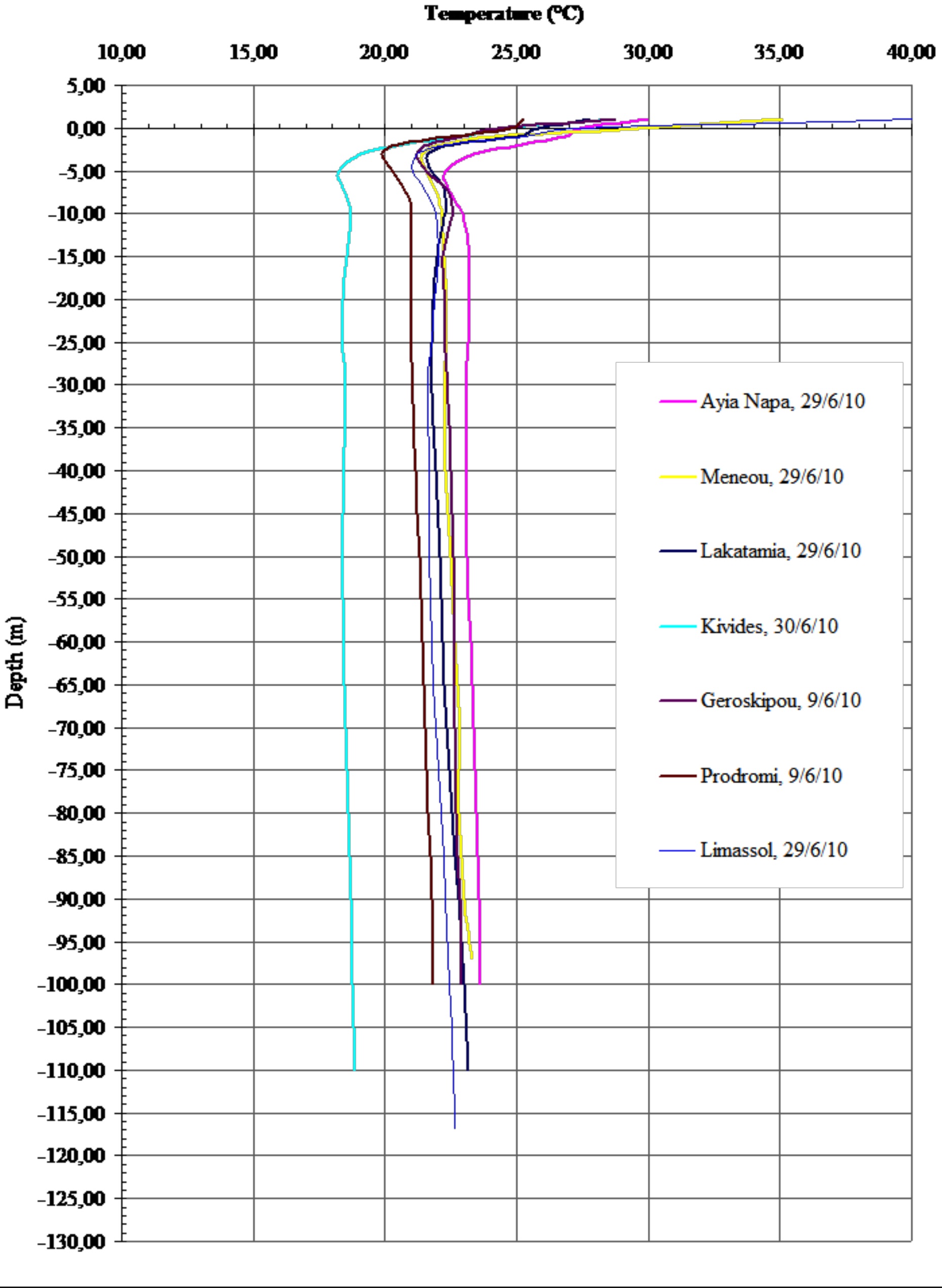

BOREHOLES TEMPERATURE COMPARISON
JULY 2010

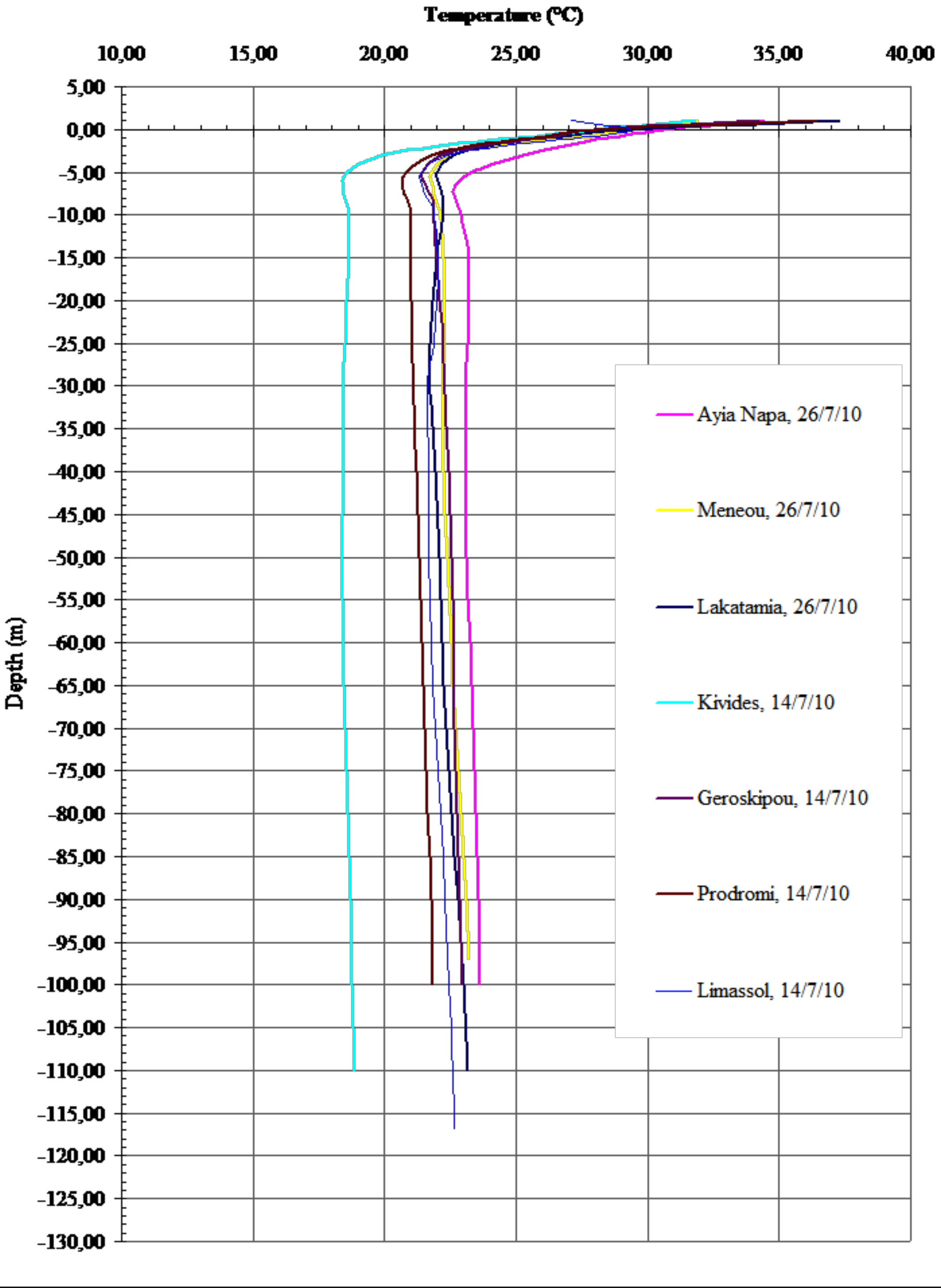

BOREHOLES TEMPERATURE COMPARISON
AUGUST 2010

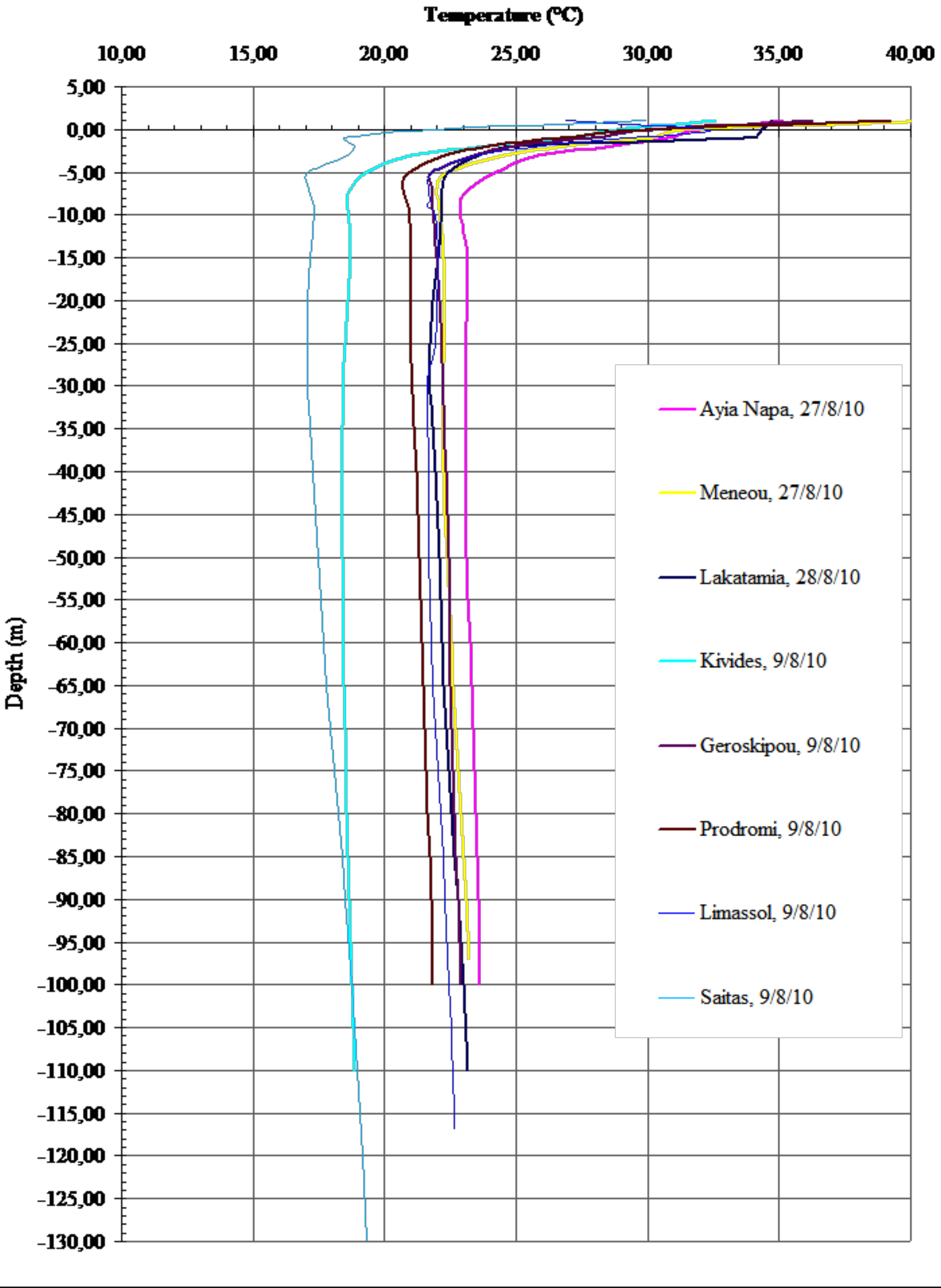

BOREHOLES TEMPERATURE COMPARISON
SEPTEMBER 2010

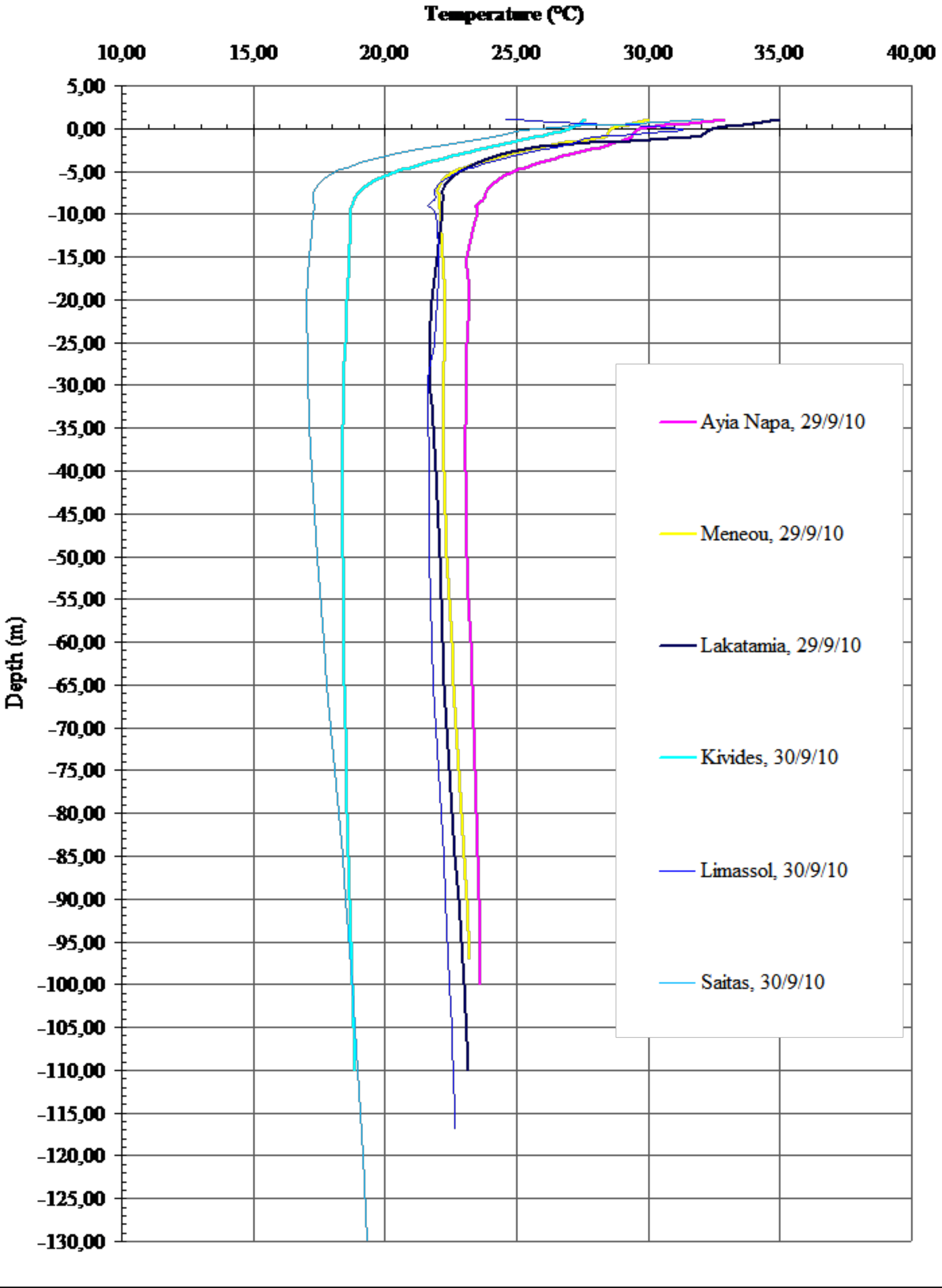

BOREHOLES TEMPERATURE COMPARISON
OCTOBER 2010

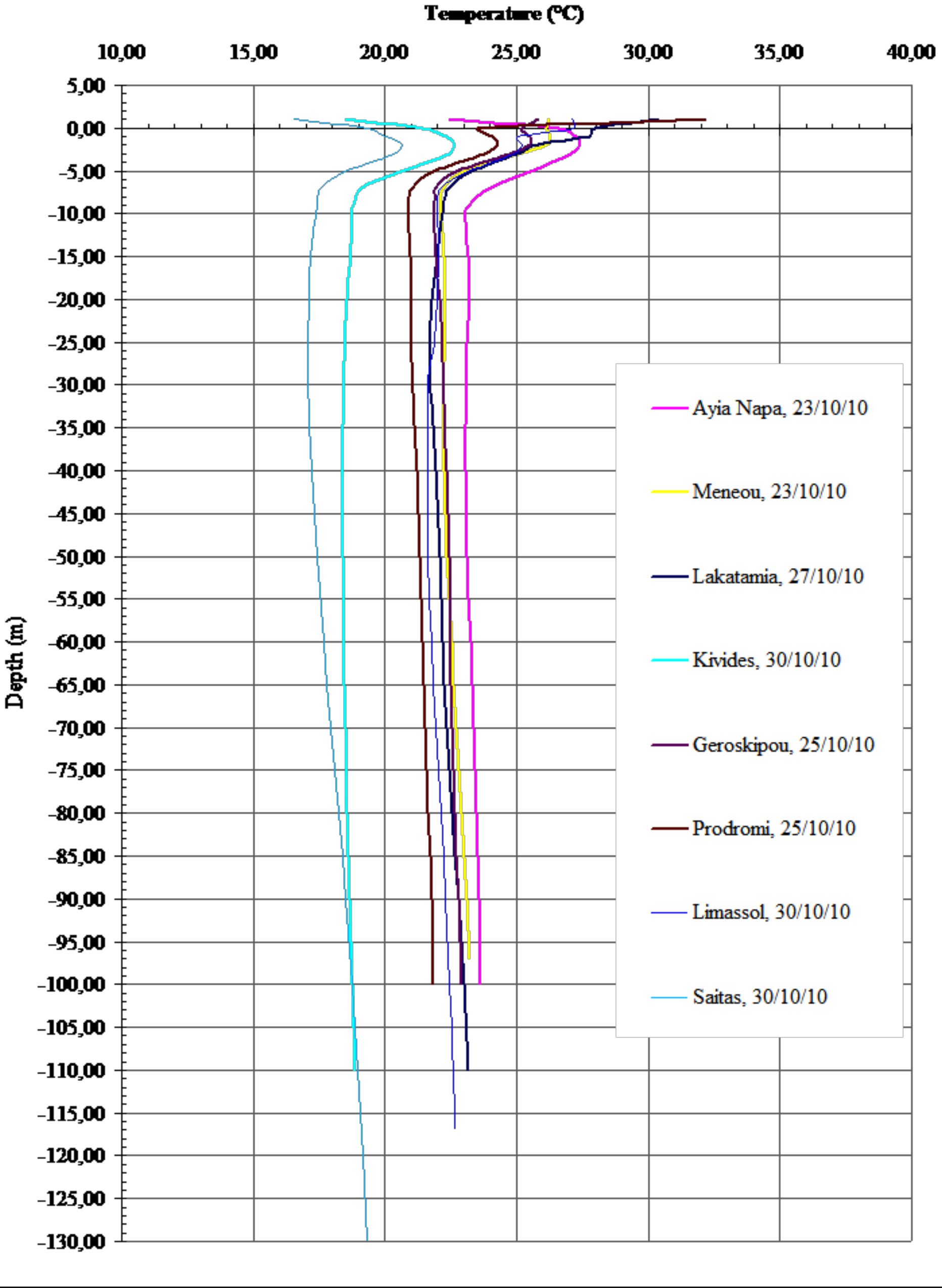

Appendix 3

The specifications of the Ground Coupled Heat Pumps (GCHP) used in the thesis are presented in this section.

1. GCHP used in the experiments in the Athalassa region in Nicosia (section 4.5: Testing of GCHP in Cyprus).
2. GCHP used in the simulations in Chapter 6, Section 6.3.

1. Specifications of the GCHP used in the experiments in the Athalassa region in Nicosia (section 4.5: Testing of GCHP in Cyprus).

PACKAGED UNITS

SPECIFICATION DATA SHEET

EX004

FHP MANUFACTURING HIGH-EFFICIENCY WATER SOURCE HEAT PUMPS

ELECTRICAL SPECIFICATIONS

Electrical Characteristics	Elect. Symbol	Compressor		Blower		Loop Pump		Min. Circuit Amps	Max. Fuse/ Breaker
		RLA	LRA	FLA	W	FLA	HP		
220-240/1/50	-8	3.30	16.00	0.90	75			5.00	15.00

MECHANICAL SPECIFICATIONS

Refrigerant: R-407C			
Air Coil			
Square M	Rows Deep	Tube O.D.	Fins/ cm
0.090	3	3/8"	5.5
Water Coil			
Type		Work Press	
Coaxial		3103 kPa	
Blower Size		Compr Type	
102 x 178		Reciprocating	
Net Weight		Ship Weight	
59 Kg		64 Kg	

BLOWER PERFORMANCE l/s

Available External Static Pressure (Pa, Gauge. Wet Coil and Filter Included)												
Blower Speed	25	50	75	100	125	150	175	200	225	250	275	300
High	126	117	106	96	85							
Medium	118	109	95	81								
Low	90	79	65									

CE

FLUID PRESSURE DROP

Fluid Flow (l/s)	Pressure Drop (kPa)
0.10	10.4
0.13	15.6
0.15	21.6
0.20	36.3
0.27	54.2

ISO 13256-1 PERFORMANCE DATA Rated at 142 l/s air and 0.19 l/s fluid flow

Water Loop				Ground Water				Ground Loop (Ext. Range Required)			
Cooling		Heating		Cooling		Heating		Cooling		Heating	
Capacity	EER	Capacity	COP	Capacity	EER	Capacity	COP	Capacity	EER	Capacity	COP
3.38	3.2	4.52	3.7	3.75	4.3	3.39	3.3	3.50	3.5	2.26	2.8

CAPACITY DATA All performance at 142 l/s air and 0.19 l/s fluid flow

COOLING

EFT Range (Standard) 10°C to 40°C — EFT Range (Ext. Range Option) 7°C to 43°C

Entering Fluid Temp. (°C)	Entering Air Temp. (°C)	Total Capacity (kW)	Sensible Capacity (kW)	Sensible to Total Ratio	Power Input (kW)	Heat of Reject (kW)	EER
10°		3.29	1.92	0.58	0.81	4.10	4.0
20°	21°db	3.08	1.83	0.59	0.93	4.00	3.3
25°	16°wb	2.97	1.79	0.60	0.98	3.95	3.0
30°		2.86	1.75	0.61	1.04	3.90	2.8
40°		2.65	1.69	0.64	1.15	3.80	2.3
10°		3.57	2.55	0.71	0.82	4.39	4.4
20°	25°db	3.34	2.42	0.73	0.93	4.27	3.6
25°	17°wb	3.22	2.37	0.74	0.99	4.21	3.3
30°		3.10	2.33	0.75	1.04	4.15	3.0
40°		2.87	2.24	0.78	1.16	4.03	2.5
10°		3.86	2.67	0.69	0.82	4.68	4.7
20°	27°db	3.60	2.54	0.71	0.94	4.54	3.8
25°	19°wb	3.48	2.49	0.72	0.99	4.47	3.5
30°		3.35	2.44	0.73	1.05	4.40	3.2
40°		3.10	2.36	0.76	1.16	4.27	2.7
10°		4.19	3.02	0.72	0.83	5.02	5.0
20°	30°db	3.91	2.87	0.73	0.95	4.86	4.1
25°	21°wb	3.78	2.81	0.74	1.00	4.78	3.8
30°		3.64	2.75	0.76	1.06	4.70	3.4
40°		3.37	2.66	0.79	1.17	4.54	2.9

Units are complete packages containing compressor, reversing valve, capillary tube metering device, and heat exchangers. Also included are safety controls: Overload protection for motors, high and low refrigerant pressure switches and solid state lock-out circuit. Refrigerant R-407C

Extended range option includes expansion valve metering device and insulated water coil

Performance based on ARI/ISO rated air flow, fluid flow and voltage. For conditions other than rated, consult the FHP EAD selection software. Due to variations in installation actual performance may vary marginally from tabulated values.

HEATING

EFT Range (Standard) 10°C to 27°C — EFT Range (Ext. Range Option) -4°C to 27°C

Entering Fluid Temp. (°C)	Entering Air Temp. (°C)	Total Capacity (kW)	Power Input (kW)	Heat of Abs. (kW)	COP
10°		3.59	1.02	2.57	3.5
15°	15°	4.18	1.12	3.06	3.7
20°		4.78	1.22	3.56	3.9
25°		5.37	1.32	4.05	4.1
10°		3.42	1.04	2.38	3.3
15°	20°	3.98	1.14	2.84	3.5
20°		4.55	1.24	3.31	3.7
25°		5.11	1.34	3.77	3.8
10°		3.22	1.06	2.16	3.0
15°	25°	3.75	1.16	2.59	3.2
20°		4.28	1.26	3.02	3.4
25°		4.81	1.37	3.45	3.5

LOW TEMP HEATING

Extended Range Option Required Antifreeze Required

-4°		1.89	0.74	1.14	2.5
0°	15°	2.35	0.82	1.53	2.9
5°		2.94	0.92	2.01	3.2
-4°		1.80	0.76	1.04	2.4
0°	20°	2.24	0.84	1.40	2.7
5°		2.80	0.94	1.86	3.0
-4°		1.69	0.77	0.92	2.2
0°	25°	2.11	0.85	1.26	2.5
5°		2.63	0.96	1.68	2.8

FHP MANUFACTURING COMPANY
601 N.W. 65th Court - Fort Lauderdale, FL 33309

2. GCHP used in the simulations in Chapter 6, Section 6.3.

Details from the specifications catalogue for the Envision NSW050 model manufactured by WaterFurnace International Inc follow.

Model Nomenclature

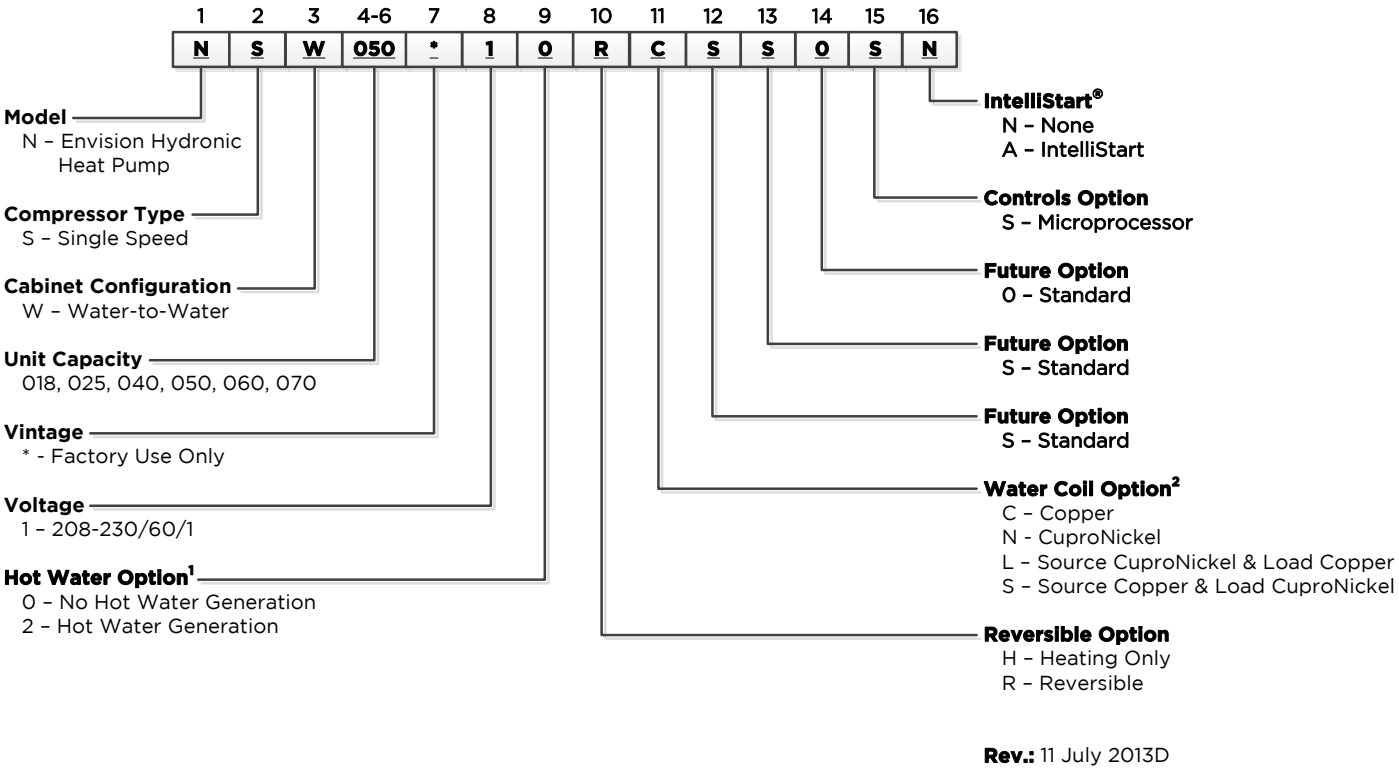

Rev.: 11 July 2013D

NOTES: 1 – Available on 040, 050, 060, and 075 only. Hot water generator requires field installed external pump kit.
2 – NSW018 and NSW025 **heating only** models are available only with copper double wall vented load coax for potable water.

All Envision Series product is safety listed under UL1995 thru ETL and performance listed with AHRI in accordance with standard 13256-2. The Envision Series is also ENERGY STAR® rated.

The Envision Series

NSW Features

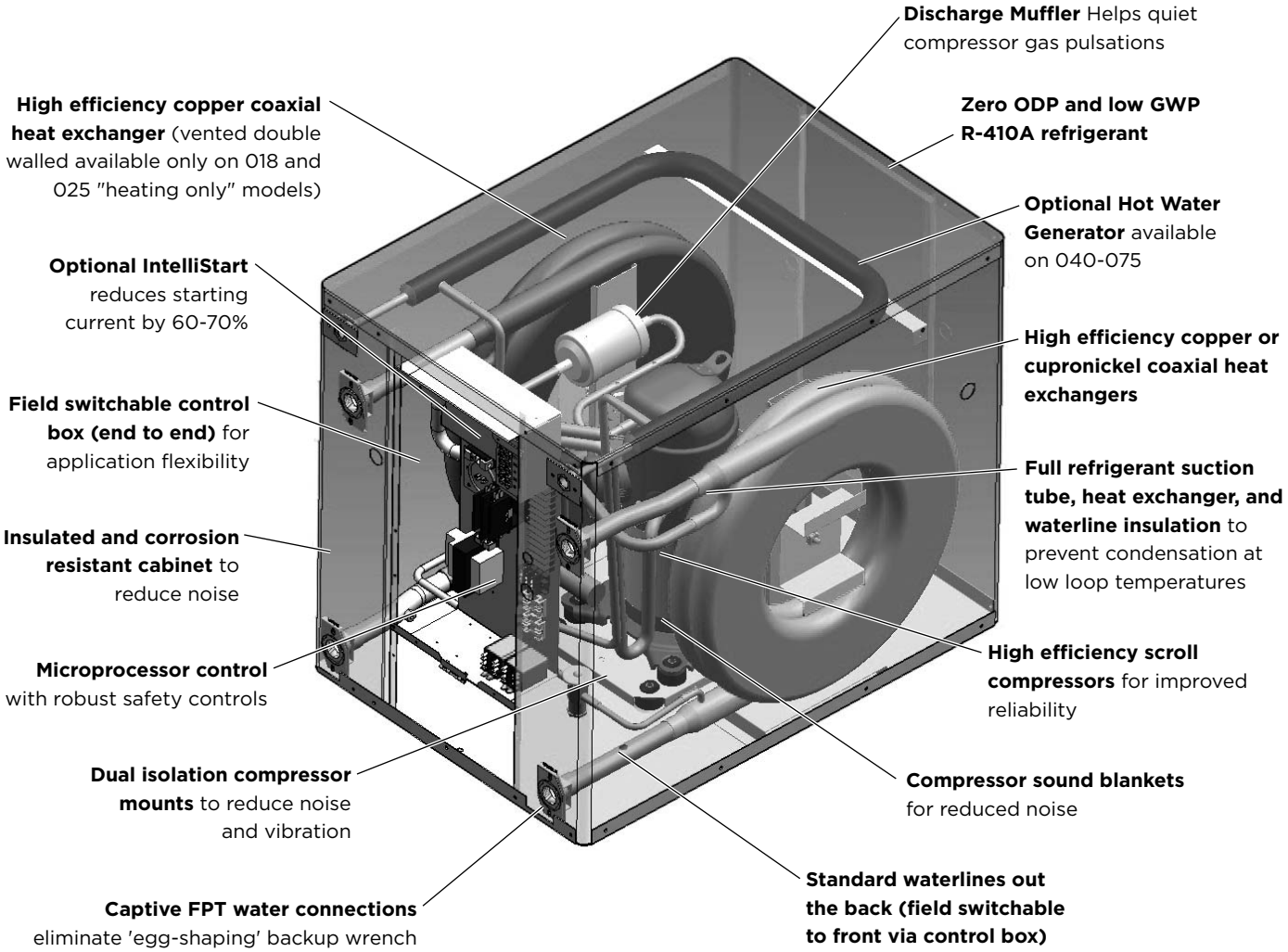

Dimensional Data

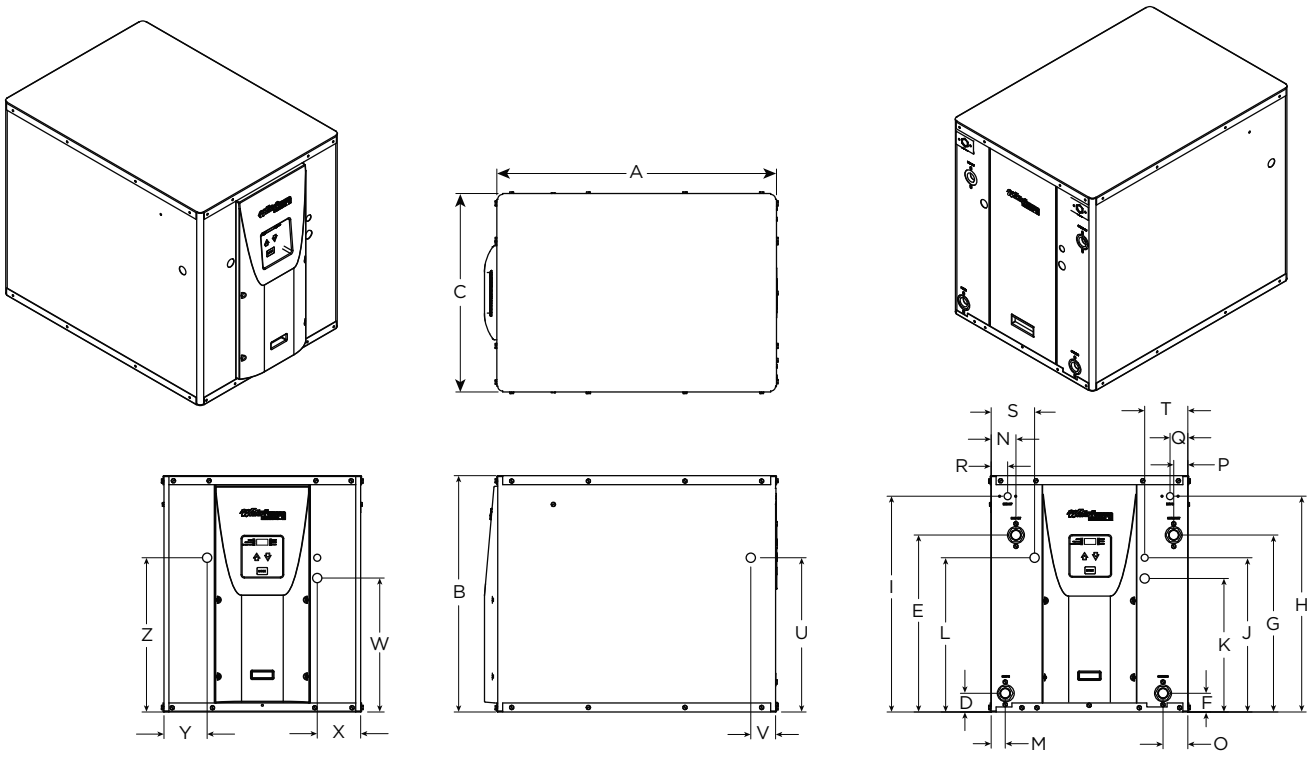

NOTE: Plastic front panel extends 1.4" (3.56 cm) beyond front of cabinet.

8/09/13

Model		Overall Cabinet			Water Connections									Electrical Knockouts		
		A	B	C	D	E	F	G	H	I				J	K	L
		Depth	Height	Width	Load Liquid In	Load Liquid Out	Source Liquid In	Source Liquid Out	HWG In	HWG Out	Load Water FPT	Source Water FPT	HWG Water FPT	1/2 in. cond Low Voltage	3/4 in. cond Ext Pump	3/4 in. cond Power Supply
018	in.	23.5	26.1	19.5	10.0	22.2	10.0	22.2	-	-	1 in.	1 in.	-	16.0	14.2	14.2
	cm.	59.7	66.3	49.5	25.4	56.4	25.4	56.4	-	-	25.4 mm	25.4 mm	-	40.6	36.1	36.1
025	in.	23.5	26.1	19.5	10.0	22.2	10.0	22.2	-	-	1 in.	1 in.	-	16.0	14.2	14.2
	cm.	59.7	66.3	49.5	25.4	56.4	25.4	56.4	-	-	25.4 mm	25.4 mm	-	40.6	36.1	36.1
040	in.	31.0	26.2	22.0	2.1	19.6	2.1	19.6	23.9	23.9	1 in.	1 in.	1/2 in.	17.1	14.8	17.1
	cm.	78.7	66.5	55.9	5.3	49.8	5.3	49.8	60.7	60.7	25.4 mm	25.4 mm	12.7 mm	43.4	37.6	43.4
050	in.	31.0	26.2	22.0	2.2	20.6	2.2	20.6	23.9	23.9	1-1/4 in.	1-1/4 in.	1/2 in.	17.1	14.8	17.1
	cm.	78.7	66.5	55.9	5.6	52.3	5.6	52.3	60.7	60.7	31.8 mm	31.8 mm	12.7 mm	43.4	37.6	43.4
060 & 075	in.	31.0	26.2	22.0	2.4	23.0	2.4	23.0	20.6	20.6	1-1/4 in.	1-1/4 in.	1/2 in.	17.1	14.8	17.1
	cm.	78.7	66.5	55.9	6.1	58.4	6.1	58.4	52.3	52.3	31.8 mm	31.8 mm	12.7 mm	43.4	37.6	43.4

Model		Water Connections										Electrical Knockouts			
		M	N	O	P	Q	R	S	T	U	V	W	X	Y	Z
		Load Liquid In	Load Liquid Out	Source Liquid In	Source Liquid Out	HWG In	HWG Out	Power Supply	Low Voltage	Side Power Supply	Side Power Supply	Ext Pump	Ext Pump	Power Supply	Power Supply
018	in.	2.4	2.4	2.4	2.4	-	-	3.5	2.9	14.9	2.6	2.1	1.8	2.9	4.1
	cm.	6.1	6.1	6.1	6.1	-	-	8.9	7.4	37.8	6.6	5.3	4.4	7.4	10.4
025	in.	2.4	2.4	2.4	2.4	-	-	3.5	2.9	14.9	2.6	2.1	1.8	2.9	4.1
	cm.	6.1	6.1	6.1	6.1	-	-	8.9	7.4	37.8	6.6	5.3	4.4	7.4	10.4
040	in.	1.6	2.8	2.8	1.6	2.0	1.8	4.8	4.8	17.1	2.8	14.9	4.8	4.8	17.1
	cm.	4.1	7.0	7.0	4.1	5.1	4.6	12.2	12.2	43.4	7.0	37.8	12.2	12.2	43.4
050	in.	1.8	3.6	3.6	1.8	2.1	1.8	4.8	4.8	17.1	2.8	14.9	4.8	4.8	17.1
	cm.	4.6	9.1	9.1	4.6	5.3	4.6	12.2	12.2	43.4	7.1	37.8	12.2	12.2	43.4
060 & 075	in.	1.8	4.0	4.0	1.8	4.2	1.4	4.8	4.8	17.1	2.8	14.9	4.8	4.8	17.1
	cm.	4.6	10.2	10.2	4.6	10.7	3.6	12.2	12.2	43.4	7.1	37.8	12.2	12.2	43.4

8/6/10

NOTE: Plastic front panel extends 1.4 in. (3.56 cm) beyond front of cabinet.

Physical Data

Model	018	025	040	050	060	075
Compressor (1 each)	Scroll					
Factory Charge R410a, oz [kg]	44.0 [1.25]	58.0 [1.64]	70 [1.98]	68 [1.93]	104 [2.95]	110 [3.12]
Coax & Piping Water Volume - gal [l]*	.52 [1.97]	.89 [3.38]	1.0 [3.94]	1.4 [5.25]	1.6 [6.13]	1.6 [6.13]
Weight - Operating, lb [kg]	191 [86.6]	225 [102.1]	290 [131.5]	325 [147.4]	345 [156.5]	345 [156.5]
Weight - Packaged, lb [kg]	213 [96.6]	247 [112.0]	305 [138.3]	340 [154.2]	360 [163.3]	360 [163.3]

NOTE: * Source or load side only.

8/6/10

Electrical Data

Model	Rated Voltage	Voltage Min/Max	Compressor			Load Pump	Source Pump	Total Unit FLA	Min Ckt Amp	Maximum Fuse/HACR
			RLA	LRA	LRA*					
018	208-230/60/1	187/253	9.0	48.0	17.0	1.8	5.4	16.2	18.5	30
025	208-230/60/1	187/253	13.5	61.0	21.4	1.8	5.4	20.7	24.1	35
040	208-230/60/1	187/253	20.0	115.0	40.3	1.8	5.4	27.2	32.2	50
050	208-230/60/1	187/253	26.4	134.0	46.9	1.8	5.4	33.6	40.2	60
060	208-230/60/1	187/253	30.1	145.0	50.8	1.8	5.4	37.3	44.8	70
075	208-230/60/1	187/253	26.9	145.0	50.8	1.8	5.4	34.1	40.8	60

7/26/13

NOTES: All fuses type “D” time delay (or HACR circuit breaker in USA).
Source pump amps shown are for up to a 1/2 HP pump.
Load pumps amps shown are for small circulators.
*LRA with optional IntelliStart installed (208-230/60/1).

Antifreeze Correction

Catalog performance can be corrected for antifreeze use. Please use the following table and note the example given.

Antifreeze Type	Antifreeze % by wt	Heating		Cooling		Pressure Drop
		Load	Source	Load	Source	
EWT - °F [°C]		**80 [26.7]**	**30 [-1.1]**	**50 [10.0]**	**90 [32.2]**	**30 [-1.1]**
Water	0	1.000	1.000	1.000	1.000	1.000
Ethylene Glycol	10	0.990	0.973	0.976	0.991	1.075
	20	0.978	0.943	0.947	0.979	1.163
	30	0.964	0.917	0.921	0.965	1.225
	40	0.953	0.890	0.897	0.955	1.324
	50	0.942	0.865	0.872	0.943	1.419
Propylene Glycol	10	0.981	0.958	0.959	0.981	1.130
	20	0.967	0.913	0.921	0.969	1.270
	30	0.946	0.854	0.869	0.950	1.433
	40	0.932	0.813	0.834	0.937	1.614
	50	0.915	0.770	0.796	0.922	1.816
Ethanol	10	0.986	0.927	0.945	0.991	1.242
	20	0.967	0.887	0.906	0.972	1.343
	30	0.944	0.856	0.869	0.947	1.383
	40	0.926	0.815	0.830	0.930	1.523
	50	0.907	0.779	0.795	0.911	1.639
Methanol	10	0.985	0.957	0.962	0.986	1.127
	20	0.969	0.924	0.929	0.970	1.197
	30	0.950	0.895	0.897	0.951	1.235
	40	0.935	0.863	0.866	0.936	1.323
	50	0.919	0.833	0.836	0.920	1.399

WARNING: Gray area represents antifreeze concentrations greater than 35% by weight and should be avoided due to the extreme performance penalty they represent.

Antifreeze Correction Example

Antifreeze solution is propylene glycol 20% by weight for the source and methanol 10% for the load. Determine the corrected heating at 30°F source and 80°F load as well as pressure drop at 30°F for an Envision Series NSW050. Also, determine the corrected cooling at 90°F source and 50°F load.

The corrected heating capacity at 30°F/80°F would be:
46,700 MBTUH x 0.913 x 0.985 = 41,998 MBTUH
The corrected cooling capacity at 90°F/50°F would be:
44,200 x 0.969 x 0.962 = 41,202 MBTUH
The corrected pressure drop at 30°F and 15 GPM would be:
5.2 psi x 1.270 = 6.60 psi

AHRI/ISO 13256-2 Performance Ratings

English (IP) Units

Model	Capacity Modulation	Flow Rate		Water Loop Heat Pump				Ground Water Heat Pump				
				Cooling 86°F Source 53.6°F Load		Heating 68°F Source 104°F Load		Cooling 59°F Source 53.6°F Load		Heating 50°F Source 104°F Load		
		Load Gpm	Source Gpm	Capacity Btuh	EER Btuh/W	Capacity Btuh	COP	Capacity Btuh	EER Btuh/W	Capacity Btuh	COP	Energy Star Compliant
018	Single	5	5	16,400	14.0	22,200	4.5	18,800	22.9	18,500	3.7	Yes
025	Single	7	7	23,700	13.6	32,800	4.6	26,700	21.2	27,100	3.8	Yes
040	Single	10	10	35,900	15.5	47,900	4.8	40,900	23.4	39,100	3.9	Yes
050	Single	15	15	49,800	13.9	65,000	4.4	55,600	21.6	54,200	3.7	Yes
060	Single	18	18	55,400	13.6	78,000	4.7	62,500	20.6	63,200	3.8	Yes
075	Single	19	19	66,000	12.3	93,100	4.2	74,100	18.0	77,100	3.5	No

Model	Capacity Modulation	Flow Rate		Ground Loop Heat Pump				
				Cooling 77°F Source 53.6°F Load		Heating 32°F Source 104°F Load		
		Load Gpm	Source Gpm	Capacity Btuh	EER Btuh/W	Capacity Btuh	COP	Energy Star Compliant
018	Single	5	5	17,300	16.6	14,700	3.1	Yes
025	Single	7	7	24,700	16.1	22,000	3.1	Yes
040	Single	10	10	37,700	17.5	30,500	3.1	Yes
050	Single	15	15	51,500	16.4	44,200	3.1	Yes
060	Single	18	18	58,000	16.1	50,100	3.1	Yes
075	Single	19	19	68,400	14.0	61,500	2.9	No

NOTE: All ratings based upon 208V operation.

01/03/12

Pressure Drop

Model	GPM	Pressure Drop (psi)				
		30°F	60°F	80°F	100°F	120°F
018R*	3.0	0.5	0.4	0.4	0.3	0.3
	4.0	1.1	0.9	0.9	0.8	0.8
	5.0	1.6	1.4	1.4	1.3	1.3
	6.0	2.1	1.9	1.9	1.8	1.8
025R*	4.0	0.7	0.6	0.4	0.3	0.3
	5.5	1.3	1.1	0.9	0.7	0.6
	7.0	1.9	1.7	1.5	1.3	1.2
	8.5	2.6	2.4	2.2	2.0	1.9
040H/R	5.0	0.9	0.6	0.6	0.5	0.5
	7.5	2.3	2.1	2.0	1.9	1.8
	10.0	3.7	3.5	3.3	3.2	3.0
	12.5	5.0	4.7	4.4	4.2	4.0
050H/R	8.0	1.7	1.4	1.4	1.3	1.3
	11.5	3.6	3.4	3.2	3.0	2.8
	15.0	5.6	5.4	5.0	4.6	4.2
	18.5	8.3	8.1	7.6	7.2	6.8
060H/R	9.0	1.4	1.1	1.0	1.0	0.9
	13.5	4.2	3.9	3.5	3.1	2.7
	18.0	6.9	6.7	6.0	5.2	4.5
	22.5	10.7	10.5	10.0	9.4	8.7
075H/R	10.0	3.2	3.0	2.8	2.7	2.5
	14.5	5.5	5.3	5.1	4.9	4.7
	19.0	7.9	7.6	7.3	7.1	6.8
	23.5	11.5	11.3	11.0	10.8	10.5

NOTES: Temperatures are Entering Water Temperatures
*Domestic water heating units source side pressure drop and reversible units load and source pressure drop.

8/9/10

NSW Vented Only Load Side

Model	GPM	Pressure Drop (psi)			
		60°F	80°F	100°F	120°F
018H	3.0	0.5	0.4	0.4	0.3
	4.0	1.4	1.3	1.2	1.2
	5.0	2.2	2.1	2.1	2.0
	6.0	3.0	2.9	2.9	2.8
025H	4.0	1.3	1.3	1.2	1.2
	5.5	3.0	2.9	2.8	2.7
	7.0	4.6	4.4	4.3	4.1
	8.5	6.7	6.5	6.4	6.2

NOTES: Temperatures are Entering Water Temperatures.
Double wall vented coax for heating potable water

7/13/09

Reference Calculations

Heating Calculations:	Cooling Calculations:
$LWT = EWT - \frac{HE}{GPM \times C^*}$	$LWT = EWT + \frac{HR}{GPM \times C^*}$
$HE = C^* \times GPM \times (EWT - LWT)$	$HR = C^* \times GPM \times (LWT - EWT)$

NOTE: * C = 500 for pure water, 485 for brine.

Legend and Notes

Abbreviations and Definitions

ELT = entering load fluid temperature to heat pump
SWPD = source coax water pressure drop
LLT = leaving load fluid temperature from heat pump
PSI = pressure drop in pounds per square inch
LGPM = load flow in gallons per minute
FT HD = pressure drop in feet of head
LWPD = load coax water pressure drop
LWT = leaving water temperature
EWT = entering water temperature
Brine = water with a freeze inhibiting solution
kW = kilowatts
EST = entering source fluid temperature to heat pump
HE = heat extracted in MBTUH
LST = leaving source fluid temperature from heat pump
HC = total heating capacity in MBTUH
COP = coefficient of performance, heating [HC/kW x 3.413]
EER = energy efficiency ratio, cooling
TC = total cooling capacity in MBTUH
HR = heat rejected in MBTUH

Notes to Performance Data Tables

The following notes apply to all performance data tables:

- Three flow rates are shown for each unit. The lowest flow rate shown is used for geothermal open loop/well water systems with a minimum of 50°F EST. The middle flow rate shown is the minimum geothermal closed loop flow rate. The highest flow rate shown is optimum for geothermal closed loop systems and the suggested flow rate for boiler/tower applications.
- Entering water temperatures below 40°F assumes 15% antifreeze solution.
- Interpolation between ELT, EST, and GPM data is permissible.
- Operation in the gray areas is not recommended.

NSW050 - Performance Data

Cooling Capacity

Source		Load Flow-8 GPM							Load Flow-11.5 GPM						Load Flow-15 GPM					
EST °F	Flow GPM	ELT °F	LLT °F	TC MBTUH	Power kW	HR MBTUH	EER	LST °F	LLT °F	TC MBTUH	Power kW	HR MBTUH	EER	LST °F	LLT °F	TC MBTUH	Power kW	HR MBTUH	EER	LST °F
30	8	50	35.8	55.2	1.98	61.9	27.9	46.0	38.8	57.0	2.00	63.8	28.6	46.4	41.9	58.8	2.01	65.7	29.3	46.9
		70	54.6	59.8	2.01	66.6	29.8	47.2	58.0	61.0	2.02	67.8	30.3	47.5	61.5	62.2	2.02	69.1	30.7	47.8
		90	73.4	64.3	2.03	71.3	31.6	48.4	77.2	64.9	2.04	71.9	31.9	48.5	81.0	65.5	2.04	72.5	32.2	48.7
		110	92.2	68.9	2.06	75.9	33.4	49.6	96.4	68.9	2.06	75.9	33.5	49.6	100.5	68.9	2.05	75.9	33.6	49.6
	11.5	50	35.9	54.6	1.90	61.1	28.8	42.1	39.0	56.3	1.92	62.8	29.3	42.5	42.0	57.9	1.94	64.5	29.8	42.8
		70	55.0	58.1	1.92	64.6	30.3	42.9	58.4	59.1	1.93	65.7	30.7	43.1	61.7	60.2	1.94	66.9	31.0	43.3
		90	74.2	61.5	1.93	68.1	31.8	43.6	77.8	62.0	1.94	68.6	32.0	43.8	81.4	62.6	1.94	69.2	32.3	43.9
		110	93.3	64.9	1.95	71.6	33.3	44.4	97.2	64.9	1.95	71.5	33.4	44.4	101.1	64.9	1.94	71.5	33.5	44.4
	15	50	36.1	54.1	1.82	60.3	29.7	38.3	39.1	55.6	1.85	61.8	30.1	38.5	42.2	57.0	1.87	63.4	30.5	38.7
		70	55.5	56.4	1.83	62.6	30.9	38.6	58.7	57.3	1.84	63.6	31.1	38.7	62.0	58.3	1.86	64.6	31.4	38.9
		90	74.9	58.6	1.83	64.9	32.0	38.9	78.3	59.1	1.84	65.4	32.2	39.0	81.8	59.6	1.84	65.9	32.3	39.1
		110	94.3	60.9	1.84	67.2	33.1	39.2	98.0	60.9	1.84	67.2	33.2	39.2	101.6	60.9	1.83	67.1	33.3	39.2
50	8	50	36.7	51.5	2.53	60.2	21.7	65.5	39.5	53.5	2.53	62.2	22.4	66.0	42.4	55.5	2.54	64.2	23.1	66.5
		70	54.6	59.9	2.58	68.7	24.4	67.7	57.9	61.5	2.59	70.4	24.9	68.1	61.3	63.1	2.60	72.0	25.5	68.5
		90	72.4	68.3	2.64	77.3	26.9	69.9	76.3	69.5	2.65	78.5	27.3	70.2	80.3	70.7	2.65	79.8	27.7	70.6
		110	90.2	76.7	2.70	85.9	29.4	72.1	94.7	77.5	2.71	86.7	29.6	72.4	99.2	78.3	2.71	87.5	29.8	72.6
	11.5	50	39.8	51.6	2.43	59.9	21.3	61.9	39.6	53.4	2.44	61.7	21.9	62.2	42.4	55.2	2.45	63.6	22.5	62.6
		70	58.3	58.9	2.47	67.4	23.9	63.4	58.2	60.3	2.48	68.8	24.4	63.7	61.5	61.7	2.48	70.2	24.9	64.0
		90	76.8	66.3	2.51	74.8	26.4	64.9	76.8	67.3	2.51	75.8	26.8	65.1	80.6	68.3	2.52	76.9	27.1	65.4
		110	95.3	73.6	2.55	82.3	28.9	66.5	95.4	74.2	2.55	82.9	29.1	66.6	99.7	74.8	2.55	83.5	29.3	66.7
	15	50	42.9	51.7	2.33	59.7	23.5	58.2	39.6	53.3	2.35	61.3	24.0	58.4	42.5	54.9	2.36	63.0	24.5	58.7
		70	62.0	58.0	2.35	66.0	25.8	59.1	58.4	59.2	2.36	67.2	26.2	59.2	61.7	60.4	2.37	68.5	26.5	59.4
		90	81.2	64.2	2.37	72.3	28.0	59.9	77.2	65.0	2.38	73.1	28.2	60.1	80.9	65.9	2.38	74.0	28.5	60.2
		110	100.3	70.5	2.39	78.6	30.2	60.8	96.0	70.9	2.39	79.1	30.3	60.9	100.2	71.4	2.40	79.5	30.5	60.9
70	8	50	37.7	47.9	3.07	58.4	15.6	85.0	40.2	50.1	3.07	60.5	16.3	85.6	42.8	52.2	3.07	62.7	17.0	86.2
		70	54.5	60.1	3.16	70.9	19.0	88.3	57.9	62.1	3.17	72.9	19.6	88.8	61.2	64.0	3.17	74.9	20.2	89.3
		90	71.4	72.3	3.25	83.4	22.2	91.5	75.5	74.1	3.26	85.2	22.7	92.0	79.6	75.9	3.27	87.0	23.2	92.4
		110	Operation not recommended																	
	11.5	50	37.5	48.6	2.96	58.7	16.4	81.6	40.1	50.6	2.96	60.6	17.1	82.0	42.8	52.5	2.96	62.6	17.7	82.4
		70	54.6	59.8	3.02	70.1	19.8	83.9	57.9	61.5	3.02	71.8	20.4	84.3	61.3	63.3	3.03	73.6	20.9	84.6
		90	71.7	71.0	3.08	81.5	23.1	86.2	75.8	72.5	3.09	83.1	23.5	86.5	79.8	74.0	3.10	84.6	23.9	86.9
		110	Operation not recommended																	
	15	50	37.3	49.3	2.84	59.0	17.4	78.1	40.0	51.1	2.85	60.8	17.9	78.4	42.7	52.8	2.85	62.5	18.5	78.6
		70	54.7	59.5	2.87	69.3	20.7	79.5	58.0	61.0	2.88	70.8	21.2	79.7	61.4	62.5	2.89	72.3	21.6	79.9
		90	72.0	69.8	2.91	79.7	24.0	81.0	76.1	71.0	2.92	80.9	24.3	81.1	80.1	72.1	2.92	82.1	24.7	81.3
		110	89.4	80.0	2.94	90.0	27.2	82.4	94.1	80.9	2.95	91.0	27.4	82.5	98.8	81.8	2.96	91.9	27.6	82.6
90	8	50	38.9	43.0	3.93	56.4	11.8	104.5	41.3	44.7	3.94	58.1	12.2	105.0	43.6	46.4	3.95	59.9	12.7	105.4
		70	56.0	54.5	4.02	68.2	14.5	107.6	59.0	56.2	4.04	70.0	14.9	108.0	62.0	58.0	4.05	71.8	15.4	108.5
		90	73.0	66.0	4.12	80.0	17.1	110.6	76.7	67.8	4.13	81.9	17.5	111.1	80.4	69.5	4.15	83.7	17.9	111.6
		110	Operation not recommended																	
	11.5	50	38.8	43.6	3.81	56.6	11.5	101.2	41.2	45.2	3.81	58.2	11.8	101.5	43.6	46.8	3.82	59.8	12.2	101.8
		70	55.9	54.7	3.87	67.9	14.1	103.4	59.0	56.3	3.88	69.6	14.5	103.8	62.0	57.9	3.89	71.2	14.9	104.1
		90	73.0	65.9	3.93	79.3	16.8	105.7	76.8	67.5	3.95	81.0	17.1	106.1	80.5	69.1	3.96	82.7	17.4	106.4
		110	Operation not recommended																	
	15	50	38.6	44.2	3.68	56.8	13.0	97.8	41.1	45.7	3.69	58.2	13.4	98.0	43.5	47.1	3.69	59.7	13.8	98.2
		70	55.8	55.0	3.72	67.7	15.9	99.3	58.9	56.5	3.72	69.2	16.3	99.5	62.0	57.9	3.73	70.7	16.7	99.7
		90	73.0	65.8	3.75	78.6	18.7	100.8	76.8	67.3	3.76	80.1	19.1	101.0	80.6	68.7	3.77	81.6	19.4	101.2
		110	Operation not recommended																	
110	8	50	40.2	38.0	4.79	54.3	7.9	124.0	42.3	39.3	4.81	55.7	8.2	124.4	44.4	40.6	4.82	57.1	8.4	124.7
		70	57.4	48.8	4.89	65.5	10.0	126.9	60.1	50.4	4.91	67.1	10.3	127.3	62.9	51.9	4.93	68.7	10.5	127.7
		90	Operation not recommended																	
		110																		
	11.5	50	40.1	38.6	4.66	54.4	8.3	120.8	42.2	39.8	4.67	55.7	8.5	121.0	44.4	41.0	4.68	57.0	8.8	121.3
		70	57.2	49.7	4.72	65.8	10.5	123.0	60.0	51.2	4.74	67.3	10.8	123.3	62.8	52.6	4.75	68.9	11.1	123.6
		90	Operation not recommended																	
		110																		
	15	50	39.9	39.1	4.52	54.5	8.7	117.5	42.1	40.3	4.53	55.7	8.9	117.7	44.3	41.4	4.53	56.9	9.1	117.8
		70	57.0	50.5	4.56	66.1	11.1	119.1	59.8	51.9	4.57	67.5	11.4	119.3	62.7	53.4	4.58	69.0	11.7	119.5
		90	Operation not recommended																	
		110																		

8/20/09

NSW050 - Performance Data cont.

Heating Capacity

Source		Load Flow-8 GPM							Load Flow-11.5 GPM						Load Flow-15 GPM					
EST °F	Flow GPM	ELT °F	LLT °F	HC MBTUH	Power kW	HE MBTUH	COP	LST °F	LLT °F	HC MBTUH	Power kW	HE MBTUH	COP	LST °F	LLT °F	HC MBTUH	Power kW	HE MBTUH	COP	LST °F
25	11.5	60	Operation not recommended																	
		80																		
		100																		
		120																		
	15	60	71.3	43.9	2.50	35.4	5.15	20.1	67.9	44.0	2.50	35.4	5.16	20.1	66.0	44.0	2.49	35.5	5.18	20.1
		80	91.0	42.6	3.41	31.0	3.66	20.7	87.6	42.6	3.37	31.1	3.71	20.7	85.9	42.6	3.33	31.3	3.75	20.7
		100	110.6	41.3	4.32	26.6	2.80	21.3	107.4	41.3	4.25	26.8	2.85	21.3	105.7	41.3	4.17	27.0	2.90	21.3
		120	130.3	40.0	5.23	22.2	2.24	22.0	127.2	40.0	5.12	22.5	2.29	21.9	125.5	39.9	5.01	22.8	2.33	21.9
30	8	60	71.8	45.7	2.36	37.6	5.67	20.3	69.0	45.8	2.43	37.5	5.53	20.3	66.3	45.8	2.49	37.3	5.39	20.4
		80	91.4	44.4	3.31	33.1	3.92	21.5	88.8	44.4	3.33	33.0	3.91	21.5	86.1	44.4	3.34	33.0	3.89	21.5
		100	111.1	43.0	4.27	28.5	2.96	22.7	108.5	43.0	4.23	28.6	2.98	22.6	105.9	43.0	4.19	28.7	3.01	22.6
		120	130.7	41.7	5.22	23.9	2.34	23.8	128.2	41.7	5.13	24.1	2.38	23.8	125.7	41.6	5.04	24.4	2.42	23.7
	11.5	60	72.2	47.2	2.50	38.6	5.53	22.4	69.3	47.2	2.49	38.7	5.56	22.4	66.5	47.3	2.48	38.8	5.59	22.4
		80	91.7	45.5	3.41	33.9	3.92	23.4	89.0	45.6	3.37	34.1	3.96	23.3	86.3	45.6	3.33	34.2	4.01	23.3
		100	111.3	43.9	4.31	29.2	2.98	24.3	108.7	43.9	4.25	29.4	3.03	24.2	106.0	43.9	4.18	29.6	3.08	24.2
		120	130.9	42.3	5.22	24.5	2.37	25.2	128.4	42.3	5.13	24.8	2.42	25.1	125.8	42.2	5.03	25.0	2.46	25.1
	15	60	72.5	48.6	2.64	39.6	5.39	24.6	69.6	48.7	2.56	40.0	5.59	24.5	66.7	48.8	2.47	40.4	5.79	24.5
		80	92.0	46.7	3.50	34.8	3.91	25.2	89.2	46.8	3.41	35.1	4.02	25.2	86.4	46.8	3.32	35.5	4.13	25.1
		100	111.5	44.8	4.36	29.9	3.01	25.9	108.9	44.8	4.27	30.2	3.08	25.8	106.2	44.8	4.17	30.6	3.15	25.8
		120	131.1	42.9	5.22	25.1	2.41	26.6	128.5	42.9	5.12	25.4	2.45	26.5	125.9	42.8	5.02	25.7	2.50	26.5
50	8	60	75.1	58.8	2.56	50.0	6.65	37.1	71.6	58.6	2.54	50.0	6.72	37.1	68.0	58.5	2.52	49.9	6.80	37.1
		80	94.5	56.3	3.47	44.4	4.71	38.5	91.1	56.2	3.42	44.6	4.80	38.5	87.7	56.2	3.36	44.7	4.88	38.5
		100	113.9	53.9	4.39	38.9	3.58	40.0	110.6	53.8	4.30	39.2	3.66	39.9	107.4	53.8	4.21	39.4	3.74	39.8
		120	133.2	51.4	5.30	33.3	2.83	41.4	130.2	51.4	5.18	33.7	2.91	41.3	127.1	51.5	5.06	34.2	2.98	41.2
	11.5	60	75.7	61.0	2.64	52.0	6.78	39.8	72.0	60.8	2.58	52.0	6.91	39.9	68.3	60.5	2.51	51.9	7.06	39.9
		80	95.0	58.1	3.53	46.1	4.83	41.0	91.5	57.9	3.44	46.2	4.93	41.0	87.9	57.8	3.36	46.3	5.04	41.0
		100	114.2	55.2	4.41	40.2	3.67	42.1	110.9	55.1	4.31	40.4	3.75	42.1	107.6	55.0	4.21	40.6	3.83	42.0
		120	133.5	52.4	5.30	34.3	2.89	43.3	130.3	52.3	5.18	34.6	2.96	43.2	127.2	52.3	5.06	35.0	3.03	43.1
	15	60	76.3	63.3	2.72	54.0	6.79	42.6	72.4	62.9	2.61	54.0	7.03	42.6	68.6	62.5	2.51	53.9	7.27	42.6
		80	95.4	59.9	3.58	47.7	4.89	43.4	91.8	59.6	3.47	47.8	5.03	43.4	88.2	59.4	3.36	47.9	5.17	43.4
		100	114.6	56.6	4.44	41.5	3.72	44.3	111.2	56.4	4.32	41.7	3.82	44.3	107.7	56.2	4.20	41.9	3.91	44.2
		120	133.7	53.3	5.30	35.2	2.94	45.2	130.5	53.2	5.18	35.5	3.01	45.1	127.3	53.1	5.05	35.8	3.07	45.1
70	8	60	78.5	71.8	2.76	62.4	7.62	53.9	74.1	71.5	2.65	62.5	7.92	53.9	69.8	71.2	2.54	62.5	8.21	53.9
		80	97.6	68.2	3.63	55.8	5.50	55.6	93.5	68.1	3.51	56.1	5.69	55.5	89.3	67.9	3.39	56.3	5.87	55.5
		100	116.7	64.7	4.51	49.3	4.20	57.3	112.8	64.6	4.37	49.7	4.34	57.2	108.9	64.6	4.23	50.2	4.47	57.1
		120	135.7	61.1	5.38	42.7	3.33	59.0	132.1	61.2	5.23	43.4	3.43	58.8	128.4	61.3	5.08	44.0	3.54	58.7
	11.5	60	79.3	74.9	2.78	65.4	7.90	57.3	74.7	74.3	2.66	65.2	8.18	57.3	70.1	73.7	2.55	65.0	8.48	57.3
		80	98.2	70.7	3.64	58.3	5.69	58.6	93.9	70.3	3.52	58.3	5.86	58.6	89.6	69.9	3.39	58.3	6.04	58.6
		100	117.2	66.6	4.51	51.2	4.32	60.0	113.1	66.3	4.37	51.4	4.44	59.9	109.1	66.1	4.24	51.6	4.57	59.9
		120	136.1	62.4	5.38	44.0	3.40	61.4	132.3	62.4	5.23	44.5	3.49	61.3	128.6	62.3	5.08	45.0	3.59	61.2
	15	60	80.1	77.9	2.79	68.4	8.18	60.6	75.3	77.1	2.67	67.9	8.47	60.7	70.5	76.2	2.55	67.5	8.76	60.7
		80	98.9	73.2	3.65	60.7	5.87	61.7	94.4	72.5	3.52	60.5	6.04	61.7	89.9	71.9	3.39	60.3	6.21	61.7
		100	117.6	68.4	4.52	53.0	4.44	62.7	113.5	68.0	4.38	53.1	4.56	62.7	109.3	67.6	4.24	53.1	4.68	62.7
		120	136.4	63.7	5.38	45.3	3.47	63.8	132.6	63.5	5.23	45.7	3.56	63.7	128.7	63.3	5.08	46.0	3.65	63.7
90	8	60	81.9	84.9	2.85	75.2	8.73	70.6	76.5	82.8	3.51	70.8	7.21	71.7	71.1	80.7	4.16	66.5	5.68	72.9
		80	100.6	80.1	3.71	67.4	6.32	72.6	95.6	78.7	4.09	64.8	5.70	73.3	90.6	77.4	4.47	62.2	5.08	74.0
		100	119.4	75.2	4.58	59.6	4.82	74.6	114.8	74.7	4.68	58.7	4.68	74.9	110.2	74.1	4.77	57.8	4.55	75.1
		120	Operation not recommended																	
	11.5	60	82.3	86.6	2.86	76.9	8.89	74.9	76.8	84.1	3.12	73.5	7.91	75.6	71.2	81.6	3.38	70.1	7.08	76.4
		80	101.1	81.8	3.72	69.0	6.43	76.5	95.9	80.2	3.84	67.1	6.12	76.9	90.8	78.6	3.95	65.1	5.83	77.3
		100	119.8	76.9	4.59	61.2	4.91	78.0	115.1	76.2	4.56	60.7	4.90	78.1	110.4	75.5	4.52	60.1	4.90	78.3
		120	Operation not recommended																	
	15	60	82.8	88.3	2.86	78.5	9.05	79.2	77.0	85.4	2.73	76.1	9.19	79.5	71.3	82.5	2.59	73.7	9.33	79.9
		80	101.5	83.4	3.73	70.7	6.55	80.3	96.2	81.6	3.58	69.3	6.68	80.5	91.0	79.7	3.43	68.0	6.81	80.7
		100	120.2	78.6	4.61	62.8	5.00	81.4	115.4	77.7	4.44	62.6	5.14	81.4	110.6	76.9	4.26	62.3	5.28	81.4
		120	Operation not recommended																	

8/19/09

Appendix 4

Soil types referred in the thesis are briefly described in the table below.

Material	Material description
Reef limestone	A limestone consisting of the remains of active reef-building organisms, such as corals, sponges, and bryozoans, and of sediment-binding organic constituents, such as calcareous algae.
Chalk	A soft, earthy, fine-textured, usually white to light-gray or buff limestone of marine origin. It consists almost wholly (90% to 99%) of calcite, formed mainly by shallow-water accumulation of calcareous remains of floating microorganisms (chiefly foraminifers) and of comminuted remains of calcareous algae, set in a structureless matrix of very finely crystalline calcite. The rock is porous, somewhat friable, and only slightly coherent.
Marl	An old term loosely applied to a variety of materials, most of which occur as loose, earthy deposits consisting chiefly of an intimate mixture of clay and calcium carbonate, formed under marine or esp. freshwater conditions; specif. an earthy substance containing 35% to 65% clay and 65% to 35% carbonate. Marl is usually gray; it is used esp. as a fertilizer for acid soils deficient in lime. In the Coastal Plain area of Southeastern United States, the term has been used for calcareous clays, silts, and sands, esp. those containing glauconite (greensand marls); and for newly formed deposits of shells mixed with clay. A soft, grayish to white, earthy or powdery, usually impure, calcium carbonate precipitated on the bottoms of present-day freshwater lakes and ponds, largely through the chemical action of aquatic plants, or forming deposits that underlie marshes, swamps, and bogs that occupy the sites of former (glacial) lakes. The calcium carbonate may range from 90% to less than 30% .
Calcarenite	A limestone consisting predominantly (more than 50%) of recycled calcite particles of sand size; a consolidated calcareous sand.
Gypsum	A monoclinic mineral, 8[CaSO4 .2H2 O] ; colorless to white in crystals, but massive beds may range from red to yellow to brown, gray, or black; the most common natural sulfate; defines 2 on the Mohs hardness scale; commonly associated with rock salt (halite) and anhydrite; forms beds and lenses interstratified with limestone, shale, and clay, esp. in rocks of Permian to Triassic age; also in volcanic fumarolic deposits; an accessory mineral in metalliferous veins.
Ochre	A name given to various native earthy materials used as pigments. They consist essentially of hydrated ferric oxide admixed with clay and sand in varying amounts and in impalpable subdivision. When carrying much manganese ocher’s grade into umbers. They are yellow, brown, or red. In general, the native yellows and browns are varieties of limonite and the native reds are varieties of hematite.
Lava	Basic lava poor in silica, generally less than 52% total SiO2; typically dark and heavy, as basalt. A rock that is composed of accidental or non-volcanic fragments in a volcanic matrix.

Gabbro	A group of dark-colored, basic intrusive igneous rocks composed principally of basic plagioclase (commonly labradorite or bytownite) and clinopyroxene (augite), with or without olivine and orthopyroxene; also, any member of that group. It is the approximate intrusive equivalent of basalt.
Hartzburgite	The ultramafic ingenious rock, harzburgite, is a variety of peridotite consisting mostly of the two minerals, olivine and low-calcium (Ca) pyroxene (enstatite); it is named for occurrences in the Hartz mountains of Germany. It commonly contains a few percent chromium-rich spinel as an accessory mineral.
Diabase	An intrusive rock whose main components are labradorite and pyroxene and that is characterized by ophitic texture. As originally applied by Brongniart in 1807, the term corresponded to what is now recognized as diorite. The word has come to mean pre-Tertiary basalt in Germany, decomposed basalt in England, and a dike-rock with ophitic texture in the United States and Canada.
Pyrites	Various metallic-looking sulphide minerals including iron pyrites (pyrite); copper pyrites (chalcopyrite); tin pyrites (stannite); white iron, cockscomb, or spear pyrites (marcasite); arsenical pyrites (arsenopyrite); cobalt pyrites (linnaeite); magnetic pyrites (pyrrhotite); and capillary pyrites (millerite). Without qualification it popularly refers to pyrite.
Umber (silisified)	A brown earth that is darker than ochre and sienna, consisting of iron oxide and oxyhydroxide with manganese oxides, clay, and lime. Highly valued as a permanent pigment, it may be used in its greenish brown natural state (raw umber) or in the dark or reddish brown calcined state (burnt umber).
Pyroxenite	A coarse-grained, holocrystalline igneous rock consisting of 90% pyroxenes. It may contain biotite, hornblende, or olivine as accessories.
Serpentinite	A rock consisting almost wholly of serpentine-group minerals, e.g., antigorite and chrysotile or lizardite, derived from the alteration of ferromagnesian silicate minerals, such as olivine and pyroxene. Accessory chlorite, talc, and magnetite may be present.